DOTTORATO DI RICERCA IN SCIENZE DELLA TERRA, DELLA VITA E DELL'AMBIENTE

Ciclo XXXII

Settore Concorsuale: 04/A2

Settore Scientifico Disciplinare: GEO/02

Palynological characterization of late Quaternary architectural elements from the Mediterranean coastal record (Arno and Po delta plains).

Presentata da:　Marco Cacciari

Coordinatore Dottorato

Prof. Giulio Viola

Supervisore

Prof. Alessandro Amorosi

Co-Supervisori

Dott.ssa Veronica Rossi
Prof. Marco Marchesini

Esame finale anno 2020

ABSTRACT

Pollen grains and spores are commonly used to study palaeoclimate variations at a high-resolution scale over rather long time intervals within continuous, fine-grained lacustrine and marine successions. On the other hand, coastal and deltaic sedimentary successions are still an underexplored archive for vegetation-based palaeoclimate reconstructions, because they are characterised by stratigraphic features considered *a priori* unfavourable for palynological studies, like the variety of depositional facies and the frequent occurrence of sand bodies and discontinuity surfaces. However, these potentially weak points can be seen as an opportunity to investigate the complex interactions among environment, vegetation and climate in areas strongly affected by late Quaternary glacio-eustatic variations. Using twenty years of high-resolution stratigraphic studies as a starting point, this Thesis explores in detail the potentiality of integrated palyno-stratigraphic analyses for an improved understanding of landscape dynamics and forcing factors in Mediterranean coastal systems at both Milankovitch and sub-Milankovitch scales. To achieve this goal, I studied two sedimentary cores retrieved in the shallow subsurface of two delta plains located at the opposite sides of the Northern Apennines: core EM2 from the Po delta plain (40 m-long) and core PA1 from the Arno delta plain (31.5 m-long).

In the Po delta plain, the stratigraphic-based palynological approach led to the detailed facies characterization of the stratigraphically expanded, freshwater paludal succession developed during the Holocene at the innermost margin of the system. In fact, the absence of other palaeobiological proxies (i.e., foraminifers and ostracods) in this portion of the basin makes palynomorphs very useful as facies indicators (i.e., halophytes, aquatics, hygrophytes, etc...). The distinction of different types of swamp facies in terms of water-table conditions, in turn, allowed the identification of the landward equivalents of flooding surfaces and of the maximum flooding surface, otherwise not traceable in such a proximal position. After filtering the facies signal and using statistical analysis, it was also possible to identify a series of Holocene cooling events in correspondence of peaks in montane taxa (e.g., mainly trees such as *Abies*, *Alnus incana* and *A. viridis*, *Fagus* and *Pinus mugo*). Although a strict continuity of the pollen record is partially hampered by the facies-aimed sampling pace, this vegetation-climate variability in the Po plain recalls the cyclicity of Bond events, especially for the early-mid Holocene (i.e., Preboreal and Boreal Oscillation, 8.2 ka event). Moreover, for the first time, pollen from a continental succession of the Adriatic area outlined the effects of the 8.2 ka cooling event on both vegetation and depositional dynamics: the former show a reaction to climate change quicker than the latter, as montane trees clearly increase before the sedimentary system's response *via* crevasse deposition. Furthermore, a change in the montane tree

pollen assemblage may suggest a vegetational succession towards more unstable conditions as the cool event unravelled.

In the Arno delta plain, Bryophyte spores were also analysed in a context of higher facies variability involving lagoonal intervals. Within the 30 m-thick succession under examination, two transgressive-regressive (T-R) depositional cycles were identified and related to the interglacial-glacial fluctuations of the MIS 5e-MIS 1 interval, mainly thanks to the varying tree species composition and the integration with sedimentological and meiofauna features. Indeed, stratigraphic intervals with dominant mixed oak – holm oak forest taxa were interpreted as interglacials, whereas the interbedded interval containing dominant Conifers and/or upland herbs was interpreted as reflecting last glacial conditions. The former invariably correspond to lagoon-deltaic deposits, whereas the latter is represented by an alluvial succession containing a vertically stacked pattern of palaeosols. Moreover, Bryophytes proved to be effective in tracking the T-R cycles boundaries, as the environmental pioneering conditions at the beginning of interglacials can be successfully exploited by this group of land plants. Furthermore, for the first time in the Arno plain, coastal deposits (lagoon) assigned to MIS 5e were detected *via* the abundance of Mediterranean elements (e.g., *Erica arborea, Quercus ilex*), fitting well with the general depositional architecture of the plain and shedding new light on the complex late Quaternary stratigraphy of the area. Interestingly, the almost synchronous response of coastal environments to the late Quaternary climate forcing was also documented at a sub-Milankovitch timescale. Indeed, a gradual increase in montane broadleaves (such as *Alnus incana, A. viridis* and *Fagus sylvatica*) occurs within the upper portion of the Holocene lagoon, peaking in correspondence of the sandy body that records the final stages of basin infilling.

The comparison between the two records suggests that Holocene subtle variations in pollen assemblages (montane *versus* lowland taxa) mainly mimic the present-day climatic differentiation at the opposite side of the Northern Apennines (sub-mediterranean in the Po Plain and meso-mediterranean in the Arno Plain), as well as the peculiar climate teleconnections of latitude zone 40-43°N with the Boreal Hemisphere's dynamics. In contrast, the last glacial vegetation landscape was rather uniform across the study sites, as pines, other conifers and steppics / Poaceae dominated with the scarce occurrence of broadleaves, mostly restricted to refugial areas.

INDEX

1. INTRODUCTION

Mediterranean delta plains are a truly effective and powerful natural laboratory on which to infer the potential response of coastal environments to future high-frequency climatic variations due to both natural and anthropogenic causes. In these areas, the combined effect of sea-level variability, subsidence and remarkable rates of sediment supply commonly favoured the deposition of stratigraphically expanded, fine-grained late Quaternary sedimentary successions, especially during the Holocene. These successions represent useful archives for high-resolution stratigraphic analysis mainly based on palaeobiological proxies such as molluscs, benthic foraminifers and ostracods, among the most common, and on a robust chronological control primarily relying on radiocarbon ages. Several studies have revealed the occurrence of recurring stratigraphic patterns (e.g., T-R depositional cycles, parasequences *sensu* Van Wagoner et al., 1988, 1990) within the postglacial sedimentary wedge buried beneath modern coastal plains (Somoza et al., 1998; Amorosi et al., 2009, 2013b, 2017; Milli et al., 2016). However, the relationship between stratigraphic architecture, the well-known high-frequency climate variability (Rapid Climate Changes *sensu* Mayewski et al., 2004 and Bond events *sensu* Bond et al., 1997) and changes in the vegetation cover, which is an important component of coastal landscape, is still a matter of debate. Similarly, peculiar late Quaternary architectural elements, including palaeosols and lagoonal horizons commonly present in the subsurface (e.g., Amorosi et al., 2016; Barbieri and Vaiani, 2018), still deserve further investigations especially to achieve a better comprehension of: *i)* processes that controlled their formation and development, *ii)* vegetation patterns and palaeoenvironmental constraints and *iii)* main active forcing factors.

In this respect, in coastal and alluvial areas we need to increase our knowledge about the complex interactions among depositional environments (and then stratal stacking patterns through time), vegetation dynamics and climate/glacio-eustatic changes at both Milankovitch (ca. 100 kyr) and sub-Milankovitch (millennial to centennial) timescales.

In pursuit of this objective, palynological analyses surely represent a strategic tool due to the high degree of preservation and the well-known capability of palynomorphs to track simultaneously palaeoenvironmental and palaeoclimate changes. Among palynomorphs, which include various groups of organic-walled microorganisms, pollen grains and spores of Pteridophytes and Bryophytes (to which I specifically refer with the word "palynological" from this point onward) are the most effective proxy to decipher the relationships among environment, vegetation and climate, as their assemblages include information about all these aspects. Over the last years, a growing interest towards the palynological content of late Quaternary coastal settings (e.g., lagoon and/or

wetland successions) has arisen. However, these studies (i.e., Di Rita et al., 2015, 2018; Dolez et al., 2015; Ejarque et al., 2016; Revelles et al., 2019) remain largely less numerous compared to those carried out in the continental/lacustrine or deep-sea realms, because of the high degree of facies variability and the common association with pronounced stratigraphic breaks. Moreover, palynological analyses are rarely performed within sedimentary successions encompassing long periods of time (i.e., one Marine Isotope Stage -MIS- or more than one).

The general purpose of this Thesis is to explore in detail the potentiality of integrated palyno-stratigraphic studies applied to subsurface successions of Mediterranean delta-coastal plains and aimed to an improved understanding of late Quaternary landscape dynamics and their forcing factors. Indeed, the landscape is a single, but complex entity shaped by both geological and biological processes, which are mainly typified by changes in depositional environments and plant communities, respectively.

In order to achieve this scope, a stratigraphic-based palynological approach was conceived and two study areas were selected from the central Mediterranean: the Po delta plain (NE Italy, N Adriatic Sea) and the Arno delta plain (NW Italy, Ligurian Sea). These areas, located at the opposite sides of the Northern Apennines, share a series of key qualities useful for the project:

– the presence of relatively thick successions of fine-grained deposits of late Quaternary age (i.e., Amorosi et al., 1999a; Aguzzi et al., 2007), favoured by rapidly subsiding settings, where palynomorphs can be highly preserved;

– availability of a robust sequence-stratigraphic framework (Amorosi et al., 2017a, Bruno et al., 2017; Rossi et al., 2017 among others), critical to the identification of key sites to be investigated through core analysis;

– advanced degree of knowledge of present-day vegetation communities (Pignatti, 1979: Ferrari, 1994; Blasi et al., 2014 among others), fundamental for an improved interpretation of palynological assemblages.

These areas were also chosen for the opportunity *i)* to investigate slightly, but significantly different (palaeo)climate settings (sub-Mediterranean for the Po delta area, Mediterranean oceanic for the Arno delta plain *sensu* Blasi et al., 2014), and *ii)* to compare stratigraphically distinct late Quaternary settings that provides different depositional facies and architectural elements prone to palynological analysis.

Taking into account these features, specific aims of this Thesis are:

- To investigate the ability of palynomorphs to improve facies characterisation of freshwater-hypohaline deposits, with a particular focus on the thick paludal successions of Holocene

age that have been extensively reported from the subsurface of the Po delta plain by Bruno et al. (2017). In particular, I will test the possibility of differentiating fine-grained lithofacies and identifying key surfaces for sequence-stratigraphic interpretation of proximal coastal successions that are typically undifferentiated due to the scarcity of the most common palaeobiological proxies (i.e., molluscs, benthic foraminifers and ostracods).

- To verify the possibility of elaborating high-resolution, vegetation-derived palaeoclimate reconstructions from unconventional archives, such as those represented by thick and laterally extensive, organic-rich coastal successions, *via* a preliminary filtering of the facies signal within the palynological assemblage. This approach could be promising in the case of the Po delta plain, where tens m-thick swampy successions of Holocene age are prone to be densely radiocarbon-dated and sampled for palynological analysis.

- To examine the stratigraphic and palaeoclimate significance of late Quaternary lagoonal intervals, widely reported from the subsurface of the Arno delta plain and containing a wealth of information to reconstruct long-term evolution trends and high-frequency dynamics of the coastal zone. The application of a stratigraphic-based palynological approach could represent the key to disentangle the relative influence of climate variability and sea-level change, among other factors, on lagoon formation, development and filling. The time and modality of palaeoenvironmental trends inside the lagoon coastal system and their relation to changing vegetation patterns will be analysed in detail across more than one interglacial.

2. STUDY AREAS: GEOLOGICAL SETTING AND VEGETATION LANDSCAPE

2.1. The Po delta plain

The Po delta plain is a flat area (about 3,000 km^2) belonging to the wider Po Plain (about 74,500 km^2) in NE Italy (Figs. 2.1, 2.2). It includes the modern Po Delta and, in the south, a triangle-shaped coastal plain that develops downstream to Pontelagoscuro village, close to Ferrara (Fig. 2.2; Bondesan et al., 1995; Correggiari et al., 2005). The Po Delta is bounded by the Adige Delta and the Venice Lagoon to the north, while the coastal plain progressively reduces its extension southwards where the Northern Apennines meet the present-day coastline (Fig. 2.1).
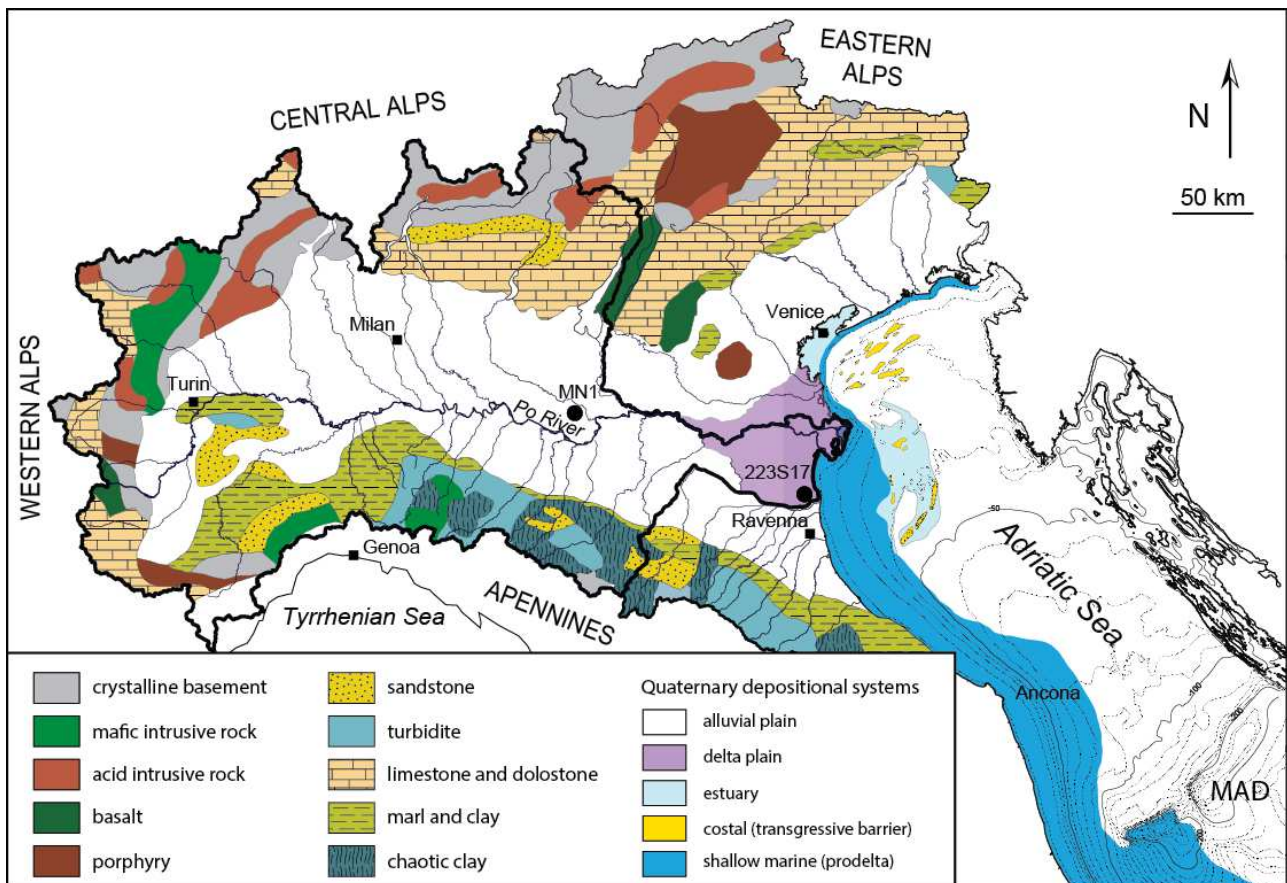
Fig. 2.1: Geological map of the Po–Adriatic system. The location of key cores 223S17 and MN1, analysed for pollen assemblages (Amorosi et al., 1999a, 2008b), are also shown. MAD: Mid-Adriatic Depression. Slightly modified after Bruno et al. (2017).

Due to the rapidly-subsiding setting (i.e., intense natural and anthropogenic subsidence; Antonellini et al., 2019) and the complex nature of the Holocene coastal progradation (Stefani and Vincenzi, 2005; Amorosi et al., 2019), the Po delta plain hosts numerous wetlands (e.g., lagoons and lakes) partly reclaimed during the last centuries. In particular, the modern Po Delta, fed by five main distributary channels (i.e., Gnocca, Goro, Maestra, Pila and Tolle), corresponds to a mixed, river- and wave-influenced system with several lagoons and bays (Fig. 2.2). It formed mainly since about

2 kyr BP in response to a rapid prograding trend, likely favoured by intense deforestation and widespread agriculture activities (Maselli and Trincardi 2013; Amorosi et al., 2019, among others).
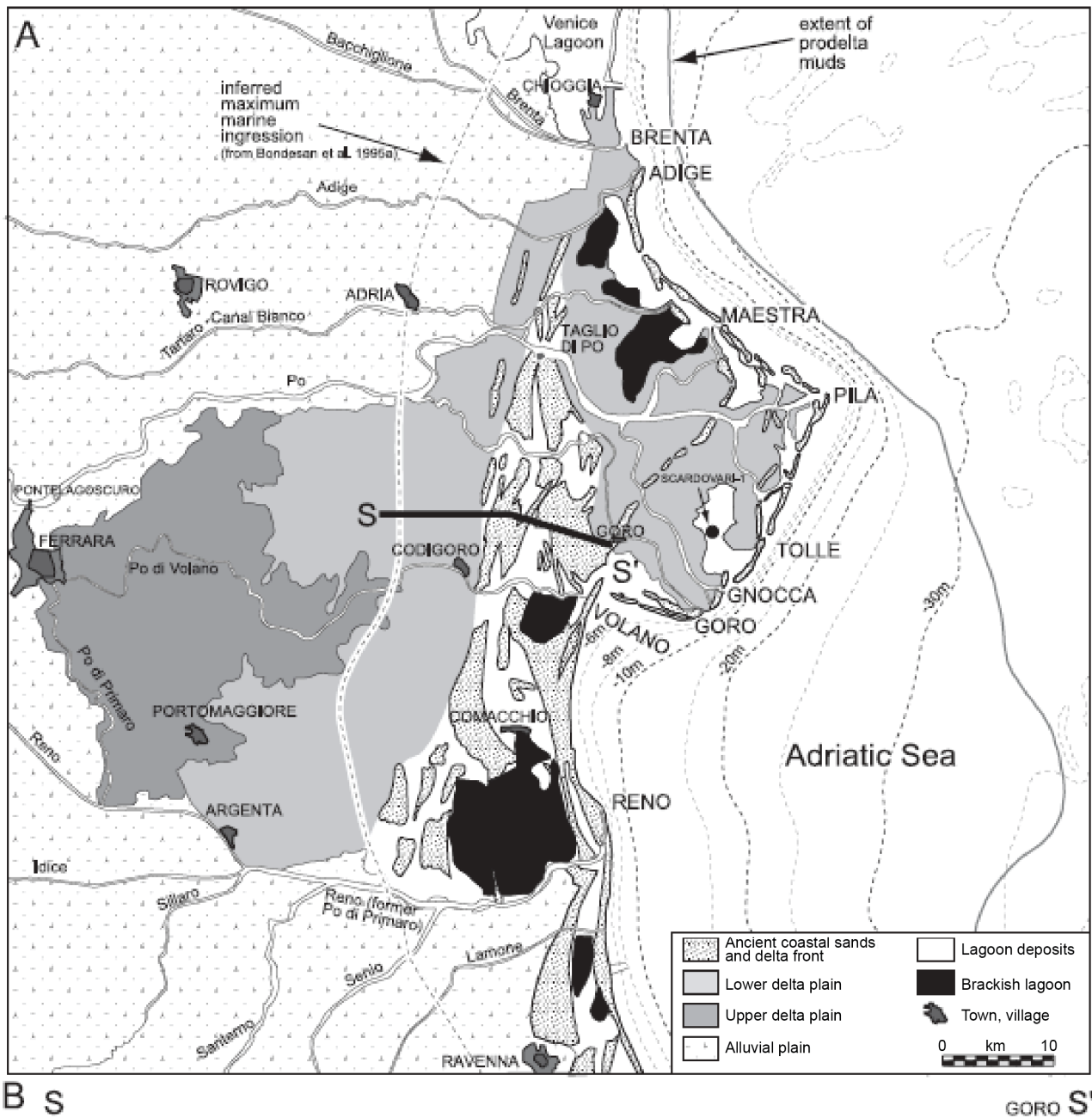
Fig. 2.2: Geomorphological map of the Po delta plain showing the main morphological elements and depositional systems by Correggiari et al. (2005).

The human impact on the delta system became overwhelming since the Porto Viro diversion (1606 AD), carried out by the Doge of Venice to preserve the Venice Lagoon from siltation (Correggiari et al., 2005; Fig. 2.2). By contrast, the southern coastal plain includes several palaeodelta lobes fed by ancient Po River branches, between about 7-2 kyr BP (among others, Po di Primaro and Po di Volano in Fig. 2.2) as testified by several stratigraphic and geomorphological studies (e.g., Stefani

and Vincenzi, 2005; Giacomelli et al., 2018; Amorosi et al., 2019). Wide wetlands (e.g., Comacchio lake in Fig. 2.2) developed behind the ancient sand ridges, some of them recently reclaimed for agro-pastoral activities (e.g., Mezzano lowlands behind the Comacchio lake; Giacomelli et al., 2018). To the east, the Po delta plain faces the northern portion of the Adriatic Sea (Figs. 2.1, 2.2), a microtidal (Paschini et al., 1993), tripartite, NW-SE elongated epicontinental basin that is about 800 km long and 200 km wide. Its northern portion is a shallow low-gradient platform (0.02°; Cattaneo et al., 2003) and goes from the Venetian-Friulian coastline to a 100-120 m deep slope, developed transversally from Pescara to the Dalmatian coast. This slope marks the northern edge of the Mid-Adriatic Depression (MAD in Fig. 2.1), the intermediate/central portion of the basin that reaches a maximum depth of 260 m. Finally, between Apulia and Montenegro the southern Adriatic portion takes place as a 1200 m deep basin.

The interactions between freshwater inputs, predominantly coming from the western side of the basin, wind forcing and the Levantine Intermediate Water (LIW), flowing in from the Eastern Mediterranean through the Otranto Strait, led to the onset of a counter-clockwise circulation. Reflecting this general pattern, the Adriatic Sea peculiar tripartite physiography leads in turn to the onset of three different circulation gyres (North-, Middle- and South-Adriatic Gyres), one for every portion of the basin, but all of them sharing a counter-clockwise direction (Poulain, 2001). This feature is responsible for sediment redistribution along the Italian coast (with an overall sediment transportation from north to south; Cattaneo et al., 2003, 2007), whereas sediments from the Dalmatian coast are negligible due to the limited size and the karstic nature of most catchments (Milliman et al., 2016).

2.1.1. Stratigraphic framework and late Quaternary dynamics

As a whole, the Po-Venetian Plain, the north, the central and the south Adriatic Sea are considered to represent the four main portions of the Alpine-Apennine and Dinarides-Hellenides foreland, resulting from the convergence between the European plate and the Adria microplate since the Cretaceous period (Carminati and Doglioni, 2012, and references therein). Specifically, the Po delta plain represents the eastern, surficial expression of the peri-sutural Po Basin bounded by the Northern Apennines to the South and the Southern Alps to the NW (Castellarin et al., 1985; Doglioni, 1993; Fig. 2.1). The Po Basin is filled with Pliocene-Quaternary deposits, up to 7-8 km thick in the major depocentres (Pieri and Groppi, 1981), that record a complex geological history strongly driven by tectonics (Mazzoli et al., 2006). This succession is significantly reduced in thickness (ca. 100 m) in correspondence of ramp anticline zones that represent the most external

deformational front of the Northern Apennines (Pieri and Groppi, 1981; Castellarin and Vai, 1986; Ori et al., 1986; Doglioni, 1993; Carminati et al., 2003). Indeed, the general structure of the basin is that of a wedge-top basin fragmented by a series of NE-verging blind thrusts and folds (Boccaletti et al., 2011), with a depocentre asymmetrically shifted towards the Apennines (Regione Emilia-Romagna and Eni-Agip, 1998; Picotti and Pazzaglia, 2008).
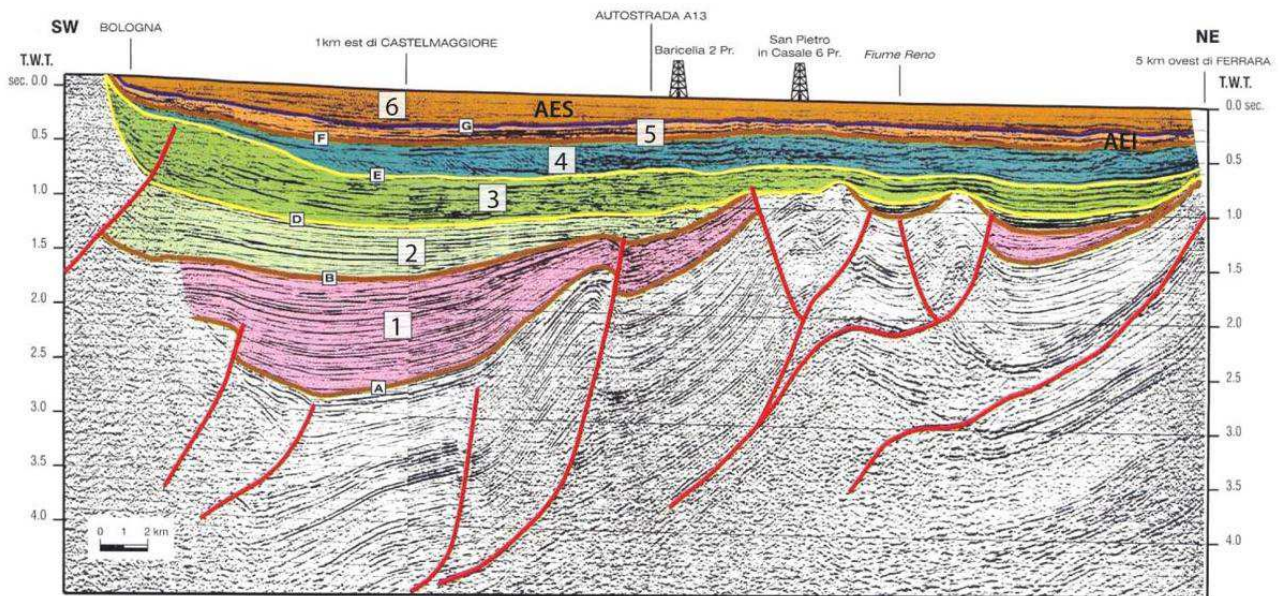
Fig. 2.3: Seismic profile interpretation showing the subdivision of the Plio-Quaternary filling succession of the Po Plain into six depositional sequences identified as UBSU (from Regione Emilia-Romagna and Eni-Agip, 1998). The depositional sequences show an upward decreasing degree of deformation.

Integrated seismic, well-log and borehole data led to a thorough investigation of the stratigraphic architecture of the Po Basin succession, characterised by an overall regressive trend from deep-marine to continental deposits (Ricci Lucchi et al., 1982; Regione Emilia-Romagna and Eni-Agip, 1998). The succession also shows a gradually decreasing degree of deformation from the Pliocene to the Late Quaternary, as clearly detected by seismic-derived stratal geometries (Fig. 2.3). An applied multivariate approach allowed the identification of six unconformity-bounded stratigraphic units (UBSU), whose boundaries mark the main phases of basin reorganisation due to intense tectonic activity (Regione Emilia-Romagna and Eni-Agip, 1998; Regione Lombardia and Eni-Divisione Agip, 2002). These units, about 100–1000 m thick, correspond to third-order depositional sequences (*sensu* Mitchum et al., 1977).

The youngest sequence is the Emilia-Romagna (ER) Supersynthem (Geological Map of Italy at 1:50000 scale), corresponding to the Cycle Qc of Ricci Lucchi et al. (1982) and chronologically dated to the last 0.87 Ma on the basis of magnetostratigraphic data (Muttoni et al., 2003). This sequence has a mean thickness of about 800 m in the present-day coastal plain subsurface and

wedges out towards the Apennines. The identification of a minor regional unconformity (dated around 0.45 Ma; Molinari et al., 2007) within the ER Supersynthem has led to its subdivision into two separate synthems, named Lower and Upper Po Synthems (Regione Emilia-Romagna and Eni-Agip, 1998; Regione Lombardia and Eni-Divisione Agip, 2002). Each synthem is composed of four fourth-order, T-R depositional cycles, known as subsynthems, whose development and cyclic vertical stacking patterns are strictly connected to the well-known Milankovitch-scale (ca. 100 kyr) glacio-eustatic variability of the Mid-Late Pleistocene period (interglacial *versus* glacial periods; Amorosi and Colalongo 2005). These T-R cycles, bounded by prominent transgressive surfaces (TSs) that can be traced across the basin from distal to proximal positions (Fig. 2.4), are more easily recognised in the subsurface of the Po delta plain, where they consist of repeated alternations of shallow marine-coastal and alluvial deposits (Amorosi et al., 1999a,b, 2004, 2016; Fig. 2.4). In terms of sequence stratigraphy, transgressive deposits (TST-transgressive systems tract) mainly include paludal, lagoonal/estuarine and coastal-shallow marine facies recording the landward migration of back-barrier systems under the forcing of an accelerating relative sea-level (RSL) rise. In contrast, deltaic and alluvial facies compose the regressive portion (HST-highstand systems tract; Fig. 2.4), tracing the seaward trajectory of the palaeocoastline.

The TSs are invariably highlighted by the abrupt superposition of back-barrier strata onto tens m-thick, pedogenized alluvial deposits that formed during the falling and lowstand stages (FSST-falling stage systems tract and LST-lowstand systems tract) owing to high rates of tectonic subsidence. The wave ravinement surface (WRS) is identified at the erosive lower limit of transgressive beach sands overlying back-barrier deposits. Faunal data (e.g., meiofauna and molluscs) demonstrated to be crucial for the identification of the MFS (maximum flooding surface) at the transition from retrogradational to progradational stacking patterns (e.g., Scarponi and Kowalewski, 2004; Rossi and Vaiani, 2008; Scarponi and Angeletti, 2008; Scarponi et al., 2013; Campo et al., 2016).

In more inland positions, where no direct marine influence is recorded over the late Quaternary period and deposits are entirely of alluvial origin, the T-R cycles consist of basal overbank facies with isolated fluvial-channel sands (TST) passing upwards to amalgamated and laterally continuous channel bodies (LST channel-belts). These abrupt shifts in channel stacking patterns mark the TSs (Fig. 2.4).
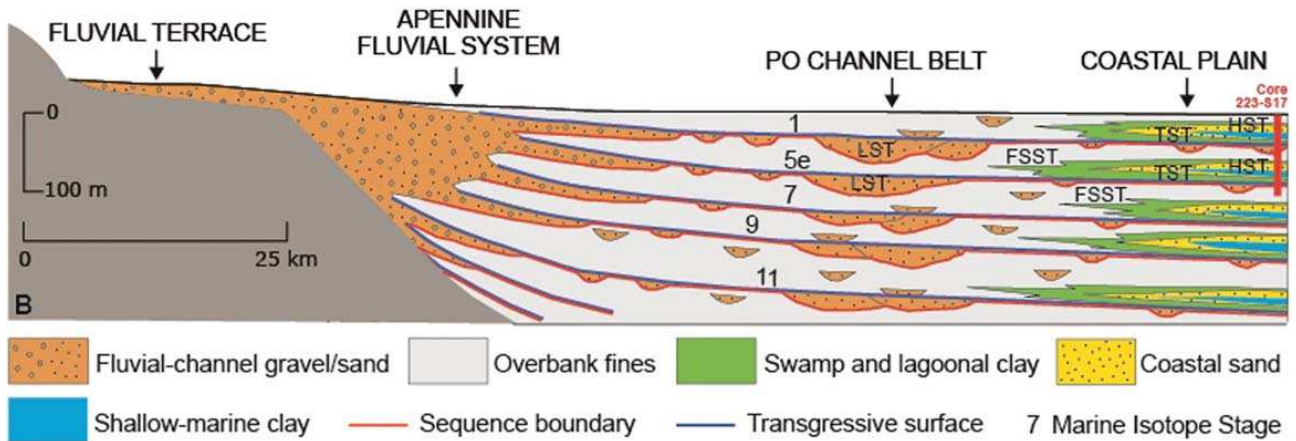
Fig. 2.4: Schematic cross-section from the Apennines to the present-day coastline of the Po delta plain. A suite of T-R cycles are identified within the Upper Po Synthem. System tracts are also reported as well as MISs attribution (from Amorosi et al., 2016).

Palynological investigations integrated with chronological data allowed to explore in greater detail the relationship between the Po Plain T-R successions and the 100 kyr-paced climate variability over the last three interglacial-glacial cycles (about the last 200-250 kyrs). Two key cores were analysed for their pollen content, one drilled about 25 km south of the Po Delta in proximity of the present-day shoreline (the 170 m-long core 223S17; Amorosi et al., 1999a; Fig. 2.1), the other in the central Po Plain, close to Mantua city about 65 km west of the inner margin of the delta plain (the 114 m-long core MN1; Amorosi et al., 2008b; Fig. 2.1). Both pollen profiles document the combined effect of sea-level and climate changes on the Po Plain facies architecture (T-R cycles), as transgressive deposits (coastal and overbank fines in distal-core 223S17 and proximal-core MN1, respectively) are invariably associated with meso-thermophilous forest expansions accompanied by high arboreal cover and pollen concentrations. By contrast, alluvial deposits formed during the FSST and LST contain high abundance of cold steppe grasses and/or conifer grains (mostly pines) indicative of cold, glacial conditions (Amorosi et al., 1999a, 2008b, 2016).

The high degree of continuity of the 223S17 pollen record allowed the precise identification of the onset of the last two interglacials (i.e., Holocene and Eemian) in correspondence of mixed oak forest expansions, while their terminations see the increase of montane trees, such as *Abies* and *Fagus,* at the expense of oaks. Noteworthy also is the higher presence of hygrophilous woods during the Holocene compared to the previous interglacial, which was characterised by more remarkable abundances of montane trees. By contrast, full glacial conditions are characterised by an abundance of grasses and *Pinus* ascribed to MISs 6, 4-2 and to substages 5d and 5b (Fig. 2.5). Less pronounced expansions of broad-leaved and/or coniferous (excluding *Pinus*) taxa reveal the occurrence of episodes of climate amelioration during the last glacial period (MIS 5c, MIS 5a, and

MIS 3 interstadials; Fig. 2.5); the most prominent one (MIS 5c) is characterised by a significant expansion of oaks and hygrophytes (Fig. 2.5). Interestingly, these pollen-derived climate events are related to minor transgressive pulses recorded by laterally extensive swamp/lagoonal horizons, strongly supporting the primary control of glacio-eustatic fluctuations on the Po plain facies architecture at different timescales (Amorosi et al., 2016).
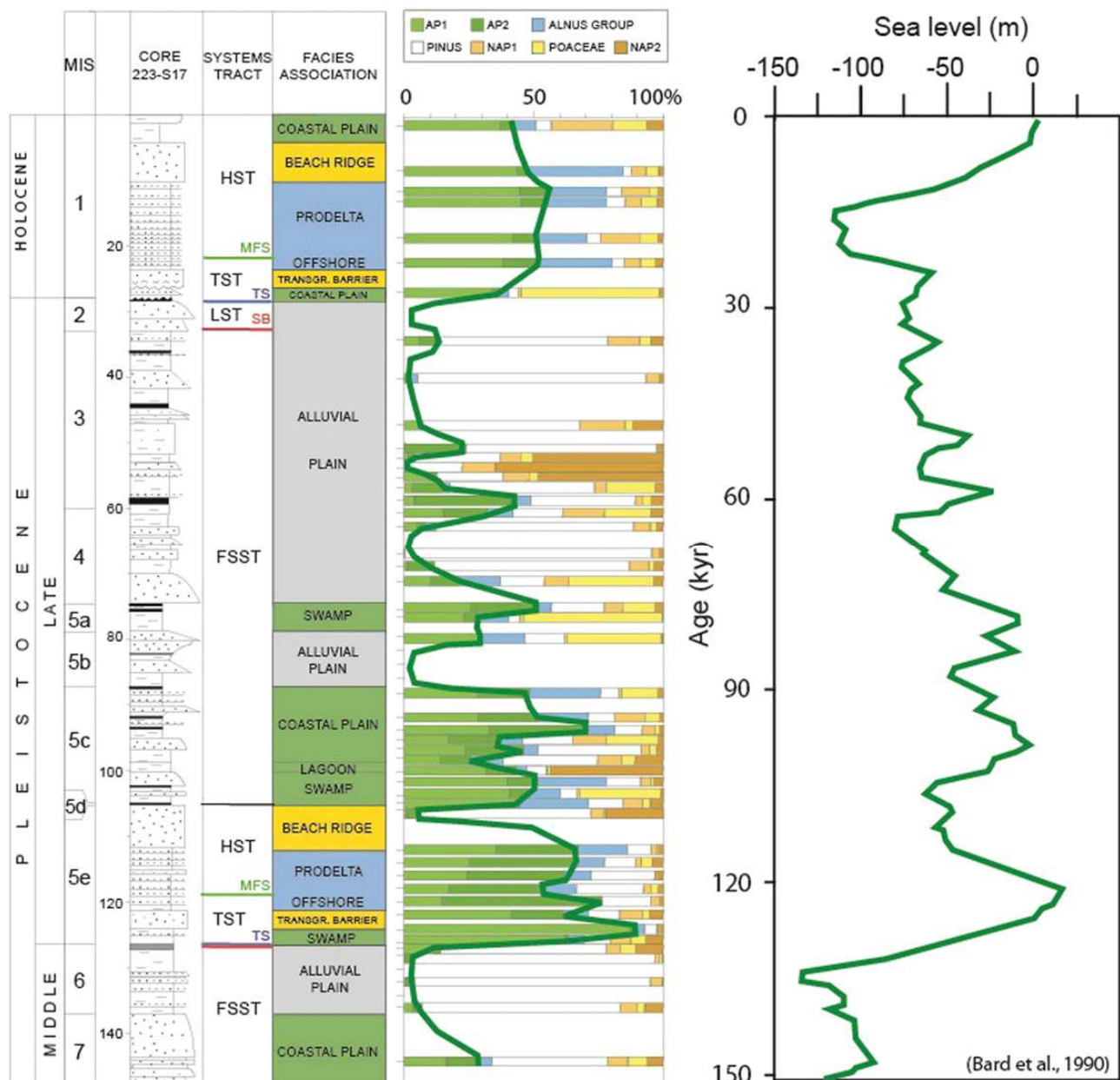
Fig. 2.5: Pollen profile of the key cored succession 223S17 (see Fig. 2.1 for location), showing vegetation changes and sequence-stratigraphic interpretation for the last 150 kyr record (MIS 6 to MIS 1). The relative sea-level curve is from Bard et al., (1990). AP1: mesophilous elements (deciduous broad-leaved trees, with *Quercus* as the main component); AP2: montane trees (*Fagus*, *Abies* and *Picea*); *Alnus*-group (riparian trees). NAP1: non-arboreal elements, excluding NAP2 and Poaceae; NAP2: shrubs and herbs withstanding dry conditions (as *Artemisia*, *Ephedra* and Chenopodiaceae). Figure from Amorosi et al. (2016).

Similarly, the inland MN1 core record, although discontinuous because of four barren intervals coinciding with fluvial-channel sand bodies, document interglacial periods (MIS 7 and 5e) characterised by high arboreal cover and pollen concentrations as well as by the abundance of the mesophilous mixed oak forest and the alder hygrophilous wood taxa. The spreading of pines and grasses (*Artemisia* among them) marks the onset of glacial conditions (e.g., MIS 6 and MIS 4), whereas interstadial conditions were inferred based on the spreading of pioneering vegetation, such as *Betula* and *Hippophae rhamnoides*.

2.1.2. High-resolution stratigraphy at the Late Pleistocene-Holocene boundary
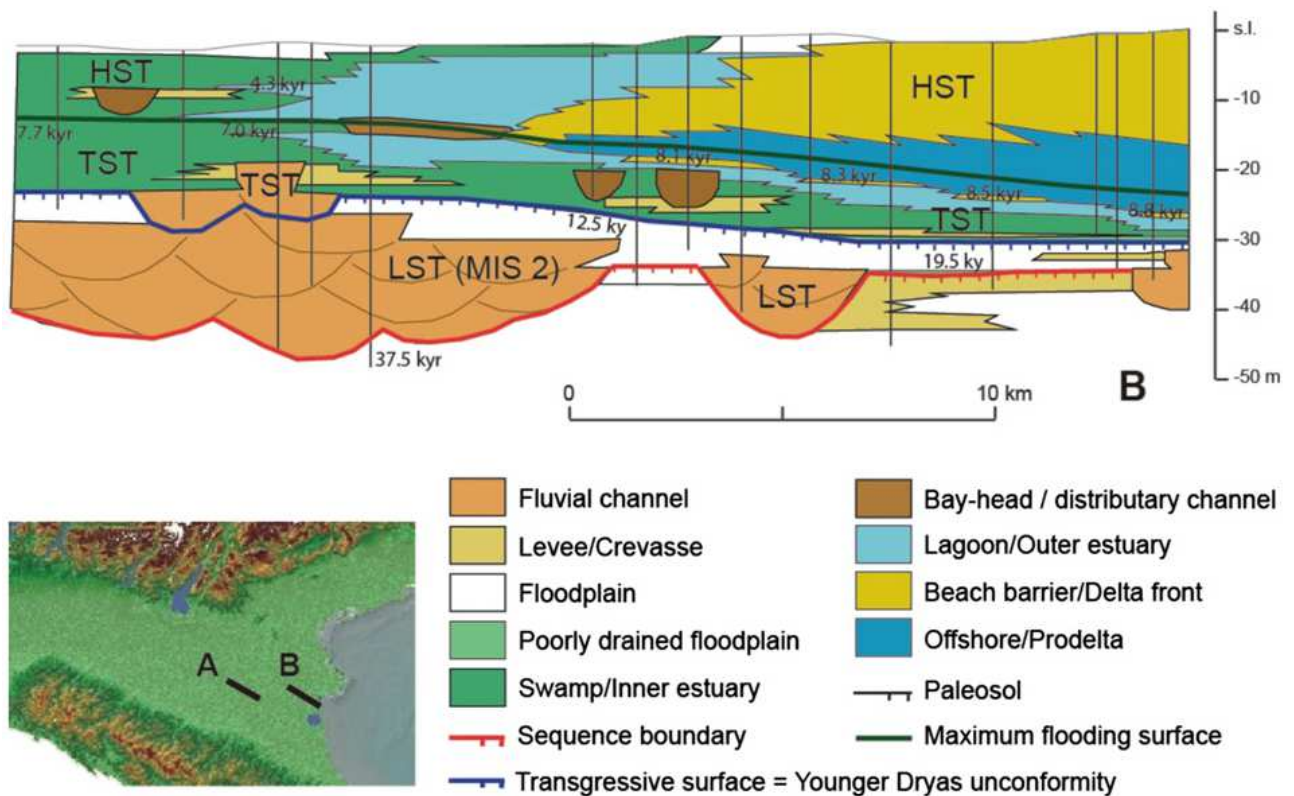
Fig. 2.6: Stratigraphic architecture and sequence-stratigraphic interpretation of the shallow subsurface of the Po delta plain (uppermost 50 m – section B) from Amorosi et al. (2016).

The Holocene succession buried beneath the Po delta plain corresponds to a ca. 30 m-thick T-R wedge that overlies Late Pleistocene deposits. Its lower boundary is generally marked by a weakly developed palaeosol formed during the Younger Dryas climate cooling (YD) and physically coincident with the TS (blue line in Fig. 2.6); a well-developed palaeosol, radiocarbon dated to the Last Glacial Maximum (LGM) period (MIS 3/2 transition), is interpreted to represent the sequence boundary (SB). This key stratigraphic surface is highly diachronous and is traceable, off the

interfluves (where palaeosols develop), at the base of coeval channel-belt sand bodies (red line in Fig. 2.6; Amorosi et al., 1999a, 2003, 2016, 2017b). Both palaeosols have been recently mapped across the Po plain, at the scale of several tens of kilometres, thanks to their pedological and geotechnical features and to the construction of a well-framed stratigraphic and chronological setting (Fig. 2.7; Amorosi et al., 2014a; Morelli et al., 2017). Within cored successions, the LGM and YD palaeosols show similar pedological features, as they are both characterised by upper dark grey/black 'A' horizons and lower 'Bk' horizons enriched in $CaCO_3$ with redoximorphic features (Morelli et al., 2017). Locally, an intermediate 'Bw' horizon can be found, showing intermediate illuviation of $CaCO_3$ from the overlying 'A' horizon. These features point to the Inceptisol category that corresponds to depositional hiatuses of a few thousands of years, in response to phases of subaerial exposure (Soil Survey Staff, 1999; Retallack, 2001). From a stratigraphic point of view, the LGM palaeosol caps a series of poorly-developed palaeosols, whose repeated stacking suggests that pedogenic processes around the MIS 3/2 transition were interrupted by alluviation (Amorosi et al., 2017b; Morelli et al., 2017). By contrast, the YD palaeosol shows a single profile. However, at the Apennines foothills, local high sedimentation rates have led to a more complicated stratigraphic setting, as three vertically-stacked Fluvisols *sensu* FAO (2014), with a slightly less mature profile than Inceptisols, developed during the warm Allerød oscillation (Cacciari et al., 2017). These palaeosols are overlain by two even less mature Regosols, assigned to the Younger Dryas on the basis of palynological analysis, whereas the older Fluvisols were assigned to the Allerød oscillation on the basis of combined palynological – radiocarbon data. This palaeosol stratigraphy can be explained by taking into account the high degree of environmental variability suitable for the development of these soils, as their main source of organic matter is n herbaceous wetland community linked to many different ephemeral, shallow stagnant water environments (Harris-Parks, 2016).

In the subsurface of the Po delta plain, the YD palaeosol (and the Holocene TS) is typically associated with a clear lithofacies contrast, as it marks the abrupt shift from Late Pleistocene alluvial exposed conditions to poorly-drained/swampy environments which finally shift to lagoons (Figs. 2.7, 2.8). This vertical stacking pattern of facies testifies to the replacement of a glacial, fluvial-dominated setting by a post-glacial, estuarine environment in response to the Melt Water Pulse (MWP) 1B and to the concomitant climate amelioration (Amorosi et al., 2003, 2017a; Bruno et al., 2017).
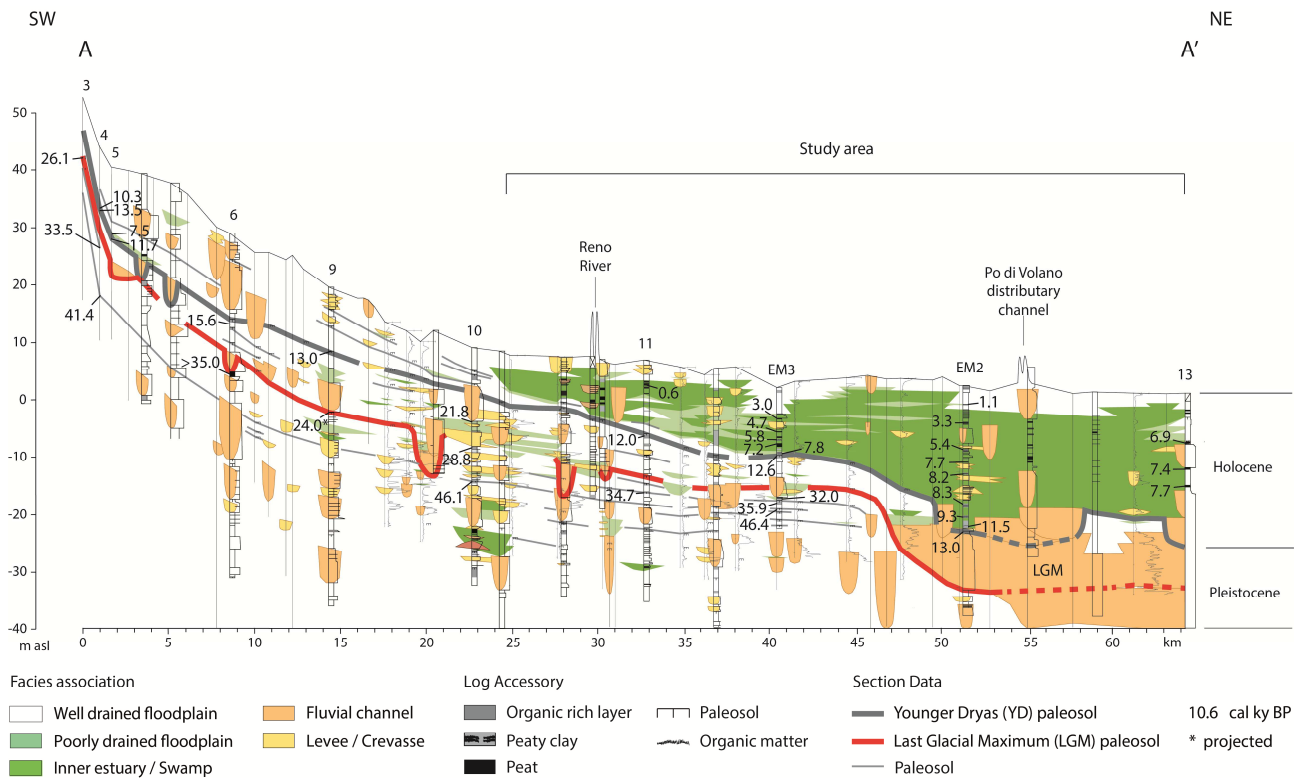
Fig. 2.7: A SW-NE cross-section showing the palaeosol-channel belt relationships within the subsurface of the Po Plain during the last 45 kyr (from Morelli et al., 2017).

2.1.3. Holocene high-resolution stratigraphy

Based on a wealth of data, including tens of high-quality core descriptions, piezocone tests, faunal and geochemical analyses and hundreds of radiocarbon ages, the Holocene T-R cycle has been investigated in detail, leading to the identification of eight millennial-scale parasequences (Fig. 2.8; Amorosi et al., 2017a; Bruno et al., 2017).

Authors refer to "parasequence" as a stratigraphic unit composed of a relatively conformable succession of genetically-related strata, bounded by flooding surfaces (FS; original definition by Van Wagoner et al., 1988, 1990). Due to the high-subsidence context of the Po Plain, a deepening upward trend is locally identified within the lower portion of some parasequences, especially within the TST. Faunal turnovers (i.e., molluscs and meiofauna, including benthic foraminifers and ostracods) allow to robustly identify and trace FSs and their landward equivalents for tens of km across both the marine and brackish realms (Fig. 2.8). In the former, the main changes in faunal assemblages document the establishment of deeper and/or more open conditions, while in the latter point to the development of higher salinity conditions.

13

Fig. 2.8: Longitudinal stratigraphic section across the Po delta plain depicting the Holocene depositional architecture. The section shows the characteristic Holocene transgressive-regressive coastal wedge that is composed of eight parasequences (PS 1-8). Radiocarbon ages are reported as calibrated yr BP.
Figure from Bruno et al. (2017).

Subtle changes in bio- and lithofacies allowed the identification of minor FSs within the eight parasequences, suggesting the occurrence of a stepped palaeoshoreline trajectory even at a centennial scale. These minor flooding episodes could reflect allogenic (e.g., smaller changes in RSL/climate conditions) and / or autogenic (e.g., changes in local subsidence rates, sediment supply) forcing factors (Amorosi et al., 2017a; Bruno et al., 2017).

Early Holocene parasequences (ca. 11.7-8 / 7.7 kyr BP; PSs 1-3 in Fig. 2.8) are organized into an overall retrogradational pattern recording alternating phases of rapid flooding and gradual shoaling within the Po River estuary (Amorosi et al., 2017a) under the forcing of the stepped sea-level rise (Vacchi et al., 2016). For this time interval, Bruno et al. (2017) elaborated a set of palaeogeographic maps (Fig. 2.9) highlighting the response of depositional systems to three main stages of marine ingression, which led the shoreline to reach its maximum inland position (about 20 km westward the present-day shoreline; Fig. 2.8) around 8-7.7 kyr BP.

After 7.7 kyr BP (approximately coinciding with the mwp-1d; Liu and Milliman, 2004), bay-head deltas started to prograde and fill the Po River estuary, thus accounting for the first phase of the three-fold coastal progradation in the study area (Amorosi et al., 2019).

Indeed, the younger, mid-late Holocene parasequences (PSs 4-8; Fig. 2.8) developed under relatively stable sea-level conditions (Vacchi et al., 2016), documenting a complex history of Po delta construction. This characterised by a dominantly aggradational phase (second phase of Po delta evolution, dated ca. 7-2 kyr BP) followed by a more recent (last ca. 2 kyr BP) rapidly prograding one (third phase of Po delta evolution). Under highstand conditions, several autogenic (e.g., delta lobe switching, human land-use activities) and allogenic (e.g., climate events) factors influenced both accommodation and sediment supply. However, the transition from an aggradational to a progradational phase (i.e., the A/P surface separating an early HST to a late HST) is marked by evident changes in palaeoenvironments and facies patterns reflecting the evolution from a wave-dominated to a river-dominated delta system.

Geomorphological studies, depicting a diachronous series of distributary channels feeding a series of sub-parallel beach ridges, and historical documents support the occurrence of these two distinct phases of evolution for the Po delta (e.g., Ciabatti, 1967; Veggiani, 1974; Bondesan et al., 1995; Stefani and Vincenzi, 2005). During the early HST (second phase of progradation) these data confirm the outbuilding of a wave-dominated delta system, with a generally linear shoreline made of arcuate ridges connected to the adjacent prograding beach ridges (Stefani and Vincenzi, 2005). Although an increasing anthropisation of the Po Plain is documented since the Iron Age onwards (ca. 2.8 kyr BP), only with the Roman Age (ca. 2.0 kyr BP) increased sediment discharge likely

influenced by land reclamation (i.e., centuriation) and agricultural activities led to the onset of a river-dominated system.
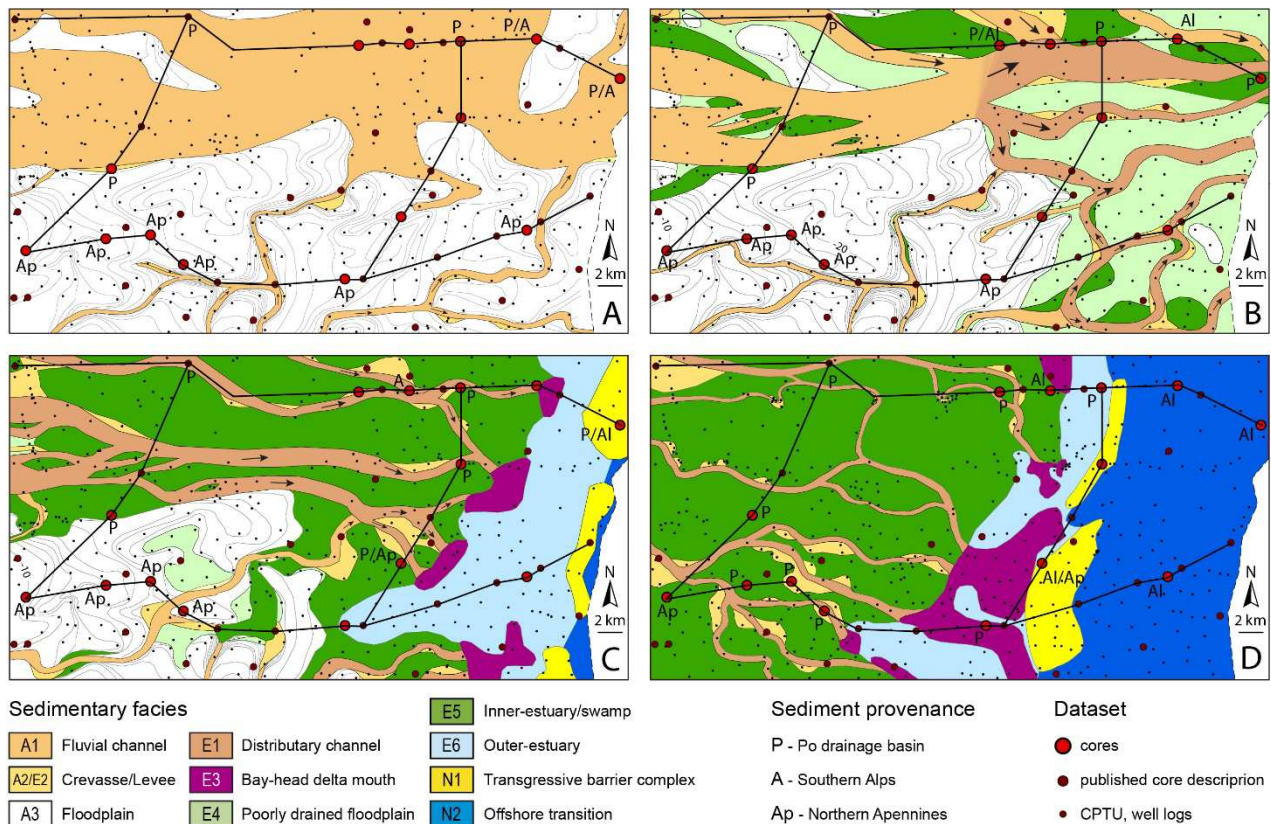
Fig. 2.9: Palaeogeographic maps showing the main stages of evolution of the Po plain between the Younger Dryas and ca. 7.5 kyr BP: A: Younger Dryas, around 12 cal kyr BP; B: around 10 cal kyr BP; C. around 8.5 cal kyr BP; D: around 7.5 kyr BP. From Bruno et al. (2017).

Further reorganisation of the hydraulic network occurred later in response to the demise of the Western Roman Empire and to the higher climate instability of the Late Antiquity – Early Middle Ages (Büntgen et al., 2011). The following Late Middle Ages, characterised by a milder climate, saw a major river avulsion close to the Ficarolo village, in 1152 AD, that shifted the Po delta system within the fluvial axis it still maintains today (Veggiani, 1974; Bondesan et al., 2005). Finally, the modern cuspate delta lobe was induced by the deviation of the Po delta mouth in a more southern position by the Republic of Venice in 1604 AD, with the aim to diminish the sediment discharge towards the northernmost portion of the Adriatic Sea and, thus, avoid the Venice lagoon siltation (Correggiari et al., 2005). Under a predominant anthropogenic influence, the delta progradation occurred very fast, since it formed its 20 km long, cuspate morphology in about 210 years (Stefani and Vincenzi, 2005).

To sum up, the detailed stratigraphic framework reconstructed for the Po plain area during the last decades represents an ideal venue where *i)* to investigate the Holocene millennial to sub-millennial

dynamics of vegetation *via* high-resolution palynological analyses and *ii)* to explore the relationships among sedimentary patterns, vegetation landscape and climate variability.

2.1.4. Present-day vegetation and climate

The study area belongs to the Emilia-Romagna region, which is characterised by a sub-Mediterranean climate, broadly diffused throughout North and Central Italy. It corresponds to a part of the Temperate Division, generally expressing central European affinities in vegetation, though with peculiar relationships with SE Europe. However, its geographic position, encased between the Po River and the Apennine orographic divide, makes it a part both of the Apennine and the Po Plain Provinces, whose boundary runs at the foot of the Apennines (Ecoregions of Italy *sensu* Blasi et al., 2014). The mean annual precipitation sum is up to 778 mm/yr and decreases during summer, with minimum values in July and August. The mean annual temperature (13.2°C) and the thermal excursion (ca. 22°C between July-January means - 23.8°C and 2°C, respectively) suggest in fact a certain degree of continentality, although much less marked than north of the Po River (Bologna site, Ubaldi, 2003). The vegetation landscape reflects these mixed climatic influences, as the study area is located at the southern margin of the Central European phytogeographic region, adjacent to the Mediterranean region (Tomaselli, 1970; Pignatti 1979, 1998). Their boundary is sharp along the Apennine ridge but becomes blurred in the East (Ferrari, 1997), where coastal vegetation occurs as a mix of Central European and euri-Mediterranean taxa. As a consequence, the present vegetation changes not only along a longitudinal gradient (distance from the Adriatic Sea), but also depending on elevation (lowlands *versus* mountains). The effects of longitude are described by Ferrari (1997) and are evident in the composition of Apennine woodlands, however in the lowlands they are less striking because of predominant anthropic landscape modifications. The anthropic impact is evident observing the different types of cultivations that cross the ER region from E to W: in fact, while Romagna is dominated by orchard crops reflecting sub-Mediterranean climate, towards the Emilia cereals and forage crops are the typical cultivations, as the climate becomes progressively more sub-continental. It is not by chance that the patriot Carlo Cattaneo noted: "The botanist can only deplore how agriculture has changed the face of the original vegetation" (Cattaneo, 1844).

As a whole, Ferrari (1997) determined four main ER vegetation belts (Fig. 10), described as follows:
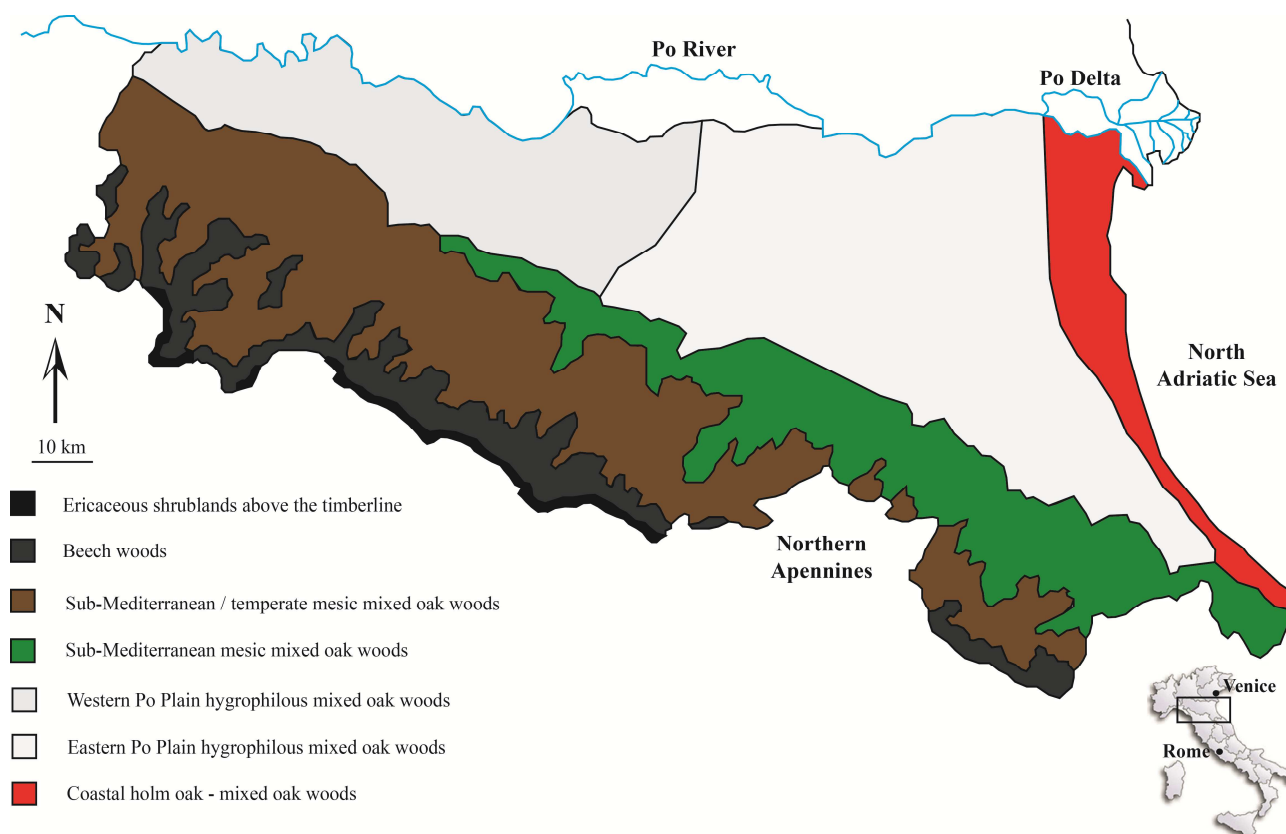
Figura 2.10: Map of the vegetation zonation of Emilia-Romagna region (partly redrawn after Ferrari, 1997 and Regione Emilia-Romagna, 1996).

- *1) Sub-Mediterranean deciduous oak woods*: belonging to the phytosociological order Quercetalia pubescent-petraeae Br.-Bl. 1931, it forms a vegetation belt in the Romagna sub-littoral foothills and along the coastline, but it is also present in the sun-exposed slopes of the eastern Emilia, becoming rare towards the west. *Quercus pubescens* (the white oak) is the dominant tree, with *Sorbus torminalis, Sorbus domestica, Acer monspessulanum, Cornus mas,* and *Viburnum lantana* as typical species of this order.

- *2a) Mixed semi-mesic oak woods*: representative of this vegetation type are the Mesola and Punte Alberete woods, south of the Po Delta, and the San Vitale pine wood, north of Ravenna. Given the high environmental differentiation of the coastal plain, landscape patchiness is also high. On the largest and youngest coastal sand dunes, the association *Orno-Quercetum ilicis* (1956) 1958 is present and is characterised by the dominance of *Quercus ilex* and *Fraxinus ornus* among the trees, while the shrub layer includes *Phyllirea angustifolia*, *Asparagus acutifolius,* and *Pyracantha coccinea*. On the oldest dunes with a retro-dunal shallow water table, *Quercus robur* and *Carpinus betulus* dominate, while *Carpinus orientalis* and *Quercus ilex* are less common. Both vegetation communities fall into the alliance Ostryo-Carpinion orientalis Horvat 1959, to be found in the

18

Balkans, on the eastern side of the central Apennines and seldom along Italy's northern Adriatic coasts.

- _2b) Lowland mixed mesic oak woods_: as previously introduced, the alluvial plain is the most heavily anthropised area, the one that has suffered the heavier losses in terms of land clearance and wood destruction through time. What now remains are remnants of the former forest that had been covering the alluvial plain for most part of the Holocene: Sant'Agostino and Traversante woods (Ferrara province), and Malalbergo wood (Bologna province). The Saliceta wood stood in the Modena province, but was destroyed shortly after the Second World War; the description by Negodi (1941) is the sole evidence of its former existence. These woods can be ascribed either to the _Cladio-Fraxinetum oxycarpae_ association, where winter waterlogging is frequent and long-lasting, or to the _Carici remotae-Fraxinetum oxycarpae_ association, where water presence is less marked. Our understanding of this scattered, patchily distributed forest cover can be enhanced by taking into account the willow and poplar hygrophilous woods bordering the banks of large rivers. The alluvial plain forest is in a state very close to the oak-hornbeam wood (_Querco-Carpinetum boreoitalicum_ Pignatti 1953), which went completely exploited by human activities due to their nutrient-rich soils ideal for agriculture. Thus, restricted woods can only have a species composition similar to the former mixed oak woods because of several disturbance effects.

- _2c) Mixed mesic and semi-mesic Apennine oak woods:_ these mixed deciduous oak woods are restricted to shady slopes in the Romagna Apennines, but become gradually dominant in the Eastern Emilia hills and foothills; in the Western Emilia Apennines this is the sole type of natural / sub-natural woods to be found. Although their tree layer is mainly composed of _Ostrya carpinifolia_ and _Laburnum anagyroides_ (alliance _Laburno-Ostryon_ Ubaldi 1988), the vegetation is highly diversified and can be subdivided into the following associations:

- _Ostryo-Aceretum opulifolii_ Ubaldi 1980, characterised by _Acer opulifolium_, _Carex digitata_, _Hepatica nobilis,_ and _Lilium croceum_. Towards the SE, between the Savio and Marecchia valleys at medium altitudes, the _Ostryo-Aceretum_ shifts to the following
- _Aceri obtusati-Quercetum cerris_ Ubaldi et Speranza 1982, a semi-mesic plant community of the same alliance.
- _Dryopterido-Ostryetym_ Ubaldi 1993 is present on steep, shady sandstone slopes, up to the 800 m-above-sea-level (a.s.l.) limit of this sub-montane vegetation; it is a highly-

diversified association, with predominant *Ostrya carpinifolia* and *Fraxinus ornus*. Subordinate are *Carpinus betulus*, *Acer campestre*, *Acer pseudoplatanus*, *Quercus cerris*, *Quercus petraea,* and *Acer opulifolium*. Noteworthy is the fact that *Ostryo-Aceretum opulifolii* woods occupy at the same altitude the sunny slopes, while the *Dryopterido-Ostryetum* occupies the shady ones.

-     *3) Beech woods:* these woods range from 800-1000 to 1700-1800 m a.s.l., where the timberline occurs, and belong to the sub-alliance *Trochiscantho-Fagenion* Gentile 1974. In the Romagna Apennines they are bipartite:

- the lower altitude community is the *Aceri platanoidis-Fagetum* Ubaldi et Speranza 1985, spanning 800-1200 m a.s.l.; it is the Apenninic beech wood with higher species richness, since it can be composed of up to 80 species, whose diagnostic ones are *Fraxinus excelsior*, *Polystichum setiferum*, *Euphorbia amygdaloides*, *Acer platanoides,* and *Arisarum proboscideum*. The most frequent trees, apart from beech, are *Tilia platyphyllos*, *Ulmus glabra,* and *Abies alba*.
- The higher altitude community is the *Polygonato verticillati-Fagetum* Ubaldi et Speranza 1985, to be found between 1200-1600 m a.s.l. and often being represented by pure or almost pure beech woods, seldom accompanied by *Abies alba* and *Acer pseudoplatanus* in nutrient-rich, well-drained soils.

The composition and bipartition of the Eastern Emilia Apennine beech woods is similar to those occurring in Romagna, except for the higher abundance of the ferns in the herbaceous layer (*Gymnocarpium-Fagetum* Ubaldi et Speranza 1985) and for the rare presence of *Picea abies* on rocky sites. Nonetheless, human clearance of these woods has transformed most of these beech woods into *Abies alba* and *Picea abies* woods.

In the Western Emilia Apennines a bipartition is also present, with the lower altitude sub-association (*seslerietosum autumnalis*, 1000-1400 m a.s.l.) not including *Acer pseudoplatanus*, *Sorbus aucuparia,* and *Abies alba*. It includes the underwood species common in the mixed mesic oak woods, such as *Primula vulgaris* and *Hepatica nobilis*, and the higher altitude sub-association (*sorbetosum aucupariae*, 1400-1700 m a.s.l.) with *Sorbus aucuparia*, *Abies alba, Acer pseudoplatanus,* and *Rosa pendulina* as diagnostic species. On a few mountain tops, *Abies alba,* and *Pinus mugo* are found on rocky sites near the timberline and are regarded as relics of an ancient upper forest belt equivalent to the Oroboreal Conifer forest belt found on the Alps and likely disappeared in the region at the Subboreal-Subatlantic cooling about 2800 years ago (Chiarugi,

1958). Therefore, the modern timberline has to be considered a real ecotone, because of the lack of a natural vegetation belt.

Finally, a human-induced modification in wood composition is represented by the replacement of the beech with the cultivated chestnut (*Castanea sativa*), nowadays forming abandoned woods.

- *4) Ericaceous dwarf shrublands above the timberline*: since only a few mountain peaks encompass the height of 2000 m a.s.l., this vegetation belt is rather sparse and discontinuous in Emilia and absent in Romagna. The vegetation is similar to the one in the Western and Central Alps (order *Rhododendro – Vaccinietalia* Braun Blanquet 1926), but impoverished in species, as it commonly occurs at the edge of geographic ranges. This vegetation belt is documented from the MIS 2 onwards (Chiarugi 1936, 1958; Bertolani Marchetti, 1963) by historical and literary sources (Panzacchi, 1585; Spallanzani, 1795). These shrublands contain three types of vegetation:

- Alliance *Loiseleurio-Vaccinion* Br.-Bl. et Jenny 1926, dominated by *Vaccinium gaultherioides*, *Vaccinium myrtillus,* and *Empetrum hermaphroditum,* with many lichens and lycopods. Linked to windier sites free from snow for 6 months per year.
- Another community similar to the previous, but devoid of *Empetrum hermaphroditum*, linked to sites where snow cover is longer, causing mosses, lichens and lycopods to be very rare.
- Alliance *Rhododendron-Vaccinion* Jenny et Br.-Bl. 1931, dominated by *Rhododendron ferrugineum*, a very rare and scattered community typical of the longest lasting snow covers.

The high altitude steppes dominated by either *Trifolium alpinum* or *Nardus stricta* or *Festuca puccinelii* are interspersed between these types of shrublands.

2.2. The Arno delta plain

The Arno delta plain (Tuscany, NW Italy; Fig. 2.11) is a ca. 450 km^2 wide, low-lying area belonging to the wider Lower Valdarno, the downstream sub-basin of the Arno River Basin, which is characterised by an overall drainage surface of ca. 8,230 km^2 (Nisi et al., 2008). The study area, transversally crossed by the lower reaches of the Arno River, is bounded by the Pisa Mountains to the east, by the Leghorn terrace and Pisa Hills - Leghorn Mountains to the south-south east and by the Serchio River - Versilia Plain to the north (Fig. 2.11).
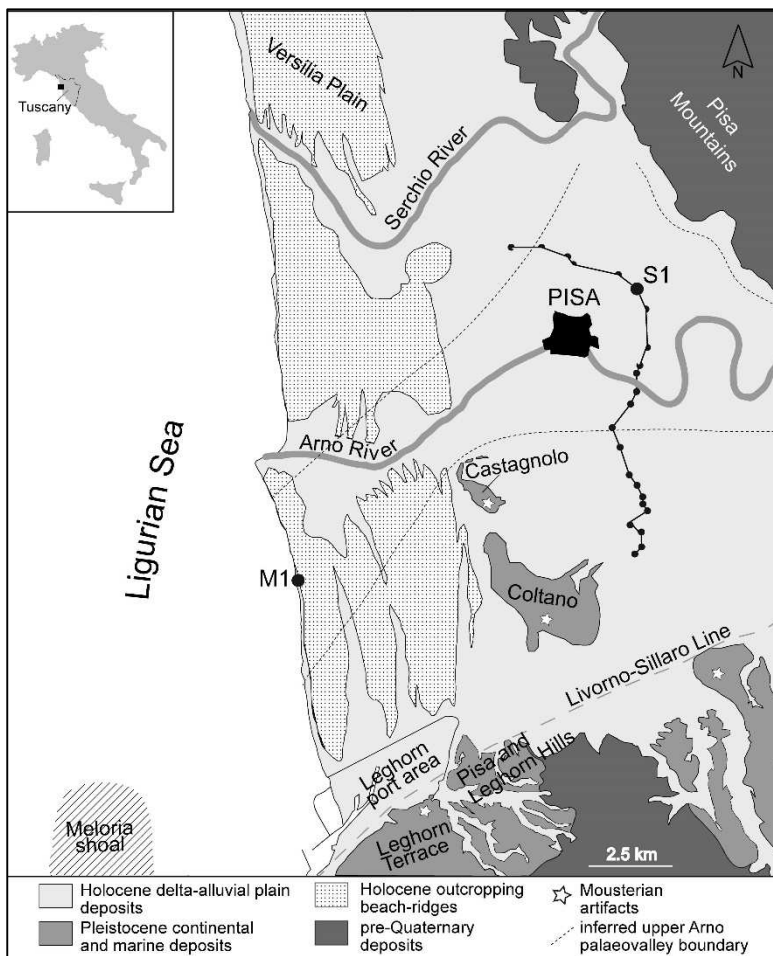
Fig. 2.11: Geological sketch map of the Arno delta plain showing the location of cores analysed for pollen content (Ricci Lucchi 2008; Amorosi et al., 2009). The section trace of Fig. 2.13 is reported (black dots correspond to the high-quality cores used for stratigraphic correlations). The inferred interfluves position of the upper Arno palaeovalley formed during the Last Glacial Maximum and filled between ca. 13-8 ka BP is also show with dotted lines. Slightly modified from Rossi et al. (2017).

To the west, the Arno delta plain faces the southernmost sector of the Ligurian Sea (Fig. 2.11) that is characterised by a relatively steep platform (average grade of ca. 0.3°-0.5°) with an almost flat sector comprised between 10-30 m water depths (Mattei, 2008). In front of the Leghorn harbour, ca. 12 km south the Arno River mouth, a 40 km^2-wide morpho-structural high (the Meloria shoal in Fig. 2.11) of uncertain origin occurs, locally perturbating the southward littoral drift of the coastal sector between the Arno River mouth and the Leghorn terrace ("convergence zone"; Casarosa et al., 2011; Gandolfi and Paganelli, 1975; Fig. 2.12). By contrast, a main northward drift occurs between

the Arno and Serchio river mouths (Gandolfi and Paganelli, 1975). By means of these longshore currents, Serchio and Arno Rivers (with a lower contribution of the Magra River, located ca. 45 km northwards) feed the present-day shoreline, which is subject to a negligible tidal excursion (maximum of 30 cm; Cipriani et al., 2001).

Nowadays, the Arno River forms a cuspate delta system with a well-developed strandplain formed by a series of juxtaposed beach ridges (Federici and Mazzanti, 1995). These ridges, cropping out up to 6 km inland from the modern coastline, can reach 10 m in elevation and record the shoreline progradation of the last 3,000 years, as suggested by archaeological-historical data (Fig. 2.12; Pranzini, 2001, 2007).
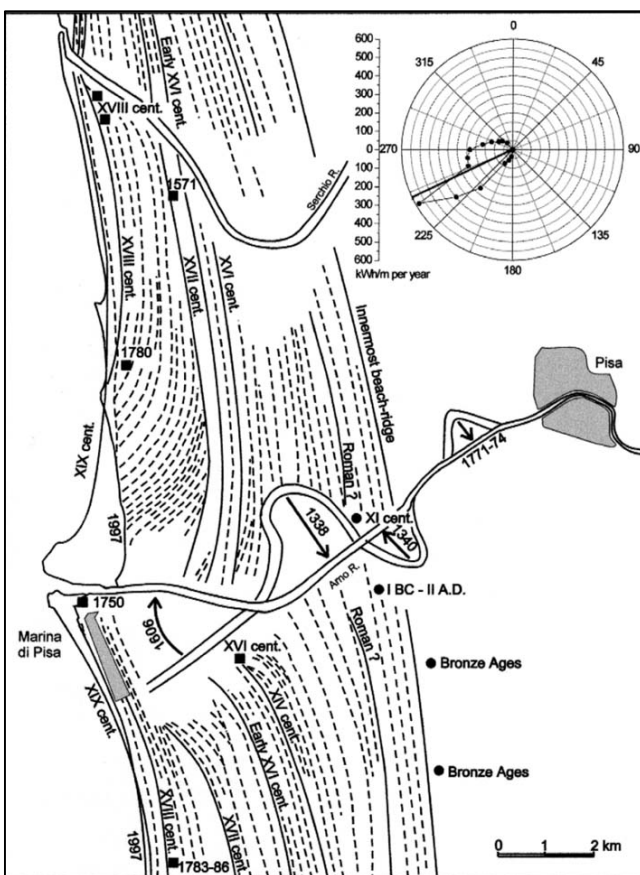
Fig. 2.12: Geomorphological sketch map of the Arno strandplain showing the main beach-ridges and relative ages. Black squares correspond to costal towers, while black dots indicate archaeological findings. From Pranzini (2011).

Behind the strandplain, a flat upper delta plain occurs grading eastwards into the alluvial plain; unique exceptions are two isolated morphological reliefs (known as "Coltano and Castagnolo islands"), rising up to 15 m above the ground level, and the Pisa city mound of recent anthropic origin (Bini et al., 2018). The "Coltano and Castagnolo islands" are composed of fluvial silts and sands, with an age older than 40 kyr BP, as deduced by the presence of Mousterian findings, but their origin is still matter of debate (Sarti et al., 2015b).

The plain is mainly composed of fine-grained overbank deposits, with subordinate fine to medium sands due to crevasse and levee bodies, located in proximity of modern and ancient river branches. Integrated stratigraphic and geomorphological studies highlight the occurrence of numerous palaeochannels that fed the plain up to the Middle Ages and belonging to the Arno and Serchio networks (e.g., Della Rocca et al., 1987; Amorosi et al., 2013a). During the Middle Ages, the palaeo-Serchio branch flowing into the Arno plain was embanked and forced to flow northwards to reduce flooding risks in the city of Pisa. During the same historical period, several other waterworks modified the fluvial landscape of the plain. Canal constructions, meander-loop cut-offs and wetland reclamations were performed in order to improve navigability, to reduce flood risk and to increase the portion of arable land (Sarti et al., 2010).

2.2.1. Stratigraphic framework and late Quaternary evolution

The Arno delta plain belongs to the onshore portion of the Viareggio Basin, a NW-SE half-graben basin (85 km long and up to 40 km wide) developed since the Late Tortonian (ca. 8-7 Myr ago) in response to the counter-clockwise migration of the Apennine foredeep-foreland system (Martini and Sagri, 1993). This extensional tectonic basin, which is still subsiding, shows a triangle shape tapering towards the Versilia plain (Pascucci, 2005). Morpho-structural highs (i.e., Pisa Mountains, Pisa Hills and Leghorn Mountains, Meloria shoal; Fig. 2.12) delimitate it, whereas a main left-lateral transverse lineament (the Livorno-Sillaro Line of Bortolotti, 1966), running at the foot of the Pisa Hills and of the Leghorn Mountains, marks its southern limit (Mariani and Prato, 1988; Argnani et al., 1997);historical earthquakes document that this lineament is still active (Pascucci, 2005). During the Quaternary, the activation of a new fault, running along the western margin of the Pisa Mountains, has contributed to the eastward extension of the basin, which shows a depocentre close to the present-day shoreline (Pascucci, 2005).

Above the Oligocene substrate, the basin fill is up to 2500 m-thick and is formed by a variety of marine, coastal and alluvial deposits organised into five unconformity-bounded units (UBSU) of late Miocene to Quaternary age, identified on the basis of seismic lines and deep wells (Pascucci, 2005). From bottom to top, Messinian littoral deposits are unconformably overlain by two Pliocene sequences composed of marine clays and sands, which in turn underlie Quaternary sequences. As a whole, the Quaternary succession is ca. 600 m thick and shows a high variability of facies, from marine to continental. The youngest sequence, chronologically attributed to the late Pleistocene-Holocene , is ca. 100 m thick (Pascucci, 2005).

Detailed multiproxy stratigraphic studies have recently been performed on the uppermost 100 metres of the Arno delta plain succession by means of sedimentological, palaeontological (i.e., molluscs, benthic foraminifers, ostracods and palynomorphs), geochemical and chronological (i.e., radiocarbon dating and ESR-Electron Spin Resonance) analyses (Aguzzi et al., 2007; Amorosi et al., 2008c, 2009, 2013b; Rossi et al., 2011, 2017; Sarti et al., 2015a among others). This approach has allowed the identification of two distinct, non-coeval palaeovalley systems (lower and upper Arno palaeovalleys) developed during non-consecutive glacial-interglacial cycles: the MISs 8 – 7 and MISs 3/2 – 1 intervals (Fig. 2.13). The palaeovalleys, which formed a multiple incised-valley system (IVS), share similar dimensions (5-8 km wide and 40-50 m thick) and terraced profiles, as well as a predominant control on their formation exerted by strong (> 100 m) sea-level falls. Accordingly, the filling successions (i.e., incised-valley fills - IVFs) accumulated during the subsequent periods of sea-level rise, corresponding to the MIS 7 and MIS 1 interglacials (ca. 225-180 kyr BP and 13-8 kyr BP, respectively). Both IVFs are mud-prone and show an overall retrogradational stacking pattern of facies (swamp-estuarine-littoral) that reflects the transformation of the palaeovalleys into wave-dominated estuaries under transgressive conditions (TST).

Subtle changes in the meiofauna, interpreted as episodes of abrupt increase of marine influence within the estuary, allow the identification of a series of flooding surfaces (FSs) within the IVFs. These FSs and related parasequences (*sensu* Van Wagoner et al., 1990) likely reflect the environmental response of the coastal system to a sub-Milankovitch glacio-eustatic cyclicity (Fig. 2.13; Amorosi et al., 2009; Rossi et al., 2017).

The turnaround from a retrogradational to a progradational facies trend, detected by micropalaeontological data and marking the MFS, is invariably located close to the palaeovalley interfluves. The Holocene post-valley fill succession, formed under highstand conditions, is well-preserved, while its MIS 7 counterpart is truncated by a series of erosive events likely related to the glacial periods occurred between MISs 6 – 2 (Fig. 2.13).
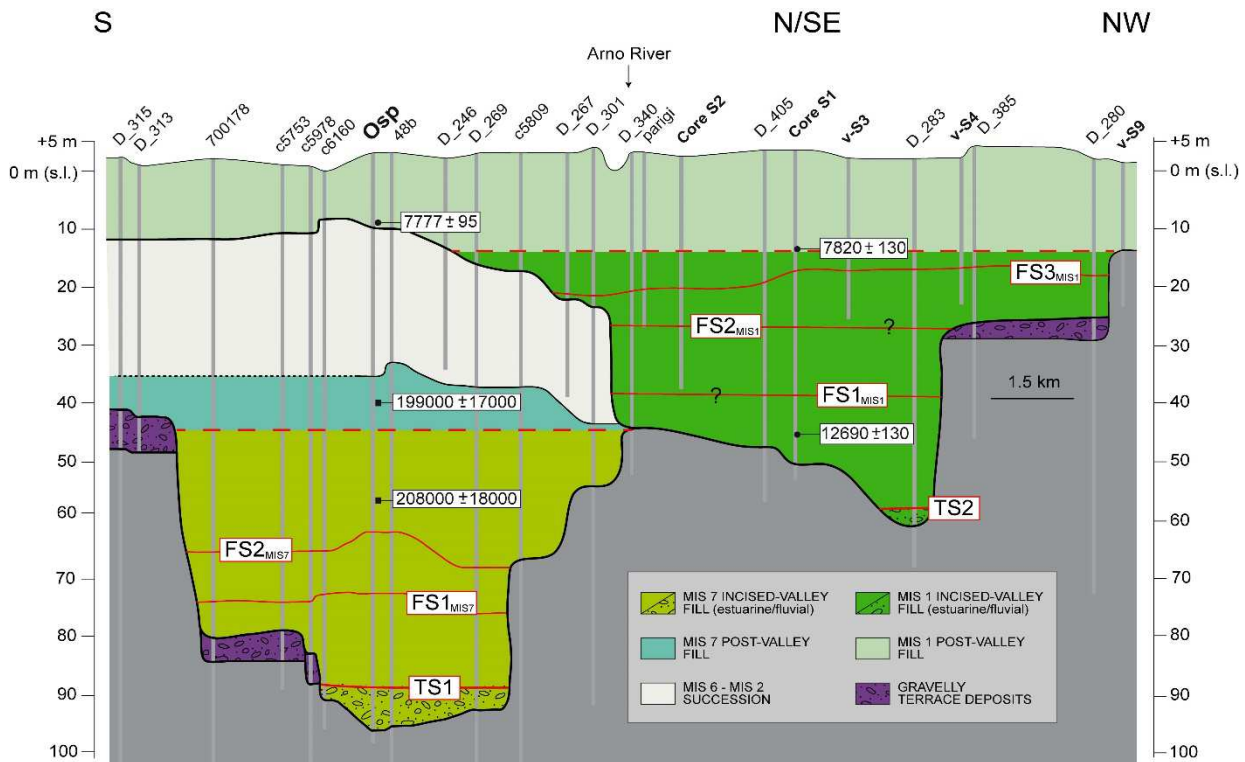
Fig. 2.13: Stratigraphic cross-section of the uppermost 100 meters of the Arno delta plain subsurface, showing the Arno multiple incised valley system with two incised valley fills dated to the present and penultimate interglacials, respectively. Black squares indicate ESR ages, while radiocarbon ages in calibrated years BP are shown as black circles. Sequence-stratigraphic interpretation and a tentative attribution to MISs are indicated. From Rossi et al. (2017).

Up to now, the stratigraphic record of the Last Interglacial (i.e., back barrier-coastal deposits assigned to MIS 5e) is missing in the shallow subsurface of the Arno plain, possibly reflecting a MIS 6 – 5 IVS in the same position as the upper Arno palaeovalley (in correspondence of the modern Arno River course; Fig. 2.11). This would imply a northward shift of the main patterns of river incision at the end of MIS 7, likely in response to a tectonic activity that could have affected the portion of the Arno Plain where the MIS 7 IVS is preserved (Argnani and Rogledi, 2012; Sarti et al., 2015b). According to Sarti et al. (2015b), stratigraphic and chronological data suggest that the southern portion of the Arno Plain (where the MIS 7 IVS is located; Fig. 2.13) would represent the transition zone between a subsiding basin, located north to the present-day Arno River course, and the uplifting area of the Pisa Hills and Leghorn Mountains. In this context, the Coltano and Castagnolo "islands" (Fig. 2.11) could represent the southern margin of the basin, where fluvial deposits older than 40 kyr extensively crop out along the foothills (Sarti et al., 2015b).

Focusing on the upper IVS, the stratigraphic cross-sections elaborated by Amorosi et al. (2008c) show that along the modern coastline the IVF is mainly composed by a monotonous, 20 m-thick succession of estuarine clays overlain by ca. 30 m of stacked littoral, shallow-marine and deltaic deposits as part of the late transgressive-regressive portion of the cycle. Landwards, between the

city of Pisa and the coastline, the IVF consists of estuarine deposits sandwiching coastal plain and bay-head delta facies. Here, the aggradational/progradational portion of the cycle is thinner (about 20 m) and mainly represented by littoral sands passing landwards to lagoon-paludal clays. Finally, in the landward-most portion (E of Pisa), the filling is made up of alternating estuarine-bay-head delta-swamp deposits organised into three different parasequences (PSs) (Fig. 2.14).

Pollen analysis were performed on two reference cores located at proximal (core S1, 56 m thick, in Amorosi et al., 2009; Fig. 2.11) and distal (core M1, 105 m thick, in Aguzzi et al., 2007; Fig. 2.11) locations in order to cover the whole spectrum of palaeoenvironments developed during the filling of the upper palaeovalley across the plain (Fig. 2.14). If on one hand pollen analysis of core S1 was performed at high-resolution aimed to characterise the small-scale depositional cycles in terms of palaeoclimate conditions (see paragraph 2.2.2.), on the other hand core M1 was analysed with a lower level of detail because the main scope of the study was to obtain a general palaeoclimate reconstruction at the Milankovitch scale. Even though M1 lies inside the upper palaeovalley (i.e., the Holocene succession is 50 m thick; Figs. 2.11, 2.14), it also intercepts older deposits belonging to previous T-R cycles: in fact, the bottom of M1 (between ca. 100-90 m core depth) is composed of a back-barrier – coastal succession characterised by a lower sandy transgressive barrier followed by a shallowing-upward, medium to coarse sandy lower shoreface-upper shoreface sequence. This succession is mainly barren of pollen grains except for its lower shoreface facies association that has a pollen assemblage dominated by *Pinus* (ca. 20-80%) with very subordinate mixed oak forest and Mediterranean taxa increasing to ca. 30% and 5%, respectively, towards the top, where an open landscape dominated by ubiquists is present. This succession is interpreted to reflect an early transgressive sand sheet passing to a shallowing-upward, high-energy delta-front environment. Its palynological content was tentatively interpreted by Ricci Lucchi (2008) as representing MIS 5e-aged, cool and wet climate conditions possibly related to a progressive cooling typical of the last portion the Eemian, as documented at La Grande Pile (eastern France, in Woillard, 1975 and in De Beaulieu and Reille, 1992), Lac du Bouchet (central France, in Reille et al., 1998) and Ioannina (western Greece, in Tzedakis et al., 2003). During the glacial periods, environmental conditions locally suitable enough to allow a refugial zone for conifers would have made their local pollen rain more abundant than expected for an interglacial. However, more recent studies (Sarti et al., 2015b; Rossi et al., 2017) have proposed an older age for these deposits (possibly MIS 9 or earlier), thus rejecting previous chronological attributions. Furthermore, older pollen samples from the underlying, 101-103 m b.s.l., swamp-lagoon succession have assemblages dominated by steppics, Poaceae and ubiquists with a very low arboreal cover and may indicate even cooler conditions, typical of a glacial period.

Above the coastal wedge, at 90-76 m b.s.l., a sedimentary succession composed of alluvial deposits contain a further basal peak in pine pollen upward decreasing at the advantage of mixed oak taxa, which finally both leave place to an open steppe related to oscillating cool-cold climates. This alluvial succession is capped by a ca. 8 m-thick fluvial-channel sand body barren of palynomorphs. Above the fluvial-channel sands, at 76-62 m b.s.l., a swamp-coastal lake-marsh succession is observed. Lake deposits are characterised by an oligotypic ostracod assemblage dominated by *Cyprideis torosa*, typical of brackish environments, and a pollen assemblage depicting an open steppic-pine woodland in the lower portion, followed by a trend of increasing, though highly variable, presence of mixed oak taxa indicative of mild conditions, suggesting an interglacial. On the basis of these considerations, the Authors are inclined to assign this succession to MIS 7 rather than to MIS 3 (dr. Veronica Rossi, personal communication, 2019).

Upwards, at 62-50 m b.s.l., an alluvial succession takes place once again, capped and topped by coarse-grained fluvial-channel facies associations. The radiocarbon age centred around 23,500 yr BP (Fig. 2.14) constrains the topmost, fluvial-channel sands and gravels to the MIS 3-2 transition and has been interpreted as the expression of a fluvial terrace belonging to the upper palaeovalley. This terrace was formed during the FSST, as confirmed by pollen associations recovered within floodplain deposits at 57-55 m b.s.l., characterised by an open pine-oak woodland indicative of a cool climate.

Finally, the Holocene record of core M1 is mainly made of an estuary-prodelta succession. Its palynological content is that of a mixed oak forest with scattered pines during the earliest Holocene; after that, the mixed oak forest reaches its maximum expansion up until 7.8 cal kyr BP. Following this phase, which ends with the maximum marine ingression (MFS), the mixed oak forest declines from a dominant position to a coordinate position to Mediterranean taxa with the concomitant re-expansion of pines and the first expansion of montane taxa (mainly *Abies* and *Fagus*) up until ca. 25 m b.s.l.. This can represent the Holocene climate optimum peak, as both the montane and the lowland plant taxa reach their maximum concentrations. Finally, up to ca. 3.2 cal kyr BP, the increase in cultivated trees, such as *Castanea* and *Olea*, suggests anthropic modifications of the montane landscape as montane taxa decline, whereas ubiquists gradually proliferate. This can represent the gradually increasing anthropic presence in the area.
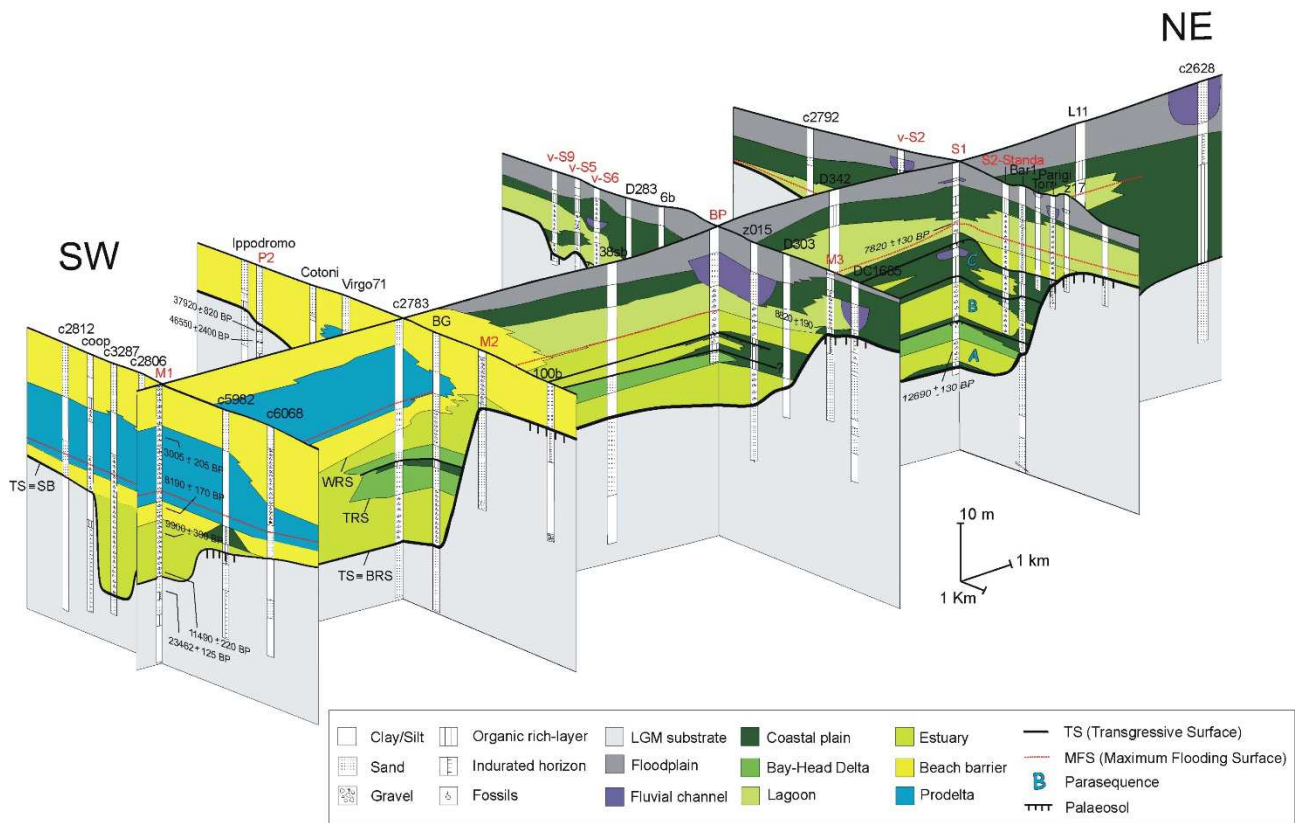
Fig. 2.14: Fence diagram showing the three-dimensional architecture of the upper incised-valley fill succession with distinctive along-dip variability in facies architecture. Reference cores, including S1 and M1 cores (see Fig. 2.11 for location), are reported in red. SB: Sequence Boundary, BRS: Bay Ravinement Surface, TRS: Tidal Ravinement Surface, WRS: Wave Ravinement Surface. Agea are reported as calibrated years BP. From Amorosi et al. (2013b).

To sum up, the stratigraphic architecture of the uppermost 100 meters of the Arno plain subsurface succession documents a complex history of multiple valley incision and filling under the predominant forcing of Milankovitch and sub-Milankovitch glacio-eustasy. Autogenic factors, including fluvial dynamics, local tectonic activity and inherited morphologies, likely played a major role in determining the location of river incisions (Rossi et al., 2017). However, the anatomy of the lower IVS is still poorly known, especially at distal locations where the two incised systems possibly nest, as well as the depositional evolution of the Arno plain during the key chronostratigraphic interval (i.e, MIS 6 – MIS 3/2) that encompasses the Last Interglacial.

2.2.2. *Postglacial high-resolution stratigraphy*

A high-resolution facies and palynological analysis of the postglacial IVF succession (dated between ca. 13-8 kyr BP) was performed within reference core S1 (Figs. 2.11, 2.14), leading to the identification and climate-characterisation of three small-scale transgressive–regressive cycles

bounded by lateral equivalents of marine flooding surfaces (i.e., parasequences in Amorosi et al., 2009, 2013b; Fig. 2.15).

The three parasequences (PS1-3 in Fig. 2.15) show an overall regressive trend, as fluvial-influenced environments are increasingly represented in a topwise direction. The lower parasequence (PS1) was chronologically constrained to the Lateglacial (radiocarbon age of 12,690±130 cal. yrs BP in Fig. 2.15) and palyno-stratigraphically subdivided into a lower transgressive estuarine portion and an upper regressive portion mainly composed of bay-head delta sands and silts. The estuarine deposits encase a pollen assemblage characterised by the abundance of mixed oak trees (45% on average), a low presence of Mediterraneans (around 5%) and pines (ca. 10-15%) and a high presence of montane trees (ca. 20-30%) interpreted as indicative of mild conditions possibly related to the Bölling-Allerød oscillation. By contrast, bay-head delta deposits are largely barren of palynomorphs and only two samples bear a pollen assemblage characterised by the dominance of pines and montane trees (20-40% and 15-40%, respectively), mostly at the expenses of Mediterraneans and, to a lesser extent, of deciduous oaks;this suggests a shifting to cooler conditions possibly attributable to the Younger Dryas. Upwards, PS2 developed under true climate optimum conditions, as the mixed oak – holm oak forest dominates pollen spectra (50-70% of deciduous oaks, 10-20% of *Quercus ilex* and *Erica arborea*) of its transgressive portion, represented by estuarine clays. The regressive portion of PS2, composed of a prograding succession of estuarine and paludal deposits, has only few pollen-bearing samples, which however show a drastic drop in climate optimum indicators paralleled by an increase in montane taxa and pines with similar proportions to the inferred Younger Dryas event. This cooling can thus be attributed to the Boreal Oscillation (estimated age of ca. 10.4 kyr in Fig. 2.15). The uppermost PS3 and the overlying late transgressive coastal deposits capped by the MFS dated at 7820±130 cal. yrs BP (Fig. 2.15) developed under recovered climate optimum conditions, although the mixed oak – holm oak forest partially left place to the hygrophilous woods (facies-modified signal due to the dominance of more continental conditions). A cooling event, recorded by a further spreading of montane taxa and pines within the regressive alluvial portion of PS3, interrupts such otherwise uniform warm climate conditions and was tentatively attributed to the 8.2 kyr event owing to a combination of factors:

- I) peak of *Abies*, also recorded in Tuscany at Lago dell'Accesa (Drescher-Schneider et al., 2007) and interpreted as an evidence of enhanced moisture;
- II) radiocarbon age of 7820±130 cal. yrs BP from the overlying, transgressive lagoonal deposit, 5 m above the PS3 upper boundary;
- III) deposition of coarse-grained sand bodies, interpreted as fluvial and distributary channels.
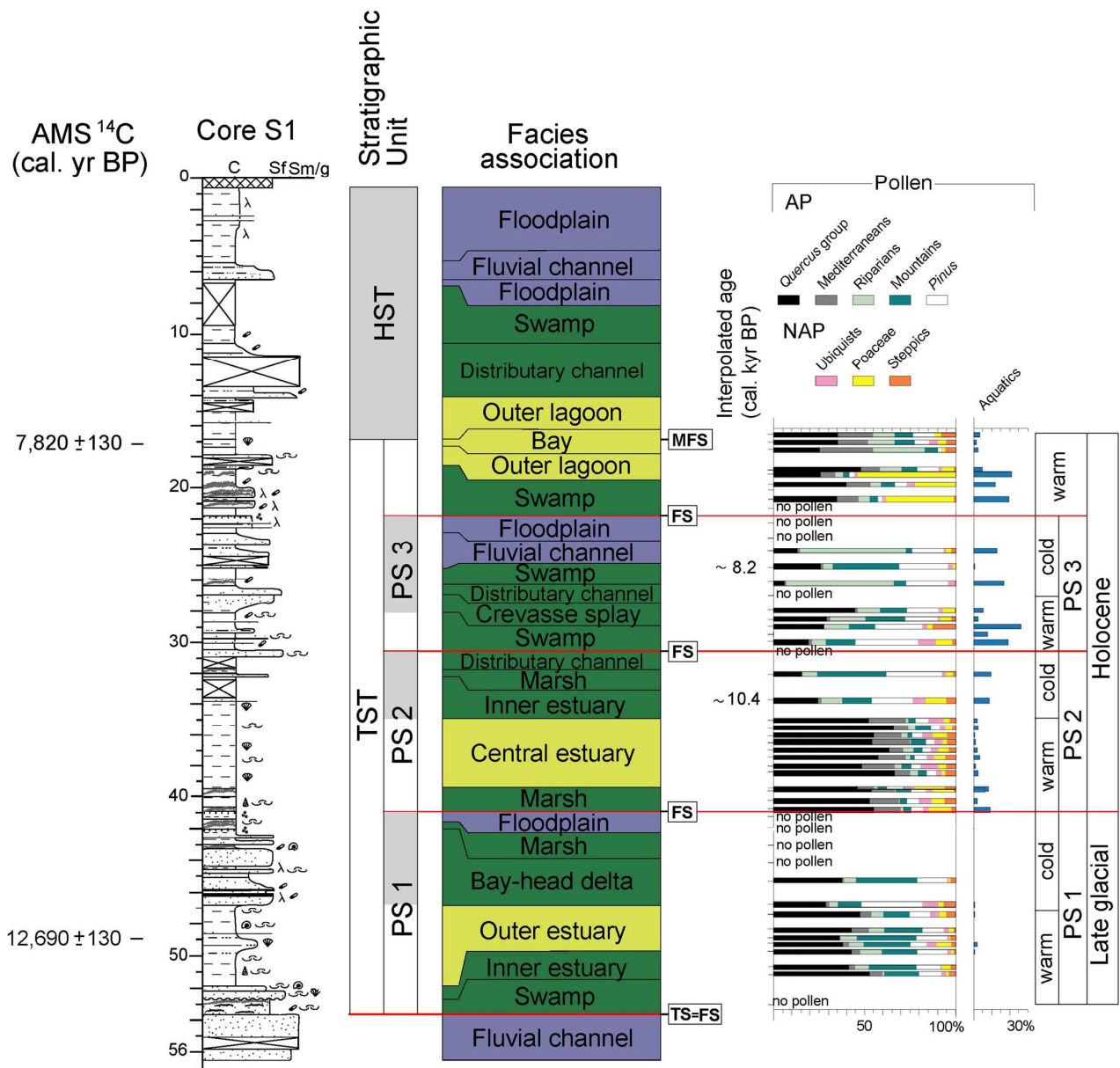
Fig. 2.15: Facies and palaeoclimate characterizations of the reference core S1 (see Fig. 2.11 for location). PS1 to PS3: parasequences (regressive portions are shown in grey), TS: Transgressive surface, FS: Flooding surface, MFS: Maximum flooding surface. Slightly modified from Amorosi et al. (2009).

It is noteworthy that the FS atop PS3 records the last transgressive pulse that completely filled the upper palaeovalley after the 8.2 kyr event. This flooding surface likely corresponds to the last acceleration phase of RSL before the achievement of relatively stable highstand conditions (i.e., MWP-1d; Liu and Milliman, 2004; Vacchi et al., 2016). In this context, a wide lagoonal basin developed and persisted up to ca. 5.0 kyr, occupying an area that extended NW-SE for 6 km and from the present coastline up to the foot of the Pisa Mountains for 18 km; at the centre of this area the city of Pisa would have developed (Rossi et al., 2011). Lagoon deposits consist of light blue-gray clays / silty clays with a variable content of organic matter (increasing towards its margins at

the transition to freshwater, paludal environments), seldom interrupted by thin fine sandy layers. Abundant *Cerastoderma glaucum* shells are found, whereas the meiofauna is mainly represented by *Ammonia tepida* and *A. parkinsoniana* (65-85%), with subordinate *Aubignyna perlucida, Cribroelphidium* spp., *Haynesina germanica,* and Miliolids; an oligotypic assemblage mainly composed of *Cyprideis torosa* also occurs. Barren horizons or oligotypic associations dominated by *Candona* and *Pseudocandona* genera are also present. This clayey deposit also shows weak geotechnical characteristics (high compressibility and low pocket penetration values), which caused the leaning of the Tower of Pisa (Sarti et al., 2012). The lagoon development encompassed the late transgressive and the early highstand periods (Figs. 2.14, 2.15). Only at ca. 5 cal. kyr BP, the complete filling was achieved and the lagoon became a wide paludal area fed by the Arno and Serchio river networks, this latter with several palaeochannels discharging from the north (Amorosi et al., 2013a). The construction of the mid-late Holocene delta plain saw alternating phases of aggradation and progradation identified within an overall progradational stacking pattern of facies: lagoon-swamp-poorly drained floodplan-floodplain deposits (Sarti et al., 2015a; Fig. 2.16).
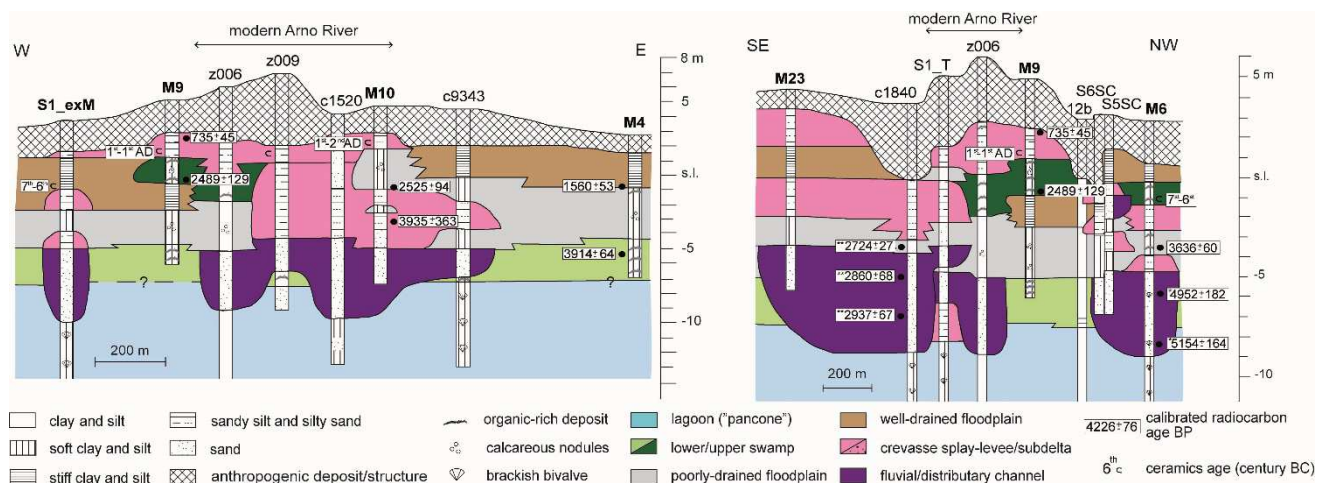
Fig. 2.16: Two representative cross-sections across the Pisa plain, showing the mid–late Holocene lithofacies distribution and stratigraphic architecture of the deltaic–alluvial prograding wedge. Radiocarbon ages are reported as calibrated yrs BP, while the archaeological data as century BC/AD. From Sarti et al. (2015a).

Two main erosive events took place between ca. 4.0-2.5 kyr BP (Fig. 2.17; Sarti et al., 2015a), reflecting centennial-scale climate variations defined by peaks in *Abies* pollen and chronologically constrained to the Eneolithic – Bronze Age and the Bronze – Iron Age transitions (about 4.0-3.8 ka BP and 2.9-2.8 ka BP, respectively). These events are represented by fluvial channel sandy bodies deeply cutting into the underlying swampy-lagoonal succession.

These two sets of palaeochannels have been mapped for the Pisa area based on the integration of core data with remote sensing (Sarti et al., 2015a). Palaeotraces document meander migrations and

fluvial avulsions. A complex fluvial channel network, consisting of separate, meandering Arno and Serchio river systems continued to feed the alluvial plain without evidence of human influence to the Roman Period, when the centuriation took place, land reclamation processes in the plain became massive and previous wetlands were drained (Baldassarri and Gattigia, 2009; Amorosi et al., 2013). During the Late Antiquity cooling, increased rainfall (Büntgen et al., 2011), strong population decrease and ceasing of land management practices led to the renewed development of wetlands (Redi, 1991; Martini et al., 2010). These humid areas, nowadays identifiable by aerial photographs and remote sensing (Bini et al., 2012; Sarti et al., 2015a), lasted up to the Middle Ages, when the Serchio river was artificially diverted northwards (Amorosi et a., 2013a); contemporaneously, the emplacement of several waterworks lasted until the Modern Age, determining the complete subaerial exposure of the floodplain.

2.2.3. Present-day vegetation and climate

The Arno delta plain belongs to the Maremma Sub-section of the Northern and Central Tyrrhenian Section of the Tyrrhenian Province, in turn falling into the Mediterranean Division of Italy (Ecoregions of Italy *sensu* Blasi et al., 2014). In this Sub-section the mean annual precipitation is 560-971 mm and the mean annual temperature is 14-17°. The hottest month is July / August with peaks of 28.9-31°C, whereas the coldest is January with temperatures of 2.2-7.1°C; the annual thermal excursion is about 14.8-17.3°C. The climate is predominantly Mediterranean oceanic. The city of Pisa and the surrounding lowlands lie in the northernmost portion of this Sub-section and are bounded by reliefs (Fig. 2.12). This combination of geographic and physiographic conditions depicts a particular setting, that of a sub-Mediterranean precipitation regime with rainfall greatly increasing with altitude, as it occurs on the Pisa Mountains where the mean annual precipitation is ca. 1252 mm versus 928-950 mm in the lowlands (Bertacchi et al., 2004). The Authors described the modern vegetation on the Pisa Mountains as dominated by chestnut woods, which replaced the natural mixed oak woods due to anthropic plantation; nowadays they are mostly used as a logging resource, however several forms of chestnut woods are present:

- *Teucrio scorodoniae-Castanetum sativae* Arrigoni et Viciani 1998 (the acidophilous community);

- *Rubo hirti-Castanetum sativae* Arrigoni et Viciani 1998 (a dense shrubby community impoverished in herbaceous taxa);

- *Ilici aquifoli-Quercetum petraeae* subass. *Castanetosum* Arrigoni 1997 (an acidophilous meso-hygrophilous wood with abundant *Quercus robus*, *Laurus nobilis* and *Ilex aquifolium*);

- *Arbuto unedi-Castanetum sativae* Arrigoni et Viciani 1998 (a thermophilous community with *Quercus ilex*, *Quercus suber* and *Arbutus unedo*);

- *Symphyto tuberosi-Castanetum sativae* Arrigoni et Viciani 1998 (an abandoned meso-hygrophilus woodland community to be found in cool valleys with *Ostrya carpinifolia* and several diagnostic herbaceous taxa);

- *Digitali australi-Castanetum sativae* Gamisans 1977 (an open thermo-heliophilous community with *Digitalis lutea* australis and *Hypericum montanum*)

Alongside the chestnut woods on the hills, *Pinus pinaster* pine woods are common beyond the *Castanea sativa* layer or in degraded portions of the woods.

Other vegetation types are:

- *Ostrya carpinifolia – Fraxinus ornus woods*, as a transition between the chestnut wood and the sub-Mediterranean holm oak forest. In fact, accessory species are *Castanea sativa, Acer campestre, Ulmus minor* and *Quercus ilex*.

- *Sambuco nigrae-Robinietum pseudoacaciae* Arrigoni 1977, an invasive association dominated by the alien species *Robinia pseudoacacia* that tends to replace the thermophilous *Quercetalia pubescent petraeae* Klika 1933 and the acidophilous *Quercetalia roboris* Tüxen 1931.

- *Roso sempervirentis-Quercetum pubescentis* Biondi 1986, a mixed oak wood association occupying limited areas nowadays because of its anthropic or human-induced substitution by chestnut, pine, *Robinia* or olive.

- *Alnion glutinosae* Mijr-Drees 1936, hygrophilous woodlands widespread along the river banks with *Corylus avellana* in the undercover and a dense herbaceous stratum made of Pteridophytes, *Carex pendula, Hedera helix* and *Ruscus aculeatus*.

- *Fraxino orni-Quercetum ilicis* Horvatic 1956, a Mediterranean holm oak forest with *Quercus ilex, Fraxinum ornus, Ostrya carpinifolia,* and less common *Quercus pubescens* in the tree layer; the shrubby layer is composed of *Arbutus unedo, Phillyrea latifolia,* and *Coronilla emerus*. Sporadic *Crataegus monogyna* and *Erica arborea* are encountered. This association has a peculiar subassociation *arbutetosum unedi* Arrigoni et Di Tommaso 1997 characterised by the constant presence of *Arbutus unedo* and *Erica arborea* and, thus, constituting a degradation of the former. A further degraded form towards the Mediterranean maquis presents the partial substitution of *Quercus ilex* by *Quercus suber*, since the latter prefers siliceous substrata where it can better compete against the holm oak;

- *Erico arboreae-Arbutetum unedi,* a maquis coenosis intermediate between the holm oak forest or other previously mentioned associations and more degraded vegetation types.

- *Cephalario leucantha-Saturejetum montanae* subass. *euphorbietum spinosae* Allegrezza, Biondi, Formica, Balleli 1997, dominated by nanophanerophytes leaving place to chamephytes and herbs. This association represents the highest degree of woodland degradation.

- *Pinus pinaster* open woodlands, with alternating *Erica arborea, Phyllirea angustifolia, Phyllirea latifolia, Castanea sativa* and various other trees and shrubs in relation to edaphic conditions and to the degree of degradation of the adjacent woods.

3. MATERIAL AND METHODS

As this Thesis focuses on past landscape dynamics of Mediterranean delta-coastal plains at both Milankovitch and sub-Milankovitch timescales, a stratigraphic-based palynological approach was conceived for the late Quaternary successions buried beneath the Po and Arno plains (40 m-long core EM2 and 31.5 m long core PA1, respectively; Fig. 3.1). This methodology relies on the palynological (i.e., pollen and spore) characterization of depositional facies and architectural elements (e.g., lagoon intervals; T-R cycles) framed into a high-resolution stratigraphic and chronological (^{14}C-based) framework. It is aimed to decipher the complex relationships among vegetation dynamics, facies architecture and climate changes.

For the two studied successions, lithological inspection of cores was integrated by the quantitative analysis of palynomorphs, which allowed: *i)* accurate facies characterization also within fully freshwater settings (core EM2 drilled ca. 40 km landward the present-day coastline; Fig. 3.1), and *ii)* robust vegetation-derived climate reconstructions in a sequence-stratigraphic perspective. Concerning core PA1, which was drilled in proximity of the Arno delta strandplain (Fig. 3.1), facies characterization also benefitted from semi-quantitative studies of the meiofauna content (i.e., ostracods and benthic foraminifers) performed on 39 samples prepared and analysed by Dr. Veronica Rossi (University of Bologna). As these faunal groups are excellent palaeonvironmental proxies within back-barrier – shallow marine settings (e.g., Holmes and Chivas, 2002; Murray, 2006), the sampling procedure was conceived alongside the palynological sampling in order to: *i)* characterise the whole spectrum of lithofacies and, where possible, *ii)* analyse the meiofauna content of the same layers sampled for palynological studies. This approach allowed integrating the information provided by these two fossil groups within the same coastal-deltaic succession. Meiofauna samples were prepared following the standard procedure reported in Amorosi et al. (2014b) and briefly explained as follows: approximately 40-50 g of sediments were dried in an oven for 8 h at 40°C, soaked in water, wet sieved through 63 μ (240 mesh) sieves and dried again. Twenty-one samples containing an autochthonous meiofauna were semi-quantitatively analysed in the size fraction > 125 μ and relative abundance categories (i.e., more than 30%; 30–10% and less than 10%) were defined. Several key papers and books were used for the identification of taxa and their autoecological characteristics (i.e., Jorissen, 1988; Athersuch et al., 1989; Albani and Serandrei Barbero, 1990; Henderson, 1990; Sgarrella and Moncharmont Zei, 1993; Montenegro and Pugliese, 1996).
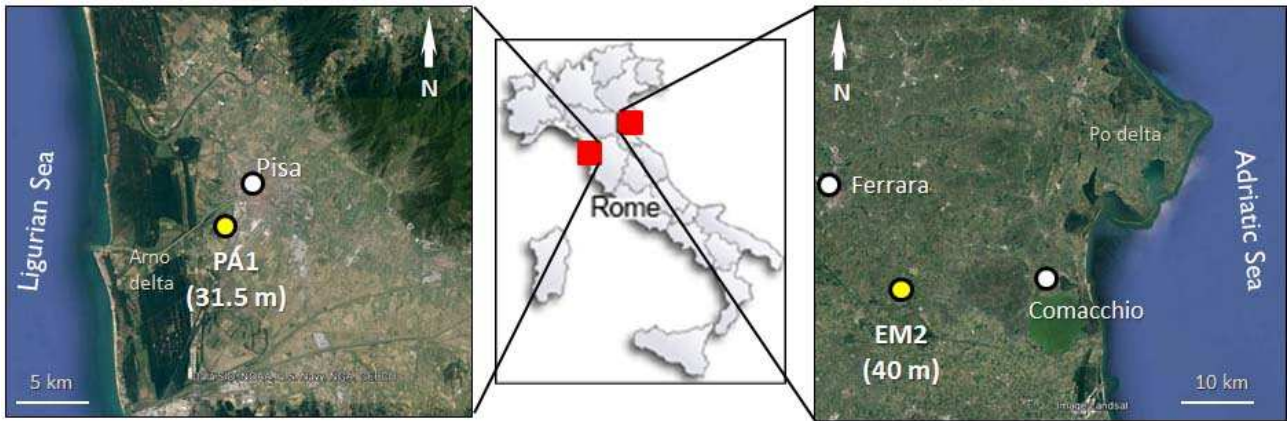
Figure 3.1: Location of the study areas and location of the cores EM2 (Po delta plain) and PA1 (Arno delta plan) analysed in the Thesis. Satellite images from Google Earth.

3.1. Core locations, recovery and logging

The 40 m-long core EM2 was recovered in 2015 in the context of a collaborative project between University of Bologna and ExxonMobil Upstream Research Company, near the Masi Torello village (ca. 15 km SE to Ferrara city) and about 40 km landward of the modern North Adriatic coastline at 2.7 m a.s.l. (Fig. 3.1). This core was selected because of *i)* its excellent chronological constraints (nine radiocarbon ages available in Amorosi et al., 2016), *ii)* the remarkable thickness of Holocene fine-grained deposits, *iii)* the cyclic occurrence of organic-rich clays and overbank/channel sands (Bruno et al., 2017) and *iv)* the lack of marine-influenced facies. This latter feature allowed me to consider the provenance of palynomorphs *via* the Adriatic Sea currents as negligible, improving the reliability of facies and palaeoclimate reconstructions in a depositional setting that lacks any other commonly-used fossils (i.e., benthic foraminifers, ostracods and molluscs) due to the freshwater, low pH and poorly oxygenized conditions (Murray, 2006; Ruiz et al., 2013 among others).

The 31.5 m-long core PA1 was recovered, as part of this Ph.D. project, in May 2017 near the city of Pisa about 1.5 m above mean sea level and about 8 km far from the coastline (Fig. 3.1). This area, immediately south to the modern Arno River course, and ca 2 km landwards of the innermost outcropping beach ridges (Fig. 3.1), was selected because of the recent identification within the near core M3 of two m-thick lagoonal successions separated by a set of palaeosols (Amorosi et al., 2014b). This vertical stacking pattern of strata was considered highly-prone to high-resolution palynological, palaeoclimate-aimed analyses due to the m-thick, fine-grained succession, furnishing the possibility to analyse a suite of facies associations including the brackish ones.

Fig. 3.2: core PA1 recovery

For the two studied cores, a continuous perforating technique guaranteed an almost undisturbed stratigraphy and very high recovery percentages (> 90%), allowing the detailed description of sedimentological features and a robust identification of the sedimentary units/lithofacies that guided the sampling strategy for palynomorphs analyses (section 3.2.). The cores were split lengthwise, photographed and described in terms of grain size, sedimentary structures, colour, type of contacts between stratigraphic intervals, pedogenic features (calcareous nodules, Fe-Mn oxides), presence of bioturbation and accessory materials (including wood fragments, decomposed organic matter, mollusc shells and fragments) in order to identify the main lithofacies. Moreover, pocket penetration (PP) values were obtained from fine-grained (silt and clay) intervals on the fresh core PA1 with the aim to characterize palaeosols and strengthen facies identification following Amorosi and Marchi (2002) and Amorosi et al. (2014a). For EM2, PP values are reported in Bruno et al. (2017).

3.2. Palynological analyses

Thirty-eight samples were analysed from core EM2 for pollen and Pteridophyte spore contents. The same analysis was performed on 49 samples from core PA1 with the addition of Bryophyte spores identification, which allowed a complete analysis of terrestrial plant palynomorphs, leading to more detailed palaeoenvironmental reconstructions within a succession with a high variety of facies. Following lithological and visual inspections of cores (section 3.1.), all lithofacies were sampled with a special focus on organic-rich- (paludal) and shell-rich (lagoon, containing the brackish bivalve *Cerastoderma glaucum*) clayey intervals, where abundant palynological assemblages were expected. Due to the high facies variability encountered in both cores, especially PA1, the sampling pace was uneven. Unique exception was represented by the m-thick, lithologically uniform, upper lagoon succession of PA1, where 1 sample per meter was evenly collected.

3.2.1. Sample preparation

Samples were prepared and analysed at "*Centro Agricoltura e Ambiente G. Nicoli*" laboratory (San Giovanni in Persiceto, BO, Italy) under the supervision of Prof. Marco Marchesini, following a standard extraction technique (Lowe et al., 1996):

1. About 3-12 g of dry sediment per sample were weighed depending on grain size (3-6 g for clays, 6-8 g for silts and 8-12 g for sands).

2. A *Lycopodium* tablet (1 tablet = 20484 spores) was added to calculate pollen concentration; lycopod spores were chosen as a concentration indicator, because they do not significantly belong to the regional flora. These spores are also useful to indicate problems occurred during sample preparation, such as mechanical damage of palynomorphs (in case they themselves present high damage rates, thus not to be adduced to natural degradation processes) or material loss (in case a few lycopods are retrieved within scarce pollen-bearing samples, thus not to be considered sterile).

3. Samples were solved in a 10% Na-pyrophosphate solution and subsequent filtered through a 0.5 mm mail sieve and a 5 μm mail nylon filter.

Fig. 3.3: 10% Na-pyrophosphate solution and sieving.

Fig. 3.4: sample filtering.

4.   Each sample then underwent repeated 24 hour-long treatments in the following order: cool 10% HCl solution to remove carbonates; hot acetolysis for excess organics and pollen reddening; hot hydrate Na-metatungstate heavy liquid floatation; cool 40% HF solution to remove silicates; ethanol suspension and evaporation at 60°C in a stove.

5. Microscope slides with glycerine jelly and paraffin were prepared, so that palynomorphs are not floating but fixed on the slides, hence they can be stored at the laboratory's collection and re-analysed anytime.

Fig. 3.5: microscope slides preparation.

3.2.2. Taxonomic identification and ecological groups

For each sample, at least 300 pollen grains were counted (where possible) at 400x magnification and recognised using the general morphological keys published by Faegri et al., (1989) and Moore et al. (1991); a 1000x magnification was used when taxonomical determination needed it. However, as a general approach, when determination at species (or genus) level was not possible (due to taphonomy, sample preparation factors, such as those previously mentioned, or to the grain's position on the fixed slide), the higher taxonomical level was conservatively chosen to avoid mis/overinterpretation. When possible, Family-aimed pollen keys were also used for determination at species level. Examples of the used pollen keys are the following:

- ASTEROIDEAE → Punt and Hoen (1999) for *Aster tripolium* type and *Tussilago farfara* type. For grains in a good preservation state, I took into account the dimensional parameters and the height of *spinulae*. When the grain had a bad preservation, a position on the slide unsuitable for species determination or intermediate values between at least two species, I referred to Asteroideae undiff. However, *Aster tripolium* type includes species with a wide range of dimensions (from a mean diameter of 19-20 μm to one of 27-28 μm), so *Bellis perennis* cf. was distinguished as a taxon including all species of minor dimensions within the pollen type. Nonetheless, if on one hand species determination was reached when possible, no autoecological considerations were inferred at species level because these two pollen types each collect different species with undistinguishable pollen grains and different autoecology.

Therefore, palaeoecological inferences were made considering the total sum of these pollen types as a single entity (i.e., non-*Artemisia* Asteroideae; see Appendix B for ecological groups of each taxon). The same approach was also used for all other herbaceous taxa (e.g., Apiaceae, Boraginaceae, Brassicaceae, Caryophyllaceae, Crassulaceae, Cyperaceae, Fabaceae, Papaveraceae, Polygonaceae, Primulaceae, Ranunculaceae and Urticaceae) that presented this issue in ecological characterisation, so that species determination could not hamper ecological inferences and *vice versa*.

- BETULACEAE → Paoli and Perini (1979) and Blackmore et al. (2003) *Alnus glutinosa, A. incana* and *A. viridis*; *A. cordata*, although having morphological parameters similar to *A. incana*, was excluded because it is endemic of southern Italy (Pignatti, 1982, 2017-2018). Nonetheless, when the grain had an intermediate position between the equatorial and the polar or was poorly-preserved, *Alnus* sp. was the conservative choice of determination.
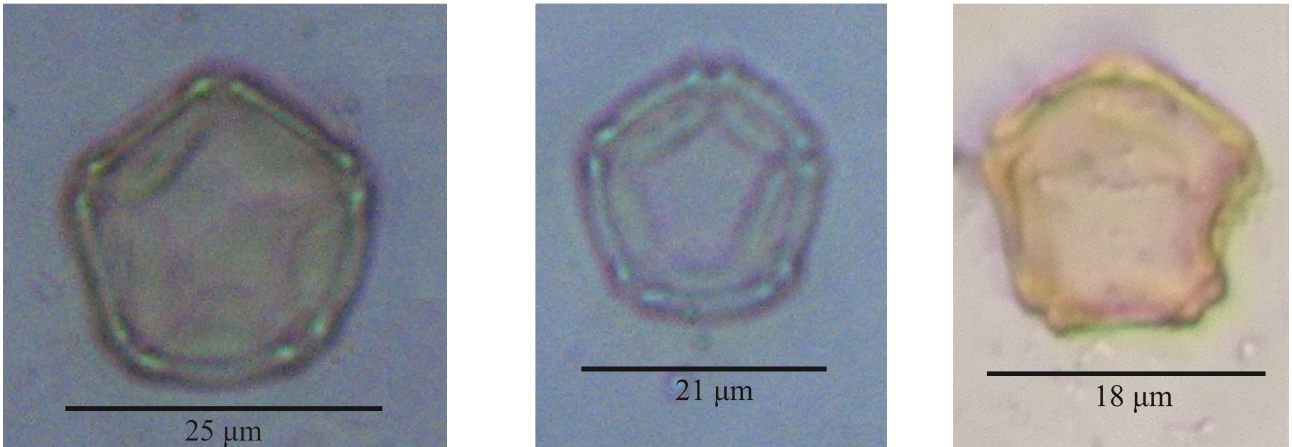
Fig. 3.6: *Alnus* pollen determination on the basis of cited pollen keys.

- FAGACEAE → Van Benthem et al. (1984) for *Quercus cerris, Q. ilex, Q. pubescens* and *Q. robur*. For grains in equatorial view, I took into account the following parameters: dimensions, shape, spatial organisation of *columellae* (distinguishable or not, organised in dark *maculae* or not) or of *verrucae* (height, organised in *maculae* or not). For grains in polar view or partially crumpled, *Quercus* sp. was chosen to avoid mis/overinterpretation.

Quercus robur (polar view)

Quercus ilex (equatorial view)
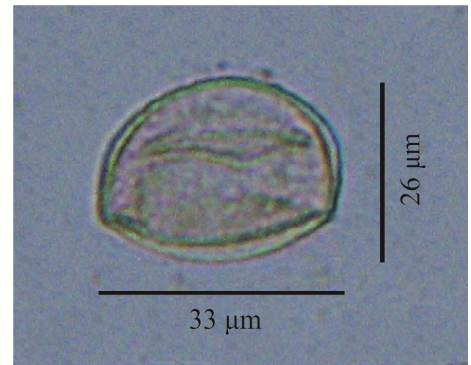
Quercus pubescens (equatorial view)
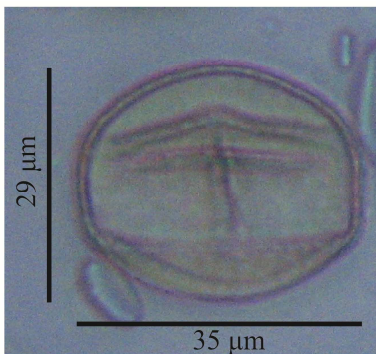
Quercus cerris (equatorial view)

Quercus sp. (polar view)
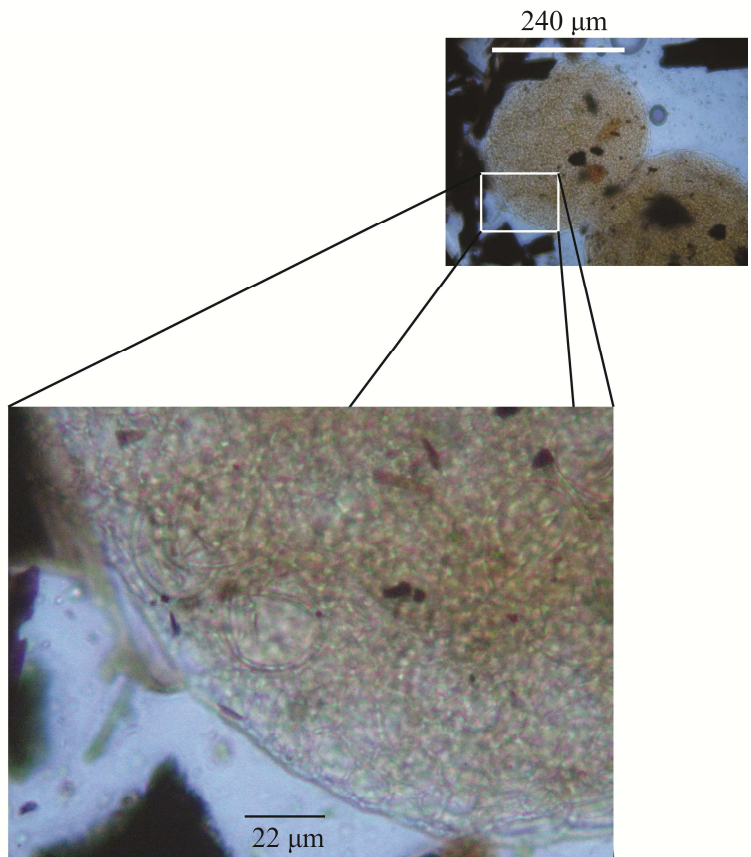
Quercus sp. (2 stamens with immature pollen grains)

Fig. 3.7: *Quercus* pollen determination on the basis of cited pollen keys.

- PINACEAE → Accorsi et al. (1979, 1983, 1994) and Arobba (1979) for *Pinus halepensis, P. mugo, P. nigra, P. pinea* and *P. sylvestris*. For grains in equatorial or polar view, I took into account dimensional parameters of *corpus* and *sacci*. Nonetheless, when preservation was poor or the position of the grain did not allow proper determination or when the measures fell into more than one species ranges, *Pinus* sp. was chosen to avoid mis/overinterpretation.

Pinus sylvestris

Pinus mugo

Pinus pinea

Pinus sp. (on the left, not measurable)
and *Pinus nigra* (on the right, measured)
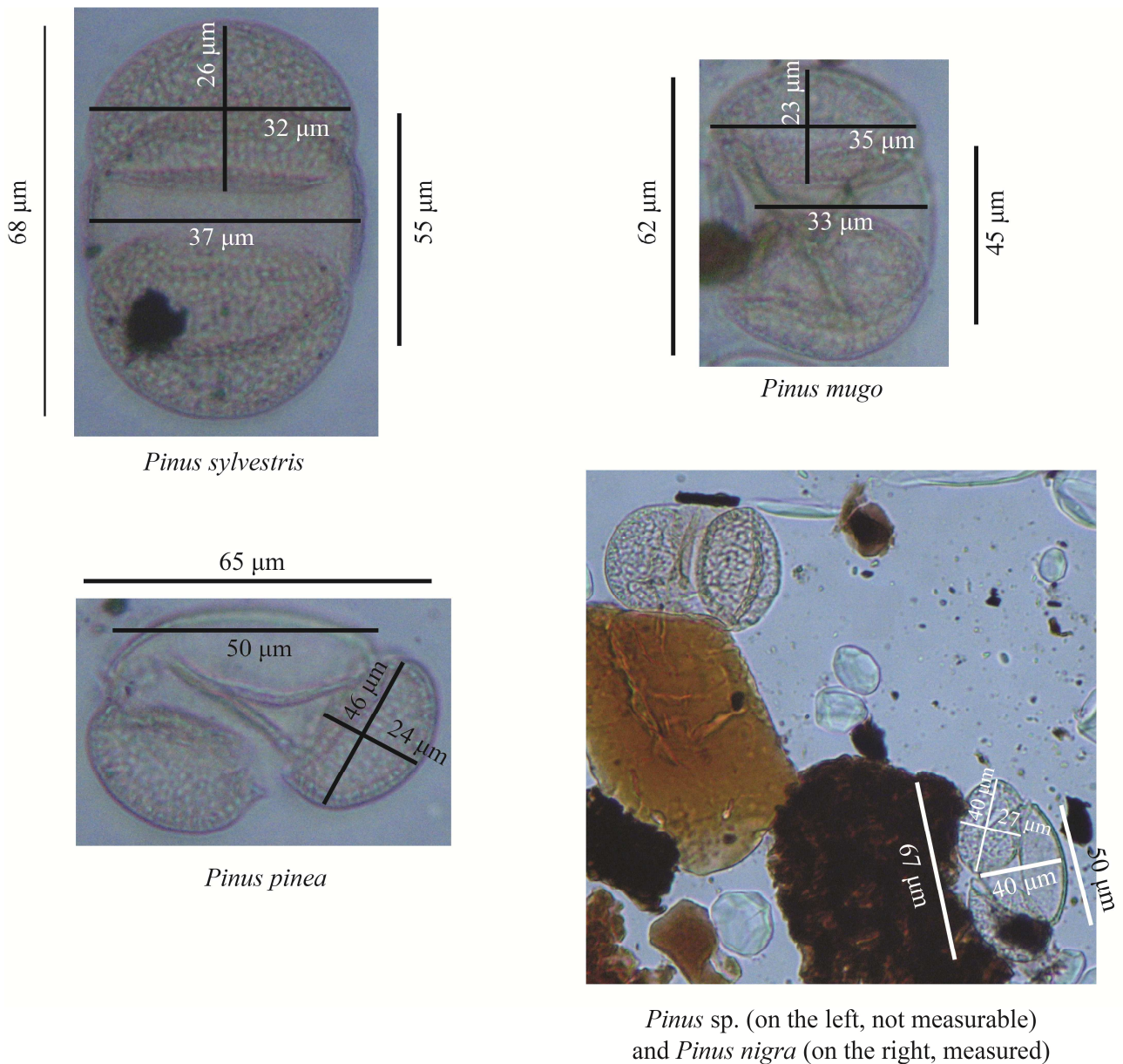
Fig. 3.8: *Pinus* pollen determination on the basis of cited pollen keys.

The laboratory's collection and published atlases (Reille, 1992, 1995, 1998) were also used to improve pollen determination.

44

Percentages of Angiosperms and Gymnosperms (Spermatophytes) were calculated on the total pollen sum and were used to elaborate pollen spectra, taxa figures and to make palaeoecological-climatic inferences. Pollen concentrations were also calculated but were used only as a general taphonomic indicator of pollen preservation within the wide variety of sedimentary facies. No palaeoenvironmental inferences were elaborated from pollen concentrations because the high variety of facies would not have allowed a proper comparison between samples.

Bryophyte spores were recognised using Boros et al. (1993) and a synthetic guide to the identification of spores comprehensive of all the species treated therein was elaborated (Appendix A). Grains were counted as undeterminable when their preservation was too poor to even determine the family taxonomical level. Secondary grains were mainly identified based on either the stronger colouring due to acetolysis or on their determination as fossil extinct taxa (i.e.: reworked; Bolkhovitina, 1956; Tschudy and Scott, 1969; Cincotta et al., 2019), and/or strong evidence of consumption likely due to fluvial transportation (i.e., transported). These types of secondary grains were not considered separately but plotted altogether in a single sum because they both do not belong to the coeval vegetation and, thus, do not contain any information on palaeoclimate and palaeoenvironment, which are the focus of this Thesis. Inferences about sediment provenance were made on the basis of reworked grains, in case they could be determined at species level and attributed to at least a group of geological formations. Percentages of Pteridophytes, Bryophytes, *Pseudoschizaea circula* (Christopher, 1976)*,* undeterminable and secondary grains were calculated on the total sum of pollen grains *plus* their respective values, a technique allowing a correct down-weighting of their presence (Berglund and Ralska-Jasiewiczowa, 1986). To sum up, 227 taxa were identified and 13497 grains were counted within core EM2, whereas analysis of core PA1 gave rise to a dataset composed of 275 taxa and 11449 grains.

Concerning taxa ecological characterisation, I relied upon several works, including Tomaselli (1970, 1987), Pignatti (1979, 1982, 1998, 2017-2018), Ferrari (1980, 1997), Berglund and Ralska-Jasiewiczowa (1986), Tutin et al. (1993), Accorsi et al. (1999, 2004), Bertoldi (2000), Ubaldi (2003), Bertacchi et al. (2004), and Pini et al. (2016). On the basis of these (palaeo)ecological information, plant ecological groups were established by summing up together all taxa with similar characteristics:

– montane taxa (Mt);
– *Quercus* + other Deciduous Trees (Q+other DT), elaborated to detect the presence of non-hygrophilous broadleaves, including the mixed-oak forest taxa;
– Mediterraneans (M);

–   woody (Hyg) and herbaceous (hyg) hygrophytes, helophytes (Aq-hel), hydrophytes (Aq-hyd);

–   halophytes (hal); one of the main halophyte taxa retrieved is *Artemisia,* whose pollen grains were considered differently depending on the general climate-stratigraphic considerations. Indeed, when an interglacial age could be inferred (by means of the combination of palynological, stratigraphic and radiocarbon data), *Artemisia* was counted as halophyte; by contrast, it was considered as a cold climate indicator when a glacial or glacial-like age could be inferred. For further information about difficulties in *Artemisia* species determination and ecological attribution, see Subally and Quézel (2002).

–   anthropic indicators (Ai), the sum includes anthropic spontaneous (As) and cultivated taxa (cc) because of the scarce anthropic presence detected throughout the samples;

–   ombrotrophic (omb), heliophilous (hel) and humicolous (hum). These last three groups were exclusively defined for Bryophytes.

In Appendix B the percentages of taxa and their attribution to specific ecological groups are reported for both studied cores. Palaeoenvironmental inferences were made by pairing taxa ecological attributions to stratigraphic facies analysis and by avoiding to consider within the local pollen rain those taxa that could only be ascribed to a regional provenance (i.e., those belonging to the Mt group, present in the lowlands mainly during glacial periods). Due to the abundance of wet environments, a peculiar attention was paid to woody and herbaceous hygrophytes, helophytes and hydrophytes, dominant in several pollen spectra.

Taking into account the definition of "swamp" and "marsh" by Howell (ed., 1960) (swamp as "*an area of saturated ground supporting dominantly trees and shrubs*"; marshes as "*shallow lakes, the waters of which are either stagnant or actuated by a very feeble current; they are, at least in the temperate zone, filled with rushes, reeds and sedges and are often bordered by trees*"), I decided to maintain the more conservative term "swamp" for the following reasons:

i) to avoid confusion along the Thesis between the botanical definitions of "swamps" and the use of this term in a general stratigraphic perspective, already published in various papers for both the study areas;

ii) to avoid the risk of overinterpretation of paludal horizons, usually sampled with an uneven, low-resolution pace mainly aimed to defining general variations in palaeoenvironmental and palaeoclimatic conditions between different facies;

iii) to be consistent with our knowledge of the Po Plain vegetation (Section 2.2.1.), as the alluvial forests with *Alnus glutinosa* and *Fraxinus excelsior* (alliances *Alno-Padion*, *Alnion*

incanae and *Salicion albae*) are more common in areas with Continental climate of Western Europe than in the Eastern Po Plain, where more Mediterranean conditions are met. Therefore, in this case we interpreted variations in hygrophytes *vs* helophytes + hydrophytes as related to relative water table oscillations mirroring the proximity / distance of trees bordering locally depressed areas.

After this careful filtering of the facies signal, an evaluation of the variations of montane taxa (Mt) and holm oak – mixed oak taxa (M and Q+other DT) was performed to make inferences about palaeoclimate variability.

3.3. Statistical elaborations

Following the method of Tarasov et al. (1998) and Kaniewski et al. (2011), statistical analyses were performed to elaborate a pollen-derived vegetation biomization and support previous identifications of autoecological groups for both palynological datasets (cores EM2 and PA1), under the supervision of Dr. David Kaniewski (University of Toulouse). Relative abundances of taxa were inserted in PAST (PAlaeontological STatistic – version 3.10 by Hammer et al., 2001) and Cluster Analysis (CA) was run in order to highlight environmental and/or climatic forcing on the assemblages. This, in turn, had the purpose to show how palynomorphs cluster together within the sampled successions in order to recognise different groups of taxa that were found most often in the same assemblage.

Paired group was used as the root, since previous considerations on the vegetation of Emilia-Romagna and Tuscany (sub-sections 2.1.4. and 2.2.3.) led me to suppose the relatively local provenance of all identified taxa. Then, I chose Correlation as similarity method to explore the temporal proximity of taxa within the stratigraphic successions characterised by high facies variability. The ecological distance between clusters was reflected by the distance between branches on the tree diagram (Kaniewski et al., 2011).

The robustness of this choice was tested by running several analyses for both datasets using different selections of taxa and samples:

- the complete dataset;
- pre-MIS 1 samples (3) and taxa (6) were excluded from EM2 because of chronological uncertainties and sample patchiness within the record;

- *Ephedra fragilis* cf. was excluded from PA1 because of occasional occurrence within the record and because of uncertainties in its Holocene distribution outside southern Italy, where nowadays it is an endemic taxon;

- occasional taxa (recorded in less than three samples with percentages lower than 1%) were excluded from both datasets;

- for the PA1 dataset only, Bryophytes were excluded after an explorative trial; then, due to the higher number of taxa with respect to EM2, a different selection (including Bryophytes) was performed by summing up within each Family all taxa with a similar ecology into a single sum, generally at the Family level. This method was chosen to minimize the dataset heterogeneity and to avoid possible overinterpretations due to taxa determination at the species level which, in this ecological-based approach, could make the dataset dispersive and, so, less informative;

- Pteridophytes, hygrophytes and aquatics were tentatively excluded from EM2 datasets in three different steps (their removal could enhance the estimation of the palaeo-rainfall *via* further statistical elaborations, following Tarasov et al., 1998, and Kaniewski et al., 2011). However, the result of the CA was poor mainly due to the high importance of these plants in fluvial-related ecosystems (and, specifically, in our records).

Taking into account the various CA outputs, I selected the final run for EM2 without pre-MIS1 and rare taxa, whereas for PA1 I kept the removal of Bryophytes and rare taxa. The resulting clusters, obtained from a final matrix of 141 taxa for EM2 and 89 taxa for PA1, allowed the identification of pollen-derived biomes (PDBs), which in turn confirmed the robustness of the autoecological plant groups and helped unravelling environmental and climatic forcing factors on the vegetation. However, although a similar mode of selection was maintained, the degree of detail of the CA was much higher for EM2 than for PA1, probably because the latter encompasses a longer time span, has higher facies variability and includes several stratigraphic discontinuities (i.e., palaeosols).

3.4. Chronological analysis

The chronological framework of the studied successions relied on radiocarbon dates (Table 1): 13 samples from core EM2 and 4 samples from core PA1 were analysed at KIGAM laboratory (Daejon City, Republic of Korea) and at CIRCE laboratory (Caserta - Naples University, Italy). The dated material was mainly represented by terrestrial organic matter (i.e., wood and plant fragments, peats, decomposed organic matter), more rarely by mollusc shells. The calibration of conventional radiocarbon ages was based on the IntCal13 dataset (Reimer et al., 2013) for terrestrial materials and Mixed Marine NoHem curves (Reimer et al., 2013) with a value of DeltaR (1±30), estimated for the Ligurian Sea (http://calib.org/marine/), for the mollusc samples. All ages are expressed in 2-sigma calibrated years BP.

For the core PA1 succession, the stratigraphic framework also benefitted from the availability of two radiocarbon ages from the nearby core Mappa3 (Bini et al., 2015, for the sample at 6.65 m core depth; Sarti et al., 2015, for the sample at 5.75 m core depth) located ca. 125 m SE (Table 3.1).

Study area	Core	Depth (m)	^{14}C age	Cal. years BP (2σ range)	Cal. years BP (mean value)	Dated material	Laboratory
Po delta plain	EM2	3.2	1180±40	1185-980	1085±100	Wood	KIGAM
	EM2	6.45	3110±80	3485-3075	3280±200	Plant fragment	KIGAM
	EM2	9.45	4480±30	5240-5035	5170±85	Wood	KIGAM
	EM2	11.1	4680±40	5480-5315	5395±80	Plant fragment	KIGAM
	EM2	13.35	6840±40	7760-7590	7675±85	Plant fragment	KIGAM
	EM2	14.65	6630±40	7575-7440	7520±35	Wood	KIGAM
	EM2	15.2	7460±40	8365-8190	8280±50	Plant fragment	KIGAM
	EM2	15.3	7070±40	7975-7825	7900±40	Peat	KIGAM
	EM2	16.6	7140±40	8025-7925	7965±35	Wood	KIGAM
	EM2	20.55	7470±50	8380-8190	8285±95	Wood	KIGAM
	EM2	22.9	8320±50	9470-9220	9335±135	Wood	KIGAM
	EM2	24.5	9990±50	11650-11260	11450±195	Plant fragment	KIGAM
	EM2	25.45	11110±50	13080-12820	12950±130	Plant fragment	KIGAM
Arno delta plain	Mappa3	5.75	3496±27	3843-3693	3768±75	Wood	CIRCE
	Mappa3	6.65	4155±64	4842-4523	4682±160	Wood	CIRCE
	PA1	13.35	6640±30	7425-7288	7380±30	*Cerastoderma glaucum*	KIGAM
	PA1	17.95	8820±40	9957-9696	9800±100	Organic clay	KIGAM
	PA1	24.1	46000±650	*50000-47825	47420±590	Gastropod shell	KIGAM
	PA1	25.02	26030±170	30757-29748	30320±270	Organic clay	KIGAM

Table 3.1: Radiocarbon ages available for core EM2 and PA1. Additional ages from the core Mappa3 are also reported for the Arno delta plain. The asterisk highlights that the sample at 24.1 m core depth is at the range limit for radiocarbon dating.

The age-depth models were constructed using a smoothing spline function in PAST (PAlaeontological STatistic – version 3.10 by Hammer et al., 2001). Differential sediment compaction was not taken into account, thus sedimentation rates were estimated on the basis of radiocarbon ages. However, it must be stressed that the age modelling was limited to the MIS 1 portion of core EM2, due to a lack of radiocarbon ages in older strata. Whereas, for core PA1 age modelling was limited to the Holocene interval because of the scarce reliability and stratigraphic reversals shown by the two oldest (pre-Holocene) samples (ages of 47420±590 and 30320±270 in Table 3.1) and of the presence of several palaeosols in the overlying strata. The highest number of available radiocarbon ages (Table 3.1), along with the lowest lithofacies variability resulted in the highest degree of accuracy for the EM2 age-depth model.

4. RESEARCH OUTLINE

The cornerstone of this project is the palynological characterization of depositional facies and architectural elements buried beneath two areas, located on the opposite sides of the Northern Apennines (Italy) and characterised by different climate conditions as reported in sections 2.1.4 and 2.2.3: *i)* the Po delta plain, facing the Adriatic Sea and *ii)* the Arno delta plain, facing the Ligurian Sea. To achieve this goal, an integrated, high-resolution stratigraphic-palynological approach supported by statistical analysis (cluster analysis) and radiocarbon dating was applied to fine-grained, stratigraphically expanded successions (Chapter 3). This methodology, designed to robustly isolate the local environmental signal from regional climate conditions, allowed to frame our data into a sequence-stratigraphic perspective and the well-known Late Pleistocene-Holocene climate history of the Mediterranean area.

The major results are reported in Chapters 5 and 6; Chapter 5 focuses on the landward portion of the Po delta plain succession (core EM2) and includes two research papers: one published in 2018 (section 5.1) and another one published in 2020 (online in 2019; section 5.2). Chapter 6 examines the Arno delta plain record (core PA1) and consists of one published research paper in 2019 (section 6.1) and a separate section (section 6.2). Section 7 provides a synthetic comparison between the palyno-stratigraphic records available from the two study areas.

Sections 5.1, 5.2, 6.1 and 6.2 correspond to specific research topics that can be summarized as follows.

Po delta plain (Chapter 5):

Research topic 1: *Late Quaternary stratigraphic patterns and vegetation dynamics at the innermost margin of the Po delta plain (section 5.1).* In this section, the shallow subsurface succession buried beneath the innermost portion of the Po delta plain (ca. 40 km landward of the present-day coastline) was investigated through the integration of sedimentological and palynological techniques on a 40 m-long core (EM2). Palynological analysis proved to be extremely useful for the facies characterisation of fine-grained deposits that mainly compose the 25 m-thick freshwater succession of Holocene age. The relative proportion of hygrophytes, aquatics and pasture-meadow herbs allowed the distinction between poorly drained floodplain, low-water table swamp and high-water table swamp (i.e., peaty swamp). The stacking patterns of facies and related water-table oscillations were used as a reference for the identification of the landward equivalents of flooding surfaces and to characterise the maximum flooding surface of the Holocene

transgressive-regressive (T-R) cycle. The identification of peak concentrations of montane trees pollen points to the possible occurrence of minor cooling events that locally correspond to phases of increased sedimentary input (e.g., crevasse splays and distributary channel deposits). Moreover, through pollen data we assigned the fluvial-channel deposit underlying the Holocene T-R cycle to the Lateglacial period, an interval of time that is commonly marked by a hiatus at onshore locations.

Research topic 2: *High-resolution record of Holocene palaeoclimate variability and depositional trends from freshwater coastal successions (section 5.2).* Given the very promising outcome of research topic 1, the further step was to test the potentiality of pollen as a palaeoclimatic tool for high-resolution studies within freshwater coastal successions, after filtering the facies signal. The application of a statistical analysis, aimed to strengthen pollen groups definition (facies indicators *versus* climate indicators), and the accurate facies characterization of the Holocene succession of core EM2 allowed the identification of a series of cooling events, consistently dated through an age-depth model based on thirteen radiocarbon ages. The observed vegetation-climate variability fits well with Bond's events, especially for the early-mid Holocene time window (i.e., Preboreal and Boreal Oscillation, 8.2 ka event), supporting a strong Mediterranean–North Atlantic climate connection. In particular, the most prominent vegetation change coincides with the well-known 8.2 ka cooling event. This finding represents the first description of the 8.2 ka event from the Adriatic continental record in terms of combined vegetation patterns and related depositional dynamics.

Arno delta plain (Chapter 6):

Research topic 3: *Palynological characterization of Late Quaternary stratigraphic cyclicity and sequence stratigraphic implications (section 6.1).* The shallow subsurface (30 m) of the southern portion of the Arno delta plain was investigated following the same methodological approach applied to the freshwater coastal succession of the Po Plain. Here, a distinctive stratigraphic cyclicity formed by alternating lagoon and alluvial deposits characterizes the 31.5 m-long core PA1, located ca. 8 km landward from the modern coastline. With the aim to assess the palaeoenvironmental, palaeoclimatic and chronological signature of these depositional cycles, palynological data, enriched by Bryophyte spores, were integrated with sedimentological features and four radiocarbon dates. Eight Bio-Sedimentary Units (BSU) and four Vegetation Phases (VP) were identified. The main palynological turnarounds along the cored succession reveal a synchronised cyclicity of palaeoenvironments and vegetation cover under the predominant forcing

of late Quaternary climatic-eustatic changes at the scale of glacial-interglacial (~100 ka) alternations. In terms of sequence stratigraphy, two T-R cycles were defined and their transgressive portions invariably associated to lagoon deposits formed during two consecutive interglacials (MIS 5e, identified for the first time in the Arno plain, and MIS 1). Palynological and sedimentological features of the regressive portions of T-R cycles highlighted strongly different evolutionary trends: the late Pleistocene lagoon turned into an interfluvial area characterised by widespread pedogenesis under glacial conditions, whereas the Holocene lagoon evolved into a delta plain at the end of the climate optimum.

Research topic 4: *High-resolution record of palaeoclimate-palaeoenvironmental trends within the MIS 5-MIS 1 interval (section 6.2).* Sixteen additional samples were collected for palynological analysis along core PA1, with a focus on lagoon intervals and palaeosol horizons. Cluster analysis highlighted five main vegetation types (pollen-derived biomes), each one related to peculiar environmental conditions and constrained to single stratigraphic intervals. Palynological analyses, strengthened by statistics, allowed: *i)* the detailed facies characterization of a suite of brackish and alluvial deposits; *ii)* the in-depth differentiation of the two interglacials in terms of mediterraneity and moisture availability; *iii)* the identification of high-resolution landscape dynamics during lagoon formation and filling across different glacio-eustatic contexts (forced regression *versus* progradation); *iv)* the identification of an almost synchronous response of coastal environments to vegetation-derived climate forcing at sub-Milankovitch timescales.

Chapter 7: *Comparison of the Arno and Po delta records.* Despite the stratigraphic and chronological discrepancies between the two records, their comparison supported *ad hoc* by other palynological data available in literature allowed to outline similar palaeoenvironmental / climatic features for the time interval covering the last two interglacials. Indeed, at the glacial-interglacial timescale the macro-climatic conditions seem to affect both areas in the same way, whereas at the interglacial timescale (mostly evident during the Holocene) the vegetation communities respond differently as warmer conditions characterise the Arno Plain. However, short-lived, lower-intensity climate variations (i.e., the 8.2 ka event and mid Holocene events) are invariably recorded by palynological changes indicative of cooler and more humid conditions. Reasonably, this complex scenario is ascribable, at least partly, to the present-day climatic separation of a sub-mediterranean (Po Plain) from a meso-mediterranean (Arno Plain) climate operated by the Northern Apennines "barrier", and the peculiar climate teleconnections of the latitude zone 40-43°N with the Boreal Hemisphere's dynamics. Minor differences encountered within the late Holocene hygrophilous

woodlands, especially in terms of relative proportion between *Alnus glutinosa* and *Salix*, could reflect the establishment of different deltaic environments at the two study sites. A low level of disturbance due to human presence is documented within both records for the last ca. 2 cal. kyr BP.

5. PALYNO-STRATIGRAPHIC RECORD OF THE PO DELTA PLAIN

5.1 Manuscript 1

Palynological characterization of the Po delta succession (northern Italy): Holocene vegetation dynamics, stratigraphic patterns and palaeoclimate variability*

Marco Cacciari, Veronica Rossi, Marco Marchesini, Alessandro Amorosi, Luigi Bruno, Bruno Campo

PALYNOLOGICAL CHARACTERIZATION OF THE PO DELTA SUCCESSION (NORTHERN ITALY): HOLOCENE VEGETATION DYNAMICS, STRATIGRAPHIC PATTERNS AND PALAEOCLIMATE VARIABILITY

Marco Cacciari [1], Veronica Rossi [1], Marco Marchesini [2], Alessandro Amorosi [1], Luigi Bruno [1], Bruno Campo [1]

1 Department of Biological, Geological and Environmental Sciences, University of Bologna, Bologna, Italy
2 Laboratorio di Palinologia e Archeobotanica - C.A.A. Giorgio Nicoli, San Giovanni in Persiceto, Bologna, Italy
Corresponding author: M. Cacciari <marco.cacciari3@unibo.it>

ABSTRACT: The 40 m-long core EM2, recovered in the innermost portion of Po delta plain, was sampled for palynological analysis, in order to link coastal-deltaic facies architecture to vegetation dynamics and Holocene climate variability. Pollen data refine facies characterization of the 25 m-thick Holocene succession: freshwater swamp clays alternating with overbank/channel sands document millennial to centennial-scale water table oscillations that invariably peak in correspondence of peaty layers. Pollen signature allows identification of the landward equivalent of the Maximum Flooding Surface atop the 7.6 ka-dated peaty interval and furnishes new insights on the relationship between coastal facies patterns and climate events.

KEYWORDS: Palynology, Holocene, Po delta plain, climate events, sequence stratigraphy

1. INTRODUCTION

Mediterranean delta plains are considered natural archives of the interactions between Holocene depositional, climate and human dynamics. In these regions, the combined effect of high sea-level conditions, remarkable rates of subsidence and sediment supply led to the deposition of stratigraphically expanded, relatively continuous fine-grained sedimentary successions, useful for high-resolution palaeoenvironmental and stratigraphic reconstructions.

The Po delta plain is one of the most studied Mediterranean deltas. A detailed characterization of sedimentary facies and a high-resolution sequence-stratigraphic framework (with the identification of a set of millennial-scale parasequences) is available for the 10-30 m-thick Holocene succession (Amorosi et al., 2017). However, the relationships between parasequence development and the well-known millennial-scale climate variability (Bond's events *sensu* Bond et al., 1997) are still matter of debate. Furthermore, palynology is a relatively unexplored stratigraphic tool for the identification of flooding surfaces within successions devoid of marine-influenced facies. Through an integrated palynological-stratigraphic approach, this study aims to reconstruct post-glacial stratigraphic patterns at the landward margin of the Po Delta and to unravel their relations with Holocene climate events.

2. MATERIAL AND METHODS

A 40 m-long core, recovered in the innermost portion of the Po delta plain (core EM2), was selected for palynological analysis, being composed of a ~25 m thick, chronologically well constrained (9 radiocarbon ages) paludal succession, framed into a robust stratigraphic context and dated to last ~13 ka (Amorosi et al., 2017; Bruno et al., 2017). Thirty-seven samples were collected, with special focus on organic-rich, fine-grained intervals, where a rich palynological association was expected. About 3-9 g of dry sediment per sample were weighed and then a *Lycopodium* tablet was added to calculate pollen concentration. Samples were mechanically disrupted in a 10% Na-pyrophosphate solution and filtered. Then, each sample underwent the following treatments: 10% HCl solution, acetolysis, enrichment with a heavy liquid, 40% HF solution, ethanol suspension and evaporation at 60 °C. Finally, microscope slides were prepared with glycerine jelly and paraffin. For each sample, at least 300 grains were counted and recognised after Reille (1992). Species ecological characterisation and pollen groups were based on Pignatti (1982, 2017). On the other hand, non-arboreal pollen (NAP) was split into herbaceous plants (H) and shrubs (sh) to better estimate the canopy thickness.

3. POLLEN SEQUENCE

The EM2 pollen spectra reported in Fig. 1 confirm the persistence, at the study site, of freshwater conditions throughout the Holocene (absence of halophytes) and highlight the vertical succession of fifteen Pollen Zones-PZs that correspond to distinct vegetation phases. In particular, a series of Lateglacial-Holocene climatic events were identified by combining high-frequency changes in relative abundance of specific pollen groups (Fig. 1) with the available radiocarbon ages. All these events are marked by relative peak concentrations of montane trees-MT (6-10%) and/or cold steppe taxa-CST (3-8%), indicative of sudden cooling, sharply followed by
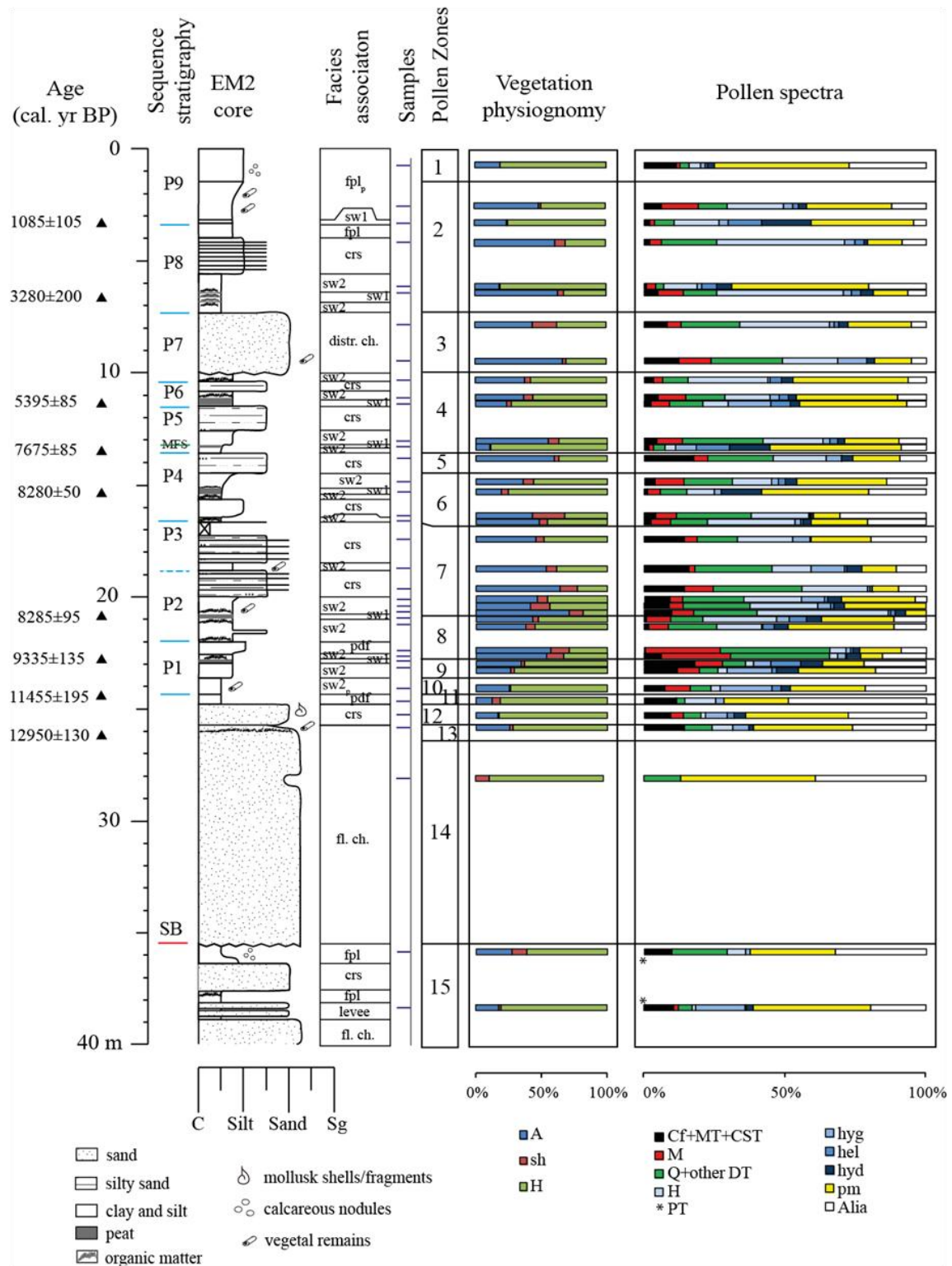
Fig. 1 - Sedimentology and pollen characteristics of core EM2: PT (Pleistocene taxa), Cf (conifers) MT (montane trees), CST (cold steppe taxa), M (Mediterranean trees), Q+other DT (mixed-oak forest and other deciduous trees), H (woody hygrophytes), hyg (herbaceous hygrophytes), hel (helophytes), hyd (hydrophytes), pm (pasture-meadow). Facies: fl. ch. (fluvial channel), distr. ch. (distributary channel), crs (crevasse splay), fpl (floodplain), pdf (poorly-drained floodplain), sw (swamp). The "p" subscript indicates a weakly pedogenised deposit. PS: parasequence (light blue lines are parasequence boundaries; dotted lines indicate minor flooding surfaces). MFS: Maximum Flooding Surface. SB: Sequence boundary from Bruno et al. (2017).

high percentages of climate optimum indicators (i.e., holm oak-mixed-oak forest, M-Q+other DT) within a relatively continuous stratigraphic interval, a few tens of centimetres thick. Along the core, conifers show similar vertical variations relative to MT+CST and, thus, were interpreted as a regional pollen rain, analogous to the cold indicators *sensu stricto.*

The oldest cold spell (PZ 13), chronologically attributed to the Younger Dryas event, occurs within the uppermost portion of the fluvial channel succession deposited under Glacial-Lateglacial conditions (Amorosi et al., 2017; PZs 14-13) and observed between ~35.5-26 m core depth (Fig. 1).

The overlying, 25 m-thick sedimentary succession, composed of alternating swamp clays and overbank/channel sands is assigned to the Holocene period, based on combined radiocarbon ages and pollen data (PZs 12-1), the latter reflecting an overall climate-optimum-like vegetal landscape. However, three distinct phases of rapid cooling are recognised and reasonably ascribed to the Preboreal Oscillation (PZ 11), Boreal Oscillation (PZ 9) and 8.2 ka event (PZ 7), respectively. More uncertain are dating and interpretation of other two cooling events recorded by PZs 5 and 3.

Finally, a relatively high concentration of MT and CST (7% total), paralleled by a sharp decrease in holm oak (from 13% to 1%), is recorded at the top (1 m) of the cored succession, within pedogenized floodplain deposits, possibly documenting the Little Ice Age event.

4. HOLOCENE VEGETATION DYNAMICS AND FACIES STACKING PATTERNS

The palynological analysis also refines facies characterization, especially of fine-grained deposits, allowing the distinction between poorly drained floodplain facies, characterised by the absence or scarcity of helophytes and hydrophytes, and swamp clays. Moreover, two types of swamp deposits were identified within the Holocene succession on the basis of the relative abundances of woody and herbaceous hygrophytes, helophytes and hydrophytes:

- *Peaty swamp* **(sw1)**: herbaceous wetland community with sparse alder carrs tolerating prolonged periods of radical drowning (helophytes) or aquatic plants (hydrophytes); subordinate hygrophytes, Poaceae and alder (mixed or not) bordering the locally flooded depressions. This pollen assemblage, invariably recorded within peaty layers (~10-30 cm thick), indicates relatively high water table conditions.
- *Swamp* **(sw2)**: open to dense alder carr with a mixed oak-holm oak ecological component in subordinate position. This pollen assemblage, found within organic-rich grey to dark grey clays, documents a relatively low water table.

Throughout the Holocene succession, sw1 peats are vertically constrained between sw2 clays, which in turn are commonly overlain by crevasse splays or distributary-channel sandy deposits containing a pollen assemblage indicative of a hygrophilous, open to dense mixed oak-holm oak forest. This repeated stacking pattern of facies tracks short-term (millennial to sub-millennial scale) oscillations in the relative water table,

allowing the identification of small-scale, T-R depositional cycles (i.e., parasequences bounded by flooding surfaces-FSs) in a fully freshwater sequence.

Specifically, each cycle is composed of basal sw2 grey-dark grey clays, commonly showing an upward increase in dispersed organic matter, and culminates into a peaty interval (sw1 that reflects the most drowned conditions). Upwards, a shallowing-upward trend is identified by pollen data, marking the progradational part of the parasequence (PS).

Furthermore, an overall increase in water table was recorded from the oldest swamp (dated around 11455±195 cal yrs BP) to the swamp recorded at ~13.35 m core depth and dated to 7675±75 cal yrs BP. This deepening-upward trend is considered as the sedimentary expression of the Maximum Flooding Surface - MFS at proximal locations. Upwards, swamps generally show less developed peat accumulation and a lower water table relative to the underlying transgressive swamps.

5. DISCUSSION AND CONCLUSIONS

Diagnostic changes in vegetation patterns enable the precise documentation of parasequence development at the landward margin of the Po delta plain during the Holocene. Therefore, because of the absence of meiofauna and molluscs in this freshwater paludal succession, the sequence-stratigraphic refinement at a millennial – sub-millennial scale was performed by palynological analysis.

Throughout core EM2, the relative abundances of woody and herbaceous hygrophytes, helophytes and hydrophytes record alternating periods of rising water table (i.e., flooding events), which peak in correspondence of cm to dm-thick peaty swamp intervals (i.e., the most drowned conditions within each PS), and which subsequently decreases. The highest relative water table was reached atop the peaty swamp deposit belonging to PS 4 and dated to ~7600 cal yrs BP (Fig. 1), which separates a set of transgressive parasequences from the highstand ones. Highstand parasequences are characterised by the development of peaty swamp intervals under lower water table conditions, reflecting the general progradation of the Po Delta system during the mid-late Holocene. These data, supported by the chronological and the stratigraphic frameworks available for the entire study area (Amorosi et al., 2017; Bruno et al., 2017; Campo et al., 2017), suggest a strong allogenic control (i.e., glacio-eustatic oscillations at the Milankovitch time-scale) on depositional dynamics ca. 35 km upstream from the modern coastline.

A unique exception is the uppermost peaty layer, recorded at 3 m core depth and dated to ~1000-1100 cal yrs BP, which reflects the local establishment of a high water table possibly related to the historical Po River avulsion in Ficarolo. The northward shift of the Po River system and the subsequent marked reduction in sediment supply reasonably induced the flooding of the southern portion of the subsiding Po delta plain, where EM2 core was recovered.

The comparison between stratigraphic and pollen-derived climatic data documents a complex interaction

between parasequence development and Holocene climate events. Not all peats (sw1-peaty swamps) developed under mild conditions, suggesting the influence of other driving mechanisms, such as early Holocene eustatic jumps (MWP-Melt Water Pulse) and autogenic factors. On the other hand, the thick alluvial successions in the uppermost portions of PSs 2, 3 and 6 saw the development of cool-temperate communities, the eldest of which was chronologically constrained to the 8.2 ka event. As a whole the three PSs suggest a strong sedimentary response to these short-term phases of climatic cooling in terms of increased sedimentary input and partial filling of paludal basins.

ACKNOWLEDGEMENTS

REFERENCES

Amorosi A., Bruno L., Campo B., Morelli A., Rossi V., Scarponi D., Hong W., Bohacs K. M., Drexler T. M. (2017) - Global sea-level control on local parasequence architecture from the Holocene record of the Po Plain, Italy. Marine and Petroleum Geology, 87, 99-111.

Bond G., Showers W., Cheseby M., Lotti R., Almasi P., deMenocal P., Priore P., Cullen H., Hajdas I., Bonani G. (1997) - A pervasive millennial-scale cycle in North Atlantic Holocene and glacial climates. Science, 278, 1257-1266.

Bruno L., Bohacs K.M., Campo B., Drexler T.M., Rossi V., Sammartino I., Scarponi D., Hong W., Amorosi A. (2017) - Early Holocene transgressive palaeogeography in the Po coastal plain (Northern Italy). Sedimentology, 64, 1792-1816.

Campo B., Amorosi A., Vaiani S.C. (2017) - Sequence stratigraphy and late Quaternary paleoenvironmental evolution of the Northern Adriatic coastal plain (Italy). Palaeogeography, Palaoclimatology. Palaeoecology, 466, 265-278.

Pignatti S. (1982) - Flora d'Italia. Edagricole, Bologna, Italy

Pignatti S. (2017) - Flora d'Italia, 1-2. Edagricole, Bologna, Italy

Reille M. (1992) - Pollen et spores d'Europe et d'Afrique du nord. Laboratoire de Botanique Historique et Palynologie, Marseille, France, pp. 331.

5.2 Manuscript 2

High-resolution record of Holocene palaeoclimate variability and depositional trends from freshwater coastal successions *

Marco Cacciari, Alessandro Amorosi, Marco Marchesini, David Kaniewski, Luigi Bruno, Bruno Campo, Veronica Rossi
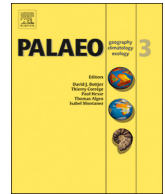
Linking Holocene vegetation dynamics, palaeoclimate variability and depositional patterns in coastal successions: Insights from the Po Delta plain of northern Italy

Marco Cacciari[a,*], Alessandro Amorosi[a], Marco Marchesini[b], David Kaniewski[c], Luigi Bruno[d], Bruno Campo[a], Veronica Rossi[a]

[a] Dipartimento di Scienze Biologiche, Geologiche e Ambientali, University of Bologna, via Zamboni 67, 40127 Bologna, Italy
[b] Department of Human and Social Sciences, University of Ferrara, via Ercole I d'Este 32, 44121 Ferrara, Italy
[c] Université Paul Sabatier-Toulouse 3, EcoLab (Laboratoire d'Ecologie Fonctionnelle et Environnement), 118 Route de Narbonne, 31062, Toulouse, cedex 9, France
[d] Department of Chemical and Geological Sciences, University of Modena, via Campi 103, 44125 Modena, Italy

ABSTRACT

Mediterranean deltaic-coastal plains represent relatively underexplored depositional archives that record the Holocene response of vegetation and depositional systems to high-frequency climate changes. In this study, we examine a 25 m-thick succession of Holocene age (core EM2) recovered in the innermost portion of the Po delta plain of northern Italy, applying an integrated palyno-stratigraphic approach. The existence of a paludal, freshwater setting inland of the line of maximum marine transgression favoured a low degree of pollen trans-portation. Application of cluster analysis to this palynological record leads to the identification of pollen-derived biomes and seven (auto)ecological groups of taxa that discriminate environmental signal (depositional facies) and regional climate conditions within a well-dated coastal record. Percentage variations of hygrophytes, aquatics and pasture-meadow herbs reveal local environmental dynamics, enabling the detailed facies char-acterisation of the cored succession, especially in terms of water table conditions. Framed into a chronologically constrained, high-resolution facies context, the proportion of montane taxa (climate degradation indicator) relative to Mediterranean taxa and *Quercus* + other deciduous trees (climate optimum indicators) highlight a vegetation-climate variability in the plain that fits with Bond events, especially for the early-mid Holocene (i.e., Preboreal and Boreal Oscillation, 8.2 ka event), supporting a strong Mediterranean–North Atlantic climate connection. For the first time, pollen from a continental succession of the Adriatic area clearly depicts the effects of the 8.2 ka cooling event on vegetation patterns (progressive degradation in high altitude communities) and depositional dynamics (increased fluvial activity), assessing the major role played by climate changes in shaping coastal landscapes in addition to glacio-eustatic variations.

1. Introduction

The diversity of palaeoclimate proxies (e.g., microfossils, molluscs, stable isotopes), the abundance of effective dating techniques (e.g., radiocarbon and other radiometric dating, amino acid racemization), and the temporal proximity to the Present have made the climate variability of Marine Isotope Stage-MIS 1 (ca. last 15 kyr) a focus of research in recent decades (e.g., Sangiorgi et al., 2003; Magny et al., 2007; Giraudi et al., 2011; Scarponi et al., 2017; Bini et al., 2019; Di Rita and Magri, 2019). Since the pioneer works of Bond and colleagues on the North Atlantic deep-sea successions (the well-known "Bond events"; Bond et al., 1997, Bond et al., 2001; Walker et al., 2018) and

the review by Mayewski and colleagues on the Holocene record (Rapid Climate Changes-RCC; Mayewski et al., 2004), the millennial to sub-millennial climate oscillations of MIS 1 and related environmental-de-positional responses have attracted increasing interest (Benito et al., 2015a, 2015b; Di Rita et al., 2015; Sarti et al., 2015; Styllas and Ghilardi, 2017; Roberts et al., 2019 among others). Special emphasis has been placed on the origin, geographical distribution, amplitude and characterisation of three major events during this period (Younger Dryas, 8.2 ka and 4.2 ka), corresponding to the chronostratigraphic limits of the Holocene subseries (Lower, Middle and Upper Holocene; Walker et al., 2012, 2018). However, several other short-term events have been identified across the globe (i.e., Preboreal and Boreal

---

Oscillations; Little Ice Age among others) and highlight a high-frequency climate variability for different regions and latitudes (e.g., Feurdean et al., 2007; Vannière et al., 2011; Magny et al., 2013).

In such a complex scenario, pollen is considered one of the most powerful palaeoclimate proxies because of its high degree of preservation (Faegri et al., 1989; Moore et al., 1991) and its capacity to furnish detailed (vegetation-derived) reconstructions. For the Mediterranean area, millennial-scale palaeoclimate patterns have been revealed mainly by a variety of lacustrine and marine pollen records (e.g., Peyron et al., 2011, 2013; Magny et al., 2012). However, pollen records from the Adriatic region very seldom encompass the whole MIS 1 (e.g., Di Rita and Magri, 2009; Magny et al., 2009; Mercuri et al., 2012; Ravazzi et al., 2013; Cremaschi et al., 2016; Pini et al., 2016; Badino et al., 2018) because of either local environmental conditions (e.g., lake formation and damming) or anthropic presence (e.g., archaeological sites), with the unique exception of a south Adriatic marine core (Combourieu-Nebout et al., 2013). Despite an abundance of relatively continuous, tens of meters thick paludal successions (Amorosi et al., 2017a), prone to preserve palynomorphs (Cacciari et al., 2018), and thorough understanding of present-day vegetation landscapes (Tomaselli, 1970; Pignatti, 1979, 1998; Ferrari, 1980, 1997), the Holocene coastal succession of the modern Po delta plain (North Italy; Fig. 1) represents a relatively underexplored depositional archive to probe vegetation-palaeoclimate reconstructions. In this area, the availability of robust, high-resolution chronological and sequence-stratigraphic frameworks (i.e., Amorosi et al., 2016, 2017a, 2017b; Bruno et al., 2017; Campo et al., 2017) makes these deposits an ideal archive to investigate climate-related palaeoenvironmental variations.

The main purpose of this work is to document the possibility of filtering the local (facies) vegetation signal from the regional (climate) record, relying upon a continuous Holocene pollen record from an unconventional (i.e., non-lacustrine and non-marine) succession of the Po delta plain (core EM2; Fig. 1), whose general palynological features (i.e., relative percentages of groups of taxa) have been published in Cacciari et al. (2018). More specifically, through an integrated, high-resolution stratigraphic-palynological approach supported by the application of statistical analyses, we aim to: i) obtain new data on vegetation-climate dynamics of the Adriatic area, verifying the timing and effects of North Atlantic climate oscillations (i.e., Bond's events), and ii) furnish insights into the effects of Holocene climate variability on the depositional dynamics of deltaic-coastal plain systems.

2. Study area

2.1. Geological setting and Quaternary stratigraphic framework

The Po delta plain is a wide flat area (ca. 3000 km^2) with around 1550 km^2 lying below mean sea level (Bondesan et al., 1995; Correggiari et al., 2005). It includes the modern Po Delta, a mixed, river- and wave-influenced system formed during the last 2 kyr (Amorosi et al., 2008; Rossi and Vaiani, 2008; Maselli and Trincardi, 2013) and the southern coastal plain occupied by palaeodelta lobes that were active between ca. 7.0–2.0 BP (Fig. 1; Stefani and Vincenzi, 2005; Amorosi et al., 2019). At the basin scale, the Po delta plain constitutes the eastern portion of the broader Po Plain, which is the surficial expression of the peri-sutural Po Basin delimitated by the Alps to the
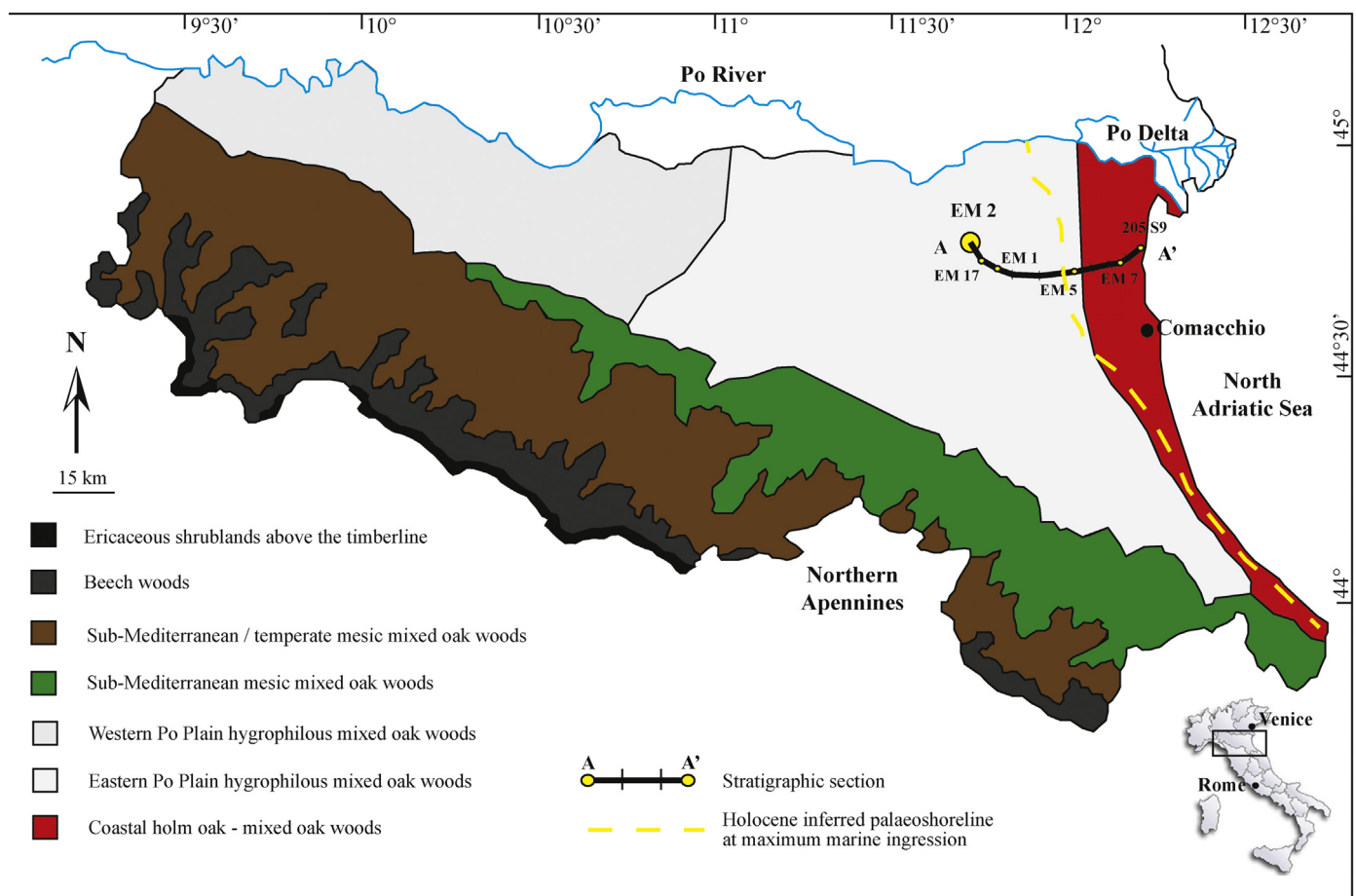
Fig. 1. Location map showing the vegetation zonation of the Emilia-Romagna region of northern Italy (partly redrawn after Ferrari, 1997 and Regione Emilia-Romagna, 1996) and location of core EM2. The inferred position of the Holocene maximum marine ingression is also shown (slightly modified from Correggiari et al., 2005 and Bruno et al., 2017). (For interpretation of the references to colour in this figure legend, the reader is referred to the web version of this article.)

north-west and by the N Apennines to the south. To the east, the Po Plain is bounded by the Adriatic Sea, a narrow (ca. 200 × 800 km) semi-enclosed epicontinental basin elongated in NW-SE direction and sandwiched between the Italian peninsula and the Balkans. As a whole, the Po Plain-Adriatic Sea system is part of the Alpine-Apennine and Dinarides-Hellenides foreland, shaped by the convergence between the European and African plates (Doglioni, 1993; Boccaletti et al., 2011). The infilling succession of the Po Basin records an overall "regressive" trend, from Pliocene deep-marine to Pleistocene-Holocene continental and coastal deposits (Ricci Lucchi et al., 1982; Regione Emilia-Romagna and Eni-Agip, 1998). The Middle Pleistocene-Holocene succession shows the repeated vertical stacking of transgressive-regressive (T-R) depositional cycles, composed of shallow marine, coastal and alluvial deposits accumulated under a predominantly glacio-eustatic control (Milankovitch 100 kyr-cycles; Amorosi et al., 2004, Lobo and Ridente, 2014). In the southern Po coastal plain, palynological analyses further support a climate control on facies architecture, as wedge-shaped coastal bodies identified between ca. 0–30 m and 100–130 m depths record phases of forest expansion associated with the last two interglacials (MIS 1 and MIS 5e, respectively). By contrast, the tens m-thick alluvial succession that separates these two nearshore bodies documents a fall in the arboreal cover and the presence of cold climate indicators, pointing to the MIS 5d-MIS 2 glacial period (Amorosi et al., 2004; Campo et al., 2017).

Recent studies (Amorosi et al., 2017a, 2019; Bruno et al., 2017) have placed the Holocene succession into a high-resolution sequence-stratigraphic framework. Above the Younger Dryas palaeosol, a prominent stratigraphic marker demarcating the transgressive surface (TS), eight parasequences (PSs) were identified (Fig. 2) based on integrated sedimentological, palaeontological (molluscs, benthic foraminifers and ostracods) and radiocarbon data. Early Holocene parasequences (PSs 1–3 in Fig. 2) are organised into a retrogradational pattern reflecting alternating periods of rapid flooding and gradual shoaling into the Po estuary, developed under the predominant control of the postglacial eustatic rise (Bard et al., 1996; Vacchi et al., 2016). By contrast, an aggradational to progradational set of mid-late Holocene parasequences (PSs 4–8 in Fig. 2) mostly controlled by changes in sediment supply, subsidence and autogenic mechanisms records the transition from a wave-dominated to a river-dominated delta system.

2.2. Present-day vegetation and climate

The study area belongs to the Emilia-Romagna (ER) region (Fig. 1) characterised by a sub-Mediterranean climate, broadly diffused throughout North and Central Italy. The annual precipitation sum is up to 778 mm/yr and decreases during summer, with minimum values in July and August. The mean annual temperature (13.2 °C) and thermal excursion (ca. 22 °C between July–January means - 23.8 °C and 2 °C, respectively) suggest a certain degree of continentality (Bologna site; Ubaldi, 2003). The vegetation landscape reflects mixed influences, as the study area is located at the southern margin of the Central European phytogeographic region, adjacent to the Mediterranean area (Tomaselli, 1970; Pignatti, 1979, 1998). The boundary between these two regions is sharp along the Apennine ridge but becomes blurred in the east (Ferrari, 1997), where coastal vegetation occurs as a mix of Central European and euri-Mediterranean taxa. The present vegetation changes not only along a longitudinal gradient (distance from the Adriatic Sea), but also along an altitudinal one (lowlands versus mountains). In order to assess the complex dynamics of vegetation communities, the concept of Potential Natural Vegetation (PNV) by Tüxen (1956) will be hereafter adopted. Though still debated (Carriòn and Fernandez, 2009; Chiarucci et al., 2010), PNV has been extensively used by several authors (Blasi et al., 2014; Hengl et al., 2018), who stressed its importance in defining both modern and past vegetation landscapes dynamics. As a whole, three main vegetation belts were identified and can be described as follows (Fig. 1; Ferrari, 1997):

a) *Ericaceous dwarf shrublands above the timberline (ca. 1800 m above sea level-a.s.l.)*: this vegetation belt is discontinuous across ER and absent in its south-eastern portion, due to lower altitudes. The vegetation is similar to the one in the Western and Central Alps (order *Rhododendro – Vaccinietalia* Braun Blanquet 1926) but impoverished in species, as it commonly occurs at the edge of geographic ranges. Since no extensive fir and/or spruce woods occur on the Apennines, the boundary between ericaceous dwarf shrublands and beech woods (Fig. 1) should be considered a real ecotone (Chiarugi, 1958).

b) *Beech woods*: beech forests occupy a relatively wide and continuous area from NW to SE, extending from 800 to 1000 m a.s.l. up to the timberline, with the exception of relict fir/spruce woods on the slopes of refugial valleys. This belt includes several species
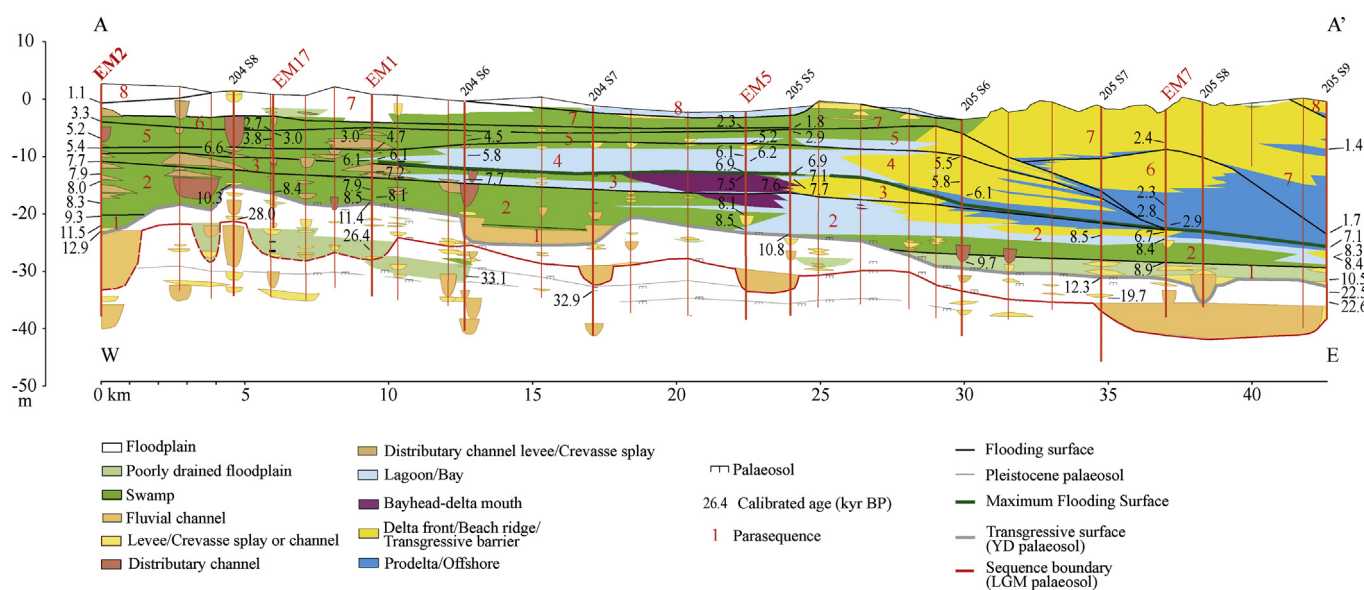
Fig. 2. Reference stratigraphic section A-A', slightly modified from Bruno et al. (2017), showing the Holocene depositional architecture of the Po delta-coastal plain. The transgressive barrier sands belonging to PS 3 mark the Holocene maximum marine ingression in Fig. 1. Key EM cores are highlighted in red; core EM2 is in bold. (For interpretation of the references to colour in this figure legend, the reader is referred to the web version of this article.)

belonging to the *Quercetum-* (*Fraxinus excelsior, Tilia platyphyllos, Ulmus glabra*) and the montane PNV (*Abies alba* and *Fagus sylvatica*), consistent with the altitude-dependent bioclimatic gradient.

c) *Mixed mesic oak woods*: as part of the *Querco – Carpinetum boreoitalicum* (Pignatti, 1953), these forests form a wide vegetation belt extending from 0 to 800 m a.s.l. that represents the Po Plain PNV (Ferrari, 1997; Pignatti, 1998). Lowland communities differ slightly from those living on the hills because of the widespread presence of humid environments. However, intense human activity has almost completely destroyed these mesophilous oak forests (Cattaneo, 1844). Seawards, on stable sand dunes along the coast, a community dominated by *Quercus ilex, Fraxinus ornus, Asparagus acutifolius* and *Pyracantha coccinea* occurs. A similar vegetation dominated by *Quercus robur, Q. ilex* and *Carpinus betulus* characterises the oldest dunes. In particular, the presence of the holm oak marks the shift from a sub-Mediterranean climate inland to a more Mediterranean one along the coast. Both communities belong to the alliance *Ostryo – Carpinion orientalis* (Horvat 1959) and represent the North Adriatic coastal form of mixed oak woodlands, which are still present in the Balkans and on the Adriatic side of the central Apennines.

Focusing on the local vegetation, the study area belongs to the Po Plain Province (ecoregions of Italy sensu Blasi et al., 2014) - Lagoon Subsection spanning about 70 km from the coastal portion of the Venetian Plain, down to the Comacchio lagoons (Fig. 1). It is mainly characterised by cultivated areas (ca. 77%, mostly *Triticum* and *Beta*).

3. Methods

In order to isolate the signal related to the depositional setting from regional climate conditions, integrated palynological and stratigraphic analyses were undertaken on a long (ca. 25 m) fine-grained succession of Holocene age, recovered in the innermost portion of the Po delta plain (core EM2; Fig. 1). Its location, ca. 25 km landward of the palaeoshoreline at the time of Holocene maximum marine ingression (Fig. 2), strongly limits the influence of marine pollen transportation according to the extreme scarcity (0–3%) of halophytes (i.e., *Artemisia* and *Beta*) already highlighted by Cacciari et al. (2018).

3.1. Core sedimentology and chronology

The 40 m-long core EM2 (44°48′ 28"N; 11°47′ 2.5″ E; Fig. 1) was recovered at 2.7 m a.s.l. by a continuous perforating system, which guaranteed an undisturbed stratigraphy and a high recovery percentage (> 90%). The core was split lengthwise and carefully described in terms of grain size, sedimentary structures, colour, organic-matter content (peat or decomposed organic matter-rich layers), stratigraphic contacts and other materials (i.e., sparse vegetation remains, calcareous and Fe−Mn nodules) in order to identify the main lithofacies. The abundance of organic-rich, peaty deposits supports a high-resolution, radiocarbon-based chronological analysis of the studied succession. Radiocarbon dating on 13 samples was performed at KIGAM laboratory (Daejon City, Republic of Korea) on wood, plant fragments and peats collected between ca. 3–25.50 m core depth (Table 1). The calibration of conventional radiocarbon ages is based on the IntCal13 dataset (Reimer et al., 2013) using OxCal 4.2. (Bronk Ramsey, 2009). All ages are expressed in 2-sigma calibrated years BP. The age-depth model was constructed using a smoothing spline function in PAST (PAlaeontological STatistic – version 3.10 by Hammer et al., 2001). Differential sediment compaction was not taken into account, thus sedimentation rates were estimated on the basis of radiocarbon ages.

3.2. Palynological analyses

Thirty-five samples from the uppermost 25 m were collected for palynological analysis. All lithofacies were analysed with a special focus on organic-rich intervals, where abundant palynological assemblages were expected. Samples were prepared and analysed at "*Centro Agricoltura e Ambiente – CAA G. Nicoli*" laboratory (Italy), following a standard extraction technique (Lowe et al., 1996): about 3–9 g of dry sediment were weighed and a *Lycopodium* tablet was added to calculate pollen concentration. Samples were mechanically disrupted in a 10% Na-pyrophosphate solution and filtered through a 0.5 mm sieve and a 5 μm nylon filter. A series of chemical treatments was then applied (10% HCl solution to remove carbonates, acetolysis for excess organics, heavy liquid, 40% HF solution, ethanol suspension for pollen grains enrichment). Following evaporation at 60 °C, microscope slides were prepared with glycerine jelly and paraffin. For each sample, at least 300 pollen grains were counted (where possible) at 400× magnification and recognised using general morphological keys (Faegri et al., 1989; Moore et al., 1991). The CAA laboratory's collection and published atlases (Reille, 1992, 1995, 1998) were also useful to improve pollen determination. If the conservation degree and orientation (i.e., polar or equatorial view) of grains were favourable, a set of morphological parameters published in literature were used for the determination at species level of alders, oaks, pines and Asteroideae (SOM-S1). If this was not possible, the conservative choice of the higher taxonomical level was made to avoid mis/overinterpretation.

Pollen percentages were calculated on the basis of the total pollen sum. Percentages of Pteridophytes, undeterminable and reworked grains were calculated on the total sum of pollen grains and themselves, a method allowing a correct weighting of their presence (Berglund and Ralska-Jasiewiczowa, 1986).

Species ecological characterisation was based on Tomaselli (1970, 1987), Pignatti (1979, 1982, 2017), Ferrari (1980, 1997), Berglund and Ralska-Jasiewiczowa (1986), Tutin et al. (1993), Accorsi et al. (1999, 2004), Bertoldi (2000), Ubaldi (2003) and Pini et al. (2016).

3.3. Statistical analysis

Following Tarasov et al. (1998) and Kaniewski et al. (2011), we performed statistical analyses to highlight pollen-derived vegetation biomization and support the identification of pollen groups. Spermatophyte and Pteridophyte taxa were calculated in PAST and grouped using Cluster Analysis. Correlation was used as similarity method to explore the temporal proximity of taxa in a facies-heterogeneous stratigraphic succession, while Paired group was used as the root by suggesting the local provenance of all identified taxa. In order to streamline the data and obtain the most informative groups, sixty occasional taxa, recorded in less than three samples with percentages lower than 1%, were excluded. The robustness of this choice was tested by running several analyses using different selections of taxa. The resulting clusters, obtained from a final matrix of 141 taxa, allowed the identification of pollen-derived biomes (PDBs) whose ecological distance is reflected by the branches on the tree diagram (Kaniewski et al., 2011). The use of present-day ER altitudinal-longitudinal vegetation belts (Fig. 1) as a reference for past associations reasonably suggests that PDBs should not be considered as separate vegetation types but, rather, as groups of plants that can thrive or decrease at the same time close to the sample site (i.e., groups of taxa that were site-dependently found together).

4. Results

4.1. Pollen data

Pollen data from core EM2 reveal a high floristic richness. Specifically, 189 taxa were identified at different taxonomic levels and raw counts are available at Mendeley Data. Consistent with the organic-rich nature of sediments, the state of preservation of pollen grains is good and the number of undeterminable grains varies from 0% to ca. 15%. The relative abundance of secondary grains reworked from older successions is generally lower than 10%.

Table 1
List of radiocarbon dated samples from core EM2.

Sample core depth (m)	Dated material	¹⁴C conventional age (yr BP)	Calibrated yr BP - 2σ range interval	Calibrated yr BP – 2σ mean value ± error	Reference
3.20	Wood	1180 ± 40	1185–980	1085 ± 105	Amorosi et al., 2017a
6.45	plant fragment	3110 ± 80	3485–3075	3280 ± 200	Amorosi et al., 2017a
9.45	Wood	4480 ± 30	5240–5035	5170 ± 85	This study
11.10	Plant fragment	4680 ± 40	5480–5315	5395 ± 80	Amorosi et al., 2017a
13.35	Plant fragment	6840 ± 40	7760–7590	7675 ± 85	Amorosi et al., 2017a
14.65	Wood	6630 ± 40	7575–7440	7520 ± 35	This study
15.20	Plant fragment	7460 ± 40	8365–8190	8280 ± 50	Amorosi et al., 2017a
15.30	Peat	7070 ± 40	7975–7825	7900 ± 40	This study
16.60	Wood	7140 ± 40	8025–7925	7965 ± 35	This study
20.55	Wood	7470 ± 50	8380–8185	8285 ± 95	Amorosi et al., 2017a
22.90	Wood	8320 ± 50	9470–9200	9335 ± 135	Amorosi et al., 2017a
24.50	Plant fragment	9990 ± 50	11,650–11,260	11,455 ± 195	Amorosi et al., 2017a
25.45	Plant fragment	11,110 ± 50	13,065–12,820	12,950 ± 130	Amorosi et al., 2017a

4.1.1. Pollen-derived biomes

In the cluster analysis of Fig. 3, the tree diagram furnishes a representation of vegetation dynamics in the plain and in the surrounding reliefs. Nine ecologically distinct PDBs were identified (Fig. 3): Poaceae humid grassland (Phg), Alder wood (Aw), Montane humid vegetation (Mhv), Mixed oak–holm oak forest (Mo-ho), Willow wood (Ww), Montane and local mesic steppe (Mlms), Swamp herbs (Swh), Mixed oak forest (Mof) and Disturbed grassland (Dg). Two PDB super-groups are recognizable at the highest ecological distance and reflect different vegetation communities developed during the climate optimum, i.e., alluvial plain vs. coastal plain PNVs. The former group of taxa mainly includes the mixed oak forest (the PNV of the Po alluvial plain and low hills), while the latter contains Mediterranean taxa (mixed oak-holm oak forest). As a whole, these super-groups are both bracketed by PDBs that reflect the lateral transition to a variety of settings differing in terms of humidity and/or levels of disturbance. Low degrees of humidity are represented by grassland biomes (Dg and Phg in Fig. 3), while high water table levels are highlighted by wetland biomes typical of swampy environments (Swh, Ww and Aw in Fig. 3). Two PDBs associated with montane taxa (Mms and Mhv in Fig. 3) interrupt this trend, suggesting they represent sudden environmental changes not related to local dynamics/lateral facies variability.

4.1.2. Pollen groups

Seven pollen groups were identified (Table 2) integrating PDBs (Fig. 3), present-day regional vegetation physiognomy (Fig. 1) and specific (auto)ecological features of the identified taxa. Each group is briefly described below.

Hygrophyte plants (Hyg): this group includes woody taxa that can tolerate only short periods of drowning (*Alnus glutinosa*, *Populus* and *Salix*) and herbs that indicate general humid conditions (Cyperaceae and most Pteridophytes). It mainly accounts for hygrophilous woods and related canopy clearings. Correspondent PDBs are Aw and Ww, both including several herbaceous hygrophytes and aquatics.

Aquatic plants (Aq): this group includes many types of plants (helophytes and hydrophytes) that grow in swampy environments adjacent to hygrophilous woods (Aw, Ww and Swh biomes). Helophytes, including *Butomus umbellatus*, *Isoetes durieui*, *I. hystrix* and various Typhaceae, can tolerate long periods of drowning and, therefore, live with the sole radical apparatus immersed. Hydrophytes consist, instead, of fully aquatic plants (mainly Callitrichaceae, *Isoetes lacustris*, Nympheaceae and *Sparganium emersum*) that live in water, either floating or immersed.

Pasture meadow (pm): this group mainly comprises Fabaceae and undetermined Asteroideae, Caryophyllaceae, Cichorioideae and Poaceae. Their attribution to biomes Phg and Dg is consistent with their ecological characteristics, as a variety of different herbs can colonise temporarily-emerged areas (e.g.: Caryophyllaceae from seaward

localities, Poaceae from a very wide range of different environments, Cichorioideae and Asteroideae from pastures).

Mediterranean taxa (M): this group mainly consists of *Quercus ilex* (falling into the Mo-ho biome) with the negligible presence of *Erica*, *Helianthemum*, *Pinus nigra* and *P. pinea*, which for this reason were not considered for elaborating PDBs (i.e., occasional taxa).

Quercus + other Deciduous trees (Q + other DT): this includes all deciduous oak taxa (*Quercus cerris*, *Q. pubescens*, *Q. robur* and *Quercus* undiff.), as well as other deciduous trees (*Carpinus betulus*, *Corylus avellana*, *Fraxinus excelsior*, *F. ornus*, *Ostrya carpinifolia*, *Tilia cordata*, *T. platyphyllos* and *Ulmus minor*) that compose the Po Plain PNV. Deciduous oak taxa (with the exception of *Q. robur*) fall into the holm oak–mixed oak biome (instead of the mixed oak), in an ecological subordinate to coordinate position with *Q. ilex*. This suggests remarkable influence of the coastal holm oak – mixed oak forest on the local environment. The attribution of *Q. robur* and *Fraxinus excelsior* to the Montane humid vegetation biome (Fig. 3) is because the sub-Mediterranean vegetation belt in ER extends up to 800 m a.s.l. (Ferrari, 1997; Pignatti, 1998).

Montane taxa (Mt): given the remarkable distance (ca. 50 km) of the core site from the Apennines, all taxa ranging in height a.s.l. from the Beech woods to the Ericaceous shrublands above the timberline were incorporated into this group. These taxa include all Conifers (*Abies alba*, *Picea excelsa* and *Pinus mugo*), montane broadleaves (*Alnus incana* and *A. viridis*) and herbs (*Dryas octopetala* and various Saxifragaceae), mainly belonging to both montane biomes (Fig. 3). *Artemisia* was not included because of uncertainties in species determination and ecology (Pignatti, 1982; Subally and Quézel, 2002). Though *Pinus* sp. falls within the mixed oak forest biome (Fig. 3), it was interpreted as part of the regional (sub-regional) pollen rain for the following reasons: *i)* temperate pine taxa, such as *P. halepensis, P. nigra* and *P. pinea*, were found in negligible amounts (< 1%) in very few samples only, *ii)* *Pinus* sp. pollen was never found in concentrations high enough to depict the onset of any pine wood, such as the one that colonized the Po Plain during the Preboreal and declined throughout the Boreal (Ferrari, 1997; Accorsi et al., 1999, 2004), and *iii)* *Pinus* sp. variations mainly follow those of the other taxa grouped into the *Mt* pollen group. *Abies alba* also falls into the mixed oak forest biome; in this case, its retrieval in the same branch of *Tilia cordata* and *T. platyphyllos* likely indicates its preference for relatively moist conditions, both in mountainous and lowland areas.

Alia: this group includes all taxa excluded from previous groups (ubiquitous taxa and others belonging to *As* - Anthropic spontaneous). Specifically, several Asteroideae (*Bellis perennis*, *Centaurea nigra* and *Tussilago farfara*), Caryophyllaceae (*Spergula arvensis*), Papaveraceae, Plantaginaceae, Polygonaceae and Urticaceae characterise this group.

In sum, according to cluster analysis (Fig. 3) all pollen groups bear a more or less marked facies signal. Only the montane taxa group can be
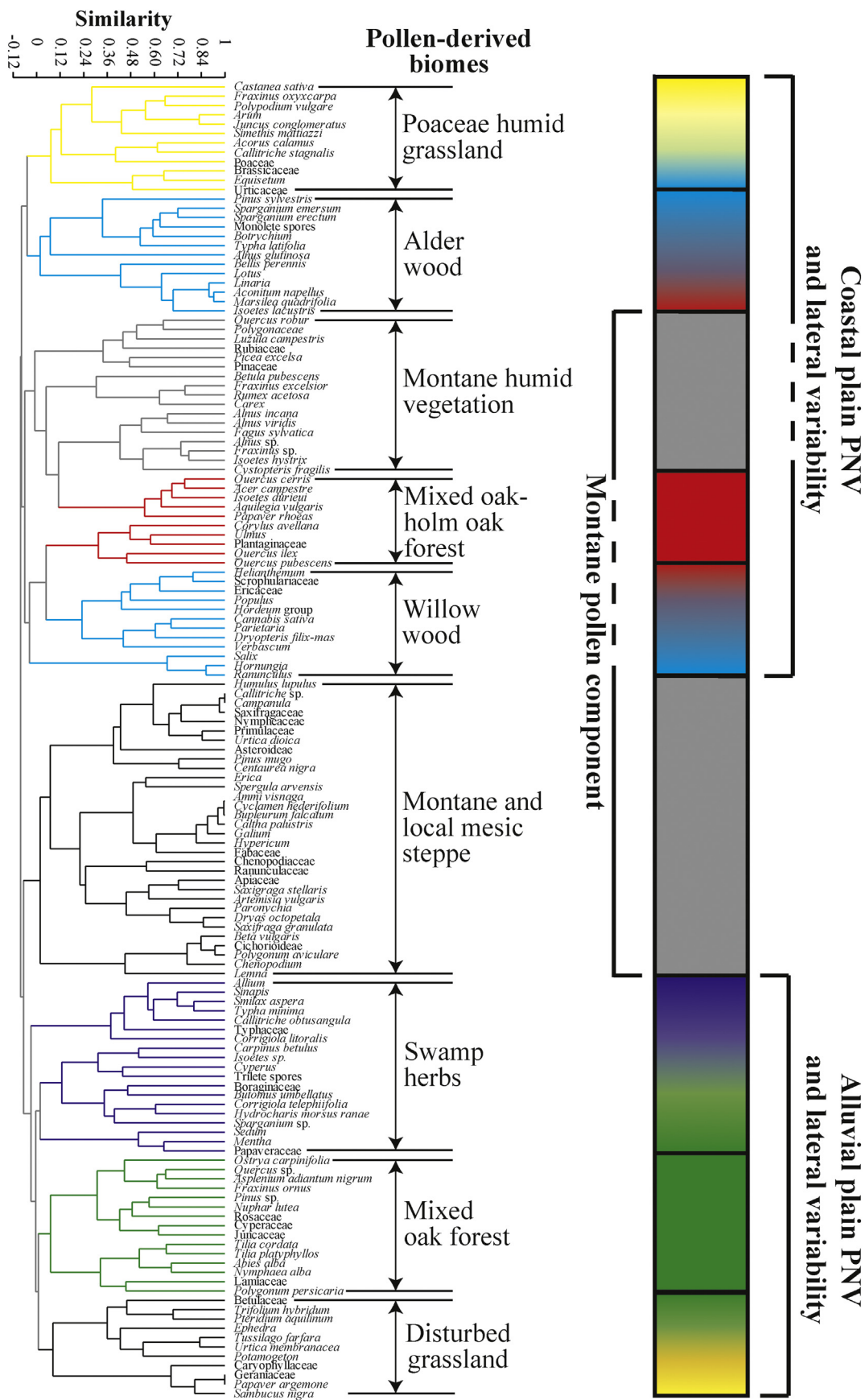
Fig. 3. Tree diagram obtained through cluster analysis performed on selected plant taxa of core EM2 (Correlation similarity method and Paired group root were used). The resulting pollen-derived biomes (PDBs) and interpreted vegetation dynamics in the Po Plain and surrounding reliefs are also shown. (For interpretation of the references to colour in this figure legend, the reader is referred to the web version of this article.)

Table 2

Pollen groups identified in core EM2 through integration of PDBs, present-day regional vegetation physiognomy and specific (auto)ecological features. Main pollen taxa and the climate and/or environmental significance of each group are reported.

Pollen groups	Main taxa	Proxy in coastal-alluvial contexts
Hyg	Sum of woody taxa (*Alnus glutinosa, Salix*) and herbs (Cyperaceae, various ferns)	Facies indicator (degree of humidity)
Aq	Sum of helophytes (*Isoetes durieui, I. hystrix, Sparganium erectum, Typha*) and hydrophytes (Callitrichaceae, *Isoetes lacustris*, Nympheaceae)	Facies indicator (water-table level)
Pm	Asteroideae, Cichorioideae, Fabaceae, Poaceae	Indicator of vegetation physiognomy
M	Mediterranean taxa (mainly *Quercus ilex;* sporadic *Pinus halepensis* and *P. pinea*)	Facies + climate indicator (climate optimum)
Q + other DT	Mixed oak forest and accessory taxa (*Carpinus betulus, Corylus avellana, Fraxinus excelsior, Ostrya carpinifolia, Quercus cerris, Q. pubescens, Q. robur, Tilia, Ulmus*)	Facies + climate indicator (climate optimum)
Mt	Mountain taxa (*Abies alba, Alnus incana, Alnus viridis, Castanea sativa, Dryas octopetala, Fagus sylvatica, Picea excelsa, Pinus mugo, Pinus* sp.-to be discussed, Saxifragaceae).	Climate indicator (cool climate)
Alia	Ubiquitous taxa + As group (anthropic spontaneous), the latter including *Bellis perennis, Centaurea nigra* and *Tussilago farfara* (Asteroideae) and Chenopodiaceae, Plantaginaceae, Polygonaceae, *Spergula arvensis,* and Urticaceae	Local disturbed environment

considered a true "outsider", an indicator of regional/sub-regional (Po Plain and surrounding reliefs) vegetation, being represented by taxa that never colonized the coastal/delta plain during the current interglacial. Thus, if stratigraphically plotted, increasing *Mt* percentages can allow the identification of climate-driven altitudinal variations on plant communities (i.e., expansions of mountain vegetation belts). Relative abundances of the identified pollen groups are reported in Fig. 4 (pollen spectra), while relative concentrations of the main taxa composing each group are reported in Figs. 5-6.

4.2. Depositional facies associations

Five main facies associations (floodplain, swamp1, swamp2, overbank/crevasse and distributary channel deposits in Fig. 4) were identified combining sedimentological and palynological data derived from the local pollen rain (Table 2). Each facies association shows particular and rather uniform vegetation communities (Figs. 4-6) defined by taxa living in the alluvial plain. The floodplain facies association (silt and clay with Fe−Mn oxides and carbonate nodules) is characterised by the dominance of pasture-meadows (ca. 14–48%) over hygrophytes and aquatics (< 10% and < 8%, respectively), pointing to a low degree of hygrophily. By contrast, swamp2 deposits (organic-rich clay) show the highest percentages (10–77%) of hygrophytes accompanied by low values of aquatics (5–11%), indicating a submerged environment with a relatively low level of the water table. The highest groundwater level characterises peat-rich swamp1 deposits, where *Aq* shows the highest percentages (9.6–32%), similar to *Hyg*. Sandy overbank/crevasse and distributary channel deposits contain relatively high abundances of hygrophytes (up to 25%), thus documenting hygrophily. More detailed palynological and sedimentological features of facies associations are reported in Table 3.

4.3. Chronology

The age model (Fig. 7) indicates that the studied succession above the thick fluvial sand body covers the whole Holocene (Table 1; Figs. 2, 4). In general, most radiocarbon dates are stratigraphically coherent, with very few exceptions. Stratigraphic reversal was observed at ca. 15 m core depth, possibly reflecting reworking of older plant remains, and the related sample was discarded. Eleven out of twelve radiocarbon ages (2-sigma calibrated years BP) were interpolated using a smoothing spline function omitting the age of ca. 12,950 cal yr BP as it belongs to the abandonment facies of a fluvial channel belt (Fig. 4), whose sedimentation rates are unclear. The resulting age-depth model suggests that three main stratigraphic intervals, reflecting rather constant sedimentation rates, can be identified (Fig. 7). The lowermost interval (ca. 11.7–8.3 cal ky BP) denotes an accumulation rate of ca. 1.4 mm/yr. Upwards, between ca. 8.3–7.7 cal ky BP, the accumulation rate strongly

increases up to ca. 10 mm/yr. Its value drops to about 1.5 mm/yr between 7.7 and 1.1 cal ky BP, though the presence of a distributary-channel deposit around 10 m partly lowers this estimation. The wood fragment sampled at the base of the channel deposit and dated to around 5.2 kyr BP probably derives from the underlying eroded swamps. Thus, this age should be considered as a *terminus post-quem*. The uppermost 3 m of the cored succession, younger than 1085 years BP, have a more uncertain chronology due to the lack of radiocarbon dates.

4.4. Vegetation phases

Opportunely framed into a high-resolution chronological-facies context, the relative proportion of *Mt* relative to *Q + other DT* and *M* allows the identification of 14 pollen zones (PZs, Fig. 4). Considering montane taxa as a good proxy for climate degradation and mixed oak-holm oak forest trees as indicators of the local achievement of the vegetation final stage (Table 2), PZs were grouped into five main vegetation phases. They are described in ascending order.

PZs 14–11 (ca. 25.50–23 m; < 12,950–9300 cal. yr BP): this interval overlies a tens m-thick alluvial succession mainly formed by fluvial-channel sands (i.e., Po channel belt) and overbank deposits constrained to the last glacial period (Fig. 4 – Amorosi et al., 2017b). The uppermost portion of the channel fill probably developed under Lateglacial conditions (Cacciari et al., 2018), characterised by the remarkable abundance of *Mt* (ca. 13.5%, with *Pinus mugo* up to 5.9%). An abrupt vegetation change is recorded within PZ 14, where montane taxa decrease (ca. 6.9%) and *Quercus ilex* appears in significant amounts (4.7%), marking the onset of the Holocene. As a whole, relative abundances of *Q + other DT* and *M* (ca. 7% and 5%, respectively) compared to that of *Mt* (ca 10%) point to an early stage of vegetation development. PZs 13 and 11 record two short-term changes in the plant community, irrespective of the facies signal. PZ 13 is characterised by a slight increase in montane taxa, which is paralleled almost by the disappearance of the mixed oak and Mediterranean taxa. By contrast, a more pronounced enrichment of *Mt* (up to 15.8%) occurs within PZ 11.

PZ 10 (ca. 23–21 m; ca. 9300–8300 cal. yr BP): even though local driving factors, mainly highlighted by aquatics and hygrophytes, may have affected the plant community, this interval records a sudden decrease in montane taxa, which are almost totally replaced by Mediterranean and deciduous broadleaves. Specifically, *Mt* drops to a minimum value of 1%, whereas *M* and *Q + other DT* peak around 26% and 37%, respectively, marking the achievement of the PNV on the plain.

PZs 9–7 (ca. 21–13.5 m; ca. 8300–7700 cal. yr BP): this interval records a period of high-frequency variability in the vegetation community that encompasses several facies in the record. Its lowermost portion (PZ 9, ca. 8285–8000 cal. yr BP) shows a pronounced peak in
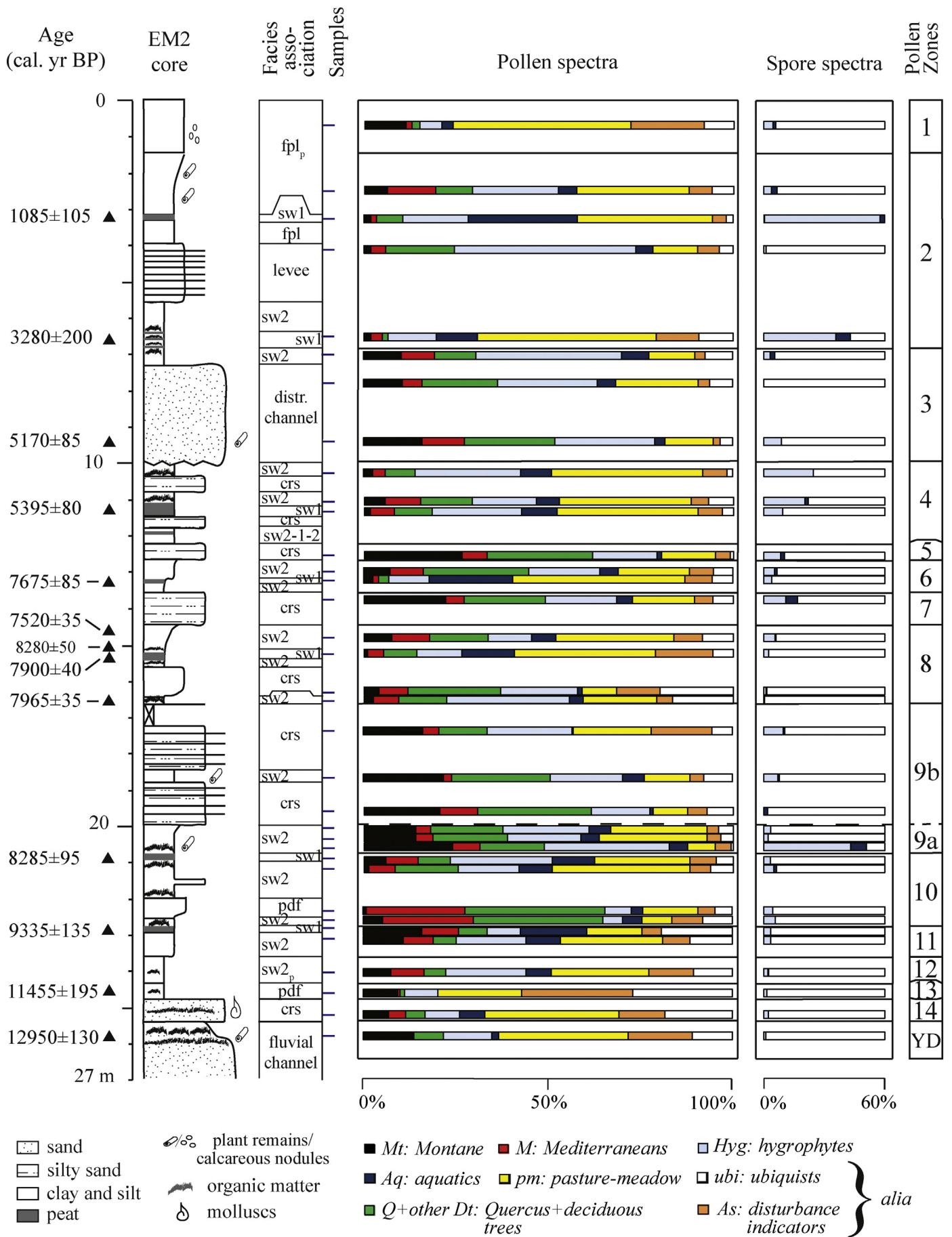
(caption on next page)

Fig. 4. Stratigraphy and main palynological features (pollen and spores) of core EM2 reported as relative abundances of pollen groups (modified after Cacciari et al., 2018; see text and Table 2). Pollen Zones were defined after filtering the facies signal with the support of cluster analysis (Fig. 3). Available radiocarbon ages are also shown as calibrated years BP (Table 1). (For interpretation of the references to colour in this figure legend, the reader is referred to the web version of this article.)
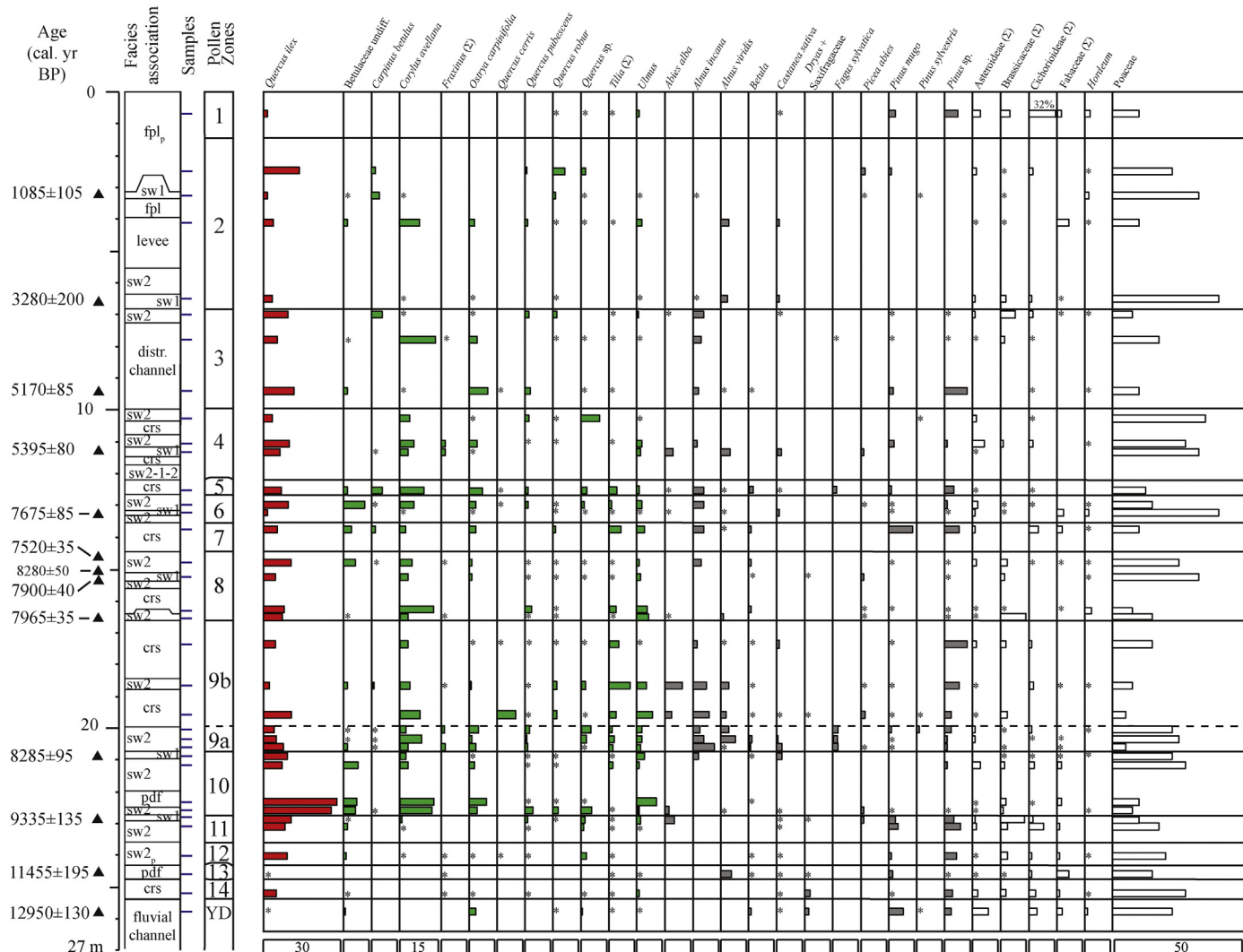
Fig. 5. Pollen percentage diagram, showing the relative abundances of *Quercus ilex* (*M* group) along with the most important oak + other deciduous (*Q + other DT*), montane (*Mt* group) and pasture meadow taxa (*pm* group). The first two groups are considered good indicators of coastal and alluvial plain PNVs, whereas the *Mt* group is a proxy for climate-driven altitudinal variations on plant communities (e.g., expansions of mountain vegetation belts). Asterisk represents percentages < 1%. Facies abbreviations: distributary channel (distr. channel), crevasse splay (crs), poorly drained floodplain (pdf), fpl (floodplain), swamp 2 (sw2), swamp 1 (sw1); the "p" subscript means pedogenised. (For interpretation of the references to colour in this figure legend, the reader is referred to the web version of this article.)

montane taxa (14–24%) that is paralleled by a decrease in Mediterraneans, while the mixed oak forest remains well represented. Upwards, PZ 8 documents the recovery of holm oak forests accompanied by a sharp decline in montane taxa. The observed concentration of *Quercus ilex* (6–10%) is also considered significant because of the locally high water-table. This interval shows an upward expansion of montane trees (ca. 22%, PZ 7).

PZs 6–3 (ca. 13.5–7 m; ca. 7700–3700 cal. yr BP): the pollen content in this interval documents high-frequency changes in vegetation communities less pronounced than in underlying PZs 9–7. Two events of *Mt* expansion (PZs 5 and 3) interrupt a pollen spectrum indicative of a mesic holm oak-mixed oak forest developed laterally to hygrophilous prairies and herbaceous wetlands (PZs 6 and 4). Specifically, PZ 5 exhibits a high concentration of *Mt* (ca. 26%) showing almost all taxa found in the studied succession (except for *Pinus sylvestris*) and accompanied by most of broadleaves. A relative increase in montane taxa is also recorded within the PZ 4, but it is not paralleled by a significant

drop in Mediterraneans.

PZs 2–1 (uppermost 7 m; < 3700 cal. yr BP): pollen data in PZ 2 point to the establishment of a holm oak-mixed oak forest without a significant peak in *Mt*. A peculiar pollen assemblage indicative of a disturbed environment with a strong reduction in forest cover to the benefit of *pm* (mainly Cichorioideae) and a remarkable peak in montane taxa are found within PZ 1.

5. Discussion

5.1. Holocene vegetation and climate dynamics

5.1.1. The onset of the Holocene (ca. 11.7–9.3 kyr BP)

The beginning of the Holocene (PZ 14 in Fig. 4) is marked by the appearance of *Quercus ilex*, accompanied by mixed oak–holm oak elements, suggesting the establishment of particularly favourable microclimatic conditions in the coastal plain. This interpretation is
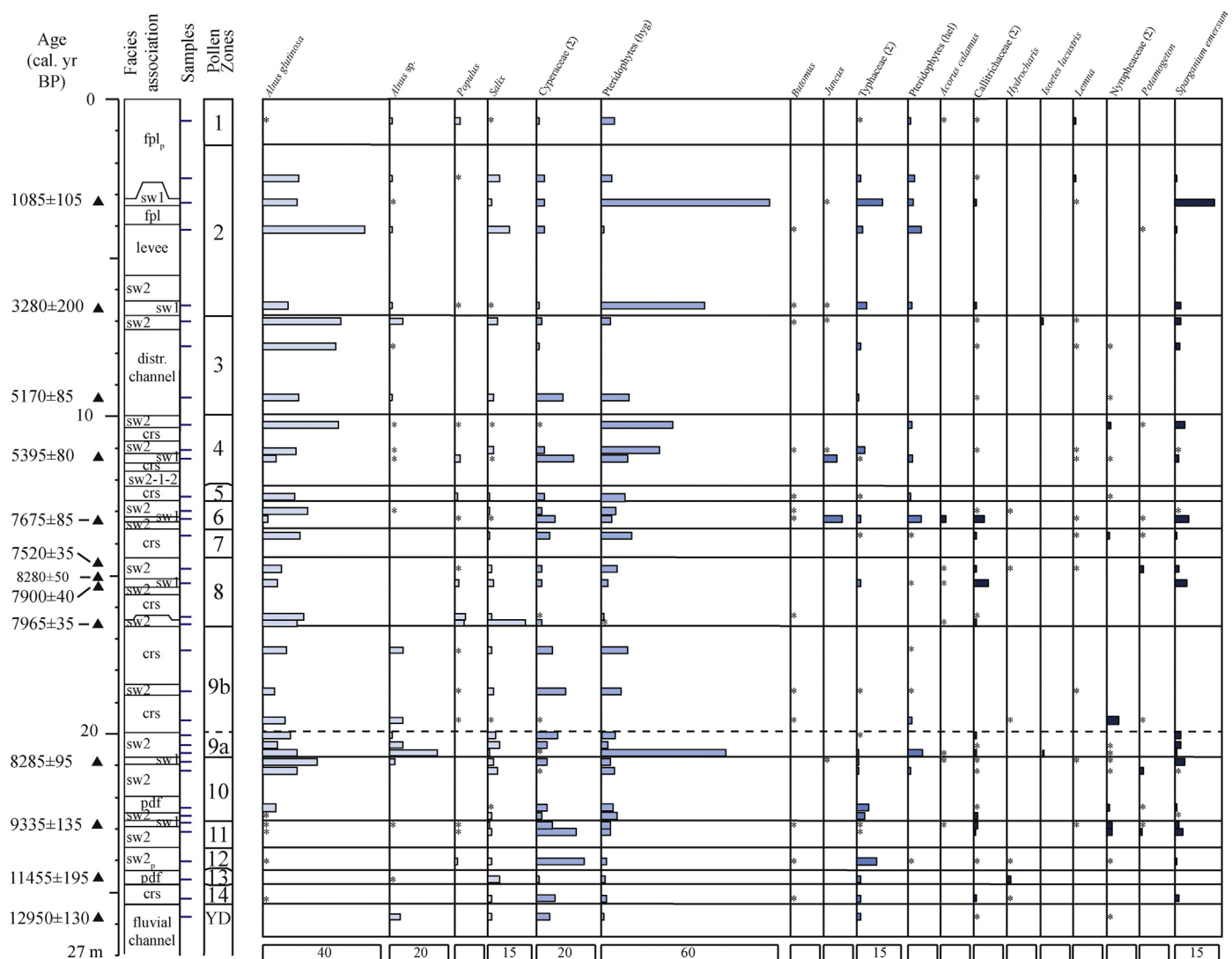
Fig. 6. Pollen percentage diagram, showing the relative abundances of hygrophytes (woody and herbaceous) and aquatics (helophytes and hydrophytes), both considered good facies indicators in terms of local humidity and water table level. Asterisk represents percentages < 1%. Facies abbreviations: distributary channel (distr. channel), crevasse splay (crs), poorly drained floodplain (pdf), fpl (floodplain), swamp 2 (sw2), swamp 1 (sw1); the "p" subscript means pedogenised. (For interpretation of the references to colour in this figure legend, the reader is referred to the web version of this article.)

strengthened by very low percentages of *Pinus* sp., compared to the coeval *Pinus sylvestris* forest developed in the Po Plain (Accorsi et al., 1999, 2004; Valsecchi et al., 2008). A partially coeval (12000–11,700 cal yrs. BP) rapid expansion of a mixed open broad-leaved forest has been recorded at Lake Ledro (southern Alps, Italy), Lake Fimon (23 m a.s.l., N Italy) and within marine deposits of the South Adriatic Sea (Valsecchi et al., 2008; Combourieu-Nebout et al., 2013; Joannin et al., 2013). An increasing trend in species richness and in the relative abundance of mixed oak-holm oak taxa, which probably reflects the vegetation response to progressively increasing temperature and precipitation, is interrupted by two peaks in montane taxa dated to around 11,400 cal yr BP and 9300 cal yr BP (PZs 13, 11 in Fig. 4). PZ13 is characterised by the strong decline of mixed oak-holm oak forests, mainly for the benefit of *Alnus viridis*, accompanied by low amounts of *Pinus mugo*, *Betula* and *Castanea*, highlighting a cool-wet climate ascribable to the Preboreal oscillation (PBO/Bond event 8; ca. 11,300–11,100 cal BP, Bond et al., 1997; Rasmussen et al., 2007a, 2007b, 2014). Interestingly, this cool and wet phase shows similar vegetation dynamics to those reconstructed in NE Europe (De Klerk et al., 2006) and the Netherlands (Bos et al., 2007), whereas cool and dry conditions commonly characterise the PBO event in the

Mediterranean record (e.g.: Lake Trifoglietti and Lake Accesa in southern and central Italy, respectively, and in several marine cores - Dormoy et al., 2009; Favaretto et al., 2009; Magny et al., 2013). The youngest (PZ11) peak in montane taxa suggests another episode of climate cooling consistent with the Boreal oscillation (Rasmussen et al., 2007a, 2007b, 2014). It is marked by a general increase in conifers (*Abies*, *Picea* and *Pinus mugo*, with *Pinus* sp. in the background), although no montane alders and no *Quercus ilex* decrease are observed. These features suggest less cool but drier conditions than during the PBO.

5.1.2. Early-mid Holocene optimum and the 8.2 ka event (ca. 9.3–7.7 kyr BP)

The abrupt expansion of mixed oak-holm oak forests on the plain around 9300 cal yr BP (PZ 10; Fig. 4) marks the rapid establishment of the PNV corresponding to the beginning of the Holocene climate optimum. Within the uppermost part of PZ 10, holm oak-mixed oak taxa are partially replaced by hygrophytes, reflecting the establishment of a hygrophilous vegetation under similar climate conditions, but in a different environment. Warm temperate oak forests characterise the latest Boreal and the early Atlantic landscape of the Po Plain (PZs

Table 3

Diagnostic sedimentological and palynological features of the main facies associations from the Holocene succession of core EM2.

Facies association	Sedimentological features	Palynological content
Peaty swamp (sw1)	Black to dark brown peat, 10 to 30 cm-thick	Arboreal cover shows low values, ranging between 10 and 47%. The *Aq* group shows the highest percentages (9.6–32%); both *Q + other DT* and *M* groups display low percentages (ca. 7% and 5%, respectively). Among woody hygrophytes, *Alnus glutinosa* is the dominant tree (ca. 8%). The *pm* group, mainly composed by Poaceae, occurs with relative abundances ranging between 11 and 49%
Swamp (sw2)	Grey to dark grey clays-silty clays, high but variable amount of decomposed organic matter and plant remains	The *Hyg* group shows high percentages (10–77%) with the dominance of *Alnus* (*A. glutinosa* and *A.* undiff.), Cyperaceae and Pteridopythes, locally accompanied by *Salix* and *Populus*. The *Aq* group occurs with percentages ranging between 5 and 11%, while the *Q + other DT* and *M* show a high range of variability (6–34% and 2–24%, respectively). *Pm*, commonly represented by Poaceae and subordinate Cichorioideae and Asteroideae, occurs with percentages that vary between 7 and 41%
Floodplain/Poorly drained floodplain (fpl/pdf)	Light grey to grey clay-silty clay and grey to brown silty clay-sandy silt. Local presence of calcareous nodules and Fe−Mn oxides, plant remains and a variable amount of decomposed organic matter	The pollen assemblage is heterogeneous with remarkable percentages of the *pm* group (ca. 14–48%), while *Aq* commonly occurs with abundances lower than 8%. *Hyg* is well represented (ca. 10–27%) with *Salix* as a significant component. *Q + other DT* and *M* show highly variable percentages between 1 and 37%
Crevasse splay/Levee (crs, lev)	Silty sand to sandy silt deposits, dm to few m-thick, organised in alternating layers (lev) or coarsening-upward (crs) successions. Scattered plant fragments and Fe−Mn oxides	The arboreal cover is generally high (51–77%). The *Hyg* dominates (i.e., *Alnus glutinosa*, *Salix*, Cyperaceae and Pteridophytes) and reach abundances of ca. 25%, while *pm* commonly stands around 12%. Various taxa belonging to *Q + other DT* and *M* occur with percentages that vary around 7 and 20%, respectively
Distributary channel (dch)	M-thick (ca. 3 m), medium to fine sandy succession. Erosional lower boundary and scattered wood fragments	Remarkable occurrence of taxa belonging to *Hyg* and *Aq*
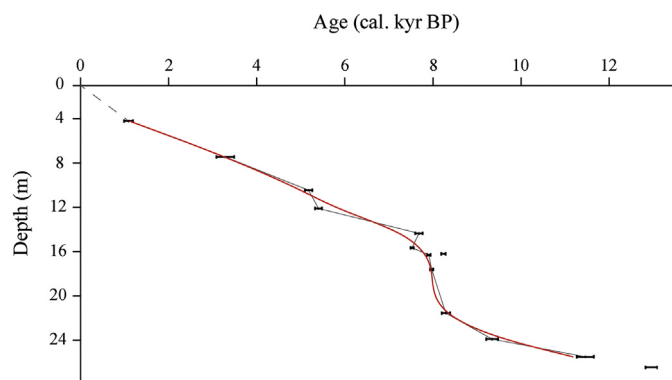
Fig. 7. Core EM2 age-depth model obtained applying the smoothing spline function (red line; smooth valour = 0.85) using the software PAST (Hammer et al., 2001). The thin black line shows the linear interpolation among ages. Radiocarbon ages are listed in Table 1. (For interpretation of the references to colour in this figure legend, the reader is referred to the web version of this article.)

10–7), as documented by several on-land pollen records from both sides of the Adriatic (Watts et al., 1996; Jahns and van der Bogaard, 1998; Sadori et al., 2011). However, two short-term periods of climate worsening occurred at the early-mid Holocene transition (*Mt* peaks around 8300–8000 cal yr BP and 7700 cal yr BP). The former has an impressive stratigraphic evidence (ca. 3 m in 300 years) that allows the detailed reconstruction of vegetation dynamics during the well-documented 8.2 ka cooling event-Bond event 5 (Bond et al., 1997; Rasmussen et al., 2007a, 2007b, 2014):

i) firstly, *Alnus incana*, *A. viridis* and *Fagus sylvatica* appeared (PZ 9a), documenting the expansion of the regional hygrophilous montane vegetation, probably favoured by slightly cooler and wetter conditions (Figs. 4, 5);

ii) shortly after *F. sylvatica* disappeared, giving way to *Abies* and *Picea*, while *A. incana* and *A. viridis* significantly increased (PZ 9b; Figs. 4, 5). These two events document the first destabilization of the montane vegetation community and further enhancement of the

annual rainfall, respectively. Our interpretation is also supported by the high variability in local re-colonisation processes, which saw different broadleaves competing for the same strongly disturbed environment (Fig. 5). Accordingly, an antagonistic behaviour of *Fagus sylvatica* and *Abies* is recorded at Lake Ledro (N Italy), where an expansion of *Abies* occurred around 8.2 ka (Joannin et al., 2013).

The second peak in montane taxa (PZ 7) shows the remarkable abundance of *Pinus mugo* (ca. 9.3%; Fig. 5), which almost completely replaced the other conifers. Although these features indicate a further degradation in high altitude vegetation communities and a possible lowering of the timberline, framing this event into a wider climate context is complicated. For the south Adriatic, Combourieu-Nebout et al. (2013) identified a short-term phase of holm oak-mixed oak forest decrease at 7.9–7.6 kyr BP, accompanied by a peak in *Abies* and *Picea*, both rapidly replaced by *Pinus*. This vegetation change was interpreted to reflect increased precipitations and lower temperatures. Interestingly, the previous decline in *Quercus* pollen is dated to around 8.3–8.2 kyr BP and linked to a decrease in temperature, which leads to the hypothesis of a local (Adriatic?) complex expression of the '8.2 ka event'. In our record this climate feature is clearer, possibly due to the influence of Siberian High outbreaks (Bora wind) on the northern Adriatic area. Indeed, Bora is a winter downslope wind that blows from the Pannonian plain through the lower portions of the Julian and Dinaric Alps into the north and central Adriatic Sea (Signell et al., 2010). Since seasonality increases during periods of climate cooling, Bora wind could also become stronger, enhancing pollen transportation from the alpine Oroboreal Conifer forest belt (*P. mugo* and *Picea* occupy the present-day shrublands above the timberline of the southern Alps; Ferrari, 1997), as well as from the Apennines (*Alnus viridis* in Mercuri, 2015) down to the Po Plain.

5.1.3. Mid Holocene optimum and transition to the late Holocene (ca. 7700–3700 cal yr BP)

After the perturbation centred at 7700 cal yr BP, the return to climate optimum conditions is recorded by the hygrophilous version of PNV, which characterised the Po Plain landscape up to ca. 5000 cal yr BP (late Atlantic). However, a short-lived, marked peak in montane

taxa (PZ 5 in Fig. 4) points to a minor climate cooling centred on 7000 cal yr BP. Although a semi-coeval climate change has been patchily recorded within the Mediterranean marine record (Fletcher and Zielhofer, 2011; Combourieu-Nebout et al., 2009, 2013; Desprat et al., 2013), our data show an impressive and peculiar tree species diversity (including *Q + other DT*), suggesting low impact of this climate oscillation on the vegetation cover. A further minor increase in montane trees occurs between ca. 5000–3800 cal yr BP (PZ 3; Fig. 4). In this instance, the absence of *Abies, Fagus* and *Picea* coupled with the high degree of chronological uncertainty due to the presence of an erosional distributary channel, prevent from in-depth palaeoclimate reconstructions.

5.1.4. Late Holocene (last 3700 years)

According to Accorsi et al. (1999, 2004), the late Holocene pollen record of the Po Plain (PZs 2–1; Fig. 4) documents the development of a vegetation landscape characterised by hygrophilous forests and by a clear shrinking of the holm oak and mixed oak woods, probably related to a heavier human land-use. Moreover, a peak of *Q. ilex* accompanied by a mixed oak forest recovery dated to around 830 cal. yr BP (Fig. 4) could represent the Medieval Climate Optimum. The following increase in montane taxa exclusively represented by *Pinus* species could be related to the Little Ice Age.

5.2. Climate imprint on landscape evolution and depositional patterns

The main shifts in Holocene vegetation, reconstructed from pollen data, fit well key depositional and palaeoenvironmental changes in the Po Plain (Fig. 8). This suggests a primary role of climate fluctuations, in addition to glacio-eustatic changes (MWPs-Melt Water Pulses), in shaping the coastal landscape. The marked warming documented by the appearance of *Q. ilex* corresponds to a phase of general drowning of the Po estuary (Figs. 2, 8; Bruno et al., 2017), revealing a simultaneous vegetation-depositional response at ca. 11.7 cal kyr BP under combined climate and eustatic forcing factors related to MWP 1B (Fairbanks, 1989; Vacchi et al., 2016). In the earliest Holocene (before 9.3 cal kyr BP), the increasing degree of hygrophily (overbank/crevasse deposits overlain by swamps; Fig. 4) reflects the landward migration of facies under the predominant forcing of relative sea-level (RSL) rise (Vacchi et al., 2016). In this context, high-frequency events of climate cooling revealed by peaks in montane taxa (e.g., PBO and BO) do not seem to affect significantly coastal depositional patterns (Fig. 8). Interestingly, a generalized phase of flooding that led to a widespread peaty sedimentation in the area (Bruno et al., 2017) is concomitant with the establishment of optimum climate conditions, marked by the PNV achievement (Fig. 8). During this period, the inner portion of the estuarine system appears to be particularly sensitive to cooling episodes (centred at ca. 8.2, 7.7 and 7.0 cal kyr BP). Indeed, increased fluvial activity led to the rapid sedimentation of thick crevasse splay sands and silts fed by a nearby distributary channel (Fig. 2) and intercalated with peaty swamp and swamp clays (average accumulation rate of ca. 6 mm/yr between 8.3 and 7.0 cal kyr BP). A marked peak in river floods has been documented by Benito et al. (2015a, 2015b) for the entire Mediterranean area between ca. 8000–7000 cal yr BP. Increased river inputs have been identified in the Adriatic Basin and correlated to the 7.7 and 7.5–7.0 cal kyr BP climate events (Combourieu-Nebout et al., 2013). Moreover, enhanced flood activity dated ca. 8.2–7.1 cal kyr BP was identified by Zhornyak et al. (2011) in the Apuan Alps (Renella cave, NW Italy). These combined climate-stratigraphic data suggest that major shifts towards enhanced fluvial activity possibly reflect phases of increased soil erodibility related to climate-driven changes in vegetation cover, as already hypothesized by Fletcher and Zielhofer, 2013.

The stratigraphically expanded sedimentary record of the Po estuary also allows the examination of depositional dynamics and their relation to vegetation patterns on sub-millennial time scales around the well-known 8.2 ka event (Fig. 8). The onset of a cooler climate is testified by

the sudden appearance, among montane taxa, of *Fagus sylvatica*, within peaty swamp deposits dated to around 8300 cal yr BP. Following a further step of montane forests degradation (*F. sylvatica* is replaced by *Abies alba*; Fig. 5), the depositional system reacts via increased fluvial (crevasse) sedimentation. These dynamics suggest a different response of coastal sedimentation compared to the vegetation community, as this latter exhibits an almost immediate response to climate cooling. By contrast, a time lag is not observed for the subsequent cooling phase centred at 7.7 cal kyr BP that possibly records a second spell of the 8.2 ka event (Figs. 4, 8).

The end of climate optimum conditions and the transition to the late Holocene (ca. 5000–3700 cal yr BP) are locally recorded by a 3 m-thick distributary-channel sand body, which is part of a complex drainage network that fed the Po delta plain during the earliest phases of progradation (Amorosi et al., 2017a, 2019). Although this stratigraphic interval is affected by a low palynological-chronological resolution due to the sandy nature of the deposit (Figs. 7, 8), our record of enhanced fluvial activity is well correlated with a major Po River avulsion and the consequent reorganization of the deltaic network reported for the same period of time (Rossi and Vaiani, 2008; Piovan et al., 2012; Amorosi et al., 2017b, 2017b). This phase was also contemporaneous to widespread deforestation induced by transhumant pastoralism during the Eneolithic (Cremaschi and Nicosia, 2012; Bruno et al., 2015)

6. Conclusions

The combined palynological and stratigraphic analysis of the Holocene depositional record from the subsurface of the modern Po delta-coastal plain (core EM2) enables differentiation of environmental (local) and climate (regional) changes, both marked by distinctive vegetation dynamics, in a key area between the continental and marine realms. Placed within a robust facies and chronological framework, shifts in vegetation communities from stratigraphically expanded (tens m-thick), organic-rich deposits that accumulated in inner estuarine-deltaic settings provide high-resolution (millennial-scale) data about Holocene palaeoclimate variations in the N Adriatic area. The major outcomes of this study can be summarised as follows:

- Nine pollen-derived biomes (PDBs) were identified from the core EM2 pollen record through cluster analysis. The resulting dendrogram mainly reflects the development of different vegetation communities under optimum conditions (PNV) and along environmental-local humidity/disturbance gradients.
- The comparison between PDBs, local present-day vegetation belts and (auto)ecological features of the identified taxa allowed us to define seven pollen groups and to interpret them in terms of environmental and/or climate forcing. Only montane taxa (*Mt*) exclusively reflect the regional/sub-regional pollen rain, whereas Mediterranean (*M*) and deciduous broadleaved (*Q + other DT*) taxa are indicative of PNV on the plain.
- Stratigraphic variations in montane taxa document changes in the altitudinal distribution of vegetation communities linked to cooling periods. This vegetation-climate variability fits well with Bond events, especially for the early-mid Holocene, suggesting a strong Mediterranean–North Atlantic climate link at high-frequency time intervals.
- One major vegetation change (dated between 8.3 and 8.0 cal kyr BP) coincides with the widespread climate perturbation attributed to the 8.2 ka cooling event.
- Climate played a major role in shaping coastal landscapes in addition to glacio-eustatic variations, determining changes in the local and regional vegetation cover, as well as triggering an increase in fluvial activity.

Supplementary data to this article can be found online at https://doi.org/10.1016/j.palaeo.2019.109468.
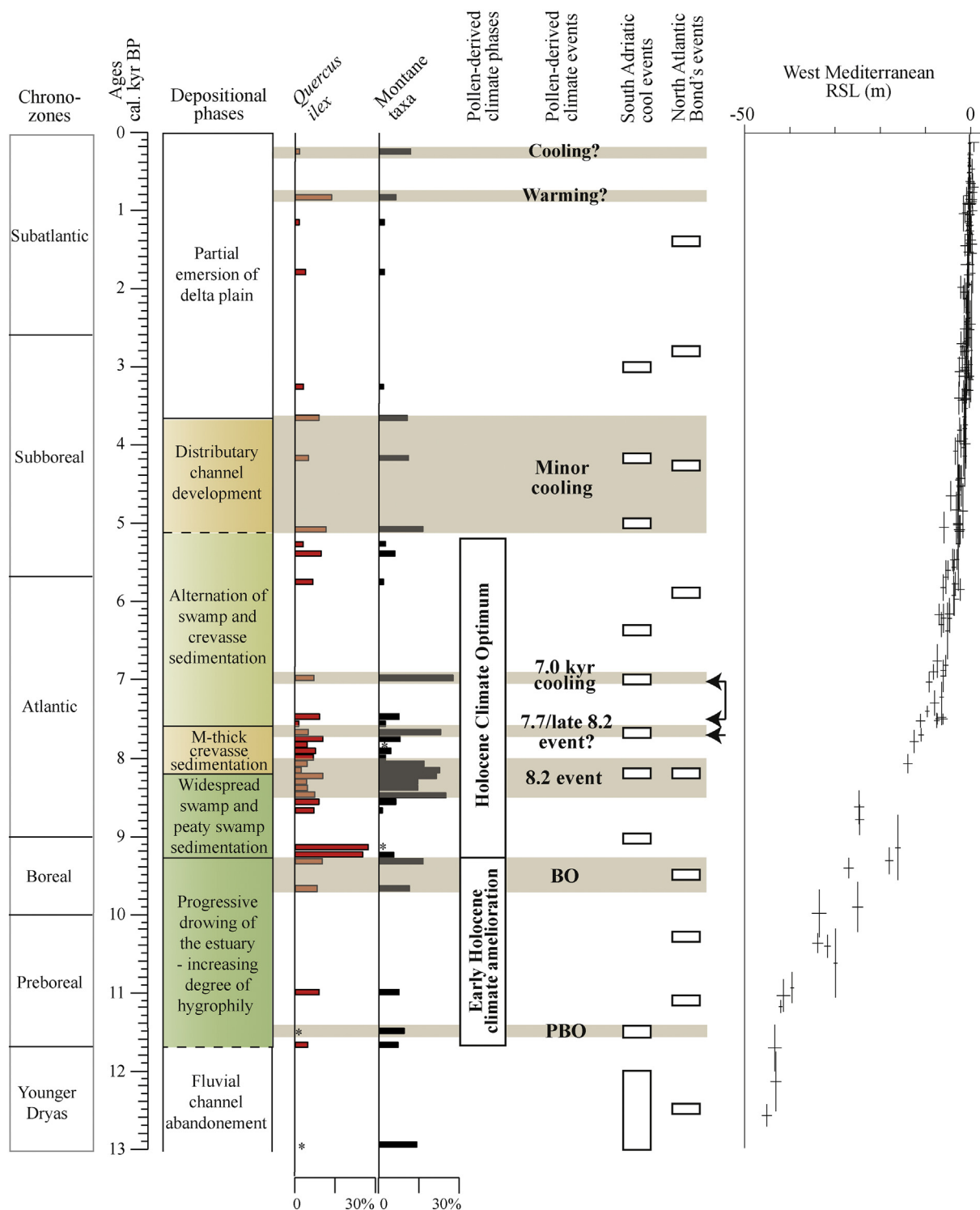
Fig. 8. Comparison between depositional dynamics (vertical stacking pattern of facies), pollen-derived climate phases and climate events recorded in core EM2. Palynological samples are plotted against time instead of depth (Figs. 4-6) applying the age-depth model reported in Fig. 7; unique exception is the sample centred at 11.7 cal kyr BP, as its chronological attribution is based on the pollen content (i.e., remarkable appearance of *Q. ilex*). Chronozones of Mangerud et al., 1974, slightly modified by Ravazzi (2003), and cooling events recorded in the North Atlantic area (Bond's events; Bond et al., 1997) and the south Adriatic Sea (Combourieu-Nebout et al., 2013) are also highlighted. Black arrows indicate phases of enhanced runoff of Po and Adriatic rivers, as reported by Combourieu-Nebout et al. (2013). Plots of RSL index points from western Mediterranean (Vacchi et al., 2016) are also shown. PBO: Preboreal Oscillation; BO: Boreal Oscillation. (For interpretation of the references to colour in this figure legend, the reader is referred to the web version of this article.)

## Declaration of competing interest

The authors declare that they have no known competing financial interests or personal relationships that could have appeared to

influence the work reported in this paper.

Acknowledgements

References

Accorsi, C.A., Bandini Mazzanti, M., Forlani, L., Mercuri, A.M., Trevisan Grandi, G., 1999. An overview of Holocene forest pollen flora/vegetation of the Emilia Romagna region – Northern Italy. Archivio Geobotanico 5 (1–2), 3–27.

Accorsi, C.A., Bandini Mazzanti, M., Forlani, L., Mercuri, A.M., Trevisan Grandi, G., 2004. Holocene forest vegetation (pollen) of the Emilia Romagna plain – northern Italy. In: Pedrotti F, Gehu J.M. (eds) La végétation postglaciaire du passé et du présent. Syngenèse, synécologie et synsystématique. Colloq. Phytosociol. 28, 1–103.

Amorosi, A., Bruno, L., Cleveland, D.M., Morelli, A., Hong, W., 2017b. Paleosols and associated channel-belt sand bodies from a continuously subsiding late Quaternary system (Po Basin, Italy): new insights into continental sequence stratigraphy. Geol. Soc. Am. Bull. 129 (3–4), 449–463.

Amorosi, A., Colalongo, M.L., Fiorini, F., Fusco, F., Pasini, G., Vaiani, S.C., Sarti, G., 2004. Palaeogeographic and palaeoclimatic evolution of the Po Plain from 150-ky core records. Glob. Planet. Chang. 40, 55–78.

Amorosi, A., Dinelli, E., Rossi, V., Vaiani, S.C., Sacchetto, M., 2008. Late Quaternary palaeoenvironmental evolution of the Adriatic coastal plain and the onset of the Po River Delta. Palaeogeogr. Palaeoclimatol. Palaeoecol. 268, 80–90.

Amorosi, A., Maselli, V., Trincardi, F., 2016. Onshore to offshore anatomy of a Late Quaternary source-to-sink system (Po Plain – Adriatic Sea, Italy). Earth-Sci. Rev. 153, 212–237.

Amorosi, A., Bruno, L., Campo, B., Morelli, A., Rossi, V., Scarponi, D., Hong, W., Bohacs, K.M., Drexler, T.M., 2017a. Global sea-level control on local parasequence architecture from the Holocene record of the Po Plain, Italy. Mar. Petroleum Geol. 87, 99–111.

Amorosi, A., Barbieri, G., Bruno, L., Campo, B., Drexler, T.M., Hong, W., Rossi, V., Sammartino, I., Scarponi, D., Vaiani, S.C., Bohaks, K.M., 2019. Three-fold nature of coastal progradation during the Holocene eustatic highstand, Po Plain, Italy – close correspondence of stratal character with distribution patterns. Sedimentology 66, 3029–3052. https://doi.org/10.1111/sed.12621.

Badino, F., Ravazzi, C., Valié, F., Pini, R., Aceti, A., Brunetti, M., Champvillair, E., Maggi, V., Maspero, F., Perego, R., Orombelli, G., 2018. 8800 years of high-altitude vegetation and climate history at the Rutor Glacier forefield, Italian Alps. Evidence of middle Holocene timberline rise and Glacier contraction. Quat. Sci. Rev. 185, 41–68.

Bard, E., Hamelin, B., Arnold, M., Montaggioni, L., Cabioch, G., Faure, G., Rougerie, F., 1996. Deglacial sea-level record from Tahiti corals and the timing of global meltwater discharge. Nature 382, 241–244.

Benito, G., Macklin, M.G., Cohen, K.M., Herget, J., 2015a. Past hydrological extreme events in a changing climate. Catena 130, 1–108. https://doi.org/10.1016/j.catena.2014.12.001.

Benito, G., Macklin, M.G., Panin, A., Rossato, S., Fontana, A., Jones, A.F., Machado, M.J., Matlakhova, E., Mozzi, P., Zielhofer, C., 2015b. Recurring flood distribution patterns related to short-term Holocene climatic variability. Sci. Rep. 5, 16398. https://doi.org/10.1038/srep16398.

Berglund, B.E., Ralska-Jasiewiczowa, M., 1986. Handbook of Holocene Palaeoecology and Palaeohydrology. Wiley-Interscience. John Wiley & Sons Ltd, Chichester (1986).

Bertoldi, R., 2000. Storia del popolamento vegetale della pianura del Po. In: Ferrari, C., Gambi, L. (Eds.), (a cura di), Un po di terra. Guida all'ambiente della bassa Pianura Padana e alla sua storia. Ed. Diabasis.

Bini, M., Zanchetta, G., Perşoiu, A., Cartier, R., Català, A., Cacho, I., Jonathan, J.R., Di Rita, F., Drysdale, N.R., Finné, M., Isola, I., Jalali, B., Lirer, F., Magri, M., Masi, A., Marks, L., Mercuri, A.M., Peyron, O., Sadori, L., Sicre, M.-A., Welc, F., Zielhofer, C., Brisset, E., 2019. The 4.2 ka BP event in the Mediterranean region: an overwiew. Clim. Past 15, 555–577.

Blasi, C., Capotorti, G., Copiz, R., Guida, D., Mollo, B., Smiraglia, D., Zavattero, L., 2014. Classification and mapping of the ecoregions of Italy. Plant Biosyst 148 (6), 1255–1345.

Boccaletti, M., Corti, G., Martelli, L., 2011. Recent and active tectonics of the external zone of the Northern Apennines (Italy). Int. J. Earth Sci. https://doi.org/10.1007/s00531-010-0545-y.

Bond, G., Showers, W., Cheseby, M., Lotti, R., Almasi, P., deMenocal, P., Priore, P., Cullen, H., Hajdas, I., Bonani, G., 1997. A pervasive millennial-scale cycle in North

Atlantic Holocene and glacial climates. Science 278, 1257–1266.

Bond, G., Kromer, B., Beer, J., Muscheler, R., Evans, M.N., Showers, W., Hoffmann, S., Lotti-Bond, R., Hajdas, I., Bonani, G., 2001. Persistent solar influence on North Atlantic climate during the Holocene. Science 294, 2130–2135.

Bondesan, M., Calderoni, G., Cattani, L., Ferrari, M., Furini, A.L., Serandrei Barbero, R., Stefani, M., 1995. Nuovi dati stratigrafici, paleoambientali e di cronologia radio-metrica sul ciclo trasgressivo-regressivo olocenico nell'area deltizia padana. Annali dell'Università di Ferrara, sezione Scienze della Terra 8 (1), 1–34.

Bos, J.A.A., Van Geel, B., Van der Plicht, J., Bohnke, S.J.P., 2007. Preboreal climate os-cillations in Europe: wiggle-match dating and synthesis of Dutch high-resolution multi-proxy records. Quat. Sci. Rev. 26, 1927–1950.

Bronk Ramsey, C., 2009. Bayesian analysis of radiocarbon dates. Radiocarbon 51 (1), 337–360.

Bruno, L., Amorosi, A., Severi, P., Bartolomei, P., 2015. High-frequency depositional cycles within the late Quaternary alluvial succession of Reno River (northern Italy). Ital. J. Geosci. 134 (2), 339–354.

Bruno, L., Bohacs, K.M., Campo, B., Drexler, T.M., Rossi, V., Sammartino, I., Scarponi, D., Hong, W., Amorosi, A., 2017. Early Holocene transgressive palaeogeography in the Po coastal plain (Northern Italy). Sedimentology 64, 1792–1816.

Cacciari, M., Rossi, V., Marchesini, M., Amorosi, A., Bruno, L., Campo, B., 2018. Palynological characterization of the Po delta succession (Northern Italy): Holocene vegetation dynamics, stratigraphic patterns and palaeoclimate variability. In: Alpine and Mediterranean Quaternary 31 (Quaternary: Past, Present, Future - AIQUA Conference, Florence, 13–14/06/2018), pp. 109–112.

Campo, B., Amorosi, A., Vaiani, S.C., 2017. Sequence stratigraphy and late Quaternary paleoenvironmental evolution of the Northern Adriatic coastal plain (Italy). Palaeogeogr. Palaeoclimatol. Palaeoecol. 466, 265–278.

Carriòn, J.S., Fernandez, S., 2009. The survival of the 'natural potential vegetation' concept (or the power of tradition). J. Biogeogr. 36, 2202–2203.

Cattaneo, C., 1844. Introduzione alle notizie naturali e civili sulla Lombardia. Milano, Bernardoni di Giovanni Tipografo. pp. 1844.

Chiarucci, A., Araùjo, M.B., Decocq, G., Beierkuhnlein, C., Fernàndez-Palacios, J.M., 2010. The concept of potential natural vegetation: an epitaph? Journal of Vegetation Science 21, 1172–1178.

Chiarugi, A., 1958. Ricerche sulla vegetazione dell'Etruria. XI: una seconda area relitta di vegetazione di Pigella (Picea excelsa Lam.) sull'Appennino Settentrionale. N. Giorn. Bot. Ital. 65, 23–42.

Combourieu-Nebout, N., Peyron, O., Domoy, I., Desprat, S., Beaudouin, C., Kotthoff, U., Marret, F., 2009. Rapid climatic variabiliry in the west Mediterranean during the last 25000 years frim high resolution pollen data. Clim. Past 5, 503–521.

Combourieu-Nebout, N., Peyron, O., Bout-Roumazeilles, V., Goring, S., Dormoy, I., Joannin, S., Sadori, L., Siani, G., Magny, M., 2013. Holocene vegetation and climate changes in the central Mediterranean inferred from a high-resolution marine pollen record (Adriatic Sea). Clim. Past 9, 2013–2043.

Correggiari, A., Cattaneo, C., Trincardi, F., 2005. Depositional patterns in the late Holocene Po delta system. River deltas – Concept, models and examples. In: SEPM Special Publications 83, pp. 365–392.

Cremaschi, M., Nicosia, C., 2012. Sub-Boreal aggradation along the Apennine margin of the Central Po Plain: geomorphological and geoarchaeological aspects. Géomorphologie 2012 (2), 155–174.

Cremaschi, M., Mercuri, A.M., Torri, P., Florenzano, A., Pizzi, C., Marchesini, M., Zerboni, A., 2016. Climate change versus land management in the Po Plain (Northern Italy) during the Bronze Age: new insights from the VP/VG sequence of the Terramara Santa Rosa di Poviglio. Quat. Sci. Rev. 136, 153–172.

De Klerk, P., Couwenberg, J., Joosten, H., 2006. Short-lived vegetational and environ-mental change during the Preboreal in the Biebrza upper basin (NE Poland). Quat. Sci. Rev. 26, 1975–1988.

Desprat, S., Combourieu-Nebout, N., Essallami, L., Sicre, M.A., Dormoy, I., Peyron, O., Siani, G., Bout Roumazeilles, V., Turon, J.L., 2013. Deglacial and Holocene vegeta-tion and climatic changes in the southern Central Mediterranean from a direct land-sea correlation. Clim. Past 9, 767–787.

Di Rita, F., Magri, D., 2009. Holocene drought, deforestation and evergreen vegetation development in the central Mediterranean: a 5500 year record from Lago Alimini Piccolo, Apulia, southeast Italy. The Holocene 19, 295–306.

Di Rita, F., Magri, D., 2019. The 4.2 ka event in the vegetation record of the central Mediterranean. Clim. Past 15, 237–251.

Di Rita, F., Celant, A., Milli, S., Magri, D., 2015. Lateglacial – early Holocene vegetation history of the Tiber delta (Rome, Italy) under the influence of climate change and sea level rise. Rev. Palaeobot. Palyno. 218, 204–216.

Doglioni, C., 1993. Some remarks on the origin of foredeeps. Tectonophysics 228, 1–20.

Dormoy, I., Peyron, O., Combourieu Nebout, N., Goring, S., Kotthoff, U., Magny, M., Pross, J., 2009. Terrestrial climate variability and seasonality changes in the Mediterranean region between 15000 and 4000 years BP deduced from marine pollen records. Clim. Past 5, 615–632.

Faegri, K., Iversen, J., Krzywinski, K., 1989. Textbook of pollen analysis. John Wiley and Sons, Chichester.

Fairbanks, R.G., 1989. A 17,000-year glacio-eustatic sea level record: influence of glacial melting rates on the Younger Dryas event and deep-ocean circulation. Nature 342, 637–642.

Favaretto, S., Asioli, A., Miola, A., Piva, A., 2009. Preboreal climatic oscillation recorded by pollen and foraminifera in the Southern Adriatic Sea. Quat. Int. 190, 89–102.

Ferrari, C. (editor), 1980. Flora e vegetazione dell'Emilia Romagna. Grafiche Zanini, Bologna (Italy), 1980.

Ferrari, C., 1997. The vegetation belts of Emilia Romagna (Northern Italy). Allionia 34, 219–231.

Feurdean, A., Wohlfarth, B., Björckman, L., Tantau, I., Bennike, O., Willis, K.J., Farcas, S.,

Robertsson, A.M., 2007. The influence of refugial populations on Lateglacial and early Holocene vegetational changes in Romania. Rev. Palaeobot. Palyno. 145, 305–320.

Fletcher, W.J., Zielhofer, C., 2011. Fragility of Western Mediterranean landscapes during Holocene rapid climate changes. Catena 103, 16–29.

Fletcher, W.J., Zielhofer, C., 2013. Fragility of Western Mediterranean landscapes during Holocene Rapid Climate Changes. Catena 103, 16–29.

Giraudi, C., Magny, M., Zanchetta, G., Drysdale, R.N., 2011. The Holocene climatic evolution of Mediterranean Italy: a review of the continental geological data. The Holocene 21 (1), 105–115.

Hammer, Ø., Harper, D.A.T., Ryan, P.D., 2001. PAST: Paleontological Statistics Software Package for Education and Data Analysis. Palaeontol. Electron. 4 (1) (9pp).

Hengl, T., Walsh, M.G., Sanderman, J., Wheeler, I., Harrison, S.P., Prentice, I.C., 2018. Global mapping of potential natural vegetation: an assessment of machine learning algorithms for estimating land potential. PeerJ 6:e5457. https://doi.org/10.7717/peerj.5457.

Jahns, S., van der Bogaard, C., 1998. New palynological and tephrostratigraphical investigations of two salt lagoons on the Island of Mljet, south Dalmatia, Croatia. Veget. Hist. Archaeobot. 7, 219–234.

Joannin, S., Vannière, B., Galop, D., Peyron, O., Haas, J.N., Gilli, A., Chapron, E., Wirth, S.B., Anselmetti, F., Desmet, M., Magny, M., 2013. Climate and vegetation changes during the Lateglacial and early-middle Holocene at Lake Ledro (southern Alps, Italy). Clim. Past 9, 913–933.

Kaniewski, D., Van Campo, E., Paulissen, E., Weiss, H., Bakker, J., Rossignol, I., Van Lerberghe, K., 2011. The medieval climate anomaly and the Little Ice Age in coastal Syria inferred from pollen-derived palaeoclimatic patterns. Glob. Planet. Chang. 78, 178–187.

Lobo, F.J., Ridente, D., 2014. Stratigraphic architecture and spatio-temporal variability of high-frequency (Milankovitch) depositional cycles on modern continental margins: an overview. Mar. Geol. 352, 215–247.

Lowe, J.J., Accorsi, C.A., Bandini Mazzanti, M., Bishop, V., Van der Kaars, S., Forlani, L., Mercuri, A.M., Rivalenti, C., Torri, P., Watson, C., 1996. Pollen stratigraphy of sediment sequences from carter lakes Albano and Nemi (near Rome) and from the central Adriatic, spanning the interval from oxygen isotope stage 2 to the present day. Mem. Ist. Ital. Idrobiol. 55, 71–98.

Magny, M., de Beaulieu, J.-L., Drescher-Schneider, R., Vannière, B., Walter-Simonnet, A.V., Miras, Y., Millet, L., Bossuet, G., Peyron, O., Brugiapaglia, E., Peyroux, A., 2007. Holocene climate changes in the Central Mediterranean as recorded by Lake-level fluctuations at Lake Accesa (Tuscany, Italy). Quat. Sci. Rev. 26, 1736–1758.

Magny, M., Galop, D., Bellintani, P., Desmet, M., Didier, J., Haas, J.N., Martinelli, N., Pedrotti, A., Scandolari, R., Stock, A., Vannière, B., 2009. Late Holocene climatic variabilità south of the Alps as recorded by lake-level fluctuations at Lake Ledro, Trentino, Italy. The Holocene 19 (4), 575–589.

Magny, M., Joannin, S., Galop, D., Vannière, B., Haas, J.N., Bassetti, M., Bellintani, B., Scandolari, R., Desmet, M., 2012. Holocene palaeohydrological changes in the northern Mediterranean borderlands as reflected by the lake-level record of Lake Ledro, northeastern Italy. Quat. Res. 77, 382–396.

Magny, M., Combourieu-Nebout, N., de Beaulieu, J.L., Bout-Roumazeilles, V., Colombaroli, D., Desprat, S., Francke, A., Joannin, S., Ortu, E., Peyron, O., Revel, M., Sadori, L., Siani, G., Sicre, M.A., Samartin, S., Simonneau, A., Tinner, W., Vannière, B., Wagner, B., Zanchetta, G., Anselmetti, F., Brugiapaglia, E., Chapron, E., Debret, M., Desmet, M., Didier, J., Essallami, L., Galop, D., Gilli, A., Haas, J.N., Kallel, N., Millet, L., Stock, A., Turon, J.L., Wirth, S., 2013. North-South palaeohydrological contrasts in the central Mediterranean during the Holocene: tentative synthesis and working hypotheses. Clim. Past 9, 2043–2071.

Mangerud, J., Andersen, S.T., Berglund, B.E., Dorrner, J.J., 1974. Quatcrnary stratigraphy of Norden, a proposal for terminology and classification. Boreas 3, 109–128.

Maselli, V., Trincardi, F., 2013. Man made deltas. Sci. Rep. 2013 (3), 1926. https://doi.org/10.1038/srep01926.

Mayewski, P.A., Rohling, E.E., Stager, J.C., Karlén, W., Maasch, K.A., Meecker, L.D., Meyerson, E.A., Gasse, F., van Kreveld, S., Holmgren, K., Lee-Thorp, J., Rosqvist, G., Rack, F., Staubwasser, M., Schneider, R.R., Steig, E.J., 2004. Holocene climate variability. Quat. Res. 62, 243–255.

Mercuri, A.M., 2015. Applied palynology as a trans-discipline science: the contribution of aerobiology data to forensic and palaeoenvironmental issues. Aerobiologia 31, 323–339.

Mercuri, A.M., Bandini Mazzanti, M., Torri, P., Vigliotti, L., Bosi, G., Florenzano, A., Olmi, L., Massamba N'siala, I., 2012. A marine/terrestrial integration for mid-late Holocene vegetation history and the development of the cultural landscape in the Po valley as a result of human impact and climate change. Veget. Hist. Archeobot. 21, 353–372.

Moore, P.D., Webb, J.A., Collinson, M.E., 1991. Pollen analysis, 2nd. Blackwell Scientific Publications, Oxford.

Peyron, O., Goring, S., Dormoy, I., Kotthoff, U., Pross, J., de Beaulieu, J.-L., Drescher Schneider, R., Vannière, B., Magny, M., 2011. Holocene seasonality changes in the central Mediterranean region reconstructed from the pollen sequences of Lage Accesa (Italy) and Tenaghi Philippon (Greece). The Holocene 21 (1), 131–146.

Peyron, O., Magny, M., Goring, S., Joannin, S., De Beaulieu, J.-L., Brugiapaglia, E., Sadori, L., Garfi, G., Kouli, K., Ioachim, C., Combourieu-Nebout, N., 2013. Contrasting patterns of climatic change during the Holocene across the Italian Peninsula reconstructed from pollen data. Clim. Past 9, 1233–1252.

Pignatti, S., 1979. I piani di vegetazione in Italia. Giorn. Bot. Ital. 113, 411–428.

Pignatti, S., 1982. Flora d'Italia. Edagricole, Bologna.

Pignatti, S., 1998. I boschi d'Italia – Sinecologia e biodiversità. UTET, Torino.

Pignatti, S., 2017. Flora d'Italia. Edagricole, Bologna.

Pini, R., Minari, E., Furlanetto, G., Gorian, F., Ravazzi, C., Rizzi, A., Valoti, F., 2016. Guida per il riconoscimento del polline negli ambienti forestali della Pianura Padana.

Tipografia Camuna S.p.A, Breno (Brescia, Italy).

Piovan, S., Mozzi, P., Zecchin, M., 2012. The interplay between adjacent Adige and Po alluvial systems and deltas in the late Holocene (Northern Italy). Géomorphologie 18 (4), 427–440.

Rasmussen, S.O., Vinther, B.M., Clausen, H.B., Andersen, K.K., 2007a. Early Holocene climate oscillations recorded in three Greenland ice cores. Quat. Sci. Rev. 26, 1907–1914.

Rasmussen, S.O., Bigler, M., Blockley, S.P., Blunier, T., Buchardt, S.L., Clausen, H.B., Cvijanovic, I., Dahl-Jensen, D., Johnsen, S.J., Fischer, H., Gkinis, V., Guillevic, M., Hoek, W.Z., Lowe, J.J., Pedro, J.B., Popp, T., Seierstad, I.K., Steffensen, J.P., Svensson, A.M., Vallelonga, P., Vinther, B.M., Walker, M.J.C., Wheatley, J.J., Winstrup, M., 2014. Dating, Synthesis, and Interpretation of Palaeoclimatic Records and Model-data Integration: advances of the INTIMATE project. Quat. Sci. Rev. 106, 14–28.

Rasmussen, S.O., Vinther, B.M., Clausen, H.B., Andersen, K.K., 2007b. Early Holocene Greenland Ice Core Chronology 2005 (GICC05) and 10 Year Means of Oxygen Isotope Data from Ice Core GRIP. PANGAEA.

Gli antichi bacini lacustri e i fossili di Leffe, Ranica e Pianico-Sellere (Prealpi Lombarde). In: Ravazzi, C. (Ed.), Quaderni di geodinamica alpina e quaternaria. CNR, Consiglio Nazionale delle Ricerche, Istituto per la dinamica dei processi ambientali.

Ravazzi, C., Marchetti, M., Zanon, M., Perego, R., Quirino, T., Deaddis, M., De Amicis, M., Margaritora, D., 2013. Lake evolution and landscape history in the lower Mincio River valley, unravelling drainage changes in the Central Po Plain (N-Italy) since the Bronze Age. Quat. Int. 288, 195–205.

Regione Emilia-Romagna & Eni–Agip, 1998. Riserve idriche sotterranee della Regione Emilia-Romagna. S.EL.CA, Firenze.

Regione Emilia-Romagna, Servizio Paesaggio, Parchi e Patrimonio Naturale, 1996. Cartografia fitoclimatica dell'Emilia Romagna. Carta 1:500.000. In: Assessorato Territorio, Programmazione e Ambiente, collana Studi e Documentazioni 47.

Reille, M., 1992. Pollen et spores d'Europe et d'Afrique du nord. Laboratoire de Botanique Historique et Palynologie, Marseille.

Reille, M., 1995. Pollen et spores d'Europe et d'Afrique du nord. Supplément 1. Laboratoire de Botanique Historique et Palynologie, Marseille.

Reille, M., 1998. Pollen et spores d'Europe et d'Afrique du nord. Supplément 2. Laboratoire de Botanique Historique et Palynologie, Marseille.

Reimer, P.J., Bard, E., Bayliss, A., Warren Beck, J., Blackwell, P.G., Bronk Ramsey, C., Buck, C.E., Cheng, H., Lawrence Edwards, R., Friedrich, M., Grootes, P.M., Guilderson, T.P., Haflidason, H., Hajdas, I., Hatté, C., Heaton, T.J., Hoffmann, D.L., Hogg, A.G., Hughen, K.A., Felix Kaiser, K., Kromer, B., Manning, S.W., Niu, M., Reimer, R.W., Richards, D.A., Marian Scott, E., Southon, J.R., Staff, R.A., Turney, C.S.M., Van der Plicht, J., 2013. Intcal13 and Marine13 radiocarbon age calibration curves 0-50,000 years cal BP. Radiocarbon 55, 1869–1887.

Ricci Lucchi, F., Colalongo, M.L., Cremonini, G., Gasperi, G., Iaccarino, S., Papani, G., Raffi, S., Rio, D., 1982. Evoluzione sedimentaria e paleogeografica nel margine appenninico. In: Cremonini, G., Ricci Lucchi, F. (Eds.), Guida alla geologia del margine Appenninico–Padano. Guida Geologica Regionale della Società Geologica Italiana, pp. 17–46.

Roberts, N., Allcock, S.L., Barnett, H., Mather, A., Eastwood, W.J., Jones, M., Primmer, N., Yiğitbaşıoğlu, H., Vannière, B., 2019. Cause-and-effect in Mediterranean erosion: the role of humans and climate upon Holocene sediment flux into a central Anatolian lake catchment. Geomorphology 331, 36–48.

Rossi, V., Vaiani, S.C., 2008. Microfaunal response to sediment supply changes and fluvial drainage reorganization in Holocene deposits of the Po Delta, Italy. Mar. Micropaleontol. 69, 106–118.

Sadori, L., Jahns, S., Peyron, O., 2011. Mid-Holocene vegetation history of the central Mediterranean. The Holocene 21 (1), 117–129.

Sangiorgi, F., Capotondi, L., Combourieu-Nebout, N., Vigliotti, L., Brinkhuis, H., Giunta, S., Lotter, A.F., Morigi, C., Negri, A., Reichart, G.-J., 2003. Holocene seasonal sea-surface temperature variations in the southern Adriatic Sea inferred from a multi-proxy approach. J. Quat. Sci. 18 (8), 723–732.

Sarti, G., Rossi, V., Amorosi, A., Bini, M., Giacomelli, S., Pappalardo, M., Ribecai, C., Ribollini, A., Sammartino, I., 2015. Climatic signature of two mid-late Holocene fluvial incisions formed under sea-level highstand conditions (Pisa coastal plain, NW Tuscany, Italy). Palaeogeogr. Palaeoclimatol. Palaeoecol. 434, 183–195.

Scarponi, D., Azzarone, M., Kowalewski, M., Huntley, J.W., 2017. Surges in trematode prevalence linked to centennial-scale flooding events in the Adriatic. Sci. Rep. 7, 5732. https://doi.org/10.1038/s41598-017-05979-6.

Signell, R.P., Chiggiato, J., Horstmann, J., Doyle, J.D., Pullen, J., Askari, F., 2010. High resolution mapping of Bora winds in the northern Adriatic Sea using synthetic aperture radar. J. Geophys. Res. 115, C04020.

Stefani, M., Vincenzi, S., 2005. The interplay of eustasy, climate and human activity in the late Quaternary depositional evolution and sedimentary architecture of the Po Delta system. Mar. Geol. 222-223, 19–48.

Styllas, M.N., Ghilardi, M., 2017. Early- to mid-Holocene paleohydrology in northeast Mediterranean: the detrital record of Aliakmon River in Loudias Lake, Greece. The Holocene 27, 1487–1498.

Subally, D., Quézel, P., 2002. Glacial or interglacial: *Artemisia*, a plant indicator with dual responses. Rev. Palaeobot. Palyno. 120, 123–130.

Tarasov, P.E., Cheddadi, R., Guiot, J., Bottema, S., Peyron, O., Belmonte, J., Ruiz-Sanchez, V., Saadi, F., Brewer, S., 1998. A method to determine warm and cool steppe biomes from pollen data; application to the Mediterranean and Kazakhstan regions. J. Quat. Sci. 13 (4), 335–344.

Tomaselli, M., 1970. Note illustrative alla carta della vegetazione naturale potenziale d'Italia. Min. Agr. Foreste, Collana verde 27, Roma.

Tomaselli, M. (Ed.), 1987. Guida alla vegetazione dell'Emilia Romagna. Collana Annali, Facoltà di Scienze MM., FF., NN. Università di Parma.

Tutin, T.G., Heywood, V.H., Burges, N.A., Valentine, D.H., 1993. Flora europaea. Cambridge University Press.

Tüxen, R., 1956. Die heutige potentielle natürliche Vegetation als Gegenstand der Vegetationskartierung. Angewandte Pflanzensoziologie (Stolzenau) 13, 4–42.

Ubaldi, D., 2003. Flora, fitocenosi e ambiente. In: Elementi di geobotanica e fitosociologia. CLUEB, Bologna.

Vacchi, M., Marriner, N., Morhange, C., Spada, G., Fontana, A., Rovere, A., 2016. Multiproxy assessment of Holocene relative sea-level changes in the western Mediterranean: sea-level variability and improvements in the defnition of the isostatic signal. Earth-Sci. Rev. 155, 172–197.

Valsecchi, V., Finsinger, W., Tinner, W., Ammann, B., 2008. Testing the influence of climate, human impact and fire on the Holocene population expansion of Fagus sylvatica in the southern Prealps (Italy). The Holocene 18 (4), 603–614.

Vannière, B., Power, M.J., Roberts, N., Tinner, W., Carrión, J., Magny, M., Bartlein, P., Colombaroli, D., Daniau, A.L., Finsinger, W., Gil-Romera, G., Kaltenrieder, P., Pini, R., Sadori, L., Turner, R., Valsecchi, V., Vescovi, E., 2011. Circum-mediterranean fire activity and climate changes during the mid-Holocene environmental transition (8500-2500 cal. BP). The Holocene 21 (1), 53–73.

Walker, M., Berkelhammer, M., Björck, S., Cwynar, L., Fisher, D.A., Long, A.J., Lowe, J.J., Newnham, R.M., Rasmussen, S.O., Weiss, H., 2012. Formal subdivision of the Holocene Series/Epoch: a discussion paper by working group of INTIMATE (Integration of ice-core, marine and terrestrial records) and the Subcommission on Quaternary Stratigraphy (International Commissiono f Stratigraphy). J. Quat. Sci. 27 (7), 649–659.

Walker, M., Head, M.J., Berkelhammer, M., Björck, S., Cheng, H., Cwynar, L., Fisher, D., Gkinis, V., Long, L., Lowe, J., Newnham, R., Rasmussen, S.O., Weiss, H., 2018. Formal ratification of the subdivision of the Holocene Series/ Epoch (Quaternary System/ Period): two new Global Boundary Stratotype Sections and Points (GSSPs) and three new stages/ subseries. Episodes 41 (4), 213–223. https://doi.org/10.18814/epiiugs/2018/018016.

Watts, W.A., Allen, J.R.M., Huntley, B., 1996. Vegetation history and palaeoclimate of the last Glacial period at Lago Grande di Monticchio, Southern Italy. Quat. Sci. Rev. 15, 133–153.

Zhornyak, L.V., Zanchetta, G., Drysdale, R.N., Hellstrom, J.C., Isola, I., Regattieri, E., Piccini, L., Baneschi, I., Couchoud, I., 2011. Stratigraphic evidence for a "pluvial phase" between ca 8200-7100 ka from Renella cave (Central Italy). Quat. Sci. Rev. 30, 409–417.

6. PALYNO-STRATIGRAPHIC RECORD OF THE ARNO DELTA PLAIN

6.1 Manuscript 3

Palynological characterization of Late Quaternary stratigraphic cyclicity and sequence stratigraphic implications*

Marco Cacciari, Alessandro Amorosi, Bruno Campo, Marco Marchesini, Veronica Rossi

Palynology of the late Quaternary succession of the Arno Plain (northern Italy): new insights on palaeoenvironmental trends and climate dynamics

Marco Cacciari, Alessandro Amorosi, Bruno Campo, Marco Marchesini & Veronica Rossi

M. Cacciari, Università di Bologna, Dipartimento di Scienze Biologiche, Geologiche e Ambientali, Via Zamboni 67, I-40126 Bologna, Italy; marco.cacciari3@unibo.it

A. Amorosi, Università di Bologna, Dipartimento di Scienze Biologiche, Geologiche e Ambientali, Via Zamboni 67, I-40126 Bologna, Italy; alessandro.amorosi@unibo.it

B. Campo, Università di Bologna, Dipartimento di Scienze Biologiche, Geologiche e Ambientali, Via Zamboni 67, I-40126 Bologna, Italy; bruno.campo2@unibo.it

M. Marchesini, Università di Ferrara, Dipartimento di Studi Umanistici, Via Ercole I d'Este 32, I-44121 Ferrara, Italy; mmarchesini@caa.it

V. Rossi, Università di Bologna, Dipartimento di Scienze Biologiche, Geologiche e Ambientali, Via Zamboni 67, I-40126 Bologna, Italy; veronica.rossi4@unibo.it

KEY WORDS - Palynology, palaeoclimate, palaeoenvironment, late Pleistocene, Holocene, Tuscany.

ABSTRACT - Palynological analyses, backed by meiofauna (ostracods and benthic foraminifers), sedimentological and radiocarbon data, enabled the identification of late Quaternary turnovers of depositional environments and coeval vegetation dynamics from a ca. 30 m-long core succession (core PA1), retrieved in the Arno delta area (N Italy), 2 km landwards of the innermost outcropping beach ridge. Based on the identification of 213 palynomorph taxa (pollen and spores), eleven ecological groups were elaborated and their relative frequencies stratigraphically plotted, allowing the identification of eight bio-sedimentary units (BSUs) and four vegetation phases dated to the late Pleistocene onwards. The former record palaeoenvironmental changes, mainly in terms of water-table level and salinity. The latter reflect different palaeoclimate conditions at both Milankovitch and sub-Milankovitch timescales, relying on the proportion of montane versus Mediterranean taxa. The vertically stacked pattern of BSUs reveals two transgressive-regressive cycles developed above an alluvial plain succession stratigraphically assigned to the penultimate glacial interval (Marine Isotope Stage-MIS 6). Both depositional cycles show a transgressive portion composed of swampy-lagoonal clays formed under interglacial conditions. Pollen (Mediterranean forest with increasing optimum-like conditions) suggests a MIS 5e age for the lowermost transgressive interval, whereas the palynological assemblage (Mediterranean/ sub-Mediterranean forest) and radiocarbon ages consistently indicate an early Holocene age (ca. 9800-7400 cal yrs BP) for the uppermost one. A climate-driven phase of subaerial exposure, likely related to the onset of the last glacial period, affected the MIS 5e lagoon, as testified by the record of an open/sparse pine forest within pedogenised alluvial deposits sandwiched between the two lagoon intervals. By contrast, the early Holocene lagoon experienced a long-term trend of sedimentary filling by river inputs under rather stable interglacial, highstand conditions. Only at the end of climate optimum conditions, marked by a peak of Fagus *dated around 5000 cal yrs BP, the lagoon turned into a delta plain. This study documents the successfully use of a multi-proxy, palynological-based approach to investigate the complex interplay between environments, vegetation and climate changes in alluvial-coastal plain contexts and within a sequence-stratigraphic perspective.*

RIASSUNTO - [Il record palinologico della successione tardo quaternaria della pianura dell'Arno (Italia settentrionale): caratterizzazione paleoambientale e paleoclimatica] - Le associazioni polliniche fossili/sub-fossili presenti nei depositi di sottosuolo delle attuali pianure deltizio-costiere sono ottimi strumenti per investigare le relazioni esistenti fra le variazioni paleoambientali e paleoclimatiche dal tardo Quaternario ad oggi. In questo lavoro sono presentati e discussi i risultati ottenuti tramite un'analisi quantitativa palinologica, comprendente pollini e spore di Pteridofite e Briofite, e semi-quantitativa del contenuto in ostracodi e foraminiferi bentonici del sondaggio a carotaggio continuo PA 1, profondo circa 30 m e ubicato 2 Km a est del cordone affiorante più antico della pianura deltizia del Fiume Arno (Toscana, Italia settentrionale).

A partire da 213 taxa di palinomorfi (145 pollini, 68 spore) sono stati elaborati undici gruppi ecologici. Integrando gli spettri pollinici e di spore coi dati sedimentologici, meiofaunistici e le datazioni al radiocarbonio, sono state identificate lungo la stratigrafia di sondaggio otto unità bio-sedimentarie (BSU-Bio Sedimentary Units) che corrispondono a specifiche condizioni paleoambientali in termini soprattutto di livello della tavola d'acqua, salinità, grado di umidità e di disturbo ambientale (naturale e/o antropico). Il dato relativo alla pioggia pollinica a carattere più regionale, ed in particolare il rapporto fra alcuni gruppi ecologici, ha inoltre permesso di identificare entro lo stesso record deposizionale quattro differenti fasi della vegetazione corrispondenti ad altrettante condizioni paleoclimatiche inquadrabili dal Pleistocene superiore ad oggi.

L'impilamento verticale delle BSU documenta lo sviluppo di due cicli trasgressivo-regressivi al di sopra di depositi di pianura alluvionale, stratigraficamente attribuibili al penultimo periodo glaciale (MIS-Marine Isotope Stage 6). Entrambi i cicli mostrano una tendenza simile sia per quanto riguarda la successione dei diversi paleoambienti sia per le concomitanti variazioni nel paesaggio vegetale. Praterie igrofile molto disturbate con un elevato numero di taxa di Briofite si sviluppano in corrispondenza delle due superfici trasgressive e indicano condizioni paleoambientali instabili nelle quali le piante erbacee pioniere formano le prime associazioni vegetali. La porzione trasgressiva di ogni ciclo è composta da depositi fini di ambiente palustre-lagunare contenenti un'associazione pollinica tipica di un periodo interglaciale (querco-lecceta mista). La stretta relazione esistente fra evoluzione paleoambientale e oscillazioni paleoclimatiche è inoltre confermata dalla concomitante transizione verso condizioni lagunari maggiormente marino-influenzate dal pieno sviluppo della querco-lecceta mista. Tuttavia, le dinamiche della vegetazione durante i due interglaciali mostrano alcune importanti differenze. Durante la formazione della laguna trasgressiva olocenica (circa 9800-7400 anni calibrati BP) la vegetazione non raggiunge mai un alto grado di sclerofillia, che è invece molto evidente nel registro pollinico della laguna formatasi precedentemente ed interpretata come espressione del MIS 5e. La stessa laguna tirreniana subisce una fase di emersione che porta alla formazione di una serie di paleosuoli e all'instaurarsi di una piana inondabile (porzione regressiva del ciclo) in concomitanza di un netto cambio nella vegetazione: la querco-lecceta viene sostituita da una rada pineta planiziale, ad indicare condizioni tipiche di un periodo glaciale.

L'espressione stratigrafica della laguna olocenica è maggiormente sviluppata nel sottosuolo della pianura dell'Arno, poiché essa registra non solo la fase trasgressiva ma anche la successiva prima fase di stazionamento alto del livello marino. Al suo interno, sia le associazioni

palinologiche sia la meiofauna documentano condizioni paleoambientali e paleoclimatiche relativamente stabili fino a circa 5000 anni calibrati fa. Solo in quel momento, in concomitanza con un periodo di deterioramento climatico suggerito dal picco del faggio e coincidente con l'uscita dall'optimum climatico, la laguna si trasforma in piana deltizia ad opera degli apporti fluviali. Il suo riempimento è ben documentato dalla diffusione del salice, a formare un bosco igrofilo, al quale si sussegue un ambiente emerso prettamente alluvionale caratterizzato da un'associazione di prateria con elementi antropici (polline di bietola ed altri elementi che indicano un ambiente generalmente disturbato) che porta alla drastica riduzione della copertura arborea.

INTRODUCTION

Palynology represents a versatile tool in Quaternary Geology, successfully exploitable in several research fields (e.g., palaeoclimate, palaeoecology and palaeobiology, sequence stratigraphy, geoarchaeology) and stratigraphic contexts from marine to continental realms (e.g., Ravazzi, 2002; Bertini et al., 2010, 2014; Combourieu-Nebout et al., 2015; Cremaschi et al., 2016; Milli et al., 2016; Sadori et al., 2016; Desprat et al., 2017; Revelles et al., 2017). In particular, the palyno-stratigraphic analysis of non-marine Mediterranean successions (e.g., lacustrine, lagoonal-paludal and floodplain deposits) allows investigating both regional (climate) and local (environment) vegetation dynamics in response to well-known Quaternary climate oscillations, at Milankovitch (i.e., 100 kyrs-cyclicity) and sub-Milankovitch timescales (10 kyrs-cyclicity or less), or to the Holocene human pressure. This latter started to accelerate around 8000 cal yrs BP with the Neolithic agriculture revolution and increased with the development of the first urban centres, especially since the Bronze age, becoming a major driver of landscape changes as much as climate at decadal to centennial timescales (Hooke, 2000).

Although the Mediterranean lacustrine record is the most exploited, being characterised by thick and relatively continuous successions prone to be robustly dated (Follieri et al., 1988; Tzedakis et al., 2006; Colombaroli et al., 2007; Magny et al., 2012 among others), coastal-delta plains and, in particular, (palaeo)lagoonal basins have undergone a growing interest by the Quaternary research community during the last decade (e.g., Bellini et al., 2009; Jalut et al., 2009; Giraudi, 2012; Di Rita et al., 2015, 2018; Dolez et al., 2015; Ejarque et al., 2016; Arobba et al., 2018; Kaniewski et al., 2018). Indeed, the subsurface successions of these areas, located at the edge between land and sea, are naturally prone to record even subtle palaeoenvironmental changes potentially forced by a combination of allogenic (e.g., RSL-relative sea level and climate) and autogenic (e.g., human activity, inherited morphology/palaeotopography, local tectonics) factors. Moreover, they commonly contain a lot of sedimentological and palaeobiological proxies other than palynomorphs, such as molluscs, meiofauna, sedimentary structures and pedogenic features, that can strongly support and improve stratigraphic reconstructions. In Italy, only few studies (Mozzi et al., 2003; Ricci Lucchi, 2008; Amorosi et al., 2009; Milli et al., 2013, 2016; Breda et al., 2016) fully applied palynology to investigate the depositional cycles buried beneath the modern coastal-delta plains with an interdisciplinary perspective comprising a sequence-stratigraphic framework for chronological intervals longer than the present interglacial (MIS-Marine Isotope Stage 1; last ca. 17000 years).

This study provides a detailed palynological characterisation (i.e., pollen and spores of Pteridophytes and Bryophytes), accompanied by a semi-quantitative meiofauna analysis, of the late Quaternary succession buried beneath a key portion of the Arno coastal plain (N Italy; newly drilled core PA1 in Fig. 1), where two lagoonal intervals separated by indurated horizons are recovered by several cores within the uppermost 30 m (e.g., core P1 in Amorosi et al., 2008; Fig. 1). Since age, forcing factors and sequence-stratigraphic implications of this stratal stacking patterns are still unknown, we aim: 1) to better characterise such stratigraphic cyclicity in terms of palaeoenvironment, palaeoclimate and chronology by means of microfossil turnovers backed by radiocarbon dates, and 2) to furnish new insights into the linkage between depositional trends and climate changes in coastal contexts. Specific aim is to contribute in reconstructing past vegetational phases of the Arno Plain, in the framework of the reference lacustrine records available for the Ligurian-Tyrrhenian coastal sector (i.e., Massaciuccoli Lake in Colombaroli et al., 2007 and Mariotti Lippi et al., 2007; Accesa Lake in Drescher-Schneider et al., 2007; Valle di Castiglione in Follieri et al., 1988 and reviews by Ribecai, 2011, and Di Rita & Magri, 2012).

STUDY SITE

Geological and stratigraphic setting

The Arno coastal plain (N Tuscany, Italy) is a 450 km^2 wide, low-lying area that belongs to the onshore portion of the subsiding Viareggio Basin (VB), a NW-SE half-graben basin developed since the late Tortonian (ca. 8-7 Myrs ago) in response to the counter-clockwise migration of the Appennine foredeep-foreland system (Martini & Sagri, 1993). A still active NE-SW transverse lineament (Livorno-Sillaro Line in Bortolotti, 1966) runs at the foothills of the Leghorn and Pisa Hills (Fig. 1), marking the southern limit of the basin. The southern portion of the VB is filled with a ca. 2500 m-thick sedimentary succession, whose superficial expression corresponds to the Arno Plain, bordered by the Pisa Mountains to the east, the Versilia Plain/Serchio River to the north and the Ligurian Sea to west (Fig. 1). The infilling succession is formed by a variety of marine, coastal and alluvial deposits organised into five unconformity-bounded units of late Miocene to Quaternary age, identified on the basis of seismic lines and deep wells (Pascucci, 2005).

The uppermost 100 meters of the Quaternary unit have been investigated in detail during the last ten years by means of a multi-proxy stratigraphic approach (sedimentology, micropalaeontology, geochemistry), which revealed a complex history of valley incision and filling with the uncommon preservation of two non-coeval incised-valley systems (IVSs), developed in different portions of the plain during non-consecutive glacial-interglacial cycles (Rossi et al., 2017). The IVSs are made up mainly of mud-prone estuarine successions (incised-valley fills-IVFs), which have been chronologically
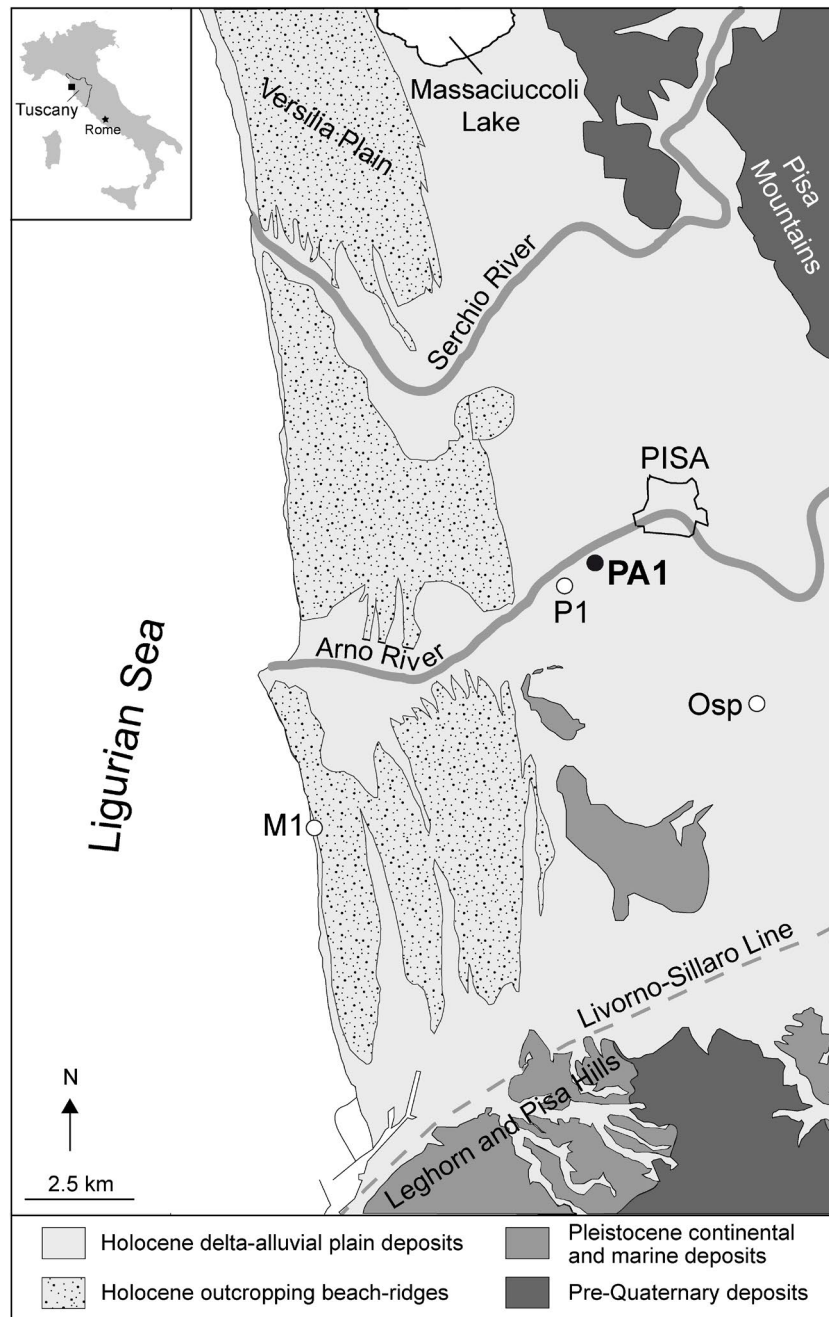
Fig. 1 - Geological sketch map of the Arno coastal plain with the location of the studied core PA1 and other reference cores (shown as white dots) mentioned in the text.

constrained to the present (MIS 1 in core M1; Fig. 1) and penultimate (MIS 7 in core Osp; Fig. 1) interglacials (Rossi et al., 2017). Each IVF exhibits a complex alternation of inner and outer estuarine deposits organised into an overall retrogradational stacking pattern of facies (transgressive systems tract), which culminates with a beach-barrier sand body that marks the maximum marine ingression (Amorosi et al., 2008; Rossi et al., 2017).

The following inundation of the interfluves, with the formation of a sea-level highstand succession (highstand systems tract), is recorded exclusively above the uppermost IVS, due to significant post-MIS 7 fluvial erosion probably related to the onset of glacial conditions.

The two palaeovalley systems are separated by a fluvial channel belt, a few tens of metres thick, built by the Arno River. These stratigraphic features point to a predominant glacio-eustatic control on the Arno plain depositional architecture at the Milankovitch scale. Local tectonism, however, possibly played a key role in determining changes of the river network (i.e., northward shift of river incision; Rossi et al., 2017).

During the mid-late Holocene period (last 8000-7000 years), a strong deceleration in relative sea-level rise (Vacchi et al., 2016), combined with autogenic factors (palaeotopography and river dynamics), led to the development and subsequent filling of a wide lagoon

superimposed on the MIS 1 IVS (Rossi et al., 2017). Lagoonal deposits, which are chronologically constrained to ca. 8000-5000 cal yrs BP (Benvenuti et al., 2006; Amorosi at al., 2013), occur between ca. 20-5 m below sea level (b.s.l.) and show seaward transition to beach-barrier sands and shallow-marine clays. Upwards, a 10-15 m thick prograding succession of swamp and floodplain deposits, locally encasing lenticular fluvio-deltaic sandy bodies (i.e., channel-fill, crevasse splay, levee), documents the growing phase of the Arno deltaic-alluvial system (Bini et al., 2015; Sarti et al., 2015).

Vegetation and climate context

The climate of the study area is Mediterranean/sub-Mediterranean, with a mean temperature of 15° C and a mean precipitation of ca. 900 mm/year as recorded at the weather station at Pisa (Fig. 1). The modern vegetation of the Arno coastal plain belongs to the meso-Mediterranean belt sensu Pignatti (1979), although many factors complicate the vegetal landscape. In fact, the proximity of the Ligurian coastal vegetation to the north, influenced by an Atlantic climate, and of a succession of altitudinal vegetation belts (similar to those described by Ubaldi, 2003 for the Emilia Romagna region and by Pignatti, 1979 for the whole Italian Peninsula), such as the sub-montane mixed oak forest and the beech woods on the Apennines to the N and NE, create a mosaic of Mediterranean/sub-Mediterranean woods. Subordinate hygro/mesophilous woods develop on inter/retrodunal areas (Garbari, 2004), as the main source of hygrophily is the presence of the Arno and Serchio rivers (Fig. 1). In this context, a mixture of xerophilous/evergreen taxa typical of the Mediterranean maquis (i.e., *Erica arborea* Linnaeus, 1753; *Quercus ilex* Linnaeus, 1753; and *Phillyrea*) thrive in association with both mesic elements composing the mixed oak woods (i.e., *Ostrya carpinifolia* Scopoli, 1772; *Quercus cerris* Linnaeus, 1753; *Q. pubescens* Willdenow, 1805; *Q. robur* Linnaeus, 1753; *Tilia* and *Ulmus*) and hygrophilous taxa like *Alnus glutinosa* Gaertner, 1790; *Populus* and *Salix* (Bellini et al., 2009; Ribecai, 2011). Beech woods (*Fagus sylvatica* Linnaeus, 1753) are in upper transition with fir-spruce and Scottish pine forests and then with the ericaceous shrublands above the timberline. The Apennine orographic divide is the vegetation symmetry axis between Emilia Romagna and Tuscany, this latter bearing, stronger degrees of mediterraneity (Ubaldi, 2003). Nonetheless, this pattern was heavily altered in recent times by anthropic activities and led to the partial substitution of beech by chestnut and pine (Arrigoni et al., 1999).

MATERIAL AND METHODS

Coring campaign and sedimentological analysis

The 31.5 m-long core PA1 was recovered immediately south to the modern Arno River course at about 1.5 m above mean sea level and ca. 2 km landwards of the innermost outcropping beach ridge (Fig. 1), archaeologically dated to the pre-Roman period (older than ca. 2000 cal yrs BP; Pranzini, 2007). The adopted continuous perforating technique guaranteed an almost undisturbed core stratigraphy and very high recovery percentages (> 95%), allowing the detailed description of sedimentological

features and a robust identification of the sedimentary units that guided the sampling strategy for palaeontological analyses (i.e., palynomorphs and meiofauna). The core was split lengthwise and described in terms of sediment texture and colour, type of contacts between units, pedogenic features (calcareous nodules, Fe-Mn oxides) and the presence of accessory materials including wood fragments, decomposed organic matter, mollusc shells and fragments. Pocket penetration values were also measured from fine-grained (silt and clay) intervals for robust palaeosol identification (Amorosi et al., 2017).

Palynological and meiofauna analyses

Palynological analyses were carried out on 33 samples to 1) obtain a detailed palaeoenvironmental characterisation of the sedimentary units using pollen (especially the local pollen rain) and non-pollen palynomorphs - NPP (mainly including Pteridophyte and Bryophyte spores), and 2) reconstruct palaeoclimate conditions on the basis of the regional pollen rain. Samples were treated following Lowe et al. (1996), and described as follows: 1) about 3-9 g of dry sediment were weighed and a *Lycopodium* tablet was added to calculate palynomorph concentration; 2) samples were then manually disrupted in a 10% Na-pyrophosphate solution and filtered through a 0.5 mm sieve and a 5 µm nylon filter; 3) a series of chemical treatments was then applied (10% HCl solution to remove carbonates, acetolysis for excess organics, hydrate Na-metatungstate heavy liquid, 40% HF solution, ethanol suspension) and 4) after an evaporation at 60 °C, microscope slides were prepared with glycerine jelly and paraffin. For each sample, 300 pollen grains were counted (where possible) and recognised using published illustrations and morphological keys (Faegri et al., 1989; Moore et al., 1991; Reille, 1992, 1995, 1998). Bryophyte spores were recognised using Boros et al. (1993).

Pollen percentages were calculated on the basis of the total pollen sum (Tab. 1 of the Supplementary Online Material [SOM]). Hygrophytes and aquatics were included for detecting the environmental characteristics, especially considering the high facies variability of the Holocene deposits and the high significance of humid environments in shaping local vegetation (Amorosi et al., 2013). However, a separate calculation of pollen percentages was elaborated excluding hygrophytes and aquatics to verify possible masking effects of local vegetation (Tab. 2 of SOM). Percentages of Pteridophytes, Bryophytes, *Pseudoschizaea circula* Christopher (1976), undeterminable and secondary grains (i.e., grains showing evidences of intense reworking) were calculated on the total sum of pollen grains and their respective values, a technique allowing a correct down-weighting of their presence (Berglund & Ralska-Jasiewiczowa, 1986). Species ecological characterisation was based on Pignatti (1979, 1982), Berglund & Ralska-Jasiewiczowa (1986) and Tutin et al. (1993). Ostracod and benthic foraminifer analyses were also performed on a total of 39 samples to support and improve palaeoenvironmental reconstructions, as these faunal groups are known to be excellent palaeoecological indicators in coastal settings, especially of changes in salinity and degree of confinement (e.g., Debenay & Guillou, 2002; Holmes & Chivas, 2002; Murray, 2006). Samples were prepared following the

standard procedure reported by Amorosi et al. (2014). Approximately 40-50 g of sediments were dried in an oven for eight hours at 40° C, soaked in water, wet sieved through 63 μ (240 mesh) sieves and dried again. Twenty-one samples showing an autochthonous meiofauna were semi-quantitatively analysed in the size fraction > 125 μ following the method adopted by Aguzzi et al. (2007). Species identification relied upon several key papers (i.e., Jorissen, 1988; Athersuch et al., 1989; Albani & Serandrei Barbero, 1990; Henderson, 1990; Sgarrella & Moncharmont Zei, 1993; Montenegro & Pugliese, 1996).

Chronology

The chronological framework was based on four AMS ¹⁴C ages performed at KIGAM Laboratory (Daejeon, Republic of Korea) on carbon-rich samples, including mollusc shells, vegetal remains and organic matter. Conventional ages were converted into calibrated ages using Calib 7.04 (Stuiver et al., 2019) with the IntCal 13 and Mixed Marine NoHem curves (Reimer et al., 2013). A value of DeltaR (1±30), estimated for the Ligurian Sea (http://calib.org/marine/) was applied to the mollusc samples. All ages with an appropriate calibration curve are reported as the highest probability range (cal yr BP) using two standard deviations-2σ (Tab. 1). The age-depth model was constructed for the sedimentary interval in between the core top and a set of indurated horizons, on the basis of two ages from PA1 and two radiocarbon dates from the nearby core Mappa 3 (2.4 m a.s.l., located ca. 125 m SE; Tab. 1) that is characterised by an identical stratigraphy. A smoothing spline function (0.725 smoothing) in PAST (PAlaeontological Statistic-version 3.10 by Hammer et al., 2001) was applied on the radiocarbon dataset and no differential sediment compaction was taken into account.

RESULTS

Arno Plain palynological and meiofauna ecological groups

In general, pollen percentages excluding hygrophytes and aquatics showed similar proportions to those calculated from the total pollen sum, so palaeoenvironmental and palaeoclimatic inferences are based on the total sum including these taxa to better characterise wet environments throughout the section. Pollen grains and

spores show a high degree of preservation and the number of indeterminable grains ranges 3-26%. More than two hundred (213) taxa were identified (i.e., 145 pollen types and 68 spore types), along with the amount of secondary grains always lower than 23%. Total palynomorph concentration values range from 82 to 434.218 grains/g and a high number of taxa was generally recorded where pollen counts exceed 100 grains, especially for what concerns Spermatophytes (Fig. 2). Based on ecological features, pollen and spore taxa were clustered into nine and eight groups, respectively. Apart from Alia, a total of eleven ecological groups-EGs (named as Mt, M, Q+other DT, Hyg, Aq, pm, Ai, hal, omb, heli, hum; Fig. 3) were identified within our dataset, as in some cases pollen and spores belong to the same group. The Mt group (Fig. 4) includes taxa living at medium and/or high altitudes on the Apennines (Pignatti, 1979), such as *Alnus incana* (Linnaeus) Moench, 1794, *A. viridis* Gaertner, 1790, *Betula pubescens* Erhart, 1789 and *Fagus sylvatica* Linnaeus, 1753 among the broadleaves, and *Abies alba* Miller, 1768, *Larix decidua* Miller, 1768, *Picea abies* Karsten, 1881 and *Pinus mugo* Turra, 1764 among conifers. Since pollen abundances of *Pinus* sp. and undetermined Pinaceae grains show a trend similar to the conifers, they were included in Mt. A few montane Bryophytes were also found (*Dicranoweisia crispula* [Hedwig] Milde, 1869, and *Mylia taylori* [Hook] Gray, 1821). The M group (Fig. 4) includes taxa belonging to the Mediterranean evergreen and sclerophyllous forest, such as *Quercus ilex* and *Erica arborea*. The Q+other DT group gathers taxa belonging to the mixed oak forest that can be found associated with Mediterranean or sub-Mediterranean woods (Pignatti, 1979). These taxa are mainly represented by *Carpinus betulus* Linnaeus, 1753, *Celtis australis* Linnaeus, 1753, *Corylus avellana* Linnaeus, 1753, *Fraxinus* spp., *Quercus* spp., *Ostrya carpinifolia, Tilia* spp. and *Ulmus* spp. Hygrophilous taxa are also present and form the Hyg group (Fig. 5). This group includes trees as *Alnus glutinosa, Populus* and *Salix*, herbs as *Carex*, undetermined Cyperaceae and *Caltha palustris* Linnaeus, 1753, Pteridophytes (*Asplenium, Isoetes durieui* Bory, 1844, and undetermined monolete and trilete spores) and Bryophytes (*Dicranella cerviculata* [Hedwig] Schimper, 1856, *Fissidens rufulus* Bruch & Schimper, 1851 and *Phaeoceros laevis* Proskauer, 1951) spores. Another ecological group includes aquatic taxa

Core_sample depth (m)	Dating materials	Conventional age (yrs BP)	Calibrated age range (cal yrs BP)	Calibration dataset	References	Coordinates
PA1_24.95	vegetal remains	26030±170	30757-29748	IntCal 13	this study	42°53'55.7806"N - 28°36'0.0421"E
PA1_24.10	mollusc shell	46000±650	*50000-47825	Mixed Marine NoHem (50%)	this study	42°53'55.7806"N - 28°36'0.0421"E
PA1_17.95	organic matter	8820±40	9957-9696	IntCal 13	this study	42°53'55.7806"N - 28°36'0.0421"E
PA1_13.35	mollusc shell	6640±30	7425-7288	Mixed Marine NoHem (50%)	this study	42°53'55.7806"N - 28°36'0.0421"E
Mappa 3_6.65	wood fragments	4155±64	4842-4523	IntCal 13	Bini et al. (2018)	42°53'53.0168"N - 28°36'3.8080"E
Mappa 3_5.75	wood fragments	3496±27	3843-3693	IntCal 13	Sarti et al. (2015)	42°53'53.0168"N - 28°36'3.8080"E

Tab. 1 - List of the radiocarbon dates reported in the paper. Local reservoir correction was applied to mollusc shells samples (DeltaR estimation: 1±30). Calibrated ages are reported as the two standard deviations range. Asterisk marks the range close to the end of the calibration data set.
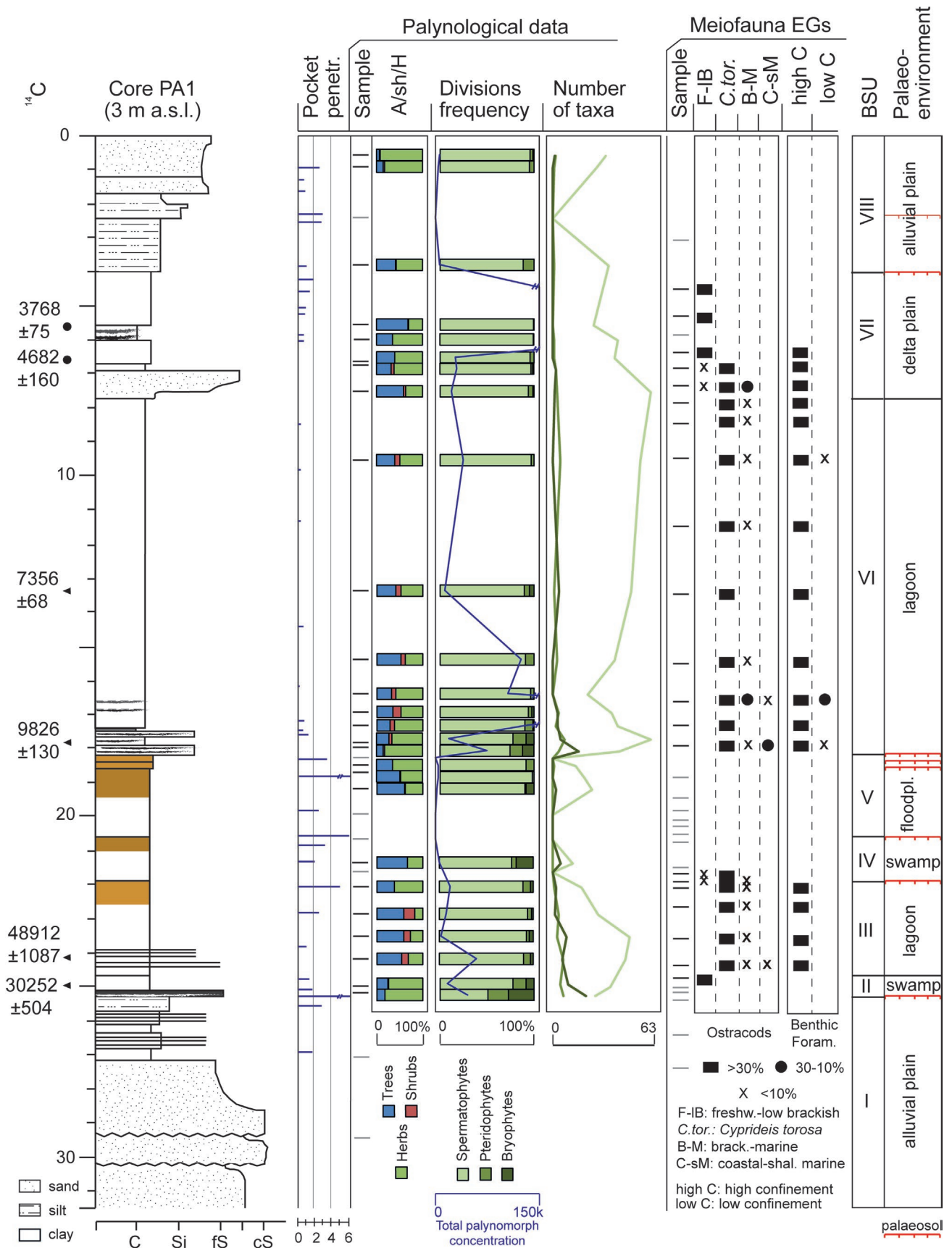
(Aq; Fig. 5), mainly *Butomus umbellatus* Linnaeus, 1753, *Callitriche* spp., *Schoenoplectus, Sparganium* spp. and *Typha* spp. among herbs, *Isoetes hystrix* Bory, 1844 and *I. lacustris* Linnaeus, 1753 among Pteridophytes and *Sphagnum* spp. among Bryophytes. *Concentricystes* algae are also present (Fig. 5). Pasture-meadow (pm group) indicators mainly include undetermined Asteroideae, Cichorioideae and Poaceae, while Anthropic indicators (Ai group), interpreted as accounting for natural disturbance when anthropic key taxa were absent, are composed of various Asteroideae, Caryophyllaceae and Polygonaceae, *Beta vulgaris* Linnaeus, 1753 and other Chenopodiaceae (Fig. 6). Finally, halophytes (hal group) are mainly represented by *Artemisia* and *Corrigiola* spp. (Fig. 6). Peculiar to Bryophytes are the omb (ombrotrophic), heli (heliophilous) and hum (humicolous) groups, always represented by rare taxa.

Concerning the meiofauna, ostracods are abundant between 25-21 m and 18-7 m core depths and are mainly represented by *Cyprideis torosa* (Jones, 1850; Fig. 2). All ostracod taxa were grouped into four categories based on their ecological characteristics, mainly driven by salinity according to Amorosi et al. (2014) and Mazzini et al. (2017): freshwater to low brackish (F-lB); euryhaline (E); brackish-marine (B-M) and coastal-shallow marine (C-sM). The F-lB group includes the following taxa: *Pseudocandona* cf. *P. albicans* (Brady, 1864), *Heterocypris salina* (Brady, 1868), *Cyclocypris* spp. and *Ilyocypris* spp. The euryhaline group is exclusively composed of *Cyprideis torosa*, a species tolerant to salinity values ranging from almost freshwater to hypersaline (Athersuch et al., 1989; Gliozzi and Grossi, 2008; Frenzel et al., 2010; Berndt et al., 2019). *Loxoconcha elliptica* Brady, 1868, *L. stellifera* Müller, 1894, and *Leptocythere bacescoi* (Rome, 1942) mainly compose the brackish-marine group, while *Palmoconcha turbida* (Müller, 1912) and *Pontocythere turbida* (Müller, 1894) represent the coastal-shallow marine taxa.

Although commonly less numerous, benthic foraminifers occur within the same stratigraphic intervals with the dominance of *Ammonia tepida* (Cushman, 1926) and *Ammonia parkinsoniana* (d'Orbigny, 1839) that are typical of high confinement settings (high confinement group-hC sensu Debenay & Guillou, 2002), along with *Haynesina germanica* (Ehrenberg, 1840) and *Quinqueloculina seminula* (Linnaeus, 1758). Other miliolids (*Adelosina* spp., *Triloculina* spp. and *Miliolinella* spp.) and *Aubignyna perlucida* (Heron-Allen & Earland, 1913) compose the low confinement (lC) species group. Poorly-preserved specimens of deep-sea taxa, interpreted as transported, are recorded within few samples collected at 24.70 m, 20.15 m and 16.55 m core depths.

Bio-sedimentary units and palaeoenvironments

Eight bio-sedimentary units (BSUs) were identified combining the micropalaeontological content (pollen, NPP and meiofauna) with the sedimentological features recorded along the cored succession (Figs 2-6). Following an ascending order, BSUs are described and interpreted in terms of palaeoenvironments (Figs 2-3). For this reason, special emphasis was placed on palynological groups/taxa strictly related to the local pollen rain (i.e., Hyg, Aq, pm and hal groups) and spores.

BSU I (31.5-25.15 m core depth) - This unit, ca. six m thick, displays an overall fining-upward trend. It consists of a lower sandy portion overlain by grey clay-silt locally interbedded with cm-thick sandy layers. The sand is organised into vertically stacked m-thick sequences, showing internal fining-upward trends from medium-coarse to medium-fine grain size. The upper fine-grained portion, which shows pocket penetration values ranging between 2-3 kg/cm^2, contains sparse iron (Fe) and manganese (Mn) oxides and calcareous nodules. The unit is capped by a stiff (penetration value > 6 kg/cm^2) dark horizon composed by silty sands. No microfossils were recovered (Fig. 2). Absolute ages are not available for this unit.

Sedimentological features and the absence of a meiofauna point to an alluvial environment, with the development of fluvial-channel sands abruptly replaced by overbank deposits. The stiff horizon atop the unit documents a prolonged subaerial exposure accompanied by soil formation.

BSU II (25.15-24.70 m core depth) - At the base of this unit, which yields a radiocarbon age of 30252±504 cal yrs BP (Tab. 1), a mm-thick sandy layer was found. Upwards, dark grey-grey silty clays occur with sparse iron and manganese oxides and vegetal remains. Palynomorphs display a total frequency ranging between 16k and 49k grains/g and document a high relative abundance and species diversity of Pteridophytes (4%; eight taxa in Fig. 2) and Bryophytes (10%; 22 retrieved taxa on a total of 49 in Fig. 2). Secondary grains show a peak (23.6%) close to the upper boundary and are mainly composed of poorly preserved Cretaceous taxa qualitatively recognised sensu Cincotta et al. (2019), such as *Piceapollenites mesophyticus* Bolkhovitina, 1956 and *Protopinus subluteus* Bolkhovitina, 1956. Among pollen, herbs are dominant (ca. 74-83%) and the local pollen rain is mainly composed of hygrophyte + aquatic and pasture-meadow taxa. The former show an upward decreasing trend (from 26-21% to 9-2%; Fig. 3) and are mainly represented by *Carex, Schoenoplectus*, Cyperaceae, *Isoetes durieui, Phaeoceros laevis* and *Sphagnum* spp. (Fig. 5). High percentages and an opposite (upward increasing) trend characterise the pm group, dominated by Poaceae (ca. 28%) and Cichorioideae (1-16%) (Fig. 6). Interestingly, halophytes were found close to the upper boundary of the unit (1.3% in Fig. 3). Mediterranean taxa also appear in the same sample with percentages of about 3%, while

Fig. 2 (color online) - Stratigraphy, general palynological features and meiofauna of core PA1 (core location is shown in Fig. 1). The main sedimentological characteristics are reported (black colour indicates organic-matter enrichment; yellowish brown colour highlights mottled indurated horizons) along with the available radiocarbon ages. Triangles indicate PA1 radiocarbon samples, while dots correspond to projected dates from the nearby core Mappa 3 (see Tab. 1). The relative frequencies of autochthonous ostracods and benthic foraminifers are shown as abundance categories of the ecological groups. The identified bio-sedimentary units (BSUs) and corresponding palaeoenvironments are also reported. Samples barren of microfossils are shown in grey.
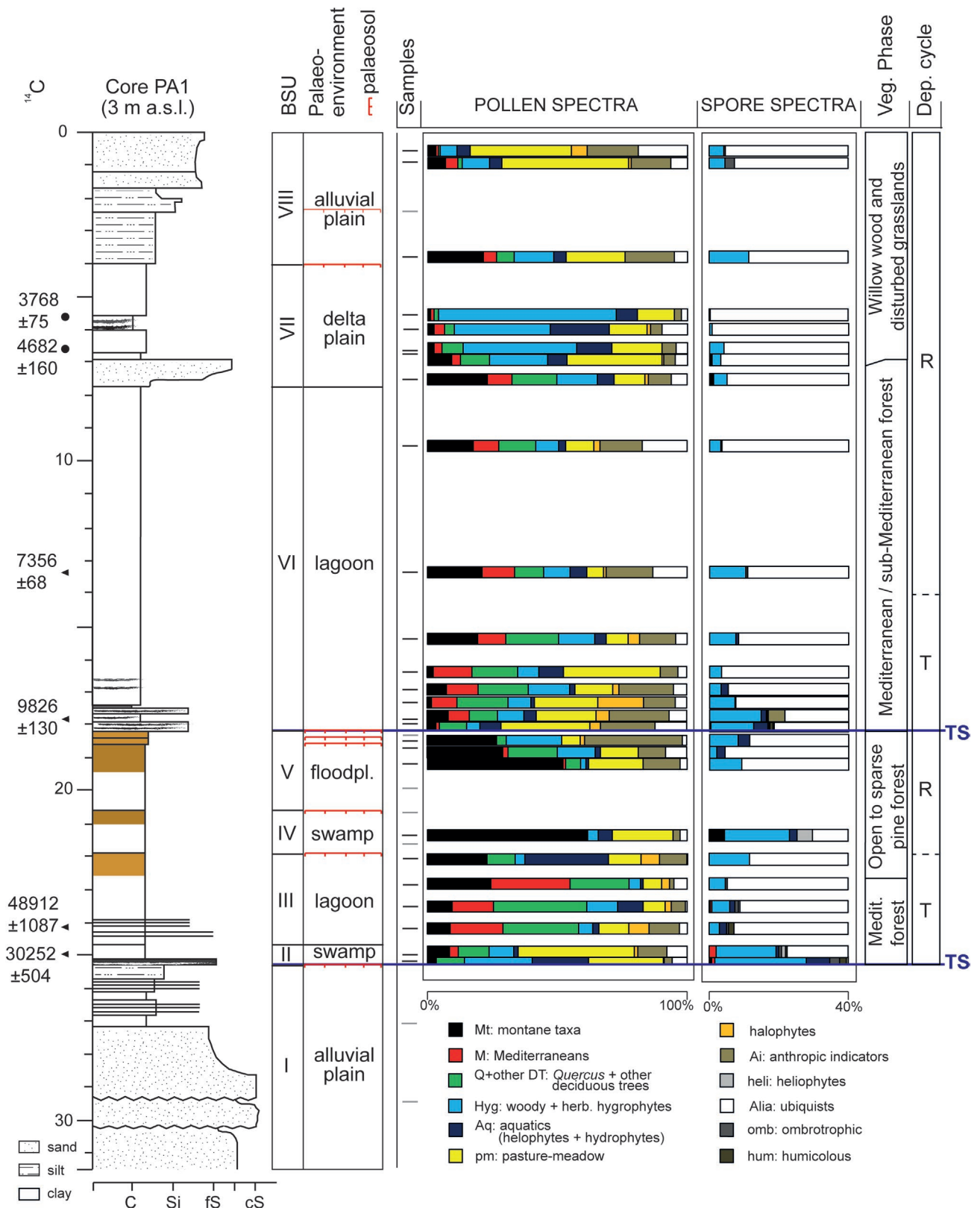
Fig. 3 - Stratigraphy and palynological spectra showing the relative abundances of pollen and spores ecological groups. Vegetation phases identified on the basis of the relative proportions among three pollen groups (Mt, M e Q+other DT) are also highlighted. Mt: montane taxa (*Abies alba*, *Pinus mugo*); M: Mediterraneans (*Quercus ilex*); Q+other DT: *Quercetum* + other dediduous trees (*Quercus pubescens*, *Tilia*); Hyg: hygrophytes (*Alnus glutinosa*, *Salix*, *Cyperaceae*); Aq: aquatics (*Sparganium emersum*, *Typha latifolia*); pm: pasture-meadow (Asteroideae, Cichorioideae, Poaceae); hal: halophytes (*Artemisia*); Ai: anthropic indicators (*Beta vulgaris*). The vertical stacking pattern of BSUs and corresponding palaeoenvironments are shown along with sequence stratigraphic interpretations (TS: Transgressive Surface; T-R cycles). Samples barren of palynomorphs are reported in grey. Keys for radiocarbon ages and sedimentological features are shown in Fig. 2 caption.

deciduous taxa stay around 11%. The abundance of the montane (Mt) group is low (3-8%). As for spores, a high number of species was recorded, especially for the lowermost sample collected at the transition with the underlying unit (Fig. 2). The Hyg+Aq group, including *Gymnocolea inflata* (Hudson) Dumortier, 1835, *Hygrohypnum lurudum* (Hedwig) Jennings, 1913 and *Phaeoceros laevis* among others, is dominant (ca. 21+7%, respectively, in the lower sample), although the subordinate occurrence of Mediterranean and humicolous taxa is remarkable (Fig. 3).

Ostracods are exclusively represented by freshwater-low brackish taxa (*Pseudocandona* cf. *P. albicans* and *Ilyocypris* spp.), while autochthonous benthic foraminifers are absent (Fig. 2).

This unit is interpreted to reflect the development of an organic-rich hypohaline environment, as a swamp characterised by a dense herbaceous layer associated with a highly diversified moss community. More specifically, the dominance of ostracods preferring stagnant waters (*Pseudocandona* cf. *P. albicans*) and hygro-helophyte mosses point to a shallow, standing aquatic body with several emerged, though persistently humid, humicolous areas. Unsteady environmental conditions are suggested by the high species diversity of spores. Episodic sediment input from the Pisa Mountains (i.e., Mesozoic sedimentary sequences; Cerratori et al., 1994) is also inferred from the Cretaceous age of secondary grains.

BSU III (24.70-21.90 m core depth) - This unit, ca. 2.5 m thick, consists of mottled grey clay with mollusc shells and fragments, passing upwards (uppermost ca. 70 cm) to yellowish brown clay with higher consistency (penetration value ranging from ca. 3 to 5 kg/cm^2) and concentration of Fe-Mn oxides (Fig. 2). Thin silty-sandy layers occur at the base of the unit where a radiocarbon date close to end of the calibration data set occurs (46000±650 yrs BP; Tab. 1). The palynomorph frequency shows variable values (4-61k grains/g) and Pteridophytes+Bryophytes significantly drop in relative abundance and number of species with respect to the underlying unit (Figs 2-3). On the other hand the arboreal component (trees+shrubs), mainly composed of *Quercus*+other deciduous taxa and Mediterranean taxa, increases up to 35% and 30%, respectively, and abruptly decreases in the uppermost sample (Figs 2-3). Secondary grains are scarce (< 7%) but a remarkable number of dinocysts, for the most part fragmented, were encountered around 23.70 m core depth. Hyg and Aq pollen and spores, mainly represented by *Alnus glutinosa*, undetermined Pteridophytes, *Lemna* and *Nymphaea alba* Linnaeus, 1753 (Fig. 5), show high percentages (ca. 11% and 10% peaks, respectively; Fig. 3) and a marked peak of the aquatics was encountered close to the upper boundary of the unit (ca. 32% in Figs 3-4). However, this topmost sample bears only qualitative information because of very low pollen counts (i.e., 56 grains). Halophytes were consistently encountered with percentages ranging from 2 to 8% (Fig. 3).

The meiofauna is abundant and dominated by *C. torosa* and *Ammonia tepida-A. parkinsoniana* (hC taxa) with the scarce occurrence (< 10%) of brackish-marine ostracods, such as *L. elliptica*. Within the uppermost

sample, few valves of *Heterocypris salina* (F-lB category) occur (Fig. 2).

The concomitant occurrence of taxa belonging to the Hyg, Aq and hal groups, along with the presence of a meiofauna (*C. torosa*+*Ammonia tepida-A. parkinsoniana*) typical of Mediterranean back-barrier settings (Ruiz et al., 2000; Debenay & Guillou, 2002; Murray, 2006), point to a brackish, permanently submerged area semi-enclosed to the sea and subject to salinity oscillations, such as a lagoon. This interpretation is supported by the occurrence of dinocysts, considered a marine proxy (Kaniewski et al., 2018), and the low relative percentages of herbs and spores that suggest the development of a relatively deep (i.e., few meters) coastal basin surrounded by vegetated areas.

The fine-grained texture is consistent with a calm environment, while the presence of mottles, oxides and the indurated horizon atop the unit are indicative of pedogenic processes due to subaerial exposure. Accordingly, an upward decrease in the water-table level is suggested by the appearance of freshwater-low brackish ostracods and by the disappearance of benthic foraminifers close to the uppermost boundary (Figs 2-3), backed by the qualitative peak of aquatic plants.

BSU IV (21.90-20.60 m core depth) - A monotonous succession of mottled silty clay with abundant Fe-Mn oxides and sparse calcareous nodules composes this unit. Its lower portion is characterised by an abundant ostracod fauna almost exclusively composed of *C. torosa* valves, some of them node-bearing. No microfossils were found up-section. The uppermost portion shows a brown-dark grey colour and a marked increase in consistency documented by pocket penetration values > 6 kg/cm^2 atop (Fig. 2). No absolute ages are available from this unit.

Despite the general scarcity of palynomorphs (95 grains, with a concentration of 3k grains/g), an evident increase in relative abundance and number of spore taxa was encountered relative to the underlying unit, with the dominance of those belonging to the Hyg+Aq groups (Figs 2-3). Among pollen, arboreal taxa show high percentages and are mainly represented by the Mt group (*Pinus* sp. and undetermined Pinaceae), however significant amounts of pasture meadow (ca. 23%) and hygrophytes+aquatics (ca. 10%) were also recorded.

Micropalaeontological and sedimentological features suggest an emerging swampy environment subject to prolonged periods of subaerial exposure that induced soil development. The related vegetal landscape is that of an open pine forest with wood clearances mainly consisting of damp areas, whose low salinity conditions are documented by the absence of halophytes and the presence of an oligotypic, euryhaline ostracod fauna including noded *C. torosa* (Frenzel et al., 2012).

BSU V (20.60-18.20 m core depth) - This unit is composed of silty clays containing Fe-Mn oxides and calcareous nodules. These latter are abundant in the uppermost portion (ca. 40 cm thick), which shows a dark grey colour. The consistency is high throughout the unit, as documented by penetration values invariably > 3 kg/cm^2 (Fig. 2). No absolute ages are available from this unit. The lower portion is barren of microfossils, while the uppermost metre contains a scarce palynological assemblage (0.08-
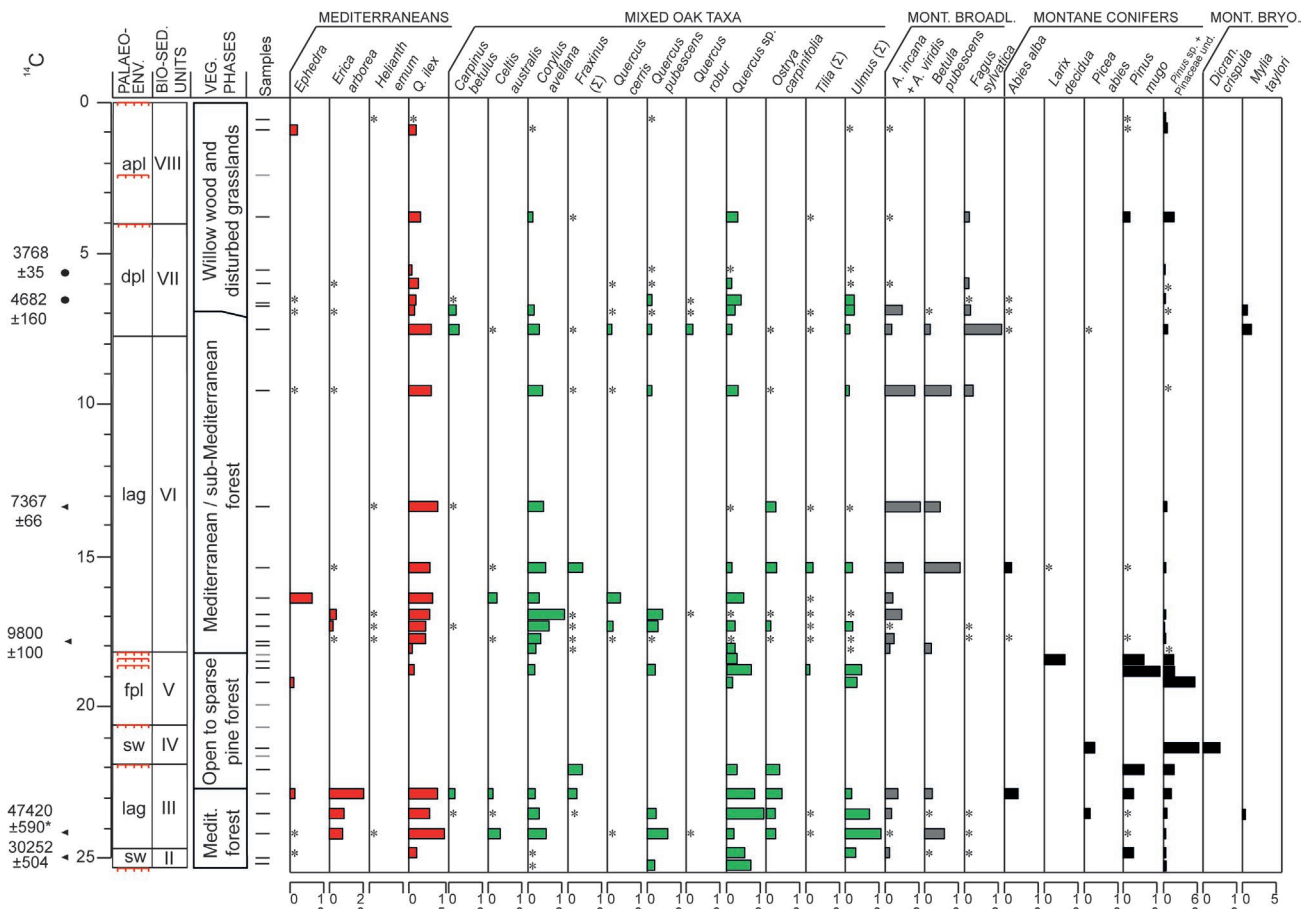
Fig. 4 (color online) - Percentage diagrams of pollen and spores of selected taxa belonging to the ecological groups M, Q+other Dt and Mt, the latter distinguished between montane broadleaves (grey) and conifers - Bryophytes (black). BSUs and corresponding palaeoenvironments and VPs are also shown along with radiocarbon ages. Samples barren of palynomorphs are reported in grey. Asterisk indicates percentages < 1%. Sw: swamp; lag: lagoon; fpl: floodplain; dpl: delta plain; apl: alluvial plain. Key for palaeosol is explained in Figs 2-3.

1.43k grains/g) mainly represented by arboreal pollen belonging to the Mt group and subordinately to Q+other DT (Figs 2-3). Hygrophytes show an upward growing trend (from 2 to 21%) driven by undetermined Cyperaceae and Pteridophytes and with the topmost appearance of *Populus*; by contrast, aquatic plants shows insignificant percentages (Fig. 4). The uppermost sample at ca. 18.4 m core depth displays a peak in taxa belonging to the Ai group (37.5%, mainly composed of *Polygonum persicaria* Gray, 1821 and Urticaceae; Fig. 6) and the scarce re-appearance of halophytes (1.8%; Fig. 3). If present, secondary grains show percentages lower than 8%.

Sedimentological features and the almost complete disappearance of aquatic plants point to the establishment of a floodplain strongly influenced by pedogenesis, although a certain degree of hygrophily is recorded close to the upper boundary. Moreover, the overall paucity of microfossils and the enhanced pedogenesis suggest persistency of poor conditions for pollen deposition. The peak in Ai taxa, concomitant with the occurrence of halophytes, possibly indicates a disturbed environment affected by variable and stressed conditions.

BSU VI (18.20-7.75 m core depth) - The basal 80 cm of this unit are made up of dark grey, organic-rich sandy silts and clays overlain by ca. 10 meters of light grey,

soft clay (penetration values generally < 1 kg/cm², but often < 0.5 kg/cm²), locally bioturbated and containing several shells and fragments of *Cerastoderma glaucum* Bruguière, 1789 (Fig. 2). The age-depth model (Fig. 7), based on radiocarbon ages (see Chronology in Material and Methods paragraph), constrain this unit between ca. 9800 and 5000 cal yrs BP.

Palynomorphs are abundant, especially in the lowermost 3 metres of the unit (18k-434k grains/g; Fig. 2), and mainly represented by Spermatophytes, although a remarkable abundance and richness of Pteridophytes and Bryophytes was observed close to the lower boundary around 18 m core depth, where the arboreal cover (trees+shrubs) is rather low (ca. 18%; Fig. 2). The latter increases constantly up to 50%, floating around this value from ca. 15.5 m core depth (Fig. 2). *Quercus*+other deciduous and Mediterranean taxa are well represented (ca. 12 and 17%, respectively) and are accompanied by variable amounts of montane trees (Fig. 4). Hygrophytes and aquatics display remarkable percentages (ca. 10% and 6%, respectively). Among the former, *Alnus glutinosa* and undetermined Pteridophytes dominate with subordinate *Salix* and undetermined Cyperaceae, while aquatics are mainly represented by *Butomus umbellatus, Callitriche* spp. and *Schoenoplectus* (Fig. 5). Halophytes show an increasing trend within the lowermost one metre,
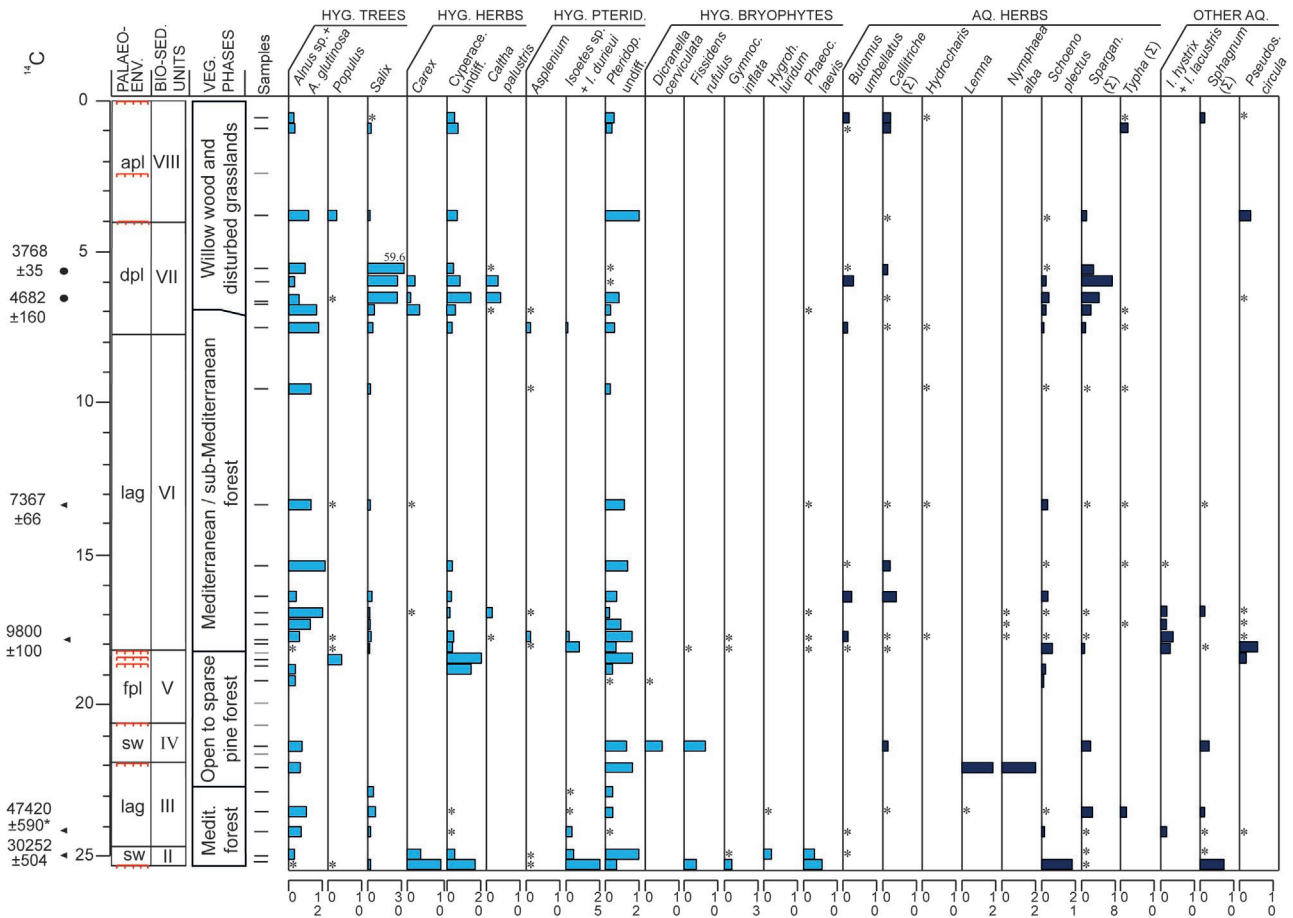
Fig. 5 (color online) - Percentage diagrams of pollen and spores of selected taxa belonging to the ecological groups Hyg and Aq. BSUs and corresponding palaeoenvironments and VPs are also shown along with radiocarbon ages. Samples barren of palynomorphs are reported in grey. Asterisk indicates percentages < 1%. Keys for palaeoenvironments are explained in Fig. 4 caption. Key for palaeosol is explained in Figs 2-3.

peaking at 4-17% and then decreasing to lower values in the remaining portion of the unit. Pasture-meadow herbs also show a similar trend (Fig. 3). The Ai group, which is mainly represented by various Asteroideae, Caryophyllaceae and Urticaceae (Fig. 6), shows a high abundance especially close to the lower boundary of the unit (ca. 20%; Fig. 3). Such high abundances and species richness were also observed for Bryophytes within the lowermost sample (Fig. 3), where 17 different species were identified. Secondary grains occur in very low percentages (< 4%).

The meiofauna is abundant and exhibits the highest species richness of the cored succession, with several secondary taxa accompanying the dominant *C. torosa* and *Ammonia tepida-A. parkinsoniana*. Among ostracods, species belonging to the B-M (e.g., *L. elliptica*, *L. stellifera*, *L. bacescoi*) and C-sM (*Palm. turbida*) categories consistently occur in the lower part of the unit. A similar trend is also recorded by low confinement foraminifers that mainly include *Cribroelphidium* species and Milioloidea (Fig. 2).

According to the sedimentological characteristics and the particular palaeontological content, this unit reflects a calm, brackish environment semi-enclosed to the sea and surrounded by humid grasslands, such as a lagoon basin, similar to BSU III. Moreover, the *C. torosa*+*Ammonia tepida-A. parkinsoniana*+*C. glaucum* assemblage is considered a sensitive and reliable indicator of back-barrier settings subject to salinity oscillations in the Mediterranean area (Amorosi et al., 2014 and references herein). A strong marine influence is documented for the lower portion (ca. 18-14 m core depth) by both the meiofauna content (remarkable abundances of brackish-marine and coastal-shallow marine ostracods and low-confinement foraminifers) and the remarkable occurrence of halophytes. This latter tends to disappear upwards and this trend is paralleled by the occurrence of a less diversified meiofauna, almost exclusively composed of *C. torosa* and high-confinement foraminifers, accounting for the transition to more restricted conditions. The basal peak in Ai pollen and Bryophyte spores suggests the occurrence of disturbed conditions during the first phases of lagoon development.

BSU VII (7.75-4 m core depth) - This unit is composed of a 70 cm-thick succession of silty sand and fine sand, rich in wood fragments and showing an internal coarsening-upward trend, overlain by grey soft to moderately consistent silty clay containing few shells and fragments of unidentifiable molluscs. An upward increase in consistency is testified by penetration values that increase from < 1 kg/cm² to ca. 1.5 kg/cm² towards the top of the unit (Fig. 2). Its lower portion (ca. 7.75-5.50 m core depth), chronologically constrained to ca. 5000-
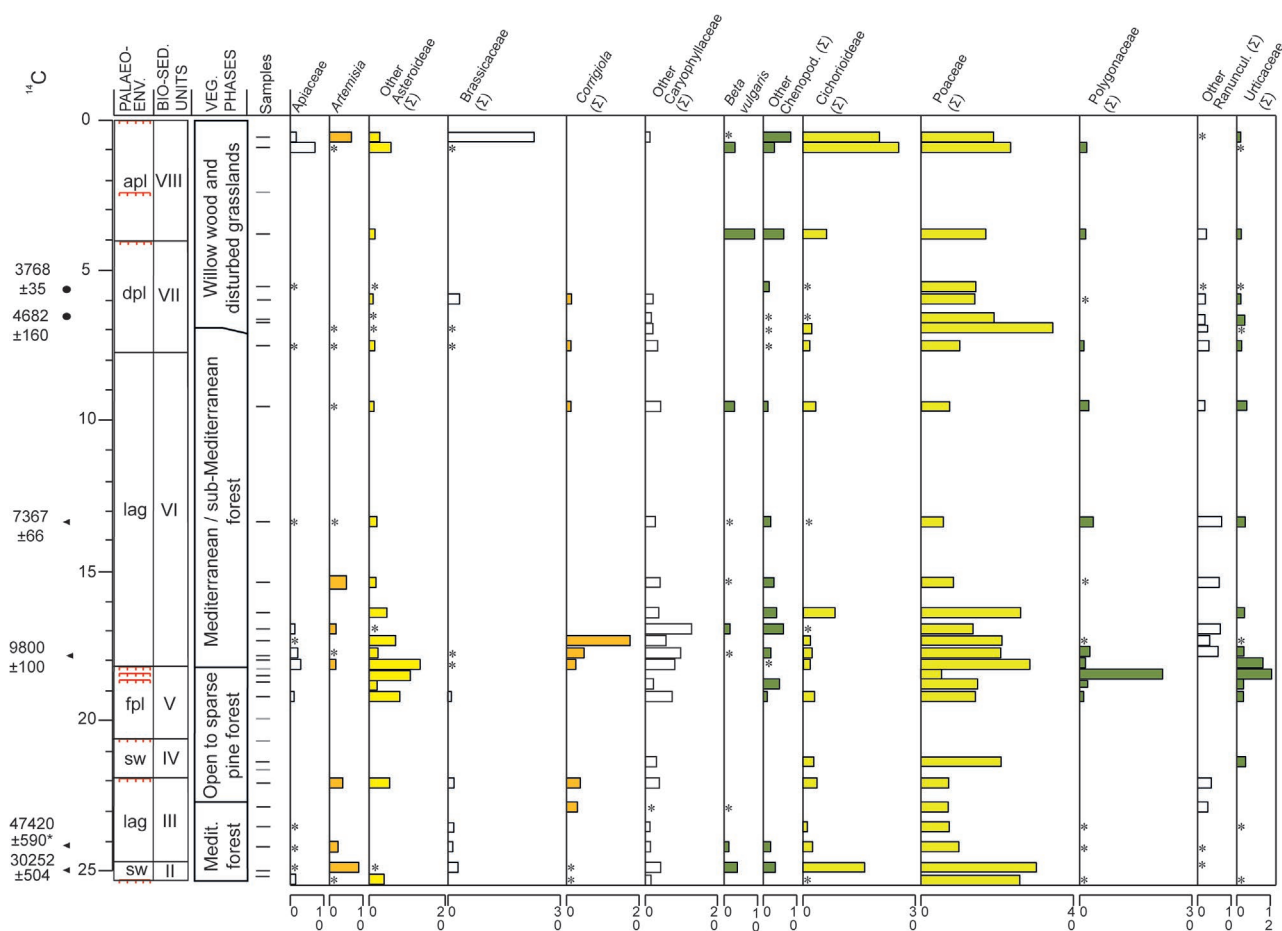
Fig. 6 - Percentage diagrams of pollen and spores of selected taxa belonging to the ecological groups pm, Ai and Alia. BSUs and corresponding palaeoenvironments and VPs are also shown along with radiocarbon ages. Samples barren of palynomorphs are reported in grey. Asterisk indicates percentages < 1%. Colours of taxa bars are those of their respective pollen group as in Fig. 3. Other Asteroideae (Σ) has both yellow and brown colours because it comprises taxa from both Ai and pm. Keys for palaeoenvironments are explained in Fig. 4 caption. Key for palaeosol is explained in Figs 2-3.

3800 cal yrs BP (Fig. 7 and Tab. 1), is characterised by diffuse organic matter, while the upper part (ca. 5.50-4 m core depth) displays an accumulation of calcareous nodules and few Fe-Mn oxides accompanied by a change towards greenish colours. Unfortunately, the chronological attribution of this interval is uncertain; however, a temporal range between ca. 3800-2500 cal yrs BP is assumable from the age-depth model (Fig. 7).

The total palynomorph frequency is generally high (> 21k grains/g), reaching a peak (> 300k grains/g) between 6-5.5 m core depth (Fig. 2). Pteridophyte and Bryophyte spores are scarce relative to pollen grains, which show variable proportions of arboreal and herbaceous taxa. Trees are mainly hygrophilous, especially *Salix* (Fig. 5), with the subordinate occurrence of Q+other DT*, M and Mt groups. In particular, *Alnus glutinosa* continues thriving up to 6.70 m, similar to the previous unit, after that it declines leaving place to *Salix* that becomes the strongly dominant tree. The accompanying herbaceous community is also varied, shifting from Pteridophyte-dominated to Cyperaceae-*Sparganium*-dominated types (Fig. 3). Halophytes are scarcely recorded (< 1.5%). Similar to the underlying unit, secondary grains are scarce (< 3%).

The meiofauna is abundant only in the lower portion of the unit and is mainly composed of ostracod valves, as benthic foraminifers are scarce and exclusively represented by *Ammonia tepida-A. parkinsoniana* (Fig. 2). The upward disappearance of benthic foraminifers is paralleled by the replacement of *C. torosa* by freshwater-low brackish taxa, which mainly include *Pseudocandona* cf. *P. albicans*.

The occurrence of ostracods tolerant to low and variable salinity conditions, along with the paucity of halophytes and benthic foraminifers, which are only represented by opportunistic high confinement species (Debenay & Guillou, 2002), suggest the development of a slightly brackish, humid environment strongly influenced by freshwater/river inputs, such as a delta plain. This interpretation is consistent with the high degree of hygrophily testified by the increased water table within the willow wood (in comparison to the previous alder wood) suggested by the spreading of Cyperaceae and *Sparganium* spp. The upward disappearance of both foraminifers and *C. torosa* paralleled by an increase in pedologic features (e.g., oxides and calcareous nodules) point to a progressively stronger influence of river inputs, leading to the almost complete subaerial exposure of the plain.

BSU VIII (4-0 m core depth) - This unit is made of mottled brown-grey, moderately consistent (penetration values between 0.7 and 2.5 kg/cm^2) silt and clay passing upwards, around 1.5 m core depth, to silty fine sands. Fe-Mn oxides and calcareous nodules are commonly encountered. Brick fragments occur within the uppermost 1.5 m. An age younger than 2500 cal yrs BP is assumed on the basis of the age-depth model (Fig. 7). Palynomorphs, generally scarce (< 4k grains/g), are absent in correspondence of an indurated horizon around 2.4 m core depth (Fig. 2). Among pollen, herbs dominate recording high percentages of pm (23-48%) and Ai (15-20%) taxa, mainly including Poaceae and Cichorioideae and various Chenopodiaceae. The other dominant family is Brassicaceae (22.5% in the topmost sample). Halophytes are almost absent, except for the uppermost sample collected 50 cm below the ground level (6%, Fig. 6). Aquatics (*Butomus umbellatus, Callitriche* spp. and *Typha* spp.) and hygrophytes (*Alnus glutinosa*, Cyperaceae and Pteridophytes) exhibit percentages around 10 and 5%, respectively, with the former showing an upward decreasing trend. Lower relative abundances were observed for hygrophytes and aquatic spores. Within the arboreal component, Q+other DT, M and Mt groups occur with generally low percentages that also show a decreasing upward trend. The only exception is represented by the peak of montane trees in the lowermost sample (Fig. 3). No autochthonous meiofauna was found.

Sedimentological features and a lack of meiofauna are suggestive of an alluvial setting, consistent with the stratigraphic position of the unit relative to the core site (Fig. 1). Despite concentrations of the anthropic taxa are not outstanding, species composition within the lowermost sample indicates a pronounced anthropic influence on the vegetal landscape. In fact, the 9% peak of *Beta vulgaris* (out of 19% Ai) suggests the presence of cultivated fields in the nearby areas, while other Chenopodiaceae (5%), Poaceae (16%) and the peak in *Pinus* sp. (ca. 16%) can account for a more widespread human presence in the alluvial plain. Furthermore, the nearly sole occurrence of undetermined pine grains (with only negligible amounts of both montane and lowland pines) can be interpreted as the result of human landscape exploitation rather than an effect of climate worsening. Finally, a certain degree of hygrophily is suggested by the relative abundance of Pteridophytes, probably reflecting the most suitable vegetation able to exploit disturbed and moist environments.

Close to the top, the pm group peaks at 48% owing to very high amounts of Cichorioideae, while the arboreal cover drops to minimum values indicating a recent transition to a vegetal impoverished environment.

Vegetation phases

Four vegetation phases (VPs) were identified focusing on the relatively regional signal derived from three pollen groups (Mt-Montane, M-Mediterranean e Q+other DT-*Quercus*+other deciduous trees; Figs 3-4) and mainly interpreted in terms of climate conditions. The VPs are briefly described below in stratigraphic order, while more detailed data are reported in Tab. 2.

The oldest vegetation phase, recorded between 25.15-22.80 m core depth and chronologically constrained
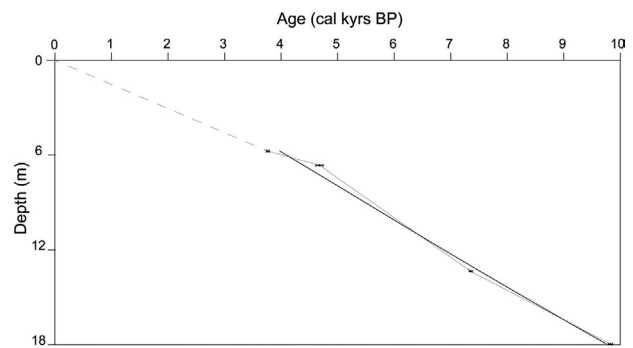
Fig. 7 - Core PA1 age-depth model, elaborated for the uppermost 18 meters applying the smoothing spline function (bold line; smooth valour = 0.725) using the software PAST (Hammer et al., 2001). The thin black line shows the linear interpolation among ages. Radiocarbon ages are listed in Tab. 1.

to the late Pleistocene (Tab. 1 and Fig. 3), is generally characterised by high amounts of Mediterranean and sub-Mediterranean taxa relative to montane ones, depicting a holm oak-mixed oak forest (Mediterranean forest in Figs 3-6). At first, *Quercus*+other deciduous and Mediterranean taxa shows ca. 10% and < 5% of relative abundances, respectively, reflecting mild conditions consistent with the very scarce presence of montane taxa. Then, the former groups (Q+other DT and M) increases reaching significantly higher values (23-36% and 16-30%, respectively), in contrast to the Mt group that remains rather low (ca. 9%). The upward replacement of *Ulmus minor* Miller, 1768 by *Erica arborea* (from 7 to 18%; Fig. 4) traces an overall trend towards more Mediterranean conditions, commonly highlighted by the turnover of sub-Mediterranean elements with a sclerophyllous vegetation typical of the climate optimum *sensu strictu* (Combourieu-Nebout et al., 2013). In this context, the topmost peak of montane taxa (24%) mainly represented by *Pinus* sp. (ca. 12%) is interpreted to reflect an increased xerophily on the mountains.

The following vegetation phase, encountered around 22.8-18.2 m core depth, marks the almost disappearance of Mediterranean taxa and the expansion of *Pinus* sp. (12.5-42%) that becomes the dominant species in all five pollen-bearing samples (Figs 3-4). The common occurrence of *P. mugo* and undetermined Pinaceae (ranging 7-12.5% and 2-21%, respectively), along with the rare presence of other conifers (Fig. 4), point to the establishment of an open to sparse pine forest in the plain under cold climate conditions.

Around 9800 cal yrs BP, a rapid spread of the holm oak-mixed oak forest (both M and Q+other DT taxa peak at ca. 15%), at the expense of conifers, took place marking the beginning of the following vegetation phase interpreted as the expression of the Holocene climate optimum (Mediterranean/sub-Mediterranean forest in Figs 3-6). If present, *Erica* remains rather low (< 5%), accompanied by very scarce and only occasional records of other Mediterranean taxa (e.g., *Phillyrea*). The montane taxa show rather low percentages during the initial stage of this VP, ranging around values of 2-8% (Fig. 3), and are mainly represented by *Alnus incana+viridis* with scarce amounts of conifers and *Fagus* (Fig. 4). Subsequently,

VP	Depth	Palynology	Main biome	Palaeoclimate inference	Inferred age
1	25.15-22.8 m	**Mt**: *Pinus* (3%, but 11% peak at the top), other conifers low or absent. *Betula pubescens* (0-4%). **Q+other DT**: *Quercus* (10-15%), *Corylus* (0-5%), *Ostrya* (0-4%), *Ulmus* (0-10%). **M**: *Q. ilex* (3-14%), *Erica* (7-18% in the upper portion). **H**: *Alnus glutinosa* (0-4%), *Salix* (0-6%). In the lowest s., Cyperaceae (44%), *Isoetes durieui* (21%) and Bryophytes (35%), then decrease.	Mediterranean holm oak - mixed oak forest	Climate optimum with initial pioneering hygrophily, then moist sub-Mediterranean, finally xerophilous Mediterranean conditions.	late Pleistocene (MIS 5e)
2	22.8-18.2 m	(Very low pollen counts and concentrations, four sterile ss. out of nine) **Mt**: *Pinus* (14-42%), *P. mugo* (7% in the lower s., 12-7% in the upper s.), *Larix decidua* (5% in the upper s.), undet. Pinaceae (4-20% in most ss.). **Q+other DT**: *Quercus* (0-8%). **M**: *Q. ilex* (0-2%). **H**: *Alnus glutinosa* (0-4%). Cyperaceae (12-18% in the two upper ss.). **Ai**: *Urtica dioica* (0-10%).	Open to sparse pine forest	Cold, hygrophilous steppe in transition to a pine forest typical of a glacial period	Last Glacial
3	18.2-6.97 m	**Mt**: *Alnus incana* (0-4%), *A. viridis* (0-5%), *Betula pubescens* (0-7%), *Fagus* (0-2%, 11.7% in the upper s.). **Q+other DT**: *Quercus* (2-9%), *Corylus* (2-11%), *Ostrya* (0-2%), *Tilia* (0-2%), *Ulmus* (0-2%). **M**: *Q. ilex* (6-11%), *Erica* (0-3%). **H**: *Alnus glutinosa* (2-11%), *Salix* (1-4%), Cyperaceae (< 8%), Bryophytes (14% in the lower s.). **hal**: *Corrigiola* (2-5-17% in the three lower ss.). **Ai**: Urticaceae (8% in the lower s.).	Mediterranean/sub-Mediterranean mixed oak - holm oak forest	Climate optimum with initial pioneering, hygrophilous conditions shifting to moist and mesophilous with an increasing degree of mediterraneity (less marked than in VP 1)	~9800-4800
4	6.97-0 m	**Mt**: *Pinus* (1-5%, 16% peak in the third s. from the top). **Q+other DT**: *Quercus* (1-5%, absent in the two upper ss.), *Ulmus* (0-2%), other taxa patchily and scarcely present. **M**: Q. *ilex* (1-4%). **H/Aq**: *Alnus glutinosa* (5-0% decreasing trend), *Salix* (23-59% in the lower portion, then < 3%), Cyperaceae (4-12%), *Sparganium* (4-17%, the scarce or absent in the three upper ss.). **Ai**: *Beta vulgaris* (9% in the third s. from the top), Cichorioideae (6-23-18% in an upward increasing trend).	Willow wood and disturbed grasslands	Hygrophilous willow wood replacing an alder wood under optimum-like conditions. In the upper portion, marked landscape anthropisation	~4800-0

Tab. 2 - Brief description of the vegetation phases established for core PA1. Main taxa are explained in an ecological group order.

around 8400 cal yrs BP (Figs 3-4, 7), a marked expansion of montane alders (5-10%) and of *Betula pubescens* (3-7%) occurs, while *Pinus* (< 6%) and *Fagus* remain scarce (Fig. 4) according to climate optimum conditions, here represented by montane broadleaves. Moreover, the presence of hygrophilous trees (mainly alders) at low and high altitudes suggests a widespread degree of moisture. A peak in *Fagus sylvatica* at 11.7%, dated around 5000 cal yrs BP (Figs 3-4, 7) and paralleled by a drop of other montane broadleaves (Fig. 4), likely indicates the occurrence of a high-frequency mid-Holocene cooling event.

The most recent vegetation phase, recorded within the uppermost 7 m core depth and dated to the last 4700 cal yrs BP, is generally characterised by a decrease in montane taxa in terms of both percentages and species richness, as most montane broadleaves and conifers disappear (Figs 3-4). However, also Mediterranean and mixed-oak taxa show relatively low percentages (1-5% and 1-11%, respectively) likely due to the pre-eminence of hygrophytes, mainly *A. glutinosa* and *Salix* (Figs 3, 5), or anthropic plants (Figs 3, 6). Thus, this vegetation phase, corresponding to a willow wood and disturbed grasslands,

mainly reflects the local environment rather than specific climate conditions.

DISCUSSION

The combined use of palynomorphs (pollen and spores) and meiofauna (ostracods and benthic foraminifers) enables the detailed reconstruction of various depositional environments (BSUs) and coeval vegetation phases (VPs) along the studied succession (Figs 2-3). The identification of both local (environment) and regional (vegetation-derived climate) signals from the same sedimentary record give us the opportunity to investigate the relationships among the palaeoenvironmental and climate changes occurring since the late Pleistocene in the Arno Plain, also within a sequence-stratigraphic perspective.

Late Quaternary palaeoenvironmental evolution of the Arno Plain

The vertical stacking pattern of BSUs, paralleled by turnovers of both palynomorphs and meiofauna ecological

groups, furnishes robust and detailed information about the depositional history of the Arno Plain since the penultimate glacial period (MIS 6) onwards, allowing the identification of a repeated alternation of coastal and alluvial deposits (i.e., depositional cycles). The alluvial deposits recorded at the core bottom and capped by a prominent palaeosol (BSU I in Figs 2-3) correlate well with the tens m-thick, fluvial sands that unconformably overlie a MIS 7 lagoonal succession intercepted by core Osp, 5 km SE of core PA1 (Rossi et al., 2017; Fig. 1).

Above this palaeosol, which reasonably formed in response to a major phase of river incision triggered by a RSL fall (MIS 6?), two transgressive-regressive (T-R) cycles (sensu Embry, 1995) chronologically constrained to the late Pleistocene and the Holocene period, respectively, are invariably characterised at the base by lagoonal-swamp deposits (BSUs II-III and VI in Figs 2-3).

Late Pleistocene depositional cycle - The thin (ca. 50 cm) swamp interval that marks the transgressive surface (TS) on top of the MIS 6? palaeosol, contains a highly diversified Bryophyte assemblage dominated by hygrophytes and aquatics with subordinate montane, Mediterranean, ombrotrophic and humicolous taxa (Fig. 3), reflecting the flooding of a subaerially exposed palaeosurface. This transgressive event, dated around 30000 cal yrs BP by a radiocarbon date (Tab. 1), led to the development of highly variable conditions that shifted from subaqueous and almost freshwater (i.e., no or very scarce halophytes and dominance of F-lB ostracods) to slightly emerged, organic-rich moss-herbs cushions with a high micro-environmental diversification. An upward increase in marine influence is clearly indicated by halophytes (Fig. 3) and by a strong meiofauna turnover (euryhaline+hC taxa replacing F-lB ostracods; Fig. 2), marking the establishment of a brackish lagoon basin whose chronology is extremely uncertain. Indeed, the available age is close to the lower limit of radiocarbon calibration data set and shows a reversal with respect the previous one (Figs 2-3; Tab. 1). The return of freshwater-low brackish ostracods around 22 m core depth (Fig. 2) suggests a shallowing-upward trend that culminates with phases of lagoon-swamp emergence and the onset of pedogenesis (top of palaeosols around 22 m and 20.60 m core depths; Fig. 2), typifying the regressive portion of the cycle. Upcore, well-drained alluvial conditions occur as documented by the disappearance of the meiofauna, the marked drop of aquatic plants and the increase in pm and Ai herbs (Figs 3, 6). A vertically stacked pattern of palaeosols caps the cycle.

Holocene depositional cycle - The abrupt superposition, onto late Pleistocene palaeosols, of lagoonal deposits containing halophytes (mainly *Artemisia*) and a euryhaline-brackish meiofauna, marks the onset of the Holocene transgression (Figs 2-3). Across the TS, dated around 9800 cal yrs BP, a peak in Bryophyte diversity reflects pioneering palaeonvironmental conditions (partially similar to those recorded at the beginning of the former T-R cycle) that rapidly stabilised as a relatively monotonous, 10 m-thick lagoonal succession developed. However, the strong decrease of halophytes recorded around 7300 cal yrs BP (i.e., from 13-14 m core depth

upwards; Figs 3, 7) suggests a progressive increase in fluvial influence within the lagoon, as confirmed by the disappearance/scarcity of brackish-marine and coastal-shallow marine ostracods, as well as of low confinement foraminifers. This environmental change highlights the transition from transgressive to regressive (progradational) conditions. The complete siltation of the lagoon basin and its transformation into a delta plain, dated around 5000 cal yrs BP, is documented by both meiofauna and palynomorphs turnovers at ca. 8 m core depth (delta plain in Figs 2-3). The meiofauna shows the progressive replacement of brackish species by freshwater-low brackish ostracods, which dominate in the uppermost portion of the delta unit (Fig. 2), reflecting a salinity decreasing trend consistent with coastal progradation. Palynomorphs support this interpretation as halophytes are absent or scarce and the presence of a riparian swampy vegetation zone is clearly revealed by significant abundances of *Alnus glutinosa* + *Alnus* sp. (6-11%; Fig. 5) and, subordinately, aquatics (1-9%). Thereafter, a rapid turnover in hygrophyte trees occurred, as *Salix* replaced *Alnus*, dominating the riparian vegetation (ca 23-59 %; Figs 3, 5) and pointing to the development of a hygrophilous woodland in the delta plain up to ca. 3800 cal yrs BP. It is noteworthy the comparison between these two types of hygrophilous woods because *Alnus* is present with rather low percentages (ca. 7-11 %), in the lower portions of the lagoon upwards, in co-dominance with several taxa of the holm oak-mixed oak forest. After that, *Salix* relegates it to a subordinate position, forming strongly dominated (ca. 23%) to pure (59.6%) willow woods. The complete subaerial exposure of the plain (alluvial plain in Figs 2-3) is marked by the disappearance of the meiofauna and by the development of an open landscape.

Timing and forcing factors of landscape changes in coastal settings as revealed by palynology

The adopted multi-proxy approach highlights a synchronised cyclicity of palaeoenvironments (i.e., late Pleistocene and Holocene T-R cycles) and vegetation dynamics in the Arno Plain (Fig. 3). In particular, palynology proves to be a key tool in deciphering the role of late Quaternary climate-eustatic changes on landscape shaping and in improving the chronological framework.

First of all, the TSs that mark the main flooding events of the plain during the last ca. 200 kyrs BP (post-MIS 7) invariably developed in concomitance of spreading phases of mixed oak-holm oak forests (Fig. 3) that are indicative of the onset of warm climate conditions (interglacials). The uppermost TS is radiocarbon dated to ca. 9800 cal yr BP, which is consistent with the general phase of acceleration in sea-level rise recorded across the W Mediterranean between ca. 10-8 kyrs BP (Vacchi et al., 2016). The vegetation community is also consistent with an early Holocene chronology, being similar to that of Lake Accesa (Drescher-Schneider et al., 2007), where the mixed oak forest makes its first appearance already during the Preboreal, while the holm oak appears slightly after at ca. 9 cal kyrs BP. The consistent presence of *Quercus ilex* is also documented in the nearby regions at Lake Massaciuccoli (Mariotti Lippi et al., 2007), although in association with *Abies alba* until ca. 6 cal kyrs BP, which

in our core is absent or scarce. A similar vegetal landscape is also recorded in the Tiber delta (Di Rita et al., 2015).

On the other hand, we are inclined to reject the MIS 3 ages available for the lowermost TS and the overlying transgressive succession (ca. 30000-49000 cal yrs BP; Fig 3), as they are inconsistent with both vegetation patterns and palaeoenvironments. Pollen data reflect a full interglacial, mixed oak-holm oak dominated landscape (Mediterranean forest; Fig. 3) with the achievement of the vegetation climax, in contrast to the Mediterranean MIS 3 pollen records that contain evidence of a more open vegetation with peaks in steppic taxa like a wooded steppe biome (Follieri et al., 1988; Magri, 2007; Combourieu-Nebout et al., 2015). Palaeoenvironmental attributions also are inconsistent with radiocarbon dating, as they would imply the unlikely development of a lagoonal basin under a global sea level tens of meters lower than the present (MIS 3 sea levels lower than 50 m b.s.l.; Antonioli et al., 2004). Moreover, higher relative abundance and an upward increasing trend of both Mediterranean (*Erica arborea*, *Quercus ilex*) and various deciduous *Quercus* and *Ulmus* taxa (Figs 3-4), characterise the late Pleistocene lagoon relative to the Holocene one (Fig. 3), suggesting a more pronounced interglacial than the Present. Allen and Huntley (2009) have inferred a similar pattern from Lago Grande di Monticchio (southern Italy). All these palynological data, if framed into the Arno Plain stratigraphic context (Rossi et al., 2017), point to a MIS 5e attribution, highlighting the importance to validate radiometric ages with other proxies for a robust chronology of pre-Holocene coastal successions. Indeed, post-mortem contamination of younger carbon can give rise to a mean value that just represents a minimum age for the deposits embedding the ${}^{14}C$ samples (Figs 2-3). More specifically, the age discrepancy (MIS 3 instead of MIS 5e) of the sample collected at 24.10 core depth (mollusc shell; Tab. 1) could be related to the precipitation of secondary carbonate produced by bacterial activities, as documented by Busschers et al. (2014) from the Rhine-Meuse plain for well-preserved mollusc shells within a comparable stratigraphic context.

Thus, similar palynological and meiofauna patterns, encountered within the transgressive portions of distinct depositional cycles, suggest a consistent response of the landscape to the last two interglacials. Conversely, different microfossil contents characterise the regressive counterparts of the same depositional cycles. In particular, MIS 5e lagoon deposits, identified in the Arno Plain subsurface for the first time, record an opposite evolution (forced regression versus progradation) if compared to the Holocene lagoon facies.

A climate-driven phase of subaerial exposure, possibly occurring at the beginning of the last glacial period (MIS 5d?), affected the MIS 5e lagoon as testified by the disappearance of Mediterranean taxa and the strong reduction of Q+other DT (onset of an open to sparse pine forest; Fig. 3) within the lowermost pedogenised horizon. Conifers (mainly *Pinus* sp. and undetermined Pinaceae) replaced the deciduous taxa within the overlying swampy deposits, which also show evidence of pedogenesis. Despite an oscillating abundance of Q+other DT, cold conditions persisted during the subsequent alluvial phase (floodplain in Figs 2-3), documenting the development

of a typical forced regressive sedimentary succession including several unconformities (i.e., palaeosols) possibly dated to the last glacial-late glacial interval. Indeed, the formation of a series of palaeosols with marked pedogenesis and a scarce palynological content (less than 3k grains/g) points to an alluvial setting affected by a low aggradation/degradation ratio and several phases of river incision under the combined influence of sea-level fall and cold climate (Amorosi et al., 2017). Similar drops in pollen concentrations have been also recorded at Valle di Castiglione (near Rome, Follieri et al., 1988) for all glacial phases between the last and present interglacials and have been interpreted as rapid declines of the vegetation cover. The absence of preserved palynomorphs in four samples out of nine enhances this interpretation. Another similarity with the Valle di Castiglione record is the dominance of pine among arboreal pollen (open pine forest in the lowlands), although local environmental conditions in the PA1 core did not allow the development and/or preservation of the cold steppe instead recorded in a more seaward position (core M1 from Aguzzi et al., 2007; Fig. 1).

If glacio-eustacy represents the triggering factor, the low subsidence context, testified by the occurrence of MIS 5e brackish deposits between ca. 20-24 m b.s.l., likely accompanied by low sediment supply favoured the transformation of the lagoon into a multi-phase interfluve (whose related incisions have not been detected yet).

According to previous studies (Amorosi et al., 2013; Sarti et al., 2015), our data document a very different environmental history for the Holocene lagoon, which was filled by Arno River inputs under a sea-level highstand context (post-8000 cal yrs BP deceleration phase; Vacchi et al., 2016) with remarkable sediment supply (normal regressive/progradational portion of the T-R cycle). A phase of generally stable environmental conditions characterised the first phase of progradation (dated between ca. 7350-5000 cal yrs BP), as documented by rather monotonous meiofauna and palynological content within the "regressive" portion of the lagoonal succession (Figs 2-3). Interestingly, the transition to a deltaic setting is matched by the end of the climate optimum and is marked by a peak in *Fagus* interpreted as a rapid expansion of the beech woods vegetation belt. A coeval rise of *Fagus* has been also identified by Dolez et al. (2015) within a lagoonal succession in France, but in this case it was interpreted as due to first deforestations on the mountains. Thus, a primary role of high-frequency climate changes (i.e., general climate deterioration and/or cool events) in triggering lagoon siltation and its turnover into a wetland area, by means of enhanced fluvial activity, can be inferred. Accordingly, other Mediterranean lagoons turned into closed water bodies or were incorporated into delta systems around 5000 cal yrs BP, suggesting an allogenic (climate *plus* sea-level stabilisation trends?) driving factor (Di Rita et al., 2011, 2015; Di Rita & Melis, 2013; Melis et al., 2017). Unfortunately, the high degree of hygrophily that characterised the Arno delta area (*Salix* 23-60%; Figs 3, 5) during the pre-protohistoric period prevents from further palaeoclimate inferences (co-occurrence of wetter periods?). As already demonstrated by Bini et al. (2015), human pressure (high percentages of cultivated plants, especially *Beta vulgaris*) seems to be the main

driving factor on the development of the well-drained alluvial plain, although the low resolution of palynological sampling does not allow to investigate in detail a potential climate influence.

CONCLUSIONS

Detailed palynological analyses (pollen and Pteridophyte and Bryophyte spores), supported by meiofauna ecological groups, allowed to identify late Quaternary turnovers of depositional environments, vegetation dynamics (both local and regional) and pollen-derived palaeoclimate changes within a subsurface stratigraphic succession (ca. 30 m-thick core PA1) of the Arno coastal plain. Two repeated suites of lagoonal/coastal-alluvial deposits, separated by a set of palaeosols, developed during the last glacial-interglacial and the present interglacial/Holocene periods, revealing a synchronised cyclicity of palaeoenvironments and vegetation cover under the prominent forcing of late Quaternary climate-eustatic changes. Our data and interpretations support the following conclusions:

1. Marked fluctuations in pollen and spores ecological groups (214 identified taxa are clustered into twelve groups), framed into the stratigraphic record, document the high sensitivity of the vegetal landscape to palaeoclimate and RSL changes in coastal-alluvial plain settings and, to a lesser extent, to human activities (i.e., land use mainly through agriculture activities). In particular, taxa/groups strictly related to the local pollen rain and spores proved to be excellent palaeoenvironmental indicators, furnishing data about the water-table level and degree of hygrophily/humidity (Hygrophytes and Aquatics), decomposed/degraded organic matter concentration (humicolous spore taxa), natural / human disturbance (Anthropic indicators) and salinity (halophytes). Palynomorph-derived palaeoenvironmental data well complement with the information about water bodies characteristics furnished by the meiofauna in terms of degree of confinement and salinity. Moreover, the relative abundances of Mediterranean, mesophilous and montane taxa track changes and trends in climate conditions at both Milankovitch and sub-Milankovitch timescales.

2. The vertically stacked pattern of 8 bio-sedimentary units, identified by means of the jointly consideration of sedimentological features and microfossils, reveals the development of two T-R cycles within the uppermost 25 m of the Arno Plain subsurface and a similar response of the environmental landscape to the establishment of consecutive interglacial conditions detected by pollen. More specifically, the TSs identified at the transition from alluvial to coastal deposits are marked by a high Bryophyte diversity indicative of unstable, changing environmental conditions.

3. Transgressive lagoon deposits, invariably formed during warm periods, are reflected by high relative abundances of holm oak-mixed oak taxa with respect to montane trees. Pollen assemblage characteristics (i.e., presence of *Q. ilex*) and radiocarbon ages confirm an early Holocene age (< 9800 cal yrs BP) for the transgressive portion of the uppermost cycle, also consistent with a coeval phase of acceleration in RSL

rise in the W Mediterranean. In contrast, the MIS 3 radiocarbon ages available from the older transgressive lagoon facies are rejected taking into account both coastal palaeoenvironments, inconsistent with low MIS 3 sea levels, and pollen-derived climate optimum conditions. The Mediterranean optimum-like vegetal composition (dense holm oak-mixed oak forest), recorded by the lowermost lagoon deposits, suggests warmer conditions than the Holocene, pointing to a MIS 5e age. These data highlight the importance to use a multi-proxy approach also for a more accurate chronological attribution of Pleistocene deposits.

4. The identification around 20 m b.s.l. of MIS 5e lagoon deposits, for the first time recorded in the Arno Plain subsurface, suggests relatively low-subsidence conditions that favoured the development of major unconformities under high-amplitude sea-level fluctuations. The coeval diffusion of an open pine forest in the plain, indicative of glacial conditions, documents climate forcing on the palaeoenvironmental evolution from a lagoon to an interfluvial area characterised by widespread pedogenesis.

5. Very different evolution trends affected the Holocene lagoon that turned into a delta plain through two main steps of progradation under the combined effect of RSL and climate oscillations. Subtle changes into the microfossil content of the lagoonal succession (i.e., halophytes almost disappear and a high-confined, euryhaline meiofauna occurs) link the beginning of siltation by river inputs around 7400 cal yrs BP, close to the beginning of deceleration in Holocene RSL rise. However, only around 5000 cal yrs BP the lagoon was completely filled with fluvial sediment in concomitance with the end of climate optimum conditions marked by a peak of *Fagus*. Pollen data also suggest a primary role of human pressure on the ultimate emersion of the delta plain and its transformation into a well-drained alluvial setting.

SUPPLEMENTARY ONLINE MATERIAL

All the Supplementary data of this work are available on the BSPI website at:

http://paleoitalia.org/archives/bollettino-spi/

REFERENCES

Aguzzi M., Amorosi A., Colalongo M.L., Ricci Lucchi M., Rossi V., Sarti G. & Vaiani C.S. (2007). Late Quaternary climatic evolution of the Arno coastal plain (Western Tuscany, Italy) from subsurface data. *Sedimentary Geology*, 202: 211-229.

Albani A.D. & Serandrei Barbero R. (1990). I Foraminiferi della Laguna e del Golfo di Venezia. *Memorie della Società Geologica*, 42: 271-341.

Allen J.R.M., Watts W.A., McGee E. & Huntley B. (2002). Holocene environmental variability – the record from Lago Grande di Monticchio. *Quaternary International*, 88: 69-80.

Amorosi A., Bini M., Giacomelli S., Pappalardo M., Ribecai C., Rossi V., Sammartino I. & Sarti G. (2013). Middle to late Holocene environmental evolution of the Pisa coastal plain (Tuscany, Italy) and early human settlement. *Quaternary International*, 303: 93-106.

Amorosi A., Bruno L., Cleveland D.M., Morelli A. & Hong W. (2017). Paleosols and associated channel-belt sand bodies from a continuously subsiding late Quaternary system (Po Basin, Italy): New insights into continental sequence stratigraphy. *GSA Bulletin*, 129: 449-463.

Amorosi A., Ricci Lucchi M., Rossi V. & Sarti G. (2009). Climate change signature of small-scale parasequences from Lateglacial-Holocene transgressive deposits of the Arno valley fill. *Palaeogeography, Palaeoclimatology, Palaeoecology*, 273: 142-152.

Amorosi A., Rossi V., Scarponi D., Vaiani S.C. & Ghosh A. (2014). Biosedimentary record of postglacial coastal dynamics: high-resolution sequence stratigraphy from the northern Tuscan coast (Italy). *Boreas*, 43: 939-954.

Amorosi A., Sarti G., Rossi V. & Fontana V. (2008). Anatomy and sequence stratigraphy of the late Quaternary Arno valley fill (Tuscany, Italy). *In* Amorosi A., Haq B.U. & Sabato L. (eds), Advances in application of sequence stratigraphy in Italy. *GeoActa, Special Publication 1*: 55-66.

Antonioli F., Bard E., Potter E.-K., Silenzi S. & Improta S. (2004). 215-ka History of sea-level oscillations from marine and continental layers in Argentarola Cave speleothems (Italy). *Global and Planetary Change*, 43: 57-78.

Arobba D. Caramiello R., Firpo M., Mercalli L., Morandi L. & Rossi S. (2018). New evidence of the earliest human presence in the urban area of Genoa (Liguria, Italy): a multi-proxy study of a mid-Holocene deposit at the mouth of the Bisagno river. *The Holocene*, 28: 1918-1935.

Arrigoni P.V., Raffaelli M., Rizzotto M., Selvi F., Foggi B., Viciani D., Lombardi L., Benesperi R., Ferretti G., Benucci S., Tommaso P.L., Di Miniati U., De Dominicis B., Tomei P.E. & Menicagli E. (1999). Carta della vegetazione forestale della Toscana. Scala 1:250.000. SELCA, Firenze.

Athersuch J., Horne D.J. & Whittaker J.E. (1989). Marine and brackish water ostracods (Superfamilies Cypridacea and Cytheracea). *In* Kermack D.M. & Barnes R.S.K. (eds), Synopsis of the British Fauna, New Series, 43: 1-343.

Bellini C., Ricci Lucchi M. & Montanari C. (2009). The Holocene landscape history of the NW Italian coasts. *The Holocene*, 19: 1161-1172.

Benvenuti M., Mariotti Lippi M., Pallecchi P. & Sagri M. (2006). Late-Holocene catastrophic floods in the terminal Arno River (Pisa, Central Italy) from the story of a Roman riverine harbour. *The Holocene*, 16: 863-876.

Berglund B.E. & Ralska-Jasiewiczowa M. (1986). Pollen Analysis and Pollen Diagrams. *In* Berglund B.E. (ed.), Handbook of Holocene Palaeoecology and Palaeohydrology: 455-484.

Berndt C., Frenzel P. & Ciner A. (2019). Intraspecific length variation and shell thickness of the ostracod *Cyprideis torosa* (Jones, 1850) as a potential tool for palaeosalinity Characterization. *Geosciences*, 9: 83-95.

Bertini A., Ciaranfi N., Marino M. & Palombo M.R. (2010). Proposal for Pliocene and Pleistocene land-sea correlation in the Italian area. *Quaternary International*, 219: 95-108.

Bertini A., Minissale A. & Ricci M. (2014). Palynological approach in upper Quaternary terrestrial carbonates of central Italy: Anything but a 'mission impossible'. *Sedimentology*, 61: 200-220.

Bini M., Rossi V., Amorosi A., Pappalardo M., Sarti G., Noti V., Capitani M., Fabiani F. & Gualandi M.L. (2015). Palaeoenvironments and palaeotopography of a multilayered city during the Etruscan and Roman periods: early interaction of fluvial processes and urban growth at Pisa (Tuscany, Italy). *Journal of Archaeological Science*, 59: 197-210.

Bolkhovitina N.A. (1956). Atlas of spores and pollen from Jurassic and Lower Cretaceous deposits of the Vilyuysk Basin. *Trudy Geologichesk Institut, Akademiya Nauk SSR, Moskva*, 2: 1-132.

Boros A., Jàrai Komlòdi M., Tòth Z. & Nilsson S. (1993). An atlas of recent European Bryophyte spores. 321 pp. Scientia Academic Press, Budapest.

Bortolotti V. (1966). La tettonica trasversale dell'Appennino. La linea Livorno-Sillaro. *Bollettino della Società Geologica Italiana*, 85: 529-540.

Bory J.-B. (1844). Sur les Isoëtes et les espèces nouvelles de cette famille découverte en Algérie. *Comptes Rendus Hebdomadaires des Séances de l'Académie des Sciences*, 18: 1166.

Brady G.S. (1864). On Species of Ostracoda new to Britain. *Annals and Magazine of Natural History*, 13: 59-64.

Brady G.S. (1868). A monograph of the recent British Ostracoda. *Transactions of the Linnean Society of London*, 26: 353-495.

Breda A., Amorosi A., Rossi V. & Fusco F. (2016) Lateglacial to Holocene depositional architecture of the Ombrone palaeovalley system (Southern Tuscany, Italy): sea level, climate and local control in valley-fill variability. *Sedimentology*, 63: 1124-1148.

Bruch P. & Schimper W.P. (1851). Bryologia Europaea Seu Genera Muscorum Europaeorum, 1. 199 pp. Stuttgartiae, sumptibus librariae E. Schweizerbart, Stuttgart.

Bruguière J.G. (1789-1792). Encyclopédie méthodique ou par ordre de matières. Histoire naturelle des vers. volume 1: 1-344 [June 1789]; 345-758 [13 Feb. 1792; dates after Evenhuis, 2003, *Zootaxa*, 166: 37; *Zootaxa*, 207], Pancoucke, Paris.

Busschers F.S., Wesselingh F.P., Kars R.H., Versluijs-Helder M., Wallinga J., Bosch J.H.A., Timmner J., Nierop K.G.J., Meijer T., Bunnik F.P.M. & De Wolf H. (2014). Radiocarbon dating of late Pleistocene marine shells from the southern North Sea. *Radiocarbon*, 56: 1151-1166.

Cerratori L., Ceccarelli Lemut M.L., Garzella G., Grifoni Cremonesi R., Mazzanti R., Morelli P., Pasquinucci M., Pescaglini Monti R., Pult Quaglia A.M., Rau A., Ronzani M. & Tozzi C. (1994). Carta degli elementi naturalistici e storici della pianura di Pisa e dei rilievi contermini. Selca, Firenze 1991.

Christopher R.A. (1976). Morphology and taxonomic status of Pseudoschizaea, Thiergart and Frantz ex R.Potonie emend. *Micropaleontology*, 22: 143-150.

Cincotta A., Pestchevitskaya E.B., Sinitsa S.M., Markevich V.S., Debaille V., Rashetova S.A., Mashchuk I.M., Frolov A.O., Gerdes A., Yans J. & Godefroit P. (2019). The rise of feathered dinosaurs: Kulindadromaeus zabaikalicus, the oldest dinosaur with "feather-like" structures. *PeerJ*, 7: 6239-6259.

Colombaroli D., Marchetto A. & Tinner W. (2007). Long-term interactions between Mediterranean climate, vegetation and fire regime at Lago di Massaciuccoli (Tuscany, Italy). *Journal of Ecology*, 95: 755-770.

Combourieu-Nebout N., Bertini A., Russo-Ermolli E., Peyron O., Klotz S., Montade V., Fauquette S., Allen J., Fusco F., Goring S., Huntley B., Joannin S., Lebretona V., Magri D., Martinetto E., Orain R. & Sadori L. (2015). Climate changes in the central Mediterranean and Italian vegetation dynamics since the Pliocene. *Review of Palaeobotany and Palynology*, 218: 127-147.

Combourieu-Nebout N., Peyron O., Bout-Roumazeilles V., Goring S., Dormoy I., Joannin S., Sadori L., Siani G. & Magny M. (2013). Holocene vegetation and climate changes in the central Mediterranean inferred from a high-resolution marine pollen record (Adriatic Sea). *Climate of the Past*, 9: 2023-2042.

Cremaschi M., Mercuri A.M., Torri P., Florenzano A., Pizzi C., Marchesini M. & Zerboni A. (2016). Climate change versus land management in the Po Plain (Northern Italy) during the Bronze Age: New insights from the VP/VG sequence of the Terramara Santa Rosa di Poviglio. *Quaternary Science Reviews*, 136: 153-172.

Cushman J.A. (1926). Recent Foraminifera from Porto Rico. *Publications of the Carnegie Institution of Wanshington, no. 344, Department of Marine Biology Papers*, 23: 73-84.

Debenay J.P. & Guillou J.-J. (2002). Ecological transitions indicated by foraminiferal assemblages in paralic environments. *Estuaries*, 25: 1107-1120.

Desprat S., Combourieu-Nebout N., Essallami L., Sicre M.-A., Dormoy I., Peyron O., Siani G., Bout Roumazeilles V. & Turon J.L. (2017). Deglacial and Holocene vegetation and climatic changes in the southern Central Mediterranean from a direct land-sea correlation. *Climate of the Past*, 9: 767-787.

Di Rita F., Celant A., Milli S. & Magri D. (2015). Lateglacial – early Holocene vegetation history of the Tiber delta (Rome, Italy) under the influence of climate change and sea level rise. *Review of Palaeobotany and Palynology*, 218: 204-216.

Di Rita F. & Magri D. (2012). An overview of the Holocene vegetation history from the central Mediterranean coasts. *Journal of Mediterranean Earth Sciences*, 4: 35-52.

Di Rita F. & Melis R.T. (2013). The cultural landscape near the ancient city of Tharros (central West Sardinia): vegetation changes and human impact. *Journal of Archaeological Science*, 40: 4271-4282.

Di Rita F., Molisso F. & Sacchi M. (2018). Late Holocene environmental dynamics, vegetation history, human impact, and climate change in the ancient Literna Palus (Lago Patria; Campania, Italy). *Review of Palaeobotany and Palynology*, 258: 48-61.

Di Rita F., Simon O., Caldara M., Gehrels W.R. & Magri D. (2011). Holocene environmental changes in the coastal Tavoliere Plain (Apulia, southern Italy): A multiproxy approach. *Palaeogeography, Palaeoclimatology, Palaeoecology*, 310: 139-151.

Dolez L., Salel T., Bruneton H., Colpo G., Devillers B., Lefèvre D., Serge D.M. & Sanchez C. (2015). Holocene palaeoenvironments of the Bages-Sigean lagoon (France). *Geobios*, 48: 297-308.

Drescher-Schneider R., de Beaulieu J.-L., Magny M., Walter-Simonnet A.-V., Bossuet G., Millet L., Brugiapaglia E. & Drescher A. (2007). Vegetation history, climate and human impact over the last 15,000 years at Lago dell'Accesa (Tuscany, central Italy). *Vegetation History and Archeobotany*, 16: 279-299.

Dumortier B.C.J. (1835). Recueil d'Observations sur les Jungermanniacées 17. 27 pp. Imprimerie de J.A. Blanquart, Tournai.

Ehrenberg C.G. (1840). Verbreitung und Einfluss des mikroskopischen Lebens in Sud- und Nord-Amerika. *Konigliche Preuss Akademie der Wissenschaften zu Berlin, Physik*, 1: 291-445.

Ejarque A., Julià R., Reed J.M., Mesquita-Joanes F., Marco-Berba J. & Riera S. (2016). Coastal Evolution in a Mediterranean Microtidal Zone: Mid to Late Holocene Natural Dynamics and Human Management of the Castelló Lagoon, NE Spain. *PLoS ONE*, 11: e0155446.

Embry A.F. (1995). Sequence boundaries and sequence hierarchies: problems and proposals. *In* Steel R.J., Felt V.L., Johannesses E.P. & Mathieu C. (eds), Sequence stratigraphy on the Northwest European Margin. *Norwegian Petroleum Society Special Publications*, 5: 1-11.

Erhart J.F. (1789). Beiträge zur Naturkunde, und den damit verwandten Wissenschaften, besonders der Botanik, Chemie, Haus- und Landwirthschaft, Arzneigelahrtheit und Apothekerkunst. 184 pp. Hannover und Osnabrück im Verlage bei Christian Ritscher.

Faegri K., Iversen J. & Krzywinski K. (1989). Textbook of pollen analysis. 328 pp. John Wiley and Sons, Chichester.

Follieri M., Magri D. & Sadori L. (1988). 250,000-year pollen record from Valle di Castiglione (Roma). *Pollen et Spores*, 30: 329-356.

Frenzel P., Keyser D. & Viehberg F.A. (2010). An illustrated key and (palaeo)ecological primer for Postglacial to Recent Ostracoda (Crustacea) of the Baltic Sea. *Boreas*, 39: 567-575.

Frenzel P., Schulze I. & Pint A. (2012). Noding of Cyprideis torosa valves (Ostracoda) – a proxy for salinity? New data from field observations and a long-term microcosm experiment. *International Review of Hydrobiology,* 97: 314-329.

Gaertner J. (1790). De fructibus et seminibus plantarum, vol. 2. Sumtibus Auctoris, Typis Academiae Carolinae: 1788-1792.

Garbari F. (2004). Viaggio al Monte Pisano: un'escursione botanica. *Studi Trentini di Scienze Naturali, Acta Biologica*, 81: 233-238.

Giraudi C. (2012). The Holocene record of environmental changes in the 'Stagno di Maccarese' marsh (Tiber river delta, central Italy). *The Holocene*, 22: 1461-1471.

Gliozzi E. & Grossi F. (2008). Late Messinian lago-mare ostracod palaeoecology: a correspondence analysis approach. *Palaeogeography, Palaeoclimatology, Palaeoecology*, 264: 288-295.

Gray S.F. (1821). A natural arrangement of British plants, according to their relations to each other, as pointed out by Jussieu, De Candolle, Brown, &c. including those cultivated for use; with an introduction to botany, in which the terms newly introduced are explained; illustrated by figures, 1: [i]-xxviii, [1]- 824, pls I-XXI plates, London: Printed for Baldwin, Cradock & Joy, Paternoster-Row.

Henderson P.A. (1990). Freshwater ostracods. *In* Kermack D.M. & Barned R.S.K. (eds), Synopses of the British Fauna, New Series, 42: 1-228.

Heron-Allen E. & Earland A. (1913). Clare Island Survey, Part. 64, Foraminifera. *Proceedings of the Royal Irish Academy*, 31: 1-188.

Holmes J.A. & Chivas A.R. (2002). The Ostracoda: applications in Quaternary research. *Geophysical Monograph Series*. 131 pp. AGU, Washington.

Hooke R. (2000). On the history of human as geomorphic agents. *Geology*, 28: 843-846.

Jalut G., Dedoubat J.J., Fontugne M. & Otto T. (2009). Holocene circum-Mediterranean vegetation changes: climate forcing and human impact. *Quaternary International*, 200: 4-18.

Jennings O.E., ed. (1913). A manual of the Mosses of Western Pennsylvania. 429 pp. Press of the City Mission, Pittsburgh.

Jones T.R. (1850). Description of the Entomostraca of the Pleistocene Beds of Newbury Copford, Clacton and Grays. *The Annals and magazine of natural history*, 6: 25-28.

Jorissen F.J. (1988). Benthic foraminifera from the Adriatic Sea; principles of phenotypic variation. *Utrecht Micropaleontology Bullettin*, 37: 1-176.

Kaniewski D., Marriner N., Morhange C., Vacchi M., Sarti G., Rossi V., Bini M., Pasquinucci M., Allinne C., Otto T., Luce F. & Van Campo E. (2018). Holocene evolution of *Portus Pisanus*, the lost Harbour of Pisa. *Scientific Reports*, 8: 11625-11639.

Karsten G.H. (1881). Deutsche Flora, vol. 2. 1284 pp. J.M. Spaeth, Berlin.

Linnaeus K. (1753). Species Plantarum. 1200 pp. Holmiae, Stockholm.

Lowe J.J., Accorsi C.A., Bandini Mazzanti M., Bishop V., Van der Kaars S., Forlani L., Mercuri A.M., Rivalenti C., Torri P. & Watson C. (1996). Pollen stratigraphy of sediment sequences from carter lakes Albano and Nemi (near Rome) and from the central Adriatic, spanning the interval from oxygen isotope Stage 2 to the present day. *Memorie Istituto Italiano Idrobiologia*, 55: 71-98.

Magny M., Joannin S., Galop D., Vannière B., Haas J.N., Bassetti M., Bellintani B., Scandolari R. & Desmet M. (2012). Holocene palaeohydrological changes in the northern Mediterranean borderlands as reflected by the lake-level record of Lake Ledro, northeastern Italy. *Quaternary Research*, 77: 382-396.

Magri D. (2007). Advances in Italian palynological studies: late Pleistocene and Holocene records. *GFF*, 129: 337-344.

Mariotti Lippi M., Guido M., Menozzi B.I., Bellini C. & Montanari C. (2007). The Massaciuccoli Holocene pollen sequence and the vegetation history of the coastal plains by the Mar

Ligure (Tuscany and Liguria, Italy). *Vegetation History and Archaeobotany*, 16: 267-277.

Martini I.P. & Sagri M. (1993). Tectono-sedimentary characteristics of Late Miocene-Quaternary extensional basins of Northern Apennines, Italy. *Earth-Science Reviews*, 34: 197-233.

Mazzini I., Rossi V., Da Prato S. & Ruscito V. (2017). Ostracods in archaeological sites along the Mediterranean coastlines: three case studies from the Italian peninsula. *In* Williams M., Hill T., Boomer I. & Wilkinson I.P. (eds), The Archaeological and Forensic Applications of Microfossils: A Deeper Understanding of Human History. *The Micropalaeontological Society, Special Publications*: 121-142.

Melis R.T., Depalmas A., Di Rita F., Montis F. & Vacchi M. (2017). Mid to Late Holocene environmental changes along the coast of western Sardinia (Mediterranean Sea). *Global and Planetary Change*, 155: 29-41.

Milde C.A.J. (1869). Bryologia Silesiaca. *Laubmoos-Flora von Nord- und Mittel-Deutschland.* 410 pp. Verlag von Arthur Felix, Leipzig.

Miller P. (1768). The gardeners dictionary. 1366 pp. Printed for the Author, 1764, London.

Milli S., D'Ambrogi C., Bellotti P., Calderoni G., Carboni M.G., Celant A., Di Bella L., Di Rita F., Frezza V., Magri D., Pichezzi R.M. & Ricci V. (2013). The transition from wave-dominated estuary to wave dominated delta: the Late Quaternary stratigraphic architecture of Tiber River deltaic succession (Italy). *Sedimentary Geology*, 284-285: 159-180.

Milli S., Mancini M., Moscatelli M., Stigliano F., Marini M. & Cavinato G.P. (2016). From river to shelf, anatomy of a high-frequency depositional sequence: the Late Pleistocene to Holocene Tiber depositional sequence. *Sedimentology*, 63: 1886-1928.

Moench K. (1794). Methodus plantas horti botanici et agri Marburgensis. A staminum situ describendi. 368 pp. Marburgi Cattorum: in officina nova libraria academiae.

Montenegro M.E. & Pugliese N. (1996). Autoecological remarks on the ostracod distribution in the Marano and Grado Lagoons (Northern Adriatic Sea, Italy). *Bollettino della Società Paleontologica Italiana*, 3: 123-132.

Moore P.D., Webb J.A. & Collinson M.E. (1991). Pollen analysis. Second edition. 128 pp. Blackwell Scientific Publications, Oxford.

Mozzi P., Bini C., Zilocchi L., Becattini R. & Mariotti Lippi M. (2003). Stratigraphy, palaeopedology and palynology of late Pleistocene and Holocene deposits in the landward sector of the lagoon of Venice (Italy), in relation to the caranto level. *Il Quaternario. Italian Journal of Quaternary Sciences*, 16: 193-210.

Müller G.W. (1894). Die Ostracoden des Golfes von Neapel und der angrenzenden Meeresabschnitte. *Fauna und Flora Golf von Neapel*, 21: 1-404.

Müller G.W. (1912). Ostracoda. *In* Schulze F.E. (ed.), Das Tierreich. 434 pp. Auftrage Konigl Press, Berlin.

Murray J. (2006). Ecology and applications of benthic foraminifera. 426 pp. Cambridge University Press, New York.

Orbigny A. d' (1839). Foraminifères. *In* Ramon de la Sagra: Historie physique, politique et Naturelle de l'Ile de Cuba. 224 pp. Arthus Bertrand, Paris 1840.

Pascucci V. (2005). Neogene evolution of the Viareggio Basin, Northern Tuscany (Italy). *GeoActa*, 4: 123-138.

Pignatti S. (1979). I piani di vegetazione in Italia. *Giornale Botanico Italiano*, 113: 411-428.

Pignatti S. (1982). Flora d'Italia. Volumes 1-3. 790 pp. 732 pp. 780 pp. Edagricole, Bologna.

Pranzini E. (2007). Airborne LIDAR survey applied to the analysis of historical evolution at the Arno River delta (Italy). *Journal of Coastal Research*, 50: 400-409.

Proskauer J.M. (1951). Studies on Anthocerotales. III. *Bulletin of the Torrey Botanical Club*, 78: 331-349.

Ravazzi C. (2002). Late Quaternary history of spruce in Southern Europe. *Review of Palaeobotany and Palynology*, 120:131-177.

Reille M. (1992). Pollen et spores d'Europe et d'Afrique du nord. Laboratoire de Botanique Historique et Palynologie, 543 pp. Marseille.

Reille M. (1995). Pollen et spores d'Europe et d'Afrique du nord. Supplément 1. Laboratoire de Botanique Historique et Palynologie, 331 pp. Marseille.

Reille M. (1998). Pollen et spores d'Europe et d'Afrique du nord. Supplément 2. Laboratoire de Botanique Historique et Palynologie. 530 pp. Marseille.

Reimer P.J., Bard E., Bayliss A., Warren Beck J., Blackwell P.G., Bronk Ramsey C., Buck C.E., Cheng H., Lawrence Edwards R., Friedrich M., Grootes P.M., Guilderson T.P., Haflidason H., Hajdas I., Hatté C., Heaton T.J., Hoffmann D.L., Hogg A.G., Hughen K.A., Felix Kaiser K., Kromer B., Manning S.W., Niu M., Reimer R.W., Richards D.A., Marian Scott E., Southon J.R., Staff R.A., Turney C.S.M. & van der Plicht J. (2013). Intcal13 and Marine13 radiocarbon age calibration curves 0-50,000 years cal BP. *Radiocarbon*, 55: 1869-1887.

Revelles J., Burjachs F., Morera N., Barceló J.A., Berrocala A., López-Bultóa O., Maichere C., Le Baillye M., Piquéa R., Palomoa A. & Terradas X. (2017). Use of space and site formation processes in a Neolithic lakeside settlement. Pollen and non-pollen palynomorphs spatial analysis in LaDraga (Banyoles, NE Iberia). *Journal of Archeological Science*, 81: 101-115.

Ribecai C. (2011). Synthesis of late Quaternary palynological studies in the Arno coastal plain and surroundings: toward a comprehensive late Quaternary palaeovegetation history. *Atti della Società Toscana di Scienze Naturali, Memorie, Serie A*, 116: 163-170.

Ricci Lucchi M. (2008). Vegetation dynamics during the last Interglacial – Glacial cycle in the Arno coastal plain (Tuscany, western Italy): location of a new tree refuge. *Quaternary Science Reviews*, 27: 2456-2466.

Rome D.R. (1942). Ostracodes marins des environs de Monaco, 2ème note. *Bulletin de l'Institut océanographique de Monaco*, 38: 1-28.

Rossi V., Amorosi A., Sarti G. & Mariotti S. (2017). Late Quaternary multiple incised-valley systems: an unusually well-preserved stratigraphic record of two interglacial valley-fill successions from the Arno plain (northern Tuscany, Italy). *Sedimentology*, 64: 1901-1928.

Ruiz F., Gonzalez-Regalado M.L., Baceta J.I., Menegazzo-Vitturi L., Pistolato M., Rampazzo G. & Molinaroli E. (2000). Los ostrácodos actuales de la laguna de Venecia (NE de Italia). *Geobios*, 33: 447-454.

Sadori L., Mazzini I., Pepe C., Goiran J.-P., Pleuger E., Ruscito V., Salomon F. & Vittori C. (2016). Palynology and ostracodology at the Roman port of ancient Ostia (Rome, Italy). *The Holocene*, 26: 1502-1512.

Sarti G., Rossi V., Amorosi A., Bini M., Giacomelli S., Pappalardo M., Ribecai C., Ribollini A. & Sammartino I. (2015). Climatic signature of two mid-late Holocene fluvial incisions formed under sea-level highstand conditions (Pisa coastal plain, NW Tuscany, Italy). *Palaeogeography, Palaeoclimatology, Palaeoecology*, 434: 183-195.

Schimper W.P. (1856). Corollarium Bryologiae Europaeae 13. 140 pp. Schweizerbart, Stuttgart.

Scopoli J.A. (1772). Flora Carniolica, Editio Secunda, 2. 244 pp. J.P. Krauss, Vienna.

Sgarrella F. & Moncharmont Zei M. (1993). Benthic Foraminifera of the Gulf of Naples (Italy): systematics and autoecology. *Bollettino della Società Paleontologica Italiana*, 32: 145-264.

Stuiver M., Reimer P.J. & Reimer R.W. (2019). CALIB 7.1 [WWW program] at http://calib.org, accessed 2019-6-30.

Tzedakis P.C., Hooghiemstra H., Pälike H. (2006). The last 1.35 million years at Tenaghi Philippon, revised chronostratigraphy and long-term vegetation trends. *Quaternary Science Reviews,* 25: 3416-3430.

Turra A. (1764). Dei vegetabili di Monte Baldo. Giornale d'Italia spettante alla scienza naturale, e principalmente all'agricoltura, alle arti, ed al commercio, 1: 144-152.

Tutin T.G., Heywood V.H., Burges N.A. & Valentine D.H. (1993). Flora europaea. 629 pp. Cambridge University Press, Cambridge.

Ubaldi D. (2003). Flora, fitocenosi e ambiente. Elementi di geobotanica e fitosociologia. 334 pp. CLUEB, Bologna.

Vacchi M., Marriner N., Morhange C., Spada G., Fontana A. & Rovere A. (2016). Multiproxy assessment of Holocene relative sea-level changes in the western Mediterranean: sea-level variability and improvements in the definition of the isostatic signal. *Earth-Science Reviews*, 155: 172-197.

Willdenow C.L. (1805). Caroli a Linné species plantarum. Ed. 4., post Reichardianam quinta. 495 pp. Berolini: Impensis G.C. Nauk, 1797-1830.

6.2. High-resolution record of palaeoclimate-palaeoenvironmental trends within the MIS 5-MIS 1 interval

6.2.1. Introduction

From a palynological perspective, late Quaternary lacustrine and deep-sea sedimentary successions are the most investigated archives for high-resolution palaeoclimatic studies (e.g., Follieri et al., 1988; Combourieu Nebout et al., 2013; Di Rita et al., 2013), owing to their low degree of facies variability and the lack of prominent erosional surfaces. Furthermore, the predominantly fine-grained nature of their successions is highly prone to preserve pollen grains due to the low degree of porosity acting as a trap (Faegri et al., 1989).

The lacustrine sedimentary record can be investigated also in terms of non-pollen palynomorphs (NPPs, such as fungal spores), siliceous or calcareous fossils (e.g., diatoms, charophytes, ostracods), sedimentary structures (e.g., varves, flood layers) and geochemistry. Changes of these parameters are considered significant for palaeoenvironmental studies, given the rather unchanging area of catchments and, thus, of sediment source. If framed into a robust and high-resolution chronological framework and opportunely calibrated, all these data allow to identify local changes in palaeohydrology (with consequent palaeoclimate inferences) and human land-use activities (e.g., Carriòn and van Geel, 1999; Joannin et al. 2013; Magny et al., 2013; Wirth et al., 2013; Mazzini et al., 2015). By contrast, marine records lack this high-resolution focus on local landscape-climate-human dynamics but can account for a strong regional definition of vegetation patterns due to the wider pollen rain (mainly coming from the surrounding catchments on the emerged portion of the basin). Climate variations detected from the marine record are of higher magnitude than those recorded within lakes and, thus, can be accounted as regional (e.g., Dormoy et al., 2009; Combourieu Nebout et al., 2013; Toti and Bertini, 2018).

As the natural joining link between lacustrine and marine realms, the sedimentary record in the subsurface of modern coastal-delta plains would represent the ideal place where to investigate the complex relationships among a set of depositional environments (from alluvial to shallow marine), vegetation dynamics and global climate-relative sea level (RSL) changes at millennial timescales. In addition, coastal plains have been densely inhabited and strongly exploited by humans since the Neolithic, leaving traces of the increasing anthropogenic impact on both ecosystems and depositional environments (Di Rita and Magri, 2012). Nonetheless, Mediterranean coastal-delta plains are still a rather underexplored archive for high-resolution palyno-stratigraphic studies over a long-term chronological interval, probably because of the common occurrence of *i)* coarse-grained

deposits (i.e., dune, beach and fluvial sands), hardly prone to palynomorph preservation, and *ii*) several sedimentary *hiatuses* or surfaces of stratigraphic condensation mainly due to sediment erosion, palaeosol formation and delta lobe shifting. In addition, alluvial and coastal regions are strongly affected by Milankovitch-scale (i.e., glacial-interglacial cycles) and sub-Milankovitch scale glacio-eustatic cyclicities, as revealed by sequence-stratigraphic studies (e.g., Catuneanu et al., 2011).

On the other hand, this supposed weakness could be seen as a unique opportunity to investigate landscape dynamics that are not recorded within any other archive and to analyse them in terms of palaeoclimate-RSL conditions. As an example, Di Rita et al. (2015) have reconstructed vegetation landscape dynamics from late Pleistocene to Holocene transgressive estuarine deposits of the Tiber delta (central Italy), linking them to a variety of sub-Milankovitch-scale climatic and environmental (i.e., water-table level and salinity conditions) processes occurring between ca. 13-8.4 cal. kyr BP. Other studies on Mediterranean highstand deposits of mid-late Holocene age (e.g., Di Rita et al., 2011, 2013, 2018; Revelles et al., 2019) have documented that sedimentary successions from brackish coastal basins / wetlands can have a high potential for high-resolution palaeoenvironmental and palaeoclimatic studies based on pollen data, as well as for reconstructing the effects of human presence.

Here I present the record of a high-resolution palyno-stratigraphic analysis from the shallow subsurface (ca. 30 m) of the Arno delta plain (core PA1 in Fig. 6.1), where the occurrence of two T-R cycles has been discussed at length in section 6.1 (Cacciari et al., 2019) and related to MIS 5 - MIS 1 glacio-eustatic variations; each cycle includes a lower transgressive lagoonal interval overlain by alluvial deposits. The main scopes of this study are to: *i)* assess the extent to which the detailed analysis of pollen and spores can improve facies characterization of a coastal-alluvial succession; *ii)* reconstruct landscape dynamics during two distinct phases of lagoon formation (i.e., MIS 5e *versus* Holocene interglacials) and subsequent infilling; and *iii)* provide new insights on the forcing factors acting during the Holocene at a sub-Milankovitch scale with a special emphasis on vegetation-derived climate and human impact data.
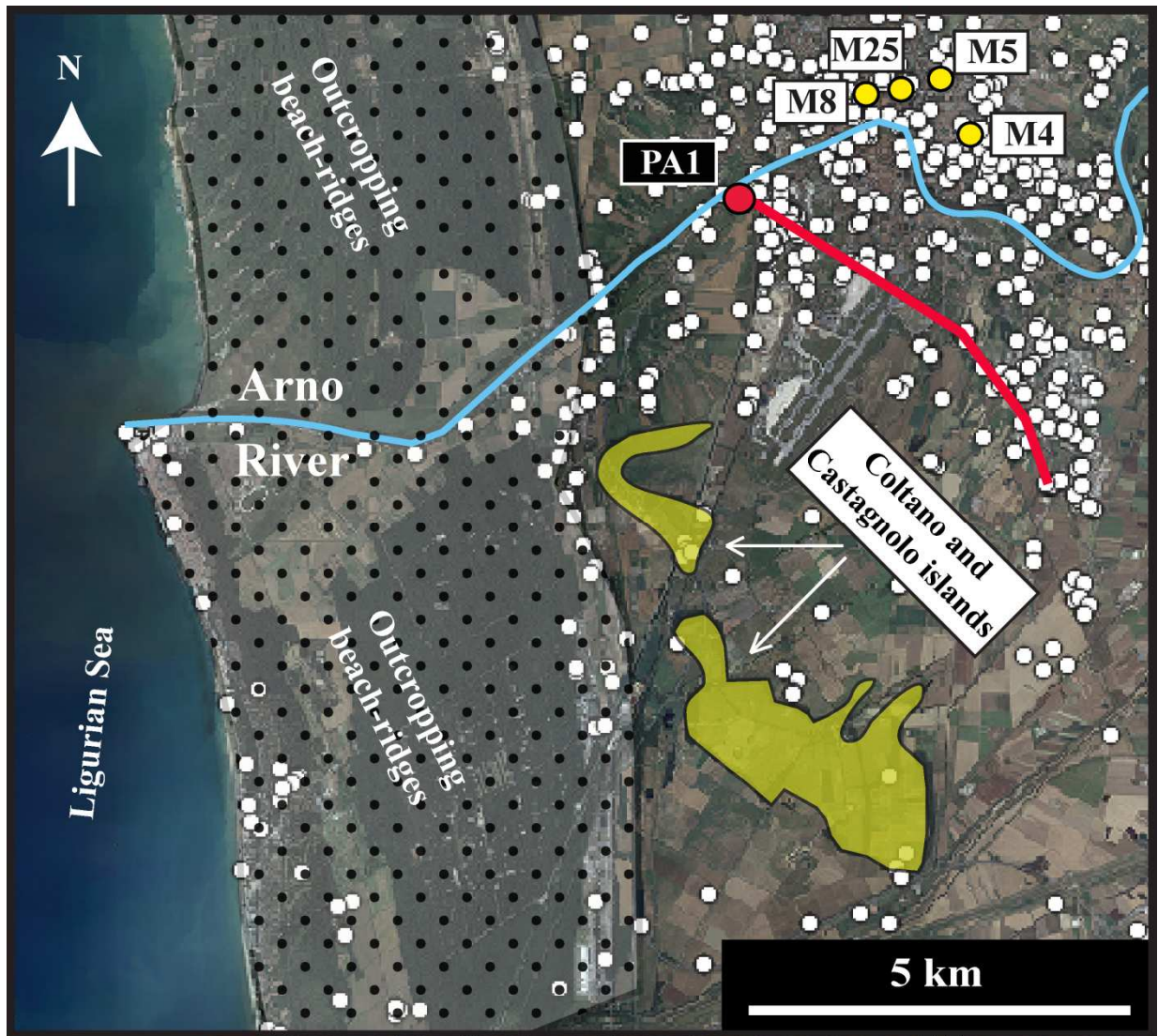
Fig. 6.1: Location map of the studied core PA1 with the trace of the stratigraphic section of Fig. 6.8 (red line). The location of the other cores discussed in text is also shown (yellow dots). White dots correspond to the Arno plain subsurface dataset (from Amorosi et al., 2013b). Satellite images are from Google Earth.

6.2.2. Methodological approach

In order to decipher the landscape dynamics at the best resolution within the PA1 cored succession, 16 samples were collected in addition to those reported in Chapter 6.1 (Cacciari et al., 2019) with a focus on two particular depositional/architectural elements recorded within the two late Quaternary T-R cycles: lagoon intervals and palaeosols. Lagoon deposits were considered very promising for our scopes, because:

-       the uniform, clayey texture makes them highly prone to palynomorph preservation;

- the expanded stratigraphic succession of the Holocene lagoon (10 m of brackish deposits covering ca. 5000 years) preserves a high-resolution, early-mid Holocene palaeoclimate record (between ca. 9800-5000 cal. yrs BP) under relatively stable environmental conditions;

- the record of the late Pleistocene lagoon, reasonably formed during the Last Interglacial, gives the opportunity to characterise for the first time Eemian palaeoclimate conditions in the Arno delta plain.

For both lagoon intervals, a constant pace in sample recovery was followed: ca. 1 sample/30 cm for the lower one and 1 sample/1 m for the thicker upper one.

Concerning palaeosols, the identification of pedological horizons was used as a guide for the uneven sampling aimed at detecting changes in vegetation communities associated to palaeosol formation and development. This approach was used for the upper regressive portions of both T-R cycles, although these intervals clearly record a different degree of pedogenesis (section 6.1; Cacciari et al., 2019). In general, pedological horizons were recognised by integrating high pocket penetration values (> 3.5 kg/cm^2) with specific colour features and accessory materials reported as follows:

- darkening of 'A' horizons, differing from swamp organic matter accumulation by the lack of clearly recognisable vegetation remains;

- reddening of 'A' and 'B' horizons due to Fe-Mn mottles;

- whitening of 'B' and 'C' horizons due to $CaCO_3$ nodules and traces of illuviation from the overlying 'A' horizon.

Cluster analysis on the whole palynological dataset (details on the applied statistical method are reported in Chapter 3) and a quantitative evaluation of secondary grains were also performed to support palaeoclimate and palaeoenvironmental (facies) inferences.

6.2.3. Depositional facies

Seven depositional facies were identified within core PA1 integrating sedimentological features and palynological data. The meiofauna content (i.e., benthic foraminifers and ostracods) reported in Cacciari et al. (2019) (section 6.1.) strongly supports facies characterization. Detailed facies descriptions and interpretations are reported below (Figs. 6.2, 6.3).

Lagoon facies association

This facies association, up to 10 m-thick, occurs at two distinct stratigraphic intervals of the cored succession (between ca. 24.5-22 m core depth and ca. 18-8 m core depth; Fig. 6.2) and is made up of bioturbated, grey-light blue silty clay with the common occurrence of disarticulated shells of bivalves, mainly *Cerastoderma glaucum*. Gastropods, lags of fragmented shells and dark organic-rich layers are locally encountered. PP values generally range within 0.2-0.6 kg/cm^2. The monotonous clayey succession is occasionally interrupted by the presence of thin (< 1 cm) sandy silt layers, locally showing organic matter laminations. The top of the 24.5-22 m deep interval is weakly pedogenized (A/C profile), as recorded by the diffuse presence of Fe mottles and higher PP values peaking at ca. 5 kg/cm^2 in the 'A' horizon. The palynological assemblage is dominated (> 15%) by Mediterranean (e.g., *Erica arborea, Quercus ilex, Olea* and *Phyllirea*) and mixed oak forest (*Carpinus betulus, Ostrya carpinifolia* and various *Quercus*, *Tilia* and *Ulmus* species) taxa. *Alnus glutinosa* and *Salix* show variable percentages (3-15%), whereas halophytes, such as *Artemisia, Beta vulgaris*, *Chenopodium* and *Corrigiola*, are a minor (2-11%) but constant component of the vegetation (Figs. 6.3, 6.6, 6.7, 6.10, 6.11). The occurrence of secondary grains is generally low (< 6%) compared to the several peaks of 20-25% recorded along the core, although an upward increasing trend is encountered within the 18-8 m core depth interval (Fig. 6.2). The meiofauna consists predominantly of the euryhaline ostracod *Cyprideis torosa* accompanied by high-confinement foraminiferal species (*sensu* Debenay and Guillou, 2002), mainly *Ammonia tepida-A. parkinsoniana*. Low abundances of brackish-marine ostracods and low confinement foraminifers occasionally occur.

Sedimentological features and the peculiar fossil content (i.e., widespread presence of halophytes and euryhaline *C. torosa*) indicate that this facies association was formed in a low-energy, brackish environment. In particular, the co-dominance of *A. tepida-A. parkinsoniana*, *C. torosa,* and *C. glaucum* is considered a sensitive and reliable indicator of semi-closed coastal basins subject to salinity oscillations such as lagoons (Russell and Petersen, 1973; Athersuch et al., 1989; Millet and Lamy, 2002; Murray, 2006). Halophytes likely colonized the brackish wetlands bordering the lagoon basins, whereas the relative abundances of *Alnus glutinosa* and *Salix* can account for the spreading of hygrophilous woods in freshwater swamps located close to the lagoon area and, to a lesser extent, to the fluvial transport from nearby riparian settings. The high percentages of Mediterranean and mixed oak forest taxa correspond to a regional vegetation signal that is not related to the depositional environment. The upward increase in secondary grains encountered within the uppermost lagoonal interval can be suggestive of increasing proximity to the source of detritus (e.g., river mouth).

Swamp facies association

This facies association, commonly less than 1 m thick, is encountered within core PA1 at different stratigraphic levels (Fig. 6.2) and is made up of dark grey silty clays with sparse vegetation remains, decomposed organic matter and occasionally Fe mottles, often found around vegetal debris and ascribed to its decay. PP values are generally in the range of 1-2 kg/cm^2, however a peak (>6 kg/cm^2) at 20.7 m core depth is suggestive of pedogenesis and CaCO$_3$ accumulation (Fig. 6.2). Palynomorph assemblages define a relatively open wetland community with a high diversification: helophytes and hydrophytes are generally abundant (Figs. 6.2, 6.3), as *Sparganium emersum* and *S. erectum* are more present alongside *Butomus umbellatus, Lemna minor, Nymphaea alba*, *Schoenoplectus* and various Isoetaceae. A highly diversified Bryophyte community, mainly characterised by *Fissidens rufulus, Phaeoceros laevis* and various *Sphagnum* species, characterises this facies at lowermost stratigraphic levels. A generally significant presence of *Alnus glutinosa* and *Salix* is also documented, although within a wide range. Humicolous taxa (e.g., *Orthodontium gracile*) are also found, whereas halophytes are very scarce (less than 2%) with the unique exception of sample collected at 24.95 m core depth, where they peak at ca. 7%. (Figs. 6.6 and 6.10). The amount of secondary grains is variable, ranging between 1-23%, with high values recorded exclusively within the lowermost intervals (Fig. 6.2). Freshwater-low brackish ostracods characterise this facies association, although valves of *C. torosa* are locally encountered.

The distinctive sedimentological features (dark colour, fine grain-size, diffuse presence of vegetal remains and organic matter) and the occurrence of abundant helophytes and hydrophytes point to a low-energy, humid setting with fresh-low brackish stagnant waters, such as a swamp. This interpretation is coherent with the general scarcity of halophytes, the ostracod fauna, and the presence of Bryophyte humicolous taxa. The highly diversified Bryophyte community found in the lowermost swamp intervals suggests pioneering conditions of wet and rather unstable (Polygonaceae and Urticaceae-rich) environments.

Bay-head delta facies association

This facies association consists of a 0.8 m-thick coarsening-upward (CU), silty-fine sand succession with wood fragments. The plant community, similar to that retrieved within lagoonal intervals, is characterised by the remarkable presence of *Fagus sylvatica,* with montane alders (*Alnus incana* and *A. viridis*) in a subordinate position (Fig. 6.11). Low amounts of secondary grains are found. A mixed brackish – freshwater ostracod fauna also occurs along with high-confinement foraminifers. Sedimentological characteristics (i.e., CU trend; presence of wood fragments), the fossil content (aquatics more abundant than halophytes, occurrence of a mixed brackish – freshwater meiofauna)

and stratigraphic position above lagoon deposits point to a bay-head delta accumulated at the distal portion of a river mouth entering the lagoon. The occurrence of *Fagus sylvatica* with montane alders is interpreted as a regional signal independent from the depositional environment.

Poorly-drained floodplain facies association

This facies association, which ranges in thickness between ca. 0.5 and 1.5 m, occurs at different stratigraphic levels throughout the core. It consists of a relatively monotonous succession of grey clays and silty clays with scarce-very scarce organic matter and vegetal debris. The occurrence of gley pedogenesis between ca. 7-4 m core depth is revealed by Agc-Cgc horizons with scarce $CaCO_3$ mm-sized nodules in the upper horizon and abundant $CaCO_3$ cm-sized nodules in the lower horizon (Fig. 6.2). Fe-Mn concretions are very scarce. PP values range between 1-2 kg/cm^2, however higher values occur in correspondence of $CaCO_3$ accumulation. A wetland vegetation community dominated by Cyperaceae, Poaceae and, less frequently Pteridophytes, with *Sparganium emersum* and *S. erectum* as subordinate taxa, is observed. Occasionally, the canopy dramatically increases, as *Salix* becomes the dominant plant by far. Secondary grains are quite abundant in its upper portion (7-26%). Freshwater-low brackish ostracods are also found (Figs. 6.6, 6.10).

This facies association is interpreted to reflect a fully terrestrial, low-energy depositional environment subject to short-lived phases of subaerial exposure (as highlighted by gley pedogenesis), such as a poorly-drained floodplain, consistent with the palynological assemblage and the ostracod fauna.

Floodplain facies association

This 2-3 m thick facies association was observed at two distinct stratigraphic intervals of the cored succession (between ca. 20.5-18 m core depth and ca. 4-2 m core depth; Fig. 6.2) and is composed of silty clay-silt with the local occurrence of mm to cm-thick sand layers. It generally shows pedogenesis, with development of both weak (A/C profiles) and mature (A-Bwc-C profiles) palaeosols. PP values are variable, ranging 1-3 kg/cm^2 within less stiff / less mature horizons and 5->6 kg/cm^2 where organic matter degradation or $CaCO_3$ accumulation is stronger; the latter case is related to the development of calcic and petrocalcic C horizons. Fe mottles are widespread across the facies, as pedogenesis often involves previously formed palaeosols, but they can be a minor component within C horizons. Mn mottles are generally much less abundant than their Fe counterparts.
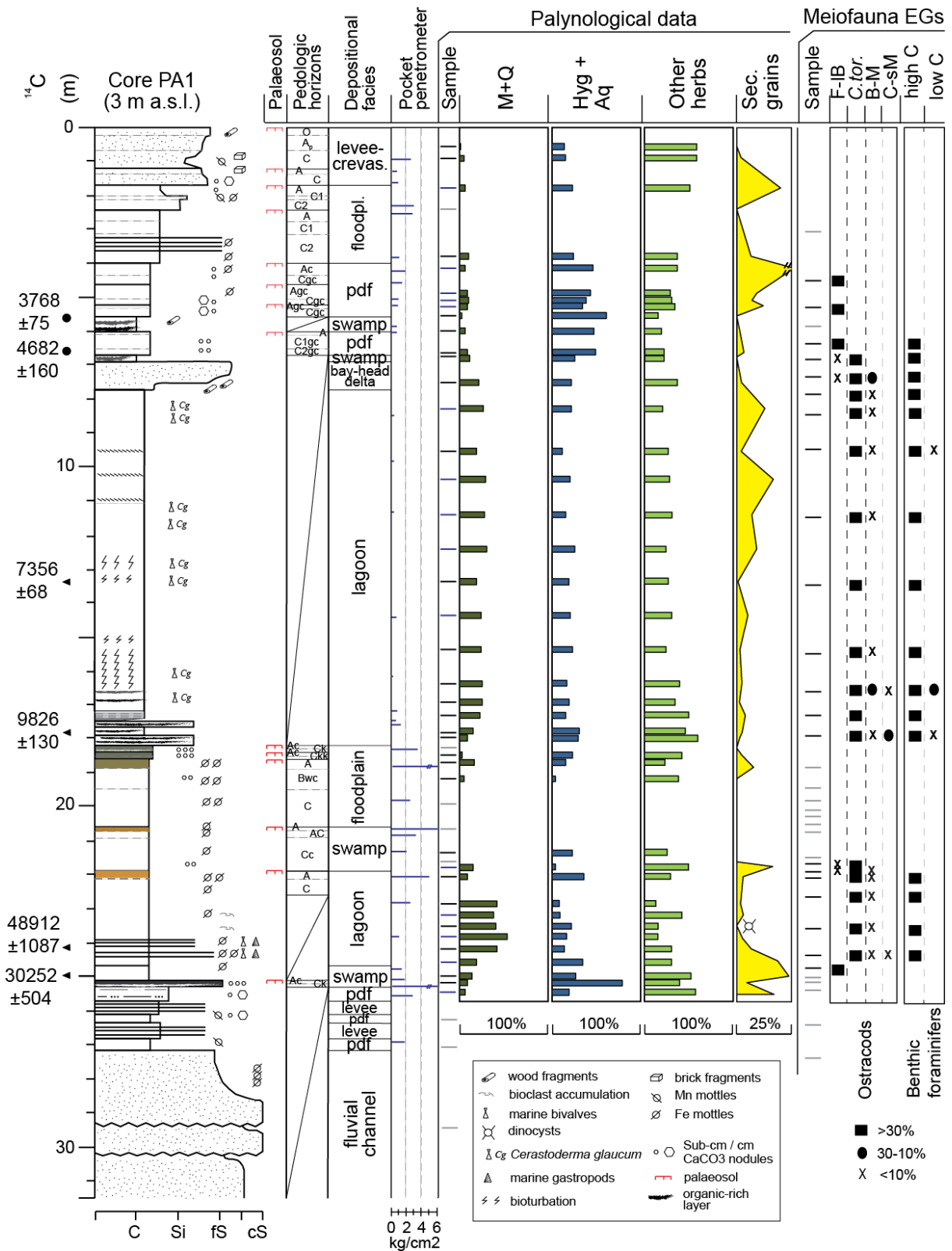
Fig. 6.2: Sedimentological and pedological features accompanied by relative percentages of selected pollen groups and ecological meiofauna groups (EGs) for the facies characterization of PA1 (core location is shown in Fig. 6.1). The stratigraphic log and the meiofauna data are slightly modified from Cacciari et al. (2019). Please refer to this paper for more detailed information about meiofauna EGs. Yellowish brown colour highlights mottled indurated horizons. Triangles indicate radiocarbon samples, while dots correspond to projected dates from the nearby core Mappa3 (see Tab. 3.1). Following Cacciari et al. (2019), the two lowermost ages should be refused. Samples barren of microfossils are shown in grey, while the 16 additional samples are reported in blue.

The main plant community found within this facies is an open woodland / wooded prairie, depending on variations in the arboreal cover. Its taxonomic composition is highly differentiated, from open pine woodlands (*Pinus mugo* and *Pinus* sp. with subordinate steppics) to disturbed prairies (Apiaceae, Brassicaceae and Poaceae) with cultivated elements (i.e., *Beta vulgaris*), the latter exclusively recorded within the uppermost interval (Figs. 6.3, 6.6, 6.7, 6.10, 6.11). Secondary grains are rather scarce and the meiofauna is absent (Fig. 6.2).

The sedimentological and palynological features point to a low-energy, well-drained alluvial depositional setting subject to various degree of pedogenesis (i.e., floodplain) and occasionally affected by river floods (sandy layers).

Levee-crevasse facies association

This facies association occurs in the lowermost (ca. 27-26 m core depth) and uppermost (ca. 2-0 m core depth) parts of the cored succession. It consists of silty sand-sandy silt couplets locally showing a general CU trend (Fig. 6.2). PP values in silt layers range between 2-3 kg/cm^2. Cm-thick CaCO$_3$ nodules are found. The meiofauna is absent. The uppermost interval contains a palynological assemblage dominated by Poaceae and Cichorioideae (pm group), with the local occurrence of Brassicaceae (alia group). Wild Chenopodiaceae (Ai / hal groups) show variable percentages ranging between ca. 2-6 % (Figs. 6.3, 6.6, 6.10). This facies association is interpreted as a channel-related deposit, such as a levee or a crevasse splay. The occurrence of a disturbed prairie with halophytes in the uppermost interval possibly indicates a process of soil salinization following agricultural practices, as confirmed by the recovery of brick fragments and by the O-Ap-C soil profile of the uppermost deposits.

Fluvial-channel facies association

This facies association exceeds 4 m in thickness and occurs in the lowermost part of the cored succession (Fig. 6.2). It is composed of grey, fine to coarse sands with the occasional evidence of widespread reddish mottles, possibly due to oscillations of the groundwater level. A suite of fining-upward (FU) sandy layers with lower erosional boundaries makes up the entire succession. One palynological sample was tentatively analysed from a fine sandy interval but it proved to be sterile. Similarly, another sample collected atop the succession was barren of microfossils. On the basis of its diagnostic sedimentological features (lithology; FU trends; lower erosional surface), this facies association is interpreted as a fluvial-channel sand body.
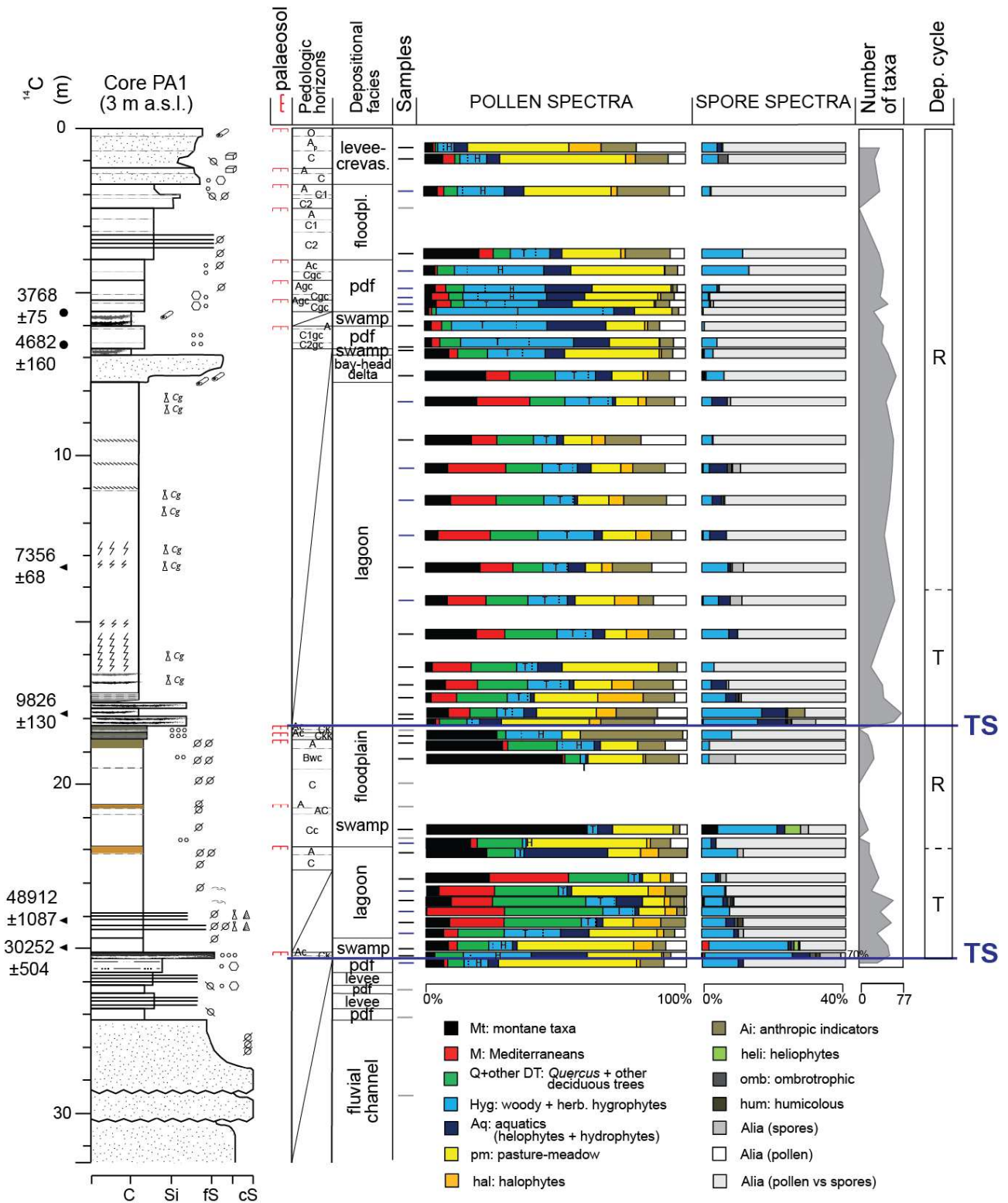
Fig. 6.3: Stratigraphy and palynological spectra showing the relative abundances of pollen and spores ecological groups. Depositional facies, T-R cycles and related TSs are shown. Please refer to Fig. 6.2 for lithological and chronological keys. Following Cacciari et al. (2019), the two lowermost ages should be refused. Samples barren of microfossils are shown in grey, whereas the 16 additional samples are reported in blue. Within hygrophytes, the letters T and H highlight whether trees or herbs dominant within the group; a dashed line separates the two portions.

108

6.2.4. Pollen and spore groups

The cluster analysis (CA) defined five pollen-derived biomes (PDBs shown in Fig. 6.4): Willow wetlands (Ww), Mesophilous disturbed grasslands (Mdg), Mediterranean oak forest (Mof), Alder woods (Aw) and Mesophilous pine wood (Mpw). These biomes are characterised as follows:

- Ww → hygrophilous wood, possibly riparian, characterised by wide canopy clearings with Cyperaceae and Poaceae and depressed, submerged areas with *Isoetes durieui* and *Sparganium* spp. Pioneering conditions are pointed to by bryophytes.

- Mdg → *Quercus cerris* and *Alnus* sp. are the main woody taxa, whereas cultivated herbs (*Beta vulgaris*) and ubiquists (Apiaceae, Brassicaceae, Cichorioideae and Chenopodiaceae) dominate both at genus/species and family levels; wetland taxa are less present and appear to be in a subordinate position (*Butomus*, *Callitriche* spp. and *Typha*).

- Mof → holm oak – mixed oak forest with a mixture of Mediterranean (*Erica arborea* and *Quercus ilex*), mesophilous (*Carpinus/Ostrya, Quercus* spp., *Tilia cordata*, and *Ulmus minor*) and wetland taxa (*Hydrocharis*, *Isoetes hystrix/lacustris* and *Myriophyllum*). Halophytes are also present (*Artemisia* and *Corrigiola* spp.), although to a lesser extent.

- Aw → meso-hygrophilous vegetation with both montane (*Alnus incana*, *A. viridis*, *Fagus sylvatica* and *Pinus sylvestris*) and lowland trees (*Alnus glutinosa*, *Carpinus betulus* and *Quercus robur*). The only Mediterranean shrub is *Pyracantha coccinea*; *Sphagnum* spp. is the sole bryophyte present.

- Mpw → Encompassing most of the Pinaceae found within the dataset (*Picea abies*, *Pinus mugo*, *Pinus* sp. and Pinaceae undiff.), in this plant association wetland herbs, such as *Lemna* and *Nymphaea alba* are also represented, suggesting a moisture availability generally intermediate between wetlands and conifer (mostly pine) woods. The degree of natural disturbance is rather high, since the presence of *Polygonum persicaria* group and Urticaceae.
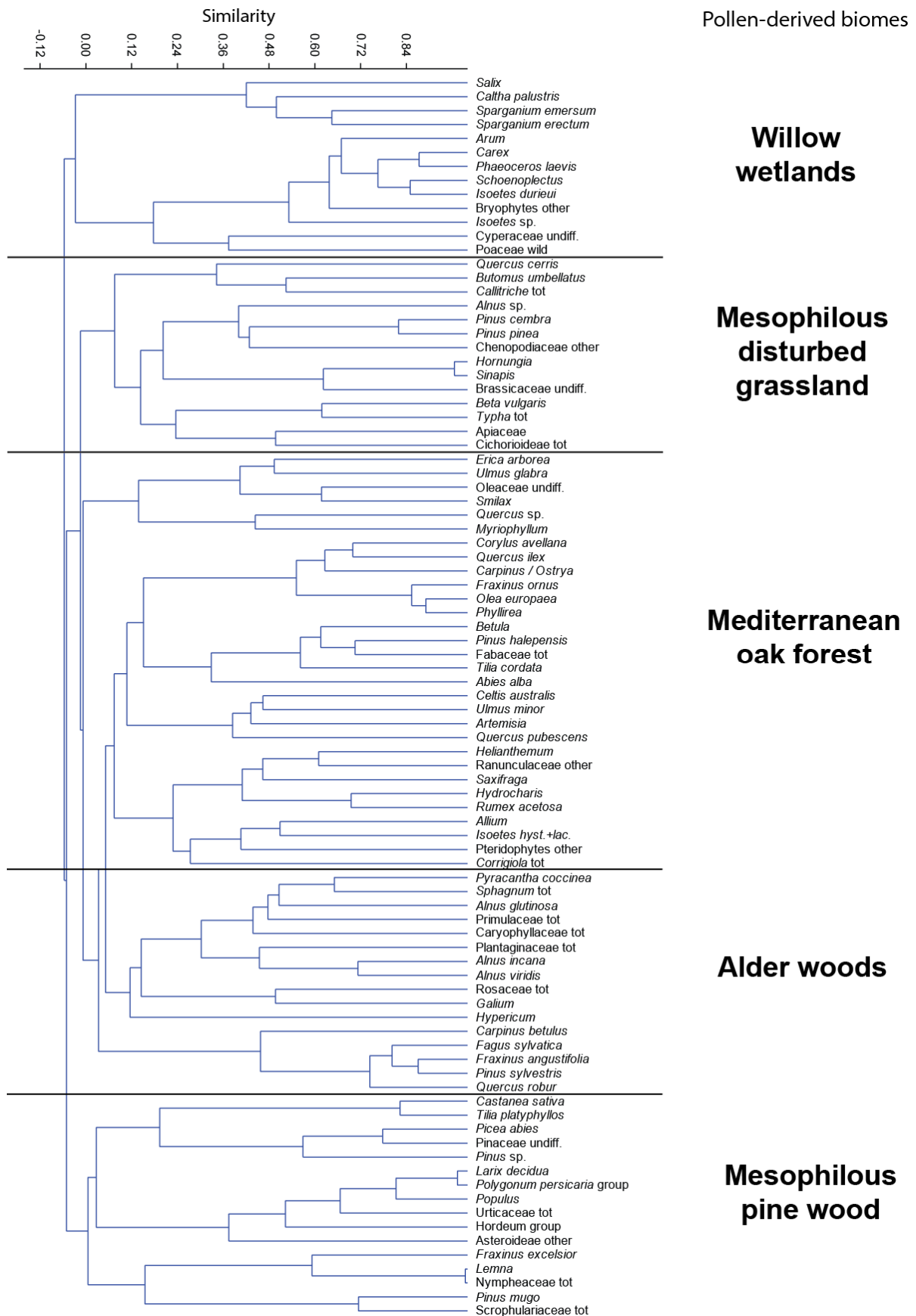
Fig. 6.4: Cluster analysis tree diagram performed on selected plant taxa of core PA1 (Correlation was used as similarity method and Paired group as root, similarly to the EM2 dataset in Chapter 5.2). The resulting pollen-derived biomes (PDBs) and interpreted vegetation dynamics in the Arno Plain and surrounding reliefs are also shown.

As a whole, the CA-derived biomization confirms and supports the ecological plant groups (shown in the pollen and spore spectra of Fig. 6.3). Biomes are interpreted as follows:

-        Ww → Willow woods and associated clearings typical of riparian, low-lying areas in alluvial/delta plains, where a certain degree of hygrophily is always present. Ecological considerations and taxa composition suggest that this biome is mostly representative of the Holocene delta plain (swamp / poorly-drained floodplain succession) and of the swamps found at the bottom of both T-R cycles where a pioneering bryophyte / wetland vegetation thrived.

-        Mdg → Herbaceous coastal community with evidence of human impact and related modifications of the vegetation landscape.

-        Mof → Interglacial-like pollen association indicative of all the vegetation types developed in the delta plain (Mediterranean, mesophilous and hygrophilous). The presence of *Erica arborea* and the high number of taxa may suggest this biome to mainly represent the Eemian vegetation associated to the lower lagoonal interval.

-        Aw → Interglacial-like pollen association indicative of a more humid climate than the Mof biome. The presence of *Sphagnum* and *Pyracantha coccinea*, found nearly just in the Holocene lagoon, and the general lesser degree of mediterraneity with respect to Mof documented by the taxa association, may suggest that this biome mainly represents the Holocene vegetation associated to the upper lagoonal interval.

-        Mpw → Vegetation typical of cool conditions (i.e., glacial periods), occasionally with local soil waterlogging. The pollen association strongly suggests this biome to represent the vegetation developed within the pedogenised floodplain of the last glacial period.

6.2.5. Late Pleistocene vegetation-environmental dynamics: trends and controlling factors
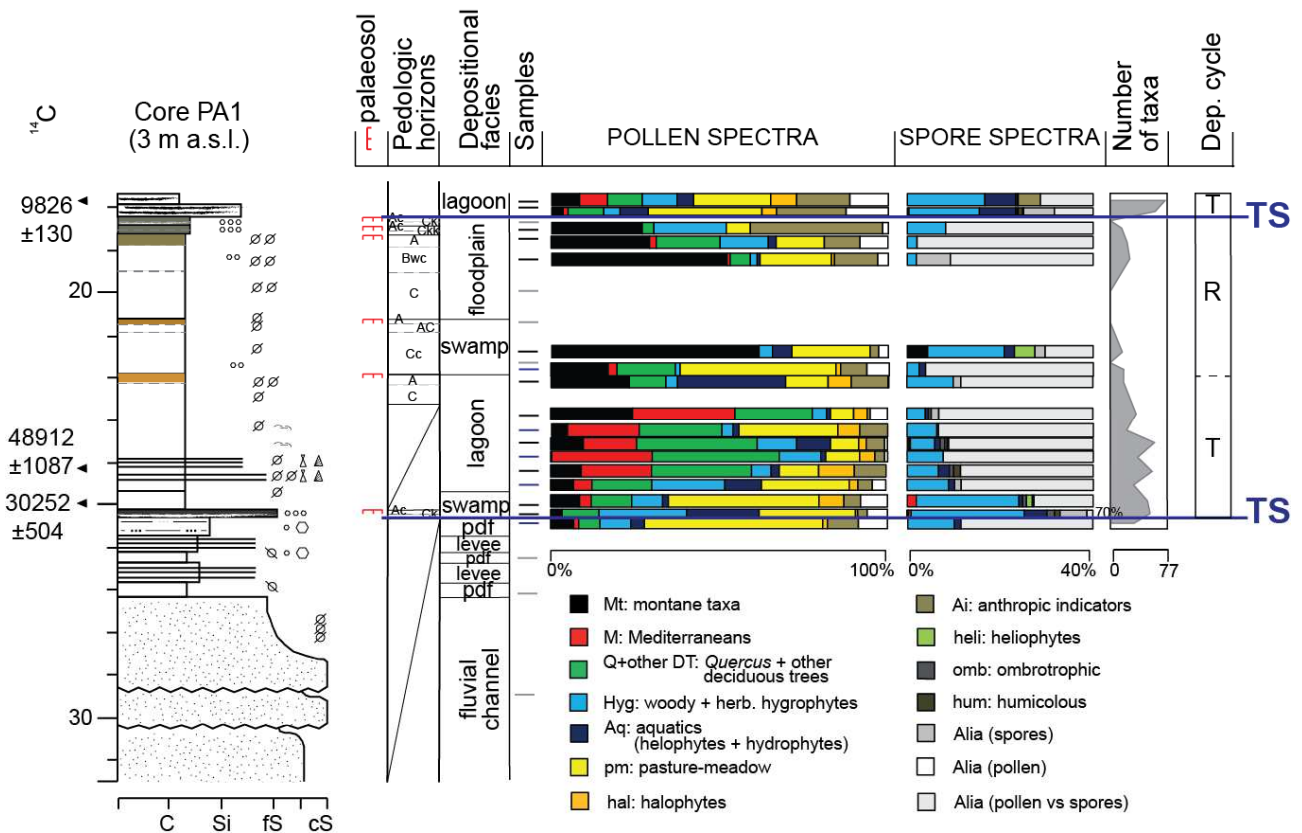
Fig. 6.5: Focus on the palyno-stratigraphic features of the lower T-R cycle. Following Cacciari et al. (2019), the two lowermost ages should be refused. Samples barren of microfossils are shown in grey, whereas the additional samples are reported in blue. Please refer to Fig. 6.2 for lithological and chronological keys and to Fig. 6.3 for hygrophyte trees/herbs ratio.

The lowermost portion of core PA1 is represented by a ca. 7 m-thick alluvial succession composed of fluvial-channel sands overlain by overbank/crevasse/poorly-drained floodplain deposits almost barren of palynomorphs. Only the topmost sample collected at 25.3 m core depth contains a plant community indicative of a humid prairie dominated by Poaceae (pm group in Figs. 6.3, 6.5, 6.6). This feature, along with the high abundance of secondary grains, is consistent with a river-dominated depositional environment developed presumably under glacial conditions. Unfortunately, no palaeoclimate inferences can be derived from palynological data due to the scarcity of climate indicators (Mediterranean and montane trees; Figs. 6.5, 6.7). However, it is noteworthy that stratigraphic correlations across the southern portion of the Arno delta plain (Figs. 6.1, 6.8) strengthen this interpretation, suggesting a MIS 6 age for the alluvial succession of core PA1, which is capped by the blackish palaeosol discussed in Cacciari et al. (2019, section 6.1) and physically coinciding with the transgressive surface (TS; Figs. 6.3, 6.5).

Fig. 6.6: Focus on the main plant taxa of the lower T-R cycle. Following Cacciari et al. (2019), the two lowermost ages should be refused. Samples barren of microfossils are shown in grey, whereas the additional samples are reported in blue. The base unit for scales is 10% when not specified.

Taxa abbreviations: *Alnus glut.* (*Alnus glutinosa*), *Caltha pal.* (*Caltha palustris*), Pteridop. (Pteridophytes), *Dicr. cervic.* (*Dicranella cerviculata*), *Fiss. ruf.* (*Fissidens rufulus*), *Gymn. infl.* (*Gymnocolea inflata*), *Hygroh. lur.* (*Hygrohypnum luridum*), *Phaeoc. lae.* (*Phaeoceros laevis*), *Callitr.* (*Callitriche*), Nymphaeac. (Nymphaeaceae), *Schoenopl.* (*Schoenoplectus*), *Sparg.* (*Sparganium*), *Sphag* (*Sphagnum*), Caryo. (Caryophyllaceae), *Beta vulg.* (*Beta vulgaris*), Chenopod. (Chenopodiaceae), Polygonac. (Polygonaceae), Ast. (Asteroideae), Brassic. (Brassicaceae), Cichorioid. (Cichorioideae), Ran. (Ranunculaceae).

Taxa colours are those of their respective ecological group.

113

Fig. 6.7: Focus on the main plant taxa of the lower T-R cycle. Following Cacciari et al. (2019), the two lowermost ages should be refused. Samples barren of microfossils are shown in grey, whereas the additional samples are reported in blue. The base unit for scales is 10% when not specified.

Taxa abbreviations: *Helianth* (*Helianthemum*), *Carpinus bet.* (*Carpinus betulus*), *Celtis austr.* (*Celtis australis*), *Q.* (*Quercus*), *Ostrya c. / C. Orientalis* (*Ostrya carpinifolia / Carpinus orientalis*), *A.* (*Alnus*), *Larix dec.* (*Larix decidua*), *Dicran. crispula* (*Dicranoweisia crispula*), *Mylia tayl.* (*Mylia taylori*).

Taxa colours are those of their respective ecological group.

Above the TS, an abrupt increase in hygrophytes and aquatics documents the development of an early transgressive swampy environment that grades from fully freshwater (Ww PDB) to freshwater-low brackish conditions, as revealed by the appearance of halophytes partly replacing the aquatics (Fig. 6.5). This palaeoenvironmental shift towards more saline and, likely, higher water-table conditions points to the gradual establishment of a lagoonal basin under a progressive climate amelioration testified by the increase of both Mediterranean and mixed oak forest taxa (Figs. 6.5, 6.7). This gradual achievement of the climate optimum is paralleled by a meiofauna turnover, from freshwater/low-brackish to euryhaline/brackish taxa typical of lagoons (Figs. 6.2, 6.5). Furthermore, during the shifting from paludal to lagoonal conditions, a peak in secondary grains (ca. 23%) is recorded at ca. 25 m core depth (Fig. 6.2). Interestingly, most of these grains (ca. 21% out of 23%) were identified as Cretaceous Pinaceae, such as *Piceapollenites mesophyticus sensu* Bolkhovitina (1956). The provenance of these palynomorphs is rather uncertain because to the north geological formations of Triassic age outcrop, whereas in the south Villafranchian - Tortonian-aged geological formations are present (Carmignani et al., 2012). A possible resedimentation from these latter can only be hypothesized. These grains eventually decrease to ca. 3% out of ca. 19% of total secondary grains at ca. 24.5 m core depth within the lowermost portion of the lagoon; after that, they completely disappear from the record, possibly marking a peculiar sedimentation pattern at the beginning of the last interglacial.

In more detail, the interglacial-like vegetation sees a first mesophilous phase of high diversification, as deciduous oak taxa peak at 24.1 m core depth alongside *Ulmus minor* (ca. 10%) and various other components of the mixed oak forest. After that, at about 23.8 m core depth, these taxa disappear or significantly decrease at the advantage of *Quercus ilex* (ca. 17%) and various Oleaceae (*Fraxinus excelsior, F. ornus, Olea* and *Phyllirea*); a concomitant peak in *Corylus avellana* (ca. 18%) suggests canopy clearing. This is followed at 23.5 m core depth by an increase in *Quercus* sp. and Betulaceae, possibly accounting for canopy recovery; at the same time, Bryophytes reach their minimum values and tree pollen reaches its maximum. A peak in reworked and fragmented dynocists is also recorded suggesting open- and/or sediment-starved conditions typical of the Maximum Flooding Zone (MFZ). As a whole, palynological data highlight a trend of increasing environmental stability characterised by a constant decrease of secondary grains and by the development of a PNV-like holm oak-mixed oak meso-Mediterranean forest.

Upwards, the degree of Mediterraneity increases up to 22.8 m core depth, where *Quercus ilex* is gradually replaced by *Erica arborea* (22% peak) as a major component of the community. This, in turn, testifies to the opening of the vegetation landscape, as the shrubby evergreen layer becomes more and more prominent within the vegetation community. Hygrophilous woods remain always

very subordinate to the meso-Mediterranean forest, further indicating a rather scarce moisture availability (Mof PDB, Fig. 6.4). Conifers, such as *Pinus* sp. and, to a lesser extent, *Pinus mugo*, appear, possibly accounting for a sparse regional presence on the hills surrounding the plain. The expansion of the meso-Mediterranean forest plummets at the topmost pedogenised portion of the lagoon deposits, where a clear decrease in mixed oak taxa is paralleled by the almost disappearance of Mediterraneans, marking an abrupt turnaround towards cooler conditions (Fig. 6.5; Mpw PDB, Fig. 6.4).

Similar vegetation dynamics have been documented by Allen et al. (2009) at Lago Grande di Monticchio (southern Italy), where Eemian deposits are constrained at 110-125 ka BP, as vegetation quickly reached the mixed oak forest community. However, pollen assemblages show how Mediterranean elements became paired to and then replaced by *Alnus* at about 121 and 116 ka BP, respectively, as wetter and more mesophilous conditions were achieved within the second portion of the interglacial. In our record, this gradual vegetation change is likely to be hinted by the palaeosol formation atop the lagoon. The vegetation dynamics recorded within the Late Pleistocene portion of core PA1 are consistent with and strengthen the attribution of the transgressive lagoon to the MIS 5e, as hypothesised in section 6.1 (Cacciari et al., 2019). Moreover, this lagoon interval (ca. 3 m thick) shows a good lateral continuity across the southern portion of the Arno delta plain, as highlighted in Fig. 6.8. Upwards, within the swamp-alluvial regressive portion of the T-R cycle, the meso-Mediterranean forest is almost completely replaced by pines, steppic herbs and, occasionally, aquatics, documenting the establishment of fully glacial conditions (Fig. 6.5).
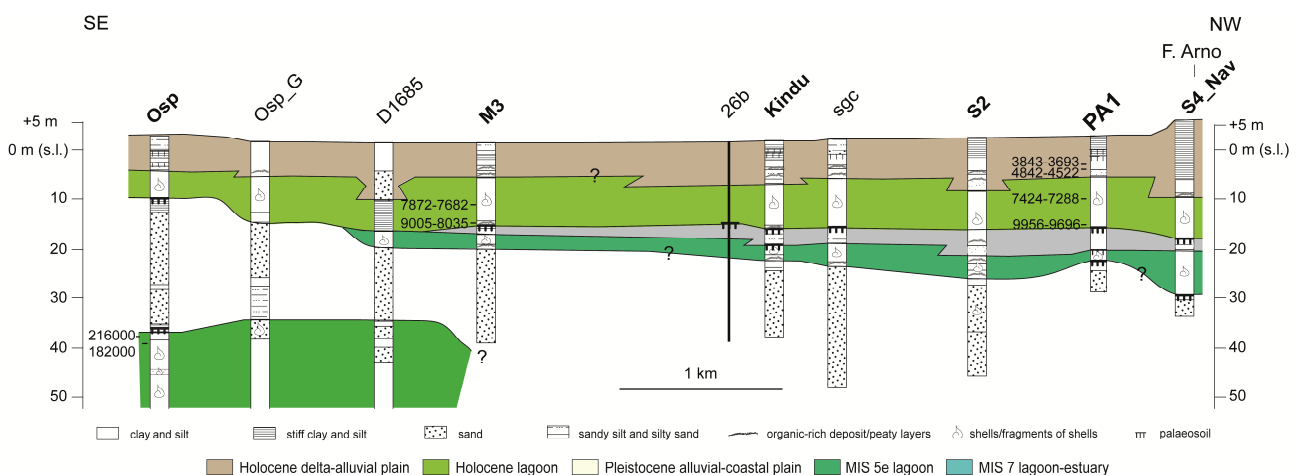
Fig. 6.8: Stratigraphic section showing the depositional architecture of the uppermost 50 meters of the Arno delta plain subsurface. At the SE margin core data document the occurrence of the lower incised-valley fill succession chronologically constrained by ESR ages to the MIS 7 (Rossi et al., 2017). Core data derive from the Arno Plain database (Amorosi et al., 2013b). Reference cores are shown in bold, as the studied core PA1. Radiocarbon ages are reported as calibrated years BP. The two refused ages from core PA1 are not shown. Section trace is reported in Fig 6.1.

To sum up, the high-resolution palyno-stratigraphic approach applied to the Late Pleistocene T-R cycle allows to highlight an almost synchronous response of coastal environments to climate forcing at sub-Milankovitch timescales The gradual retrogradational facies pattern of transgressive deposits is paralleled by a progressive achievement of climate optimum conditions, observed within lagoon deposits. The first phase of climate cooling corresponds to the lagoon emersion and to the subsequent establishment of cold conditions into a widespread alluvial plain (Fig. 6.86) characterised by an increasing degree of pedogenesis (Fig. 6.2).

6.2.6. Holocene vegetation and environmental dynamics: trends and controlling factors

The Holocene transgression (TS in Fig. 6.9) is marked by the abrupt superposition of lagoon silty clays onto stiff pedogenised floodplain deposits and physically coincides with the uppermost Late Pleistocene palaeosol (Cacciari et al., 2019; section 6.1), widely recognised across the plain (Fig. 6.8). The six additional palynological samples confirm the decreasing trend in halophytes within the lagoonal succession since ca. 7350 cal yrs BP, indicating the establishment of more fluvial-influenced conditions within the basin. This is further documented by the concomitant disappearance of both coastal-shallow marine ostracods and low-confinement foraminifers (Fig. 6.2). A synchronous expansion of freshwater wetlands bordering the lagoon is sustained by the constant presence of *Sphagnum* and, in general, the palynological assemblages indicate that freshwater environments were a rather important component of the vegetation (Figs. 6.9 and 6.10; Aw PDB in Fig. 6.4). In particular, *Alnus glutinosa* is always represented within the 5-14% range and accompanied by 1-4% of *Salix* and 3-15% of *Corylus avellana*, a tree assemblage possibly indicative of the alliance *Alnion glutinosae* Mijr-Drees 1936 (sub-section 2.2.3). However, no detailed palynological-phytosociological inferences about these freshwater wetlands can be made because the herbaceous layer is highly facies-dependent and, thus, cannot be properly defined in the record.
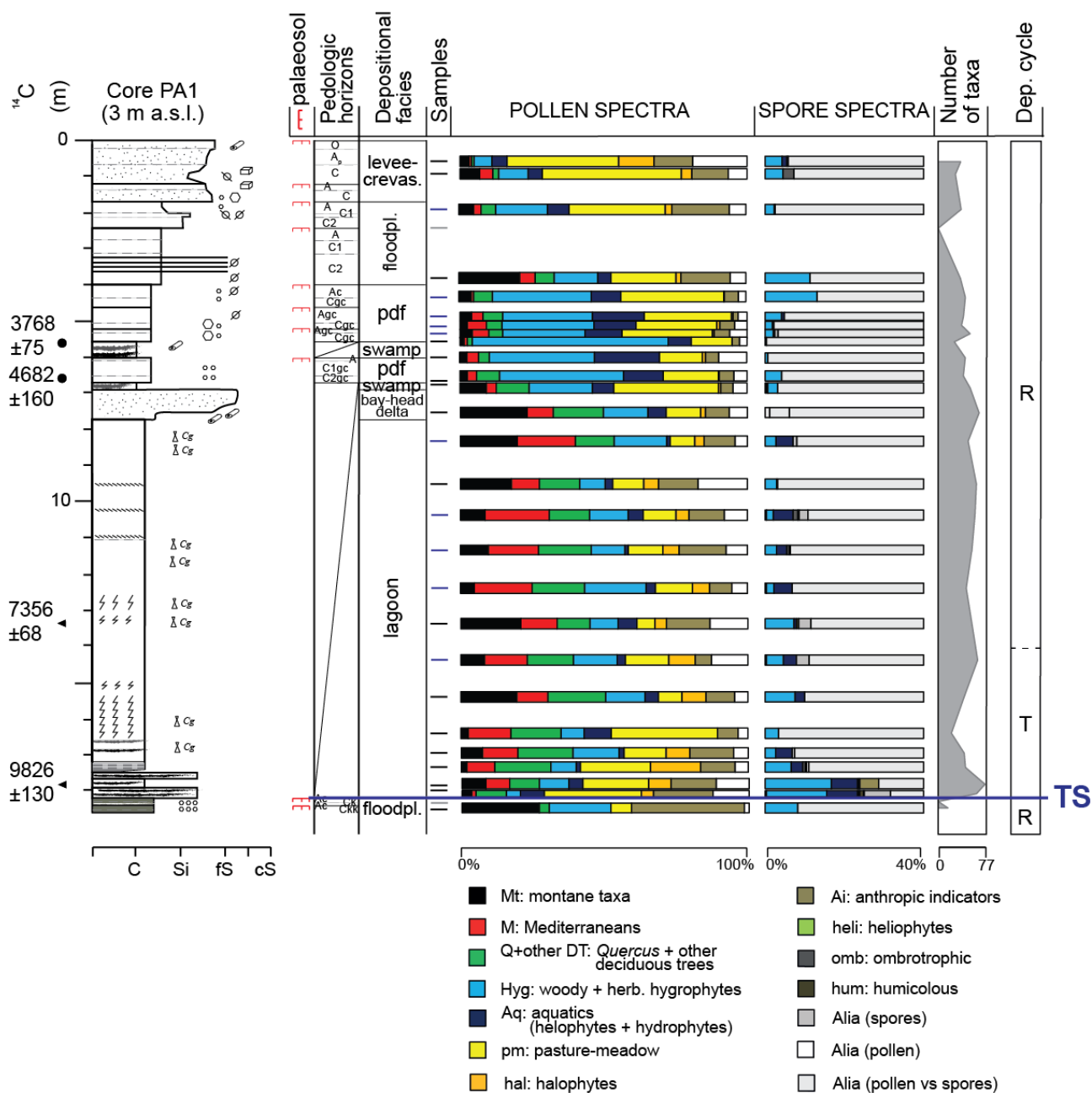
Fig. 6.9: Focus on the palyno-stratigraphic features of the upper T-R cycles of Holocene age. Samples barren of microfossils are shown in grey, while the additional samples are reported in blue. Please refer to Fig. 6.2 for lithological and chronological keys and to Fig. 6.3 for hygrophyte trees/herbs ratio.

Contrary to this clear palaeoenvironmental trend reconstructed from the lagoon succession, climate indicators suggest stable optimum conditions, as the arboreal cover is high, always ranging 50-70%, and mainly composed by Mediterraneans and mixed oak forest taxa (Fig. 6.9 and 6.11). Unique exception is represented by two samples collected at 15.35 and 13.35 m core depth, containing peaks of Mt (19-21%, mainly *Betula, Alnus incana* and *A. viridis*) dated around 8400 cal. yrs BP (interpolated from the age-depth model in Cacciari et al., 2019) and at around 7300 cal. yrs BP (radiometric age), respectively.
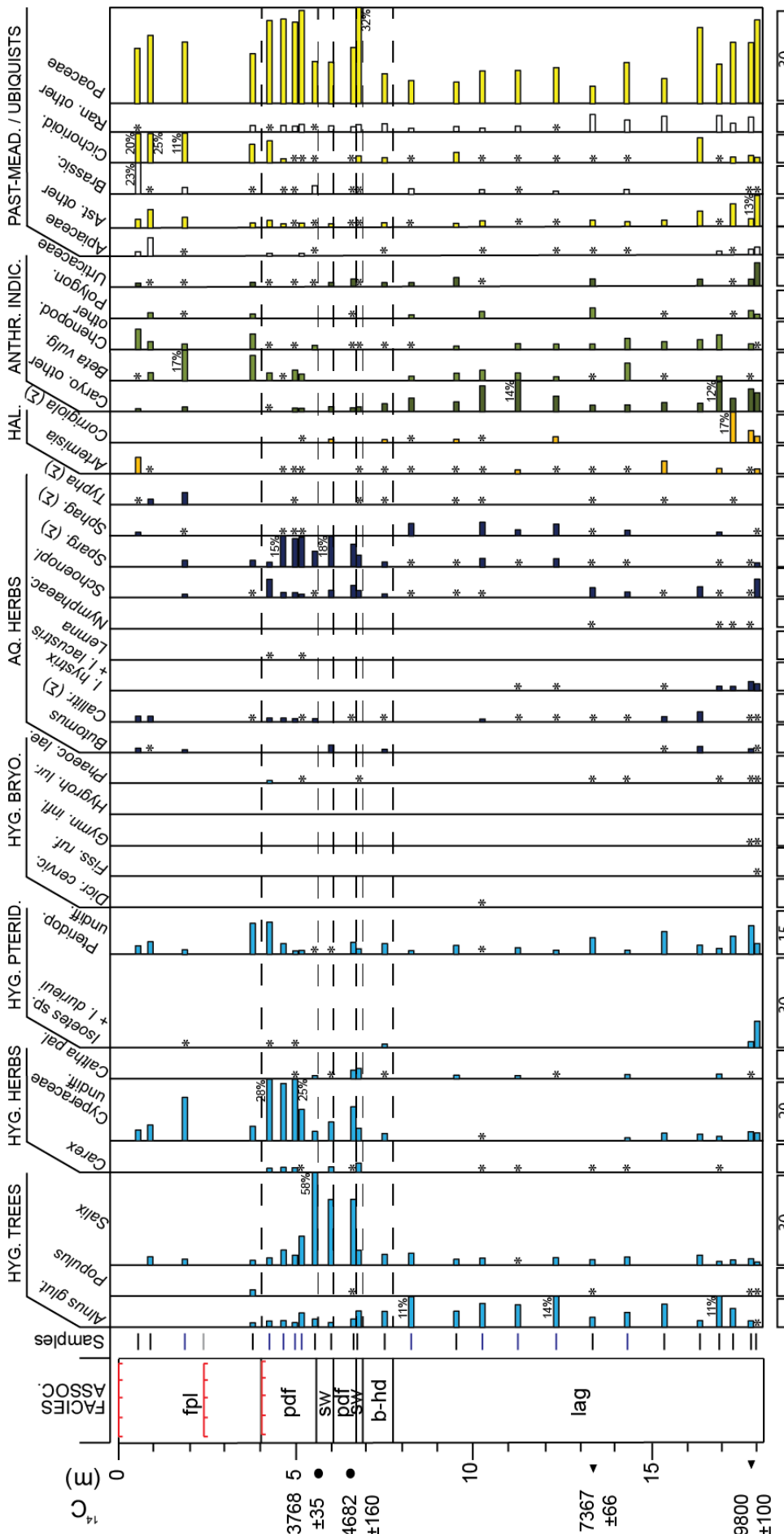
Fig. 6.10: Focus on the main plant taxa of the upper T-R cycle. Samples barren of microfossils are shown in grey, whereas the additional samples are reported in blue. The base unit for scales is 10% when not specified.

Taxa abbreviations: *Alnus glut.* (*Alnus glutinosa*), *Caltha pal.* (*Caltha palustris*), Pteridop. (Pteridophytes), *Dicr. cervic.* (*Dicranella cerviculata*), *Fiss. ruf.* (*Fissidens rufulus*), *Gymn. infl.* (*Gymnocolea inflata*), *Hygroh. lur.* (*Hygrohypnum luridum*), *Phaeoc. lae.* (*Phaeoceros laevis*), *Callitr.* (*Callitriche*), Nymphaeac. (Nymphaeaceae), *Schoenopl.* (*Schoenoplectus*), *Sparg.* (*Sparganium*), *Sphag* (*Sphagnum*), Caryo. (Caryophyllaceae), *Beta vulg.* (*Beta vulgaris*), Chenopod. (Chenopodiaceae), Polygonac. (Polygonaceae), Ast. (Asteroideae), Brassic. (Brassicaceae), Cichorioid. (Cichorioideae), Ran. (Ranunculaceae).

Taxa colours are those of their respective ecological group.

Fig. 6.11: Focus on the main plant taxa of the upper T-R cycle. Samples barren of microfossils are shown in grey, whereas the additional samples are reported in blue. The base unit for scales is 10% when not specified.

Taxa abbreviations: *Helianth* (*Helianthemum*), *Carpinus bet.* (*Carpinus betulus*), *Celtis austr.* (*Celtis australis*), *Q.* (*Quercus*), *Ostrya c. / C. Orientalis* (*Ostrya carpinifolia / Carpinus orientalis*), *A.* (*Alnus*), *Larix dec.* (*Larix decidua*), *Dicran. crispula* (*Dicranoweisia crispula*), *Mylia tayl.* (*Mylia taylori*).

Taxa colours are those of their respective ecological group.

120

Interestingly, the additional samples have revealed the presence of *Pyracantha coccinea*, a shrub living in association with *Quercus ilex* in meso-Mediterranean forests. This pollen assemblage could be a fossil expression of the *Fraxino orni-Quercetum ilicis* Horvatic 1956 alliance (sub-section 2.2.3), as scarce *Erica arborea* is also found. By contrast, the Eemian lagoon has an opposite pollen signature, as no *Pyracantha coccinea* was found, whereas *Erica arborea* is often significantly present, if not dominant. The latter pollen assemblage type could represent the *Erico arboreae-Arbutetum unedi* alliance (sub-section 2.2.3), an intermediate plant community between the holm oak forest and more degraded maquis and garrigues. In this light, the higher abundance of hygrophilous woods during the Holocene climate optimum compared to the Eemian period can be interpreted as a real climatic difference, reflecting an Eemian warmer than the Holocene (see Fig. 6.4 for further comparisons between Mof and Aw PDBs, respectively). Interestingly, the Holocene vegetation dynamics documented by Allen et al. (2002) at Lago Grande di Monticchio (southern Italy) are very similar in timing and composition to their Eemian counterparts, whereas at Valle di Castiglione (Rome) Follieri et al. (1988) record an Eemian much warmer than the Holocene, a situation more similar to that found in our record. The chance that a local environmental palynological under-representation of wetlands might have taken place during the Eemian should be discarded taking into account the very similar meiofauna content of the two lagoons. Indeed, both are characterised by high abundances of *Cyprideis torosa* and high-confinement foraminifers, whereas coastal-shallow marine and brackish-marine ostracods, as well as low-confinement foraminifers, are very scarce.

If no evident vegetation-derived climate changes seem to be responsible for the first phases of slow lagoon infilling (between ca. 7300-5000 cal. yr BP), the rapid final stage of lagoon siltation took place in concomitance of a local cooling event centred around ca. 5 cal. kyr BP, whose timing and expression was strengthened by the higher sampling frequency. The additional sample has allowed to highlight an increasing abundance of *Fagus sylvatica*, at first recorded at 9.5 m (2.7%), then at 8.25 m (5.2%) and peaking at 7.45 m (11.7%). After the lagoon closure, *F. sylvatica* rapidly decreases at 6.7 m (2%) and finally becomes negligible or disappears (Fig. 6.11). Stratigraphic data in the area document the complete filing of the lagoon around ca. 5 cal. kyr BP and the subsequent onset of a delta plain without a direct marine influence (Rossi et al., 2019).

Upwards, palaeoenvironmental dynamics within the developing delta plain (swamp-poorly-drained floodplain deposits and associated gley pedogenesis) are mainly expressed by variations of hygrophytes, helophytes and hydrophytes which document water table variations. The highest is recorded within the swamp dated around 3800 cal. yrs BP (helophytes ca. 10.5% and hydrophytes ca. 12%). Upwards, two couplets of Agc/Cgc gley palaeosols develop (Fig. 6.2): the youngest

couplet shows an increasing amount of aquatics compared to the eldest, as the willow wood becomes partially replaced by a herbaceous community. Very similar dynamics occur between 'A' and 'C' horizons, the latter denoting a shallower water table than the former. Finally, the topmost 'A' horizon shows, instead, a decreasing water table, reasonably due to the progradation of the alluvial system, as it emerged shortly after. As a general trend, *Salix* dominates in the lower portion of this delta plain succession, where an alternation of swamps and poorly drained floodplains occurs, and becomes substituted by a predominant herbaceous wetland community in the upper portion, where no swamps are recognised (Ww PDB, Fig. 6.4). This trend is not evident in Sarti et al. (2015a, core M5 in Fig. 6.1), where the three poorly-drained floodplain pollen samples only document a slight decrease in "riparians", which are however higher in the underlying swamp and lagoon, possibly accounting for a higher relative water table within swamps. This is also in tune with what was recorded in core M5 and M19 (MAPPA Project, Allevato et al., 2013), where high abundances of hygrophytes and aquatics are recorded until the Roman Age, although in a decreasing trend. It is hard to discern the climate influence on this type of mid-late Holocene vegetation landscape due to the strong facies signal and the consequent scarce representation of climate indicators (especially Mediterranean and montane taxa). The subsequent establishment of well-drained, alluvial conditions (i.e., floodplain, levee and crevasse facies) is characterised by a constant, marked drop in arboreal cover, as human presence increases and is likely related to the onset of the Roman *centuriatio*. In this case, the record of core M5 (Sarti et al., 2015a; Fig. 6.1), where an open vegetation develops in concomitance with the establishment of well-drained conditions and pine spreads similar to what was reconstructed at the base of floodplain deposits in PA1. Concerning pine, in the context of the geoarchaeological MAPPA Project a series of archaeological layers were analysed in terms of pollen and anthracological content: in core M4 (Fig. 6.1) pine pollen was commonly found from the Iron Age to the Middle Ages and charcoals revealed the presence of *Pinus sylvestris* on the plain, now a relict species on Monte Pisano (sub-section 2.2.3). Also in tune with our record is the dominance of the hygrophilous wood relative to the Mediterranean taxa, which are scarce in this period. The scarcity or absence from the pollen record of core PA1 of cultivated trees (e.g., *Castanea sativa* and *Olea europaea*, Fig. 6.11), which were found, instead, in cores M4 and M25, may suggest an extrasite position of our cored succession (like cores M8 and partially M25 in Fig. 6.1, where Cichorioideae are abundant) if compared to the real centre of the anthropic presence (namely, the urban area). In this case, a first human settlement can be hypothesized from the significant presence of *Beta vulgaris* that in turn leaves place to a generally degraded vegetation landscape where ubiquists dominate (see Fig. 6.4 for Mgd PDB composition and Fig. 6.10 for taxonomic composition of the topmost portion of core PA1).

7. COMPARISON OF THE ARNO AND PO DELTA RECORDS

EM2 and PA1 cored successions show a partial chronological overlap so a thorough comparison of the two records can be performed only for their most recent portions, corresponding to the Holocene interval (from ca. 10 cal. kyrs BP to the Present). Furthermore, this discussion requires cautiousness because of: *i)* the different facies associations involved and stratigraphic framework, *ii)* the diverse degree of chronological resolution (i.e., 13 *vs* 6 radiocarbon ages for EM2 and PA1, respectively) and *iii)* the different climate (and vegetation) conditions at the two sides of the Northern Apennines. The complexity of present-day and past climate conditions in the Po Plain and the Arno Plain is briefly introduced in the first section of this chapter (section 7.1.), while a comparison of the two palyno-stratigraphic records is reported in sections 7.2. (Holocene time interval) and 7.3. (Pleistocene time interval). I make reference to Chapters 5 and 6 for any specific palaeoenvironmental and/or palaeoclimatic considerations on single datasets.

7.1. *Present-day and past climate teleconnections*

The Arno and Po delta plains belong to two different provinces of the Italian ecoregions *sensu* Blasi et al. (2014): the Tyrrhenian and the Po Plain provinces, respectively, which differ both in terms of climate and vegetation. Even though both provinces have mean annual temperatures above 10°C, the Po Plain has higher precipitations (up to 1400 mm/yr *vs* ca. 1000 mm/yr) and a marked continental regime with respect to the Mediterranean one in the Tyrrhenian area. Furthermore, the Po River marks a clear bipartition in the plain, as continentality decreases to the south (towards the Apennines) and to the east (towards the Adriatic Sea). The two provinces involved in this thesis are geographically separated by the Northern Apennines, stretching in a NW-SE direction and constituting themselves a bioclimatic province as well, having mixed characters of continentality and oceanicity depending on latitude, E-W orientation of single slopes and elevation (Blasi et al., 2014).

For what concerns the recent past, several palaeoclimatic studies from the Mediterranean basin (e.g., Magny et al., 2002, 2013; Peyron et al., 2013, among others) show a very complex spatial-temporal pattern of variability. First of all, a bipartite Holocene is generally observed, with the first half characterised by generally wet conditions and a second half, since ca. 6 cal. kyrs BP, progressively drier (Mayewski et al., 2004). The shifting from wetter to drier conditions, however, was not immediate because a transition phase took place around 7.5-4.5 cal kyrs BP, as recorded in several multi-proxy records (Jalut et al., 2000; Magny et al., 2013).

For what concerns Italy, Magny et al. (2013) identified a general contrasting pattern of palaeohydrological changes with respect to the 40°N latitude zone during the middle part of the

Holocene. Palaeoclimate data suggest humid winters and dry summers to the north at 9-4.5 cal. kyr BP and humid winters and summers to the south at 10.3-4.5 cal. kyr BP. However, several palaeoclimate investigations document the occurrence of a wider latitude zone between ca. 40-43°N (the latter roughly corresponding to the Northern Apennines area) characterised by complex climatic teleconnections. Indeed, in this zone extremely sensitive to the North Atlantic Oscillation (NAO), Holocene climate events can show features alternately similar either to those occurring in southernmost Italy or in central Europe (e.g., Vannière et al., 2011):

- positive NAO values imply an increased storminess in Northern Europe by a northward shift of the Icelandic Low, while the African-Asian monsoon shifts north and brings humidity to the Southern Mediterranean (dry conditions are sandwiched between 40°-43°N);
- conversely, negative NAO values imply an opposite pattern, as the Icelandic Low shifts south and brings an increase in storminess to Southern Europe, while the African-Asian monsoon becomes weaker and brings dryness to the Southern Mediterranean (wet conditions are sandwiched between 40°-43°N).

Thus, our study areas (Po and Arno plains) are located close to the upper boundary of this key zone, where dual responses can be expected with respect to the Holocene climate variability. As a final remark, the current state of the art on the knowledge of these climatic dynamics suggests to properly consider the local importance of orographic divides and to conservatively choose the present-day climatic tripartition of Italy (sub-mediterranean above 43°N, meso-mediterranean in central Italy and thermo-mediterranean below 40°N) when making palaeoclimate inferences on recent past records. Since modern vegetation mirrors this climatic tripartition, this approach can be especially effective when analysing palaeovegetation patterns preserved in pollen records as those reported in the following sections.

7.2. Holocene time interval

From a general stratigraphic point of view, the Holocene records of EM2 and PA1 cores are extremely different in terms of facies associations and depositional patterns (Chapters 5 and 6; Cacciari et al., 2019, 2020) mainly due to their position in the respective plains (i.e., distance from the present-day coastline) and to the plain's physiography/geological setting (Chapter 2). The Po delta plain is a wide, flat area faintly bounded by the Apenninic river courses to the south and by the Adige River to the north. These features, which favour large-scale river avulsions, along with high subsidence rates reasonably promote the formation of laterally extended areas where waters flow very slowly or remain stagnant. Instead, the Arno delta plain is a rather narrow, triangle-shaped area sandwiched by two mountain ranges and fed by a complex fluvial network including palaeoSerchio

branches up to the late Middle Ages. These different contexts reasonably explain the widespread occurrence in the Po Plain of peaty swamps, marked by increasing amounts of aquatics peaking within peaty layers; by contrast, in the Arno Plain no true peats developed. Indeed, within the Holocene portion of PA1, the swamp facies association dated between ca. 4600-3700 cal yrs BP (Fig. 6.9) just reflects episodes of temporary deepening of the relative water table in a poorly-drained delta setting (i.e., poorly-drained floodplain), as recorded by an increase in aquatics and in the accumulation of blackened vegetal debris. Consistently, a vertically stacked series of Ag/Cg palaeosols with evidence of gley pedogenesis is documented within the lower portion of the Arno delta succession.

In-depth, vegetation-based inferences about similarities/differences in the Holocene palaeoenvironmental-palaeoclimate-human pressure dynamics, recorded by EM2 and PA1 successions, are reported below.

- Palaeoenvironmental and palaeoclimate dynamics
  - *Wetlands and hygrophilous woods* → as stated in Chapters 5 and 6 (Cacciari et al., 2019, 2020), relative water table variations were tracked *via* pollen content mainly by the presence of aquatics. Both records show an increase of this pollen group when the accumulation of vegetal organic matter becomes stronger: in EM2 this is particularly evident when comparing grey clay swamps (sw2) with peaty swamps (sw1), whereas in PA1 this trend characterizes the poorly-drained floodplain deposits with respect to the swamps. In both cases, the shift towards deposits with a higher content of vegetal organic matter always marks an augmentation of relative water table. However, a certain degree of tree cover is also mostly present, as alder and willow pollen grains were commonly found throughout freshwater deposits of both records in concentration significant enough to assess that these trees were always a component of the local vegetation. Interestingly, the EM2 core has a different pattern of distribution of these two taxa along the Holocene record, as *Alnus glutinosa* appears around 9 cal. kyr BP and persistently remains the dominant hygrophilous tree relegating *Salix* in a subordinate position. Similarly, in the PA1 core *Alnus glutinosa* appears significantly around 9.4 cal. kyr BP, possibly indicating that during the lowest portion of the Holocene this tree had yet to fully colonise both the Po and the Arno plains. This suggestion is supported by the cluster analyses, where the alder woods are always depicted as related to the PNV of each site (Fig. 3 in Cacciari et al., 2019, and Fig. 6.4). However, differently from EM2, in PA1 *Alnus glutinosa* remains the dominant component of the hygrophilous woods up to about

5 cal. kyr BP, when *Salix* replaces it mostly completely in concomitance with the filling of the lagoon and the subsequent onset of a delta plain. This different behaviour could be explained by taking into account the fact that *Salix* prefers riparian contexts, whereas *Alnus glutinosa* thrives better near / within low-lying areas with stagnant or slow-flowing waters. In the Arno Plain, the former conditions would be more widespread as the lagoon shifted to a delta plain, whereas before ca. 5 cal. kyr BP the persistent presence of a wide back-barrier system would have strongly reduced fluvial influence in favour of freshwater swampy areas bordering the brackish lagoon.

- *PNV* → the expression of the Potential Natural Vegetation at the two sites is rather different, as in the Po delta plain an alder hygrophilous wood is the main vegetation type alongside a mixed oak forest with *Quercus ilex* as the sole Mediterranean element. By contrast, in the Arno delta plain a holm oak – mixed oak forest is dominant with subordinate hygrophilous trees. This feature is also confirmed by the two cluster analyses (Fig. 3 in Cacciari et al., 2019, and Fig. 6.4). The degree of Mediterraneity is thus more prominent south of the Apennines than north of them, as mirrored by the present-day separation of a sub-mediterranean climate in Emilia-Romagna and a meso-mediterranean climate in Tuscany.

- *The 8.2 ka event* → even if with a diverse degree of confidence and resolution, the main climate event of the Holocene (i.e., 8.2 ka event - Bond event 5) is recorded within both the studied successions and significant differences in terms of associated vegetation and environmental/depositional dynamics are highlighted. The EM2 cored succession records at first a series of peaks in *Fagus sylvatica* within swampy deposits and, after that, the depositional system reacts *via* crevasse deposition (3 m thick) while *Fagus sylvatica* becomes replaced by *Abies alba*. Finally, after ca. 200 years, a second late cooling is recorded by a 1 m-thick crevasse splay and the replacement of *Abies alba* by *Pinus mugo* in an apparent trend of mountain forests degradation. On the other hand, in the PA1 succession the 8.2 ka event is less evident in terms of vegetation dynamics because only one sample, chronologically constrained to ca. 8.4 cal. kyr BP, records an increase in montane alders, *Betula* and, to a lesser extent, of *Abies alba* and *Pinus* sp. Moreover, this vegetation change was not accompanied by any stratigraphic expression, as no alteration in sedimentation/environmental dynamics is documented within the lagoon succession (Cacciari et al., 2019). To sum up, since the 8.2 ka event is generally recorded in central Italy as an increase in humidity (similarly to northern Italy and central Europe), both our records are consistent with this general pattern because montane indicators as *Abies alba,*

Alnus incana and *Fagus sylvatica* require rather moist climates and expand towards the lowlands when climate becomes cooler and moister. So, I suggest that the Arno delta plain, within the transition zone at 40°-43°N, reacted to the main Holocene climate event similarly to the Po delta plain and, thus, had a stronger climatic affinity to northern Italy and central Europe than to the southern Mediterranean (section 7.1). However, it is clear that a higher resolution analysis is needed to better investigate these dynamics in deeper detail within the Arno Plain subsurface record.

The same reason can be advocated for the difficulty in comparing vegetation dynamics for the lowermost Holocene: even though EM2 is a rather continuous record from the Younger Dryas onwards, only single samples document the early Holocene coolings in the Po delta plain (YD, PBO and BO), whereas in PA1 no record clearly attributable to this time interval is present.

– *Middle Holocene climate variability* → in the millennium following the 8.2 ka event, a minor cooling is recorded in both areas showing similar dynamics (i.e, increases in montane alders and beech – humidity increases). This climate change is dated at ca. 7.0 cal. kyr BP and at ca. 7.3 cal. kyr BP within the EM2 and PA1 records, respectively. It is noteworthy the presence of all the montane trees, except from *Pinus sylvestris*, within the EM2 record, suggesting a complete achievement of the PNV not only in the lowlands but also on the mountains. This feature possibly accounts for the complete establishment of altitudinal vegetation belts by the first millennium of the Middle Holocene, at least for what concerns the Northern Apennines. This cool event is not present among the Bond's events but has also been recorded with similar features in other regional records (i.e., mid-Adriatic marine core in Combourieu-Nebout et al., 2013), possibly accounting for a regional climate oscillation.

Another cooling event (i.e, increases in montane trees) is recorded within both datasets and chronologically constrained within the 5-4 cal. kyr BP interval, when *Alnus incana* and *Pinus* sp. dominated the Po delta plain montane pollen rain and *A. incana*, *A. viridis*, *Betula* and *Fagus* dominated the Arno delta plain's. Interestingly, these vegetation-derived events corresponds to periods of enhanced fluvial activity: a 3 m thick distributary channel developed in the Po sites, marking the end of the swamp –crevasse splay alternation; instead, in the Arno a bay-head delta formed, determining the lagoon filling. Furthermore, in the Arno record a peculiar vegetation dynamic could be hypothesized since the first peaks of montane alders are followed by a semi-concomitant peak in beech pollen, possibly suggesting a minor cooling associated to a major increase in moisture availability (precipitations?) in the mountainous areas. Thus, even if the PA1 record shows a Holocene vegetation with a clear Mediterranean affinity, its reactions to high-

frequency cooling events during the mid Holocene seem to reflect a range of teleconnections more linked to northern Italy and central Europe than to southern Italy and, to a wider, extent, to the southern Mediterranean (section 7.1.). Furthermore, this may suggest that the Northern Apennines can effectively prove to be a bioclimatic barrier in a N-S direction by generating different climate regimes and vegetations (sub- *vs* meso-mediterranean) but are ineffective against climate oscillations at the centennial-millennial timescales.

The low-resolution sampling pace kept within the late Holocene successions prevents any effective comparisons between the two palynological records.

- Anthropic presence → both records show a scarce or absent human impact, as pollen assemblages generally document a widespread level of disturbance due to natural factors, such as pioneering conditions at the beginning of the Holocene, crevasse splay emplacement or changes in facies associations. Nonetheless, evidences of human presence occur within the uppermost metres of the two studied successions (i.e., the last ca. 2 kyrs). Specifically, within the EM2 record there is the appearance of *Hordeum* in increasing amounts to the top and a peak in Asteroideae and Cichorioideae paralleled by a marked drop in arboreal cover; these features are possibly ascribable to widespread land clearances linked to pastures and cultivations. Within the topmost samples of the PA1 core, a sudden peak of *Beta vulgaris* can be indicative of cultivations in the intrasite area or in the nearsite area. This peak is followed by a gradual replacement of *Beta* by other chenopods, Apiaceae, *Artemisia*, Brassicaceae and Cichorioideae that can point to a general abandonment of the site following an increasing soil salinization (*Artemisia* and chenopods) as documented by the development of a herbaceous community typical of semi-natural pastures.

7.3. Late Pleistocene time interval
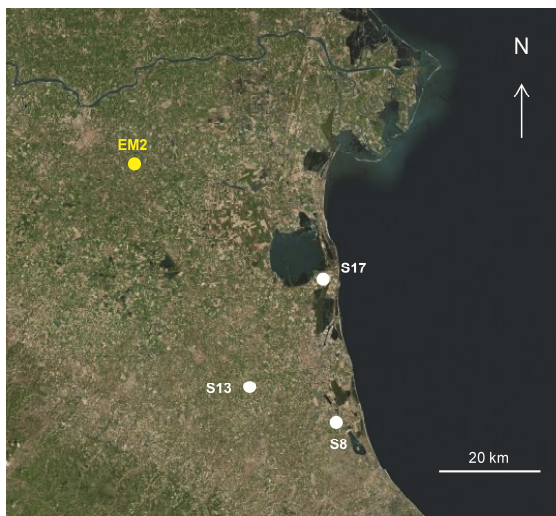
The Late Pleistocene records of EM2 and PA1 are not directly comparable because in the Po delta plain record only two samples were analysed within the alluvial succession placed below the Transgressive Surface and stratigraphically constrained to the MIS 3 (Bruno et al., 2017; Cacciari et al., 2018). Comparisons can be consequently drawn exclusively on the basis of other records available in literature for the Po plain (mainly cores S8, S13 and S17; Figure 7.1.) and showing a chronological resolution similar to that characterising the PA1 dataset.

Fig. 7.1: Location map of the cores S8, S13and S17, palynologically investigated in Amorosi et al. (2004). Location of the EM2 core is also highlighted. The image is from Bing Maps.

A brief discussion is reported below following a chronological/climate subdivision:

- Glacial period → for what concerns the interval preceding the Holocene period, cores S8, S13 and S17 (Amorosi et al., 2004; Fig. 7.1) in the Po coastal plain and core MN1 (Amorosi et al., 2008; Fig. 2.1) in the central Po plain mainly record an alluvial plain characterised by the dominance of *Pinus* sp., among trees, and of Poaceae and steppics among herbs. Mesophilous mixed oak elements are either to be found in low concentrations or absent. Pollen concentrations are very scarce and sterile samples are frequent. Local, punctuated peaks of hygrophytes and aquatics can account for short-lived episodes of moisture availability. This landscape is highly coherent with core PA1 record, where very similar pollen assemblages are recorded and sterile samples are frequent. These features, commonly present during glacial periods on both sides of the Apennines, suggest that glacial conditions equally affected vegetation on both sides of the mountain chain.

- Last interglacial → the MIS 5e depositional record of cores S8, S13 and S17 is rather expanded and contains a palynological signature typical of an interglacial, thanks to the dominance of mixed oak taxa that are partially substituted in the most recent portion of the Eemian by montane and hygrophilous trees. A similar pattern is recorded in the MN1 cored succession, although montane trees peak higher probably because of the more proximal position of the core within the Po Plain. Oppositely, in the PA1 Mediterranean elements co-dominate pollen spectra with mesophilous broadleaves, pointing that the previous interglacial was warmer in Tuscany than in the Po Plain similarly to the Holocene.

8. CONCLUSIONS

The application of pollen and spores as a powerful tool for vegetation-derived palaeoclimate reconstructions is widespread within continental/lacustrine and deep-sea settings. By contrast, subsurface successions buried beneath delta-coastal plains are still relatively underexplored, although they represent natural archives of the complex interactions among vegetation dynamics, climate-RSL variability, depositional patterns and, also, human activities. Moreover, within transitional contexts palynological data can provide useful information about palaeoenvironmental trends and possibly shed new light on their relationships with the most important palaeoclimate changes (e.g., interglacial-glacial cycles, Bond's events).

In the Mediterranean area, the Po delta plain (NE Italy) and the Arno delta plain (NW Italy) represent great laboratories where the potentiality of an integrated palyno-stratigraphic approach for late Quaternary palaeoenvironmental and palaeoclimate studies can be explored at both Milankovitch and sub-Milankovitch timescales. Indeed, these areas are characterised by relatively expanded, fine-grained successions of late Quaternary age, where palynomorphs can be nicely preserved, and their stratigraphic settings have been extensively studied over the last years. Moreover, the phytosociological background of present-day plant communities at these two sites, located at the opposite sides of the Northern Apennines, is well-known, which favours robust and in-depth palaeoenvironmental and palaeoclimatic reconstructions.

In this perspective, tens m-long sedimentary cores, performed through a continuous perforating system (40 m-long core EM2 in the Po delta plain and 31.5 m long-core PA1 in the Arno delta plain), were analysed in my Ph.D. project by means of a stratigraphic-based palynological study (38 samples for EM2 and 49 samples for PA1). To achieve a detailed palynological characterization of depositional facies and subsurface architectural elements (e.g., peaty swamp successions, lagoon intervals and T-R depositional cycles), the sampling procedure relied upon a preliminary lithofacies identification and the subsequent definition of plant ecological groups was validated *via* cluster analysis and pollen-derived biomes recognition. This methodology allowed to discern the environmental (local) signal from the climate (more regional) one throughout the studied successions, which cover long-term chronological intervals spanning the entire MIS 1 (Po Plain) and the MIS 5-MIS 1 period (Arno Plain). Accurate chronological analyses based on radiocarbon ages and the development of age-depth models permitted to reconstruct separately depositional, palaeoenvironmental and paleoclimate dynamics as well as to assess their relationships with the well-known late Quaternary glacio-eustatic and climate variability. If promptly framed into the

stratigraphic context of each area, all these data proved to be extremely informative also in terms of sequence stratigraphy.

The analysis of core EM2, drilled at the innermost margin of the Po delta plain (ca. 40 km landward the modern coastline), revealed the extent to which an integrated palyno-stratigraphic approach can be useful for the detailed facies characterization of freshwater paludal successions, where other palaeobiological proxies are commonly scarce, and for the identification of depositional patterns and key sequence-stratigraphic surfaces (section 5.1). The resulting stratigraphic framework was the base for high-resolution palaeoclimate analyses and in-depth reconstructions of Holocene landscape dynamics (section 5.2). On the other hand, results from core PA1, which is located just behind (ca. 2 km) the innermost outcropping beach-ridge of the Arno delta, highlighted the capability of palynomorphs to trace palaeoenvironmental trends in salinity and degree of hygrophily (i.e., water-table level) within brackish and hypohaline sedimentary successions, especially if integrated with meiofauna data (i.e., benthic foraminifers and ostracods; section 6.1). At the same time, pollen and spore (including Bryophytes) data strongly improved the identification of even subtle palaeoenvironmental and palaeoclimate turnovers supporting a robust sequence-stratigraphic analysis and the reconstruction of landscape dynamics (section 6.2). Four major outcomes can be summarized for the Po delta plain (points 1-4) and three for the Arno delta plain (points 5-7). All are summarised as follows, along with a last key point (point 8) that focuses on the comparison of late Quaternary landscape dynamics at the two study sites:

1.   Within the 25 m-thick, freshwater paludal succession of Holocene age recovered in the innermost portion of the Po delta plain, the palynological analysis strongly refines facies identification, allowing the clear distinction of poorly-drained floodplain, low water-table swamp and high water-table swamp (or peaty swamp), mainly on the basis of the relative proportion of hygrophytes, helophytes and hydrophytes. Floodplain clays-silts also show a peculiar pollen content dominated by pasture-meadows taxa, indicating a disturbed environment with a very low degree of hygrophily. Each facies association shows peculiar and rather uniform vegetation communities defined by the local pollen rain. Facies characterization also benefitted from the results of cluster analysis (CA) that enabled the identification of 9 pollen-derived biomes, supporting the pollen groups subdivision and their interpretation in terms of environmental and/or climate forcing. In this perspective, hygrophytes and aquatics (helophytes + hydrophytes) proved to be the most reliable facies indicators in freshwater coastal environments.

2.   The distinction of poorly-drained floodplain, low water-table swamp and high water-table swamp (or peaty swamp) facies associations, alongside overbank/crevasse and distributary channel

deposits, highlights the occurrence of a repeated stacking pattern of facies that tracks short-term (millennial-scale, at least) oscillations in the water table. This high-resolution stratigraphic framework enables the identification of landward equivalents of flooding surfaces (FS), which could not be otherwise recognised in a fully freshwater sequence barren of calcareous fossils (e.g., molluscs, ostracods). Throughout the Holocene succession, an overall increase in water-table level is recorded from the lowermost swamp deposit, dated around 11.5 cal. kyr BP, to that dated around 7.6 cal. kyr BP, which is interpreted as the landward equivalent of the MFS. This inference is consistent with the general stratigraphic framework available from the literature. Upwards, the reconstructed palaeo-water level shows a general decrease.

3.   The identification of pollen-derived biomes within the Holocene succession of the Po delta plain also permits to identify in the montane taxa group (Mt) the one that exclusively reflects the regional pollen rain at the core site (cool climate indicator). Whereas, Mediterraneans (M) and deciduous broadleaves (Q+other DT) are interpreted as indicators of a mixed facies + climate optimum signal, being indicative of the Potential Natural Vegetation on the coastal plain and alluvial plain, respectively. Therefore, peaks in Mt can be used as indicators of changes in the altitudinal distribution of vegetation communities linked to cooling periods. Their high-resolution chronology points to the identification of a series of Bond Events especially for the early-mid Holocene (i.e., Preboreal Oscillation, Boreal Oscillation and 8.2 ka event), supporting a strong Mediterranean-North Atlantic climate link at millennial timescales. Thus, our data document that expanded, organic-rich successions buried beneath the innermost portion of coastal-delta plains can be used as high-resolution palaeoclimate archives, if they are framed into a robust facies and chronological context.

4.   For the first time in a continental succession of the Adriatic area, vegetation patterns and depositional dynamics related to the 8.2 ka event were identified. Specifically, pollen assemblages mark the progressive deterioration of high altitude communities (a time-succession of *Fagus*, *Abies* and *Pinus mugo*-dominance among Mt) that is followed by an increased fluvial activity of the Po River (*via* crevasse sedimentation at the core site), assessing the major role played by climate changes in shaping coastal landscapes in addition to glacio-eustatic variations.

5.   Within the uppermost 30 meters of the Arno delta plain succession (core PA1), the palyno-stratigraphic approach backed by semi-quantitative meiofauna analyses (undertaken by my co-supervisor Dr. V. Rossi) and radiocarbon ages allowed the identification of key turnovers in depositional environments (facies associations) and vegetation patterns from the late Pleistocene onwards. The former mark changes in salinity and water-table conditions/degree of hygrophily, highlighted by the relative proportion of halophytes, aquatics and hygrophytes and supported by

meiofauna data. The latter are mainly traced by relative variations in Mediterraneans, mixed oak forest broadleaves and montane trees (similarly to the Po dataset, all the plant groups are validated also by the CA-derived biomization), indicating a clear alternation of glacial-interglacial conditions within the core record. The vertically stacked pattern of depositional facies and the identification of palaeosols reveal the occurrence of two T-R cycles developed above an alluvial plain succession stratigraphically constrained to the MIS 6. Both cycles show a lower, transgressive portion formed by lagoon deposits, radiocarbon-dated to the early Holocene and MIS 3, respectively. However, the MIS 3 ages were rejected because of the inconsistency of climate optimum-like vegetation with the presence of coastal environments during a period when the mean sea level was about 50 m b.s.l. and estimated temperatures were lower than during an interglacial. On these considerations, the lower lagoonal interval was attributed to the MIS 5e interglacial also thanks to the support of general stratigraphic data; however, further investigations should be useful to support this evidence and map the lagoon succession across the plain. The lowermost cycle is capped by a set of palaeosols; the prominent uppermost palaeosol coincides with the Holocene Transgressive Surface (TS). Interestingly, Bryophytes show a great increase in species diversity across the two TSs, suggesting particularly unstable, changing environmental conditions that fit well with the abrupt flooding of subaerially exposed palaeosurfaces. Bryophytes distribution deserves further investigations as a potentially new tool for sequence-stratigraphic studies.

6.   In the context of the Arno T-R cycles, palynology proved to be a key tool to assess the role of climate/glacio-eustatic changes on main landscape variations, as transgressive lagoonal intervals invariably contain optimum-like pollen assemblages indicative of fully interglacial conditions: a meso-Mediterranean forest with a higher degree of mediterraneity especially for the lower lagoon deposit. Furthermore, pollen strongly improved the chronological framework of the Pleistocene sequence, as the assemblage indicative of a meso-mediterranean climate (*Quercus ilex* and *Erica arborea* are the major component) is inconsistent with the MIS 3 attribution resulting from two radiocarbon ages, which also show stratigraphic reversal. These palynological features, backed by stratigraphic considerations (i.e., inconsistency of lagoon formation under MIS 3 low sea levels) and correlations across the plain, allow to chronologically constrain the lowermost lagoon to MIS 5e. This leads, for the first time in the Arno Plain, to the identification of a MIS 5e coastal deposit, shedding new light on the complex late Quaternary stratigraphy of the area.

7.   The almost synchronous response of the Arno plain coastal environments to late Quaternary climate forcing, derived from high-resolution palynological analysis, is documented also at a sub-Milankovitch timescale. Indeed, the retrogradational pattern of transgressive deposits is paralleled within lagoon intervals by a trend towards the achievement of climate optimum conditions.

Accordingly, the first phase of climate cooling (last glacial beginning) coincides with the MIS 5e lagoon emersion and to the subsequent establishment of cold conditions into a widespread alluvial plain. Concerning the Holocene lagoon, the stratigraphically expanded clayey succession (ca. 1 m/500 years) seems to develop under relatively stable optimum-like conditions. Interestingly, lagoon siltation occurred in correspondence of the *acme* of a progressive deterioration in climate conditions defined by the upward increase of *Fagus sylvatica* and dated around 5000 cal yr BP.

8.   Finally, it is noteworthy that the applied methodological approach proved to be successful within two different Mediterranean coastal settings that differ in general by stratigraphy, climate, vegetation, degree of facies variability and sea-level influence during the late Quaternary. At the scale of the interglacial period, all these differences between the two records prevented a uniform recording of the Holocene palaeoclimate variability, both as pollen signature and as stratigraphic expression, and the PNV mirrors the present-day sub-mediterranean (Po Plain) and meso-mediterranean (Arno Plain) conditions occurring at the opposite sides of the Northern Apennines. Specifically, the most important Holocene climate event (the 8.2 ka) left a clear and impressive signature on the Po Plain landscape or, at least, at its innermost margin (studied core EM2; point 4). By contrast, any stratigraphic change was detected within the Arno lagoon succession in correspondence of a peak in montane trees, dated around the 8.2 ka event by the age-depth model. Interestingly, a remarkable cooling event is recorded around 5000 cal yr BP (marking the end of the climate optimum) in both the study areas, although showing different pollen and stratigraphic signatures. In the Po delta plain a 3 m-thick distributary channel cuts the underlying swampy succession and is characterised by a strong pine presence, while in the Arno delta plain the final stage of lagoon filling takes place (*via* bay-head delta deposition) in concomitance of an increasing amount of montane alders, gradually replaced by beech upwards. Nonetheless, the sole other cooling event recorded at both sites is that centred around 7000 cal. yr BP. This implies in turn that delta-coastal systems have the potentiality to record subtle palaeoclimatic changes at a high-resolution scale but also that an interaction of local factors can prevent these changes to be recorded at all. Furthermore, the anthropic pressure seems to have always been low throughout the whole Holocene in both delta plains. It became significant, although not impressive at all, only during the last one-two millennia with evidence of a sparse cultivation (*Beta vulgaris*), a general degradation in the vegetation community and/or soil salinization (ubiquists and halophytes). In this most recent portion of the core records, the presence of pines retrieved at low-resolution can account for both pine plantations in the lowlands and/or cool oscillations linked to the Little Ice Age.

Finally, applying a wider scale of observation and integrating the EM2 record with other published palynological data from the Po Plain, it can be stated that a similar vegetation characterised the two

sites during the last glacial period. This vegetation was dominated by a sparse to dense pine/conifer forest accompanied by a cold prairie with Poaceae and steppics. By contrast, warmer conditions can be hypothesised for the last interglacial period in the Arno Plain with respect to the Po Plain, possibly matching with the recent past (i.e., Holocene) and present-day climate differences.

9. REFERENCES

Accorsi C.A., Bandini Mazzanti M., Forlani L., 1978. Modello di schede palinologiche di pini italiani (*Pinus cembra* L., *Pinus pinea* L., *Pinus sylvestris* L. subsp. *Sylvestris* L. ecotipo emiliano). Archivio Botanico e Biogeografico Italiano 54 (3-4), 65-101.

Accorsi C.A., Aiello M., Bandini Mazzanti M., Bertolani Marchetti D., De Leonardis W., Forlani L., Piccione V., 1983. Flora palinologica italiana. Schede elaborate tramite computer. Archivio Botanico e Biogeografico Italiano 59 (1-2), 55-104.

Accorsi C.A., Bandini Mazzanti M., Forlani L., Randazzo G., 1994. Flora palinologica italiana, sezione aeropalinologica: S205 – *Pinus pinea* L. (Pinaceae). Aerobiologia 10 (1), 97-111.

Accorsi C.A., Bandini Mazzanti M., Forlani L., Mercuri A.M., Trevisan Grandi G., 2004. Holocene forest vegetation (pollen) of the Emilia Romagna plain – northern Italy. In: Pedrotti F, Gehu J.M. (editors), La végétation postglaciaire du passé et du présent. Syngenèse, synécologie et synsystématique. Colloques Phytosociologiques 28, 1-103.

Aguzzi M., Amorosi A., Colalongo M.L., Ricci Lucchi M, Rossi V., Sarti G., Vaiani S.C., 2007. Late Quaternary climatic evolution of the Arno coastal plain (Western Tuscany, Italy) from subsurface data. Sedimentary Geology 202, 211-229.

Albani A.D., Serandrei Barbero R., 1990. I foraminiferi della Laguna e del Golfo di Venezia. Memorie della Società Geologica Italiana 42, 271-341.

Allen J.R.M., Watts W.A., McGee E., Huntley B., 2002. Holocene environmental variability – the record from Lago Grande di Monticchio. Quaternary International 88, 69-80.

Allen J.R.M., Huntley B., 2009. Last Interglacial palaeovegetation, palaeoenvironments and chronology: a new record from Lago Grande di Monticchio, southern Italy. Quaternary Science Reviews 28, 1521-1538.

Allevato E., Arobba D., Di Pasquale G., Pappalardo M., Ribecai C., 2013. Indicazioni paleovegetazionali dai carotaggi MAPPA. MapPapers 3-III, 107-118.

Amorosi A., Colalongo M.L., Fusco F., Pasini G., Fiorini F., 1999a. Glacio-eustatic control of continental-shallow marine cyclicity from Late Quaternary deposits of the south-eastern Po Plain (northern Italy). Quaternary Research 52, 1-13.

Amorosi A., Colalongo M.L., Pasini G., Preti D., 1999b. Sedimentary response to Late Quaternary sea-level changes in the Romagna coastal plain (northern Italy). Sedimentology 46 (1), 99-121.

Amorosi A., Marchi N., 1999. High-resolution sequence-stratigraphy from piezocone tests: an example from the Late Quaternary deposits of the southeastern Po Plain. Sedimentary Geology 128, 67-81.

Amorosi A., Centineo M.C., Colalongo M.L., Pasini G., Sarti G., 2003. Facies architecture and latest Pleistocene-Holocene depositional history of the Po delta (Comacchio area, Italy). Journal of Geology 111, 39-56.

Amorosi A., Colalongo M.L., Fiorini F., Fusco F., Pasini G., Vaiani S.C., Sarti G., 2004. Palaeogeographic and palaeoclimatic evolution of the Po Plain from 150 ky-core records. Global and Planetary Change 40, 55-78.

Amorosi A., Colalongo M.L., 2005a. The linkage between alluvial and coeval near-shore marine succession: evidence from the late Quaternary record of the Po River Plain, Italy. In: Blum M.D., Marriott S.B., Leclair S.F. (editors), Fluvial Sedimentology 7. IAS Special Publication, pp. 257-275.

Amorosi A., Centineo M.C., Colalongo M.L., Fiorini F., 2005b. Millennial-scale depositional cycles from the Holocene of the Po Plain. Marine Geology 222-223, 7-18.

Amorosi A., Dinelli E., Rossi V., Vaiani S.C., Sacchetto M., 2008a. Late Quaternary palaeoenvironmental evolution of the Adriatic coastal plain and the onset of the Po River Delta. Palaeogeography Palaeoclimatology Palaeoecology 268, 80-90.

Amorosi A., Pavesi M., Ricci Lucchi M., Piccin A., 2008b. Climatic signature of cyclic fluvial architecture from the Quaternary of the central Po Plain, Italy. Sedimentary Geology 209, 58-68.

Amorosi A., Sarti G., Rossi V., Fontana V., 2008c. Anatomy and sequence stratigraphy of the late Quaternary Arno valley fill (Tuscany, Italy). In Amorosi A., Haq B.U. and Sabato L. (editors), Advances in application of sequence stratigraphy in Italy. GeoActa, Special Publication 1, 55-66.

Amorosi A., Ricci Lucchi M., Rossi V., Sarti G., 2009. Climate change signature of small-scale parasequences from Lateglacial-Holocene transgressive deposits of the Arno valley fill. Palaeogeography, Palaeoclimatology, Palaeoecology 273, 142-152.

Amorosi A., Bini M., Fabiani F., Giacomelli S., Pappalardo M., Ribecai C., Ribolini A., Rossi V., Sammartino I., Sarti G., 2012. I carotaggi MAPPA: un'integrazione interdisciplinare. MapPapers 4-II, 96-148. Doi:10.4456/MAPPA.2012.32

Amorosi A., Bini M., Giacomelli S., Pappalardo M., Ribecai C., Rossi V., Sammartino I., Sarti G., 2013a. Middle to late Holocene environmental evolution of the Pisa coastal plain (Tuscany, Italy) and early human settlements. Quaternary International 303, 93-106.

Amorosi A., Rossi V., Sarti G., Mattei R., 2013b. Coalescent valley fills from the late Quaternary record of Tuscany (Italy). Quaternary International 288, 129-138.

Amorosi A., Bruno L., Campo B., Morelli A., 2014a. The value of pocket penetration tests for the high-resolution palaeosol stratigraphy of late Quaternary deposits. Geological Journal, 2014. DOI: 10.1002/gj.2585.

Amorosi A., Rossi V., Scarponi D., Vaiani S.C., Ghosh A., 2014b. Biosedimentary record of postglacial coastal dynamics: high-resolution sequence stratigraphy from the northern Tuscan coast (Italy). Boreas 43, 939-954.

Amorosi, A., Maselli, V., Trincardi, F, 2016. Onshore to offshore anatomy of a Late Quaternary source-to-sink system (Po Plain – Adriatic Sea, Italy). Earth-Science Reviews 153, 212-237.

Amorosi A., Bruno L., Campo B., Morelli A., Rossi V., Scarponi D., Hong W., Bohacs K.M., Drexler T.D., 2017a. Global sea-level control on local parasequence architecture from the Holocene record of the Po Plain, Italy. Marine and Petroleum Geology 87, 99-111.

Amorosi A., Bruno L., Cleveland D.M., Morelli A., Hong W., 2017b. Paleosols and associated channel-belt sand bodies from a continuously subsiding late Quaternary system (Po Basin, Italy): new insights into continental sequence stratigraphy. Geological Society of America Bulletin 129 (3-4), 449-463.

Antonellini M., Giambastiani B.M.S., Greggio N., Bonzi L., Calabrese L., Luciani P., Perini L., Severi P., 2019. Processes governing natural land subsidence in the shallow coastal aquifer of the Ravenna coast, Italy. Catena 172, 76–86.

Antonioli F., Amorosi A., Correggiari A., Doglioni C., Fontana A., Fontolan G., Ruggieri G., Spada G., 2009. Relative sea-level rise and asymmetric subsidence in the northern Adriatic. Rendiconti Online della Società Geologica Italiana 9, 5-8.

Argnani A., Bernini M., Di Dio G.M., Papani G., Rogledi S., 1997. Stratigraphic record of crustal scale tectonics in the Quaternary of the Northern Apennines (Italy). Il Quaternario 10, 595-602.

Argnani A., Rogledi S., 2012. Imversion tectonics in the Neogene basins of Tuscany (northern Apennines, Italy): insights from the Pisa-Viareggio basin. Gephysical Research Abstracts 14, EDU2012-4462, 2012. Egu General Assembly, 2012.

Arobba, D., 1979. Determinazione di *Pinus halepensis* Miller e *Pinus pinaster* Aiton sulla base di differenze palinologiche. Archivio Botanico e Biogeografico Italiano 55 (3), 83-91.

Athersuch J., Horne D.J., Whittaker J.E., 1989. Marine and brackish water ostracods (Superfamilies Cypridacea and Cytheracea). In, D.M. Kermack, R.S.K. (eds), Barnes Synopsis of the British Fauna, New Series, 43, 1-343. Brill E.J., Leiden.

Baldassarri M., Gattigia G., 2009. Tra i fiumi e il mare. Lo sviluppo di Pisa nel suo contesto ambientale tra VII e XV secolo. In Volpe G., Favia P. (editors), Atti del V Congresso Nazionale di Archeologia Medievale, Firenze, 181-187.

Barbieri G., Vaiani S.C., 2018. Benthic foraminifera or Ostracoda? Comparing the accuracy of palaeoenvironmental indicators from a Pleistocene lagoon of the Romagna coastal plain (Italy). Journal of Micropalaeontology 37, 203–230.

Baroni C., Zanchetta G., Fallick A.E., Longinelli A., 2006. Mollusca steble isotope record of a core from Lake Frassino, northern Italy: hydrological and climatic changes during the last 14 ka. The Holocene 16, 827-837.

Berglund B.E. and Ralska-Jasiewiczowa M., 1986. Handbook of Holocene palaeoecology and palaeohydrology. Wiley-Interscience. John Wiley & Sons Ltd., Chichester 1986.

Bertacchi A., Sani A., Tomei P.E., 2004. La vegetazione del Monte Pisano. Felici Editore, Ospedaletto (Pisa, Italy). pp. 34.

Bertolani Marchetti D., 1963. Analisi polliniche in relazione a reperti paletnologici al Monte Cimone (Appennino Tosco-Emiliano). Giornale Botanico Italiano 70, 578-586.

Bertoldi R., 2000. Storia del popolamento vegetale della pianura del Po. In: Ferrari C., Gambi L. (a cura di), Un po di terra. Guida all'ambiente della bassa Pianura Padana e alla sua storia. Ed. Diabasis.

Bini M., Capitani M., Pappalardo M., 2012. La carta geomorfologica (doi:10.4456/MAPPA.2012.37) online webgis www.mappaproject.com

Bini M., Rossi V., Amorosi A., Pappalardo M., Sarti G., Noti V., Capitani M., Fabiani F., Gualandi M.L., 2015. Palaeoenvironments and palaeotopography of a multi-layered city during the Etruscan and Roman periods: early interactions of fluvial processes and urban growth at Pisa (Tuscany, Italy). Journal of Archaeological Science 59, 197-210.

Bini M., Fabiani F., Pappalardo M., Schuldenrein J., 2018. Special issue of Geoarchaeology: urban geoarchaeology in the Mediterranean basin. Geoarchaeology 33 (1), 3-12.

Blackmore S., Steinmann J.A.J., Hoen P.P., Punt W., 2003. The Northwest European pollen flora, 65. Betulaceae and Corylaceae. Review of Palaeobotany and Palynology 123, 71-98.

Blasi C., Capotorti G., Copiz R., Guida D., Mollo B., Smiraglia D., Zavattero L., 2014. Classification and mapping of the ecoregions of Italy. Plant Biosyst. 148 (6), 1255-1345.

Boccaletti M., Corti G., Martelli L., 2011. Recent and active tectonics of the external zone of the Northern Apennines (Italy). International Journal of Earth Sciences 100, 1331-1348.

Bolkhovitina N.A., 1956. Atlas of spores and pollen from Jurassic and Lower Cretaceous deposits of the Vilyuysk Basin. Trudy Geologichesk Institut, Akademiya Nauk SSR, Moskva, vol. 2, 1- 132.

Bond G., Showers W., Cheseby M., Lotti R., Almasi P., deMenocal P., Priore P., Cullen H., Hajdas I., Bonani G., 1997. A pervasive millennial-scale cycle in North Atlantic Holocene and glacial climates. Science 278, 1257-1266.

Bondesan M., Favero F., Viňals M.J., 1995. New evidence on the evolution of the Po coastal plain during the Holocene. Quaternary International 29-30, 105-110.

Boros A., Jàrai Komlòdi M., Tòth Z. & Nilsson S., 1993. An atlas of recent European Bryophyte spores. 321 pp. Scientia Academic Press, Budapest.

Bortolotti V., 1966. La tettonica trasversale dell'Appennino. La linea Livorno–Sillaro. Bollettino della Società Geologica Italiana 85, 529-540.

Bronk Ramsey, C., 2009. Bayesian analysis of radiocarbon dates. Radiocarbon, 51(1), 337-360.

Bruno L., Bohacs K.M., Campo B., Drexler T.M., Rossi V., Sammartino I., Scarponi D., Hong W., Amorosi A., 2017. Early Holocene transgressive palaeogeography in the Po coastal plain (Northern Italy). Sedimentology 64, 1792-1816.

Büntgen U., Tegel W., Nicolussi K., McCormick M., Frank D., Trouet V., Kaplan J.O., Herzig F., Heussner K.U., Wanner H., Luterbacher J., Esper J., 2011. 2500 years of European climate variabilità and human susceptibility. Science 331, 578-582.

Cacciari M., Cremonini S., Marchesini M., Vianello G., Vittori Antisari L., 2017. When a pedomarker is lacking: palynological and chimica multianalysis of a Lateglacial-Holocene buried soils suite. Environmental Quality 24, 47-73.

Cacciari M., Rossi V., Marchesini M., Amorosi A., Bruno L., Campo B., 2018. Palynological characterization of the Po delta succession (Northern Italy): Holocene vegetation dynamics, stratigraphic patterns and palaeoclimate variability. Alpine and Mediterranean Quaternary 31 (Quaternary: Past, Present, Future - AIQUA Conference, Florence, 13-14/06/2018), 109-112.

Cacciari M., Amorosi A., Campo B., Marchesini M., Rossi V., 2019. Palynology of the late Quaternary succession of the Arno Plain (northern Italy): new insights on palaeoenvironmental trends and climate dynamics. Bollettino della Società Paleontologica Italiana 58 (2), 201-221.

Campo B., Amorosi A., Bruno L., 2016. Contrasting alluvial architecture of Late Pleistocene and Holocene deposits along a 120-km transect from the central Po Plain (northern Italy). Sedimentary Geology 341, 265-275.

Carminati E., Doglioni C., 2012. Alps vs Apennines: the paradigm of a tectonically asymmetric Earth. Earth Science Reviews 112, 67-96-

Carminati E., Martinelli G., Severi P., 2003. Influence of glacial cycles and tectonics on natural subsidence in the Po Plain (northern Italy): insights from ^{14}C ages G^3 4. http://dx.doi.org/10.1029/2002GC000481.

Carmignani L., Conti P., Cornamusini G., 2012. Carta Geologica della Toscana. Scala 1:250.000, LAC, Firenze.

Carriòn J.S., van Geel. B., 1999. Fine-resolution Upper Weichselian and Holocene palynological record from Navarrès (Valencia, Spain) and a discussion about factors of Mediterranean forest succession. Review of Palaeobotany and Palynology 106, 209-236.

Casarosa N., Bini M., De Blasi A.M., 2011. Morfologie relitte e antiche linee di riva delle Secche della Meloria. Studi Costieri 18, 45-54.

Castellarin A., Vai G.B., 1986. South alpine versus Po Plain apenninic arcs. In: Wezel F.C. (editor), The origin of the arcs, development in geotectonics. Elsevier, Amsterdam, pp. 253-280.

Cattaneo A., Correggiari A., Langone L., Trincardi F., 2003. The late-Holocene Gargano subaqueous delta, Adriatic shelf: sediment pathways and supply fluctuations. Marine Geology 193, 61-91.

Cattaneo A., Trincardi F., Asioli A., Correggiari A., 2007. The Western Adriatic shelf clinoform: Energy-limited bottomset. Continental Shelf Reasearch 27, 506-525.

Cattaneo, C., 1844. Introduzione alle notizie naturali e civili sulla Lombardia. Milano, Bernardoni di Giovanni Tipografo, 1844.

Catuneanu O., Galloway W.E., Kendall C.G.St.G., Miall A.D., Posamentier H.W., Strasser A., Tucker M.E., 2011. Sequence Stratigraphy: methodology and nomenclature. Newsletters on Stratigraphy 44 (3), 173-245.

Chiarugi A., 1936. Ricerche sulla vegetazione dell'Etruria marittima. Cicli forestali postglaciali nell'Appennino Etrusco attraverso l'analisi pollinica di torbe e depositi lacustri presso l'Alpe delle Tre Potenze e il Monte Rondinaio. Giornale Botanico Italiano 43, 3-61.

Chiarugi A., 1958. Ricerche sulla vegetazione dell'Etruria. XI: una seconda area relitta di vegetazione di Pigella (Picea excelsa Lam.) sull'Appennino Settentrionale. Giornale Botanico Italiano 65, 23-42.

Christopher R.A., 1976. Morphology and taxonomic status of *Pseudoschizaea*, Thiergart and Frantz ex R. Potonie emend. Micropaleontology 22, 143-150.

Ciabatti M., 1967. Ricerche sull'evoluzione del delta padano. Giornale di Geologia 34, 381-406.

Cincotta A., Pestchevitskaya E.B., Sinitsa S.M., Markevich V.S., Debaille V., Rashetova S.A., Mashchuk I.M., Frolov A.O., Gerdes A., Yans J. & Godefroit P., 2019. The rise of feathered dinosaurs: Kulindadromaeus zabaikalicus, the oldest dinosaur with "feather-like" structures. PeerJ 7, 6239-6259.

Cipriani L. E., Ferri S., Iannotta P., Paolieri F. and Pranzini E., 2001. Morfologia e dinamica dei sedimenti del litorale della Toscana settentrionale. Studi Costieri 4, 119-156.

Combourieu-Nebout N., Peyron O., Bout-Roumazeilles V., Goring S., Dormoy I., Joannin S., Sadori L., Siani G., Magny M., 2013. Holocene vegetation and climate changes in the central Mediterranean inferred from a high-resolution marine pollen record (Adriatic Sea). Climate of the Past, 9: 2023-2042.

Correggiari A., Cattaneo A., Trincardi F., 2005. The modern Po delta system: lobe switching and asymmetric prodelta growth. Marine Geology 222-223, 49-74.

De Beaulieu J.L., Reille M., 1992. The last climatic cycle at La Grande Pile (Vosges, France). A new pollen profile. Quaternary Science Reviews 11, 431-438.

Della Rocca B., Mazzanti R., Pranzini E., 1987. Studio geomorfologico della pianura di Pisa. Geografia Fisica e Dinamica Quaternaria 10, 56-84.

Di Rita F., Simone O., Caldara M., Gehrels R.W., Magri D., 2011. Holocene environmental changes in the coastal Tavoliere Plain (Apulia, Southern Italy): a multiproxy approach. Palaeogeography, Palaeoclimatology, Palaeoecology 310, 139-151.

Di Rita F., Magri D., 2012. An overview of the Holocene vegetation history from the central Mediterranean coasts. Journal of Mediterranean Earth Sciences, 4: 35-52.

Di Rita F., Anzidei A.P., Magri D., 2013. A Lateglacial and Early Holocene pollen record from Valle di Castiglione (Rome): vegetation dynamics and climate implications. Quaternary International 288, 73-80.

Di Rita F., Celant A., Milli S. and Magri D., 2015. Lateglacial – early Holocene vegetation history of the Tiber delta (Rome, Italy) under the influence of climate change and sea level rise. Review of Palaeobotany and Palynology 218, 204-216.

Di Rita F., Molisso F., Sacchi M., 2018. Late Holocene environmental dynamics, vegetation history, human impact and climate change in the ancient Literna Palus (Lago Patria; Campania, Italy). Review of Palaeobotany and Palynology 258, 48-61.

Doglioni C., 1993. Some remarks on the origin of foredeeps. Tectonophysics 228, 1-20.

Dolez L., Salel T., Bruneton H., Colpo G., Devillers B., Lefèvre D., Serge D.M., Sanchez C., 2015. Holocene palaeoenvironments of the Bages-Sigean lagoon (France). Geobios, 48: 297-308.

Dormoy I., Peyron O., Combourieu Nebout N., Goring S., Kotthoff U., Magny M., Pross J., 2009. Terrestrial climate variability and seasonality changes in the Mediterranean region between 15000 and 4000 years BP deduced from marine pollen records. Climate of the Past 5, 615-632.

Drescher-Schneider R., de Beaulieu J.-L., Magny M., Walter- Simonnet A.-V., Bossuet G., Millet L., Brugiapaglia E. & Drescher A. (2007). Vegetation history, climate and human impact over the last 15,000 years at Lago dell'Accesa (Tuscany, central Italy). Vegetation History and Archeobotany 16, 279- 299.

Ejarque A., Julià R., Reed J.M., Mesquita-Joanes F., Marco-Berba J., Riera S., 2016. Coastal Evolution in a Mediterranean Microtidal Zone: Mid to Late Holocene Natural Dynamics and Human Management of the Castelló Lagoon, NE Spain. PLoS ONE 11: e0155446.

Faegri K., Iversen J. & Krzywinski K., 1989. Textbook of pollen analysis. 328 pp. John Wiley and Sons, Chichester.

Federici P.R., Mazzanti R., 1995. Note sulle pianure costiere della Toscana. Memorie della Società Geografica Italiana 53, 165-270.

Ferrari C. (editor), 1980. Flora e vegetazione dell'Emilia Romagna. Grafiche Zanini, Bologna (Italy), 1980.

Ferrari C. 1997. The vegetation belts of Emilia Romagna (Northern Italy). Allionia 34, 219-231

Follieri M., Magri D., Sadori L., 1988. 250,000-year pollen record from Valle di Castiglione (Roma). Pollen et Spores, 30: 329-356.

Food and Agricultural Organization of the United Nations, 2014. World reference base for soil resources 2014. World Soil Resources Reports 106, 181 pp., FAO, Rome 2014.

Gandolfi G. and Paganelli L., 1975. Il litorale pisano-versiliese (area campione Alto Tirreno); composizione, provenienza e dispersione delle sabbie. Bollettino della Società Geologica Italiana 94, 1273-1295.

Garbari F., 2004. Viaggio al Monte Pisano: un'escursione botanica. Studi Trentini di Scienze Naturali, Acta Biologica 81, 233-238.

Geological Map of Italy at 1:50.000 scale (Geological Survey of Italy and CARG Project)

Giacomelli S., Rossi V., Amorosi A., Bruno L., Campo B., Ciampalini A., Civa A., Hong W., Sgavetti M., De Souza Filho C.R., 2018. A mid-late Holocene tidally-influenced drainage system revealed by integrated remote sensing, sedimentological and stratigraphic data. Geomorphology 318, 421-436.

Hammer Ø., Harper D.A.T., Ryan P.D., 2001. PAST: Paleontological Statistics Software Package for Education and Data Analysis. Palaeontologia Electronica 4 (1), 9pp.

Harris-Parks E., 2016. The micromorphology of Younger Dryas-aged black mats from Nevada, Arizona, Texas and New Mexico. Quaternary Research 85, 94-106.

Henderson P.A., 1990. Freshwater ostracods. In D.M. Kermack & R.S.K. (eds), Barnes Synopses of the British Fauna, New Series 42, 1–228. Brill E.J., Leiden.

Holmes J.A., Chivas A.R., 2002. The Ostracoda: applications in Quaternary research. Geophysical Monograph Series. 131 pp. AGU, Washington.

Howell J.V. (editor). Glossary of Geology and related Sciences. American Geological Institute, 2nd ed., 1960. Washington D.C.

Jalut G., Esteban Amat A., Bonnet L., Gauquelin T., Fontugne M., 2000. Holocene cimatic changes in the Western Mediterranean from south-east France to south-east Spain. Paleogeography, Palaeoclimatology, Palaeoecology 160, 255-290.

Joannin S., Vannière B., Galop D., Peyron O., Haas J.N., Gilli A., Chapron E., Wirth S.B., Anselmetti F., Desmet M., Magny M., 2013. Climate and vegetation changes during the Lateglacial and early-middle Holocene at Lake Ledro (southern Alps, Italy). Climate of the Past 9, 913-933.

Jorissen F.J., 1988. Benthic foraminifera from the Adriatic Sea; principles of phenotypic variation. Utrecht Micropaleontology Bullettin 37, 1-176.

Kaniewski D., Van Campo E., Paulissen E., Weiss H., Bakker J., Rossignol I., Van Lerberghe K., 2011. The Medieval climate anomaly and the Little Ice Age in coastal Syria inferred from pollen-derived palaeoclimatic patterns. Global and Planetary Change 78, 178-187.

Liu J.P., Milliman J.D., 2004. Reconsidering Melt-water pulses 1A and 1B: global impacts on rapid sea-level rise. Oceanic and Coastal Sea Research 3 (2), 183-190.

Lowe J.J., Accorsi C.A., Bandini Mazzanti M., Bishop V., Van der Kaars S., Forlani L., Mercuri A.M., Rivalenti C., Torri P., Watson C., 1996. Pollen stratigraphy of sediment sequences from carter lakes Albano and Nemi (near Rome) and from the central Adriatic, spanning the interval from oxygen isotope Stage 2 to the present day. Memorie dell'Istituto Italiano di Idrobiologia 55, 71-98.

Magny M., Miramont C., Sivan O., 2002. Assessment of the impact of climate and anthropogenic factors on Holocene Mediterranean vegetation in Europe on the basis of palaeohydrological records. Palaeogeography, Palaeoclimatology, Palaeoecology 186, 47-59.

Magny M., Combourieu-Nebout N., de Beaulieu J. L., Bout-Roumazeilles V., Colombaroli D., Desprat S., Francke A., Joannin S., Ortu E., Peyron O., Revel M., Sadori L., Siani G., Sicre M A., Samartin S., Simonneau A., Tinner W., Vannière B., Wagner B., Zanchetta G., Anselmetti F., Brugiapaglia E., Chapron E., Debret M., Desmet M., Didier J., Essallami L., Galop D., Gilli A., Haas J.N., Kallel N., Millet L., Stock A., Turon J.L., Wirth S., 2013. North-South palaeohydrological contrasts in the central Mediterranean during the Holocene: tentative synthesis and working hypotheses. Clim. Past 9, 2043-2071.

Mariani M., Prato R., 1988. I bacini neogenici costieri del margine tirrenico: approccio sismico stratigrafico. Memorie della Società Geologica Italiana 41, 519-531.

Martini I.P., Sagri M., 1993. Tectono-sedimentary characteristics of Late Miocene – Quaternary extensional basins of Northern Apennines, Italy. Earth-Science Reviews 34, 197-233.

Martini I.P., Sarti G., Pallecchi P., Costantini A., 2010. Environmental influences on the development of the Medieval-early Renaissance city states of Pisa, Florence and Siena. In Martini I.P., Chesworth W. (editors), Landscape and societies. Selected cases. Springer, Dordrecht, 203-222.

Maselli V., Trincardi F., 2013. Man made deltas. Science Reports 2013; 3: 1926. doi: 10.1038/srep01926.

Mattei R., 2008. Analisi dei depositi tardo quaternari del bacino di Viareggio: dalla creazione di una banca dati georeferenziata alla realizzazione di un modello stratigrafico-deposizionale. Laurea Specialistica in Scienze Geologiche, Università di Pisa.

Mayewski P.A., Rohling E.E., Stager J.C., Karlén W., Maasch K.A., Meecker L.D., Meyerson E.A., Gasse F., van Kreveld S., Holmgren K., Lee-Thorp J., Rosqvist G., Rack F., Staubwasser M., Schneider R.R., Steig E.J., 2004. Holocene climate variability. Quaternary Research 62, 243-255.

Mazzanti R., Pasquinucci M., 1983. L'evoluzione del litorale lunese-pisano fino alla metà del XIX secolo. Bollettino della Società Geologica Italiana 12, 605-628.

Mazzini I., Gliozzi E., Koci R., Soulie-Märsche I., Zanchetta G., Baneschi I., Sadori L., Giardini M., Van Welden A., Bushati S., 2015. Historical evolution and Middle to Late Holocene environmental changes in Lake Shkodra (Albania): New evidences from micropaleontological analysis. Palaeogeography, Palaeoclimatology, Palaeoecology 419, 47-59.

Mazzoli D., Koyi H.A., Barchi M.R., 2006. Structural evolution of a fold and thrust belt generated by multiple décollements: analogue models and natural examples from the northern Apennines (Italy). Journal of Structural Geology 28, 185-199.

Millet B., Lamy N., 2002. Spatial patterns and seasonal strategy of macrobenthic species relating to hydrodynamics in a coastal bay. Journal de Rechèrche Océanographique 27, 30–42.

Milli S., Mancini M., Moscatelli M., Stigliano F., Marini M., Cavinato G.P., 2016. From river to shelf, anatomy of a high-frequency depositional sequence: the Late Pleistocene to Holocene Tiber depositional sequence. Sedimentology 63, 1886–1928.

Milliman J.D., Bonaldo D., Carniel S., 2016. Flux and fate of river-discharged sediments to the Adriatic Sea. Advances in Oceanography and Limnology 7.

Mitchum Jr. R.M., Vail P.R., Thompson III, S., 1977. The depositional sequence as a basic unit for stratigraphic analysis. In: Payton C.E. (editor), Seismic stratigraphy – application to hydrocarbon exploration. AAPG Momoir 26, 53-62.

Molinari F.C., Boldrini G., Severi P., Dugoni G., Rapti Caputo D., Martinelli G., 2007. Risorse idriche sotterranee della Provincia di Ferrara. In: Dugoni G., Pignone R. (Editors), Risorse idriche sotterranee della Provincia di Ferrara, 7–61.

Montenegro M.E., Pugliese N., 1996. Autoecological remarks on the ostracod distribution in the Marano and Grado Lagoons (Northern Adriatic Sea, Italy). Bollettino della Società Paleontologica Italiana 3, 123-132.

Moore P.D., Webb J.A., Collinson M.E., 1991. Pollen analysis. Second edition. Blackwell Scientific Publications, Oxford, 1991.

Morelli A., Bruno L., Cleveland D.M., Drexler T.M., Amorosi A., 2017. Reconstructing Last Glacial Maximum and Younger Dryas paleolandscapes through subsurface paleosol stratigraphy: an example from the Po coastal plain, Italy. Geomorphology 295, 790-800.

Murray J., 2006. Ecology and applications of benthic foraminifera. 426 pp. Cambridge University Press, New York.

Muttoni G., Carcano C., Garzanti E., Ghielmi M., Piccin A., Pini R., Rogledi S., Sciunnach D., 2003. Onset of major Pleistocene glaciations in the Alps. Geology 31, 989-992.

Negodi G., 1941. La vegetazione dei boschi planiziari del modenese. Studi sulla vegetazione dell'Appennino emiliano e della pianura adiacente. Memorie III dell'Archivio Botanico 17, 125-149.

Nisi B., Vaselli O., Buccianti A., Minissale A., Delgado Huertas A., Tassi F., Montegrossi G., 2008. Indagine geochimica ed isotopica del carico disciolto nelle acque di scorrimento superficiale della valle dell'Arno: valutazione del contributo naturale ed antropico. Memorie Descrittive della Carta Geologica d'Italia 74, pp. 160.

Ori G.G., Roveri M., Vannoni F., 1986. Plio-Pleistocene sedimentation in the Apenninic-Adriatic foredeep (central Adriatic Sea, Italy). In: Allen P.A., Homewood P. (editors), Foreland Basins. IAS Special Publication 8, 243-254.

Panzacchi A., 1585. Relazione al Senato Bolognese sulle selve del Belvedere, Capugnano e Granaglione. Archivio dello Stato, Ufficio Contado ms 3, Bologna.

Paoli P., Perini T., 1979. Ricerche biometriche e morfologiche sul polline degli Ontani italiani. Webbia 33 (2), 221-233.

Paschini E., Artegiani A., Pinardi N., 1993. The mesoscale eddy field of the middle Adriatic during fall 1988. Deep-Sea Research Part I, 40, 1365–1377.

Pascucci V., 2005. Neogene evolution of the Viareggio Basin, Northern Tuscany (Italy). *GeoActa* 4, 123-138

Picotti V., Pazzaglia F.J., 2008. A new active tectonic model for the construction of the Northern Apennines mountain front near Bologna (Italy). Journal of Geophysical Research 113, B08412.

Pieri M., Groppi G., 1981. Subsurface geological structure of the Po Plain, Italy, Consiglio Nazionale delle Ricerche, Progetto Finalizzato Geodinamica 414, 1-23.

Pignatti S., 1979. I piani di vegetazione in Italia. Giornale Botanico Italiano 113, 411-428.

Pignatti, S., 1982. Flora d'Italia. Edagricole, Bologna.

Pignatti, S., 1998. I boschi d'Italia – Sinecologia e biodiversità. UTET, Torino.

Pignatti, S., 2017-2018. Flora d'Italia. Edagricole, Bologna.

Pini R., Minari E., Furlanetto G., Gorian F., Ravazzi C., Rizzi A., Valoti F., 2016. Guida per il riconoscimento del polline negli ambienti forestali della Pianura Padana. Tipografia Camuna S.p.A., Breno (Brescia, Italy).

Poulain P.-M., 2001. Adriatic Sea surface circulation as derived from drifter data between 1990 and 1999. Journal of Marine Systems 29, 3-32.

Pranzini E., 2001. Updrift river mouth migration on cuspate deltas: two examples from the coast of Tuscany (Italy). Geomorphology 38, 125-132.

Pranzini E., 2007. Airborne LIDAR survey applied to the analysis of the historical evolution of the Arno river delta (Italy). Journal of Coastal Research 50 (50), 400-409.

Pranzini E., 2011. Archaeological heritage, landscape value, beach use and recreational boating in Baratti Bay (Italy): synergy or conflicting interests? Journal of Coastal Research 64, 1406-1410.

Punt, W., Hoen, P.P., 2009. The Northwest European pollen flora, 70. Asteraceae – Asteroideae. Review of Palaeobotany and Palynology 157 (1-2), 22-183.

Redi F., 1991. Pisa com'era: archeologia, urbanistica e strutture materiali (secoli V-XIV), Napoli, 1-552.

Regione Emilia-Romagna, Servizio Paesaggio, Parchi e Patrimonio Naturale, 1996. Cartografia fitoclimatica dell'Emilia Romagna. Carta 1:500.000. Assessorato Territorio, Programmazione e Ambiente, collana Studi e Documentazioni 47.

Regione Emilia-Romagna and Eni-Agip, 1998. Riserve idriche sotterranee della Regopme Emilia-Romagna. S.EL.CA., Firenze.

Regione Lombardia and Eni-Divisione Agip, 2002. Geologia degli acquiferi padani della Regione Lombardia. S.EL.CA., Firenze.

Reille M., 1992. Pollen et spores d'Europe et d'Afrique du nord. Laboratoire de Botanique Historique et Palynologie, Marseille.

Reille M., 1995. Pollen et spores d'Europe et d'Afrique du nord. Supplément 1. Laboratoire de Botanique Historique et Palynologie, Marseille.

Reille M., 1998. Pollen et spores d'Europe et d'Afrique du nord. Supplément 2. Laboratoire de Botanique Historique et Palynologie, Marseille.

Reille M., Andrieu V., De Beaulieu J.L., Guenet P., Goeury C., 1998. A long pollen record from Lac du Bouchet, Massif Central, France, for the period ca. 325 to 100 ka BP (OIS 9c to 5e). Quaternary Science Reviews 17, 1107-1123.

Reimer P.J., Bard E., Bayliss A., Warren Beck J., Blackwell P.G., Bronk Ramsey C., Buck C.E., Cheng H., Lawrence Edwards R., Friedrich M., Grootes P.M., Guilderson T.P., Haflidason H., Hajdas I., Hatté C., Heaton T.J., Hoffmann D.L., Hogg A.G., Hughen K.A., Felix Kaiser K., Kromer B., Manning S.W., Niu M., Reimer R.W., Richards D.A., Marian Scott E., Southon J.R., Staff R.A., Turney C.S.M. & van der Plicht J., 2013. Intcal13 and Marine13 radiocarbon age calibration curves 0-50,000 years cal BP. *Radiocarbon*, 55: 1869-1887.

Retallack G.J., 2001. Soils of the past: an introduction to palaeopedology. 2nd edition. Blackwell, Oxford, pp. 404.

Revelles J., Ghilardi M., Rossi V., Curràs A., Lòpez-Bultò O., Brkojewitsch G., Vacchi M., 2019. Coastal landscape evolution of Corsica Island (W. Mediterranean): palaeoenvironments, vegetation history and human impacts since the early Neolithic period. Quaternary Science Reviews 225, 1-26.

Ricci Lucchi F., Colalongo M.L., Cremonini G., Gasperi G., Iaccarino S., Papani G., Raffi I., Rio D., 1982. Evoluzione paleogeografica e sedimentaria del margine appenninico. In: Cremonini G., Ricci Lucchi F. (editors), Guida alla geologia del margine appenninico-padano. Guide geologiche regionali della Società Geologica Italiana, pp. 17-46.

Ricci Lucchi M., 2008. Vegetation dynamics during the last Interglacial – Glacia cycle in the Arno coastal plain (Tuscany, western Italy): location of a new tree refuge. Quaternary Science Reviews 27, 2456-2466.

Rossi V., 2009. Ostracod assemblages from Holocene subsurface deposits of modern Po Delta: a palaeoenvironmental proxy record. Bollettino della Società Paleontologica Italiana 48 (2), 95-103.

Rossi V., Amorosi A., Bini M., Cacciari M., Campo B., Demurtas L., Giacomelli S., Sarti G., 2019. Lateral variabilità in depositional processes and coastal configuration during the Holocene Arno delta evolution. 34th IAS Meeting of Sedimentology: "Sedimentology to face societal challenges on risk, resources and record of the past". Roma, 2019.

Rossi V., Amorosi A., Sarti G., Potenza M., 2011. Influence of inherited topography on the Holocene sedimentary evolution of coastal systems: an example from Arno costal plain (Tuscany, Italy). Geomorphology 135, 117-128.

Rossi V., Amorosi A., Sarti G., Romagnoli R., 2012. New stratigraphic evidence for the mid-late Holocene fluvial evolution of the Arno coastal plain (Tuscany, Italy). Géomorphologie 2, 201-214.

Rossi V., Amorosi A., Sarti G., Mariotti S., 2017. Late Quaternary multiple incised valley systems: an unusually well-preseved stratigraphic record of two interglacial valley-fill successions from the Arno Plain (northern Tuscany, Italy). Sedimentology 64, 1901-1928.

Rossi V., Vaiani S.C., 2008. Microfaunal response to sediment supply changes and fluvial drainage reorganization during the Holocene transgression in subsurface deposits of the Po delta (Italy). Marine Micropalaeontology 69, 106-118.

Ruiz F., Gonzalez-Regalado M.L., Baceta J.I., Menegazzo-Vitturi L., Pistolato M., Rampazzo G., Molinaroli E., 2000. Los ostrácodos actuales de la laguna de Venecia (NE de Italia). Geobios, 33: 447-454.

Russel P.J., Petersen G.H., 1973. The use of ecological data in the elucidation of some shallow water European Cardium species. Malacologia 14, 223–232.

Sarti G., Bini M., Giacomelli S., 2010. The growth and decline of Pisa (Tuscany, Italy) up to the Middle Ages: correlations with landscape and geology. Il Quaternario 23 (2bis), 2010 – volume speciale, 311-322.

Sarti G., Rossi V., Amorosi A., 2012. Influence of Holocene stratigraphic architecture on ground surface settlements: a case study from the city of Pisa (Tuscany, Italy). Sedimentary Geology 281, 75-87.

Sarti G., Rossi V., Amorosi A., Bini M., Giacomelli S., Pappalardo M., Ribecai C., Ribolini A., Sammartino I., 2015a. Climatic signature of two mid-late Holocene fluvial incisions formed under sea-level highstand conditions (Pisa coastal plain, NW Tuscany, Italy). Palaeogeography, Palaeoclimatology, Palaeoecology 424, 183-195.

Sarti G., Rossi V., Giacomelli S., 2015b. The upper Pleistocene "Isola di Coltano sands" (Arno coastal plain, Tuscany Italy): review of stratigraphic data and tectonic implications for the southern margino f the Viareggio basin. Atti della Società Toscana di Scienze Naturali, Memorie serie A 122, 75-84.

Scarponi D., Kowalewski M., 2004. Stratigraphic palaeoecology: bathymetric signatures and sequence overprint of mollusk associations from upper Quaternary sequences of the Po Plain, Italy. Geology 32 (11), 989-992.

Scarponi D., Angeletti L., 2008. Integration of palaeontological patterns in the sequence stratigraphy paradigm: a case study from Holocene deposits of the Po Plain (Italy). GeoActa 7, 1-13.

Scarponi D., Kaufman D., Amorosi A., Kowalewski M., 2013. Sequence stratigraphy and the risolution of the fossil record. Geology 41, 239-242.

Sgarrella F., Moncharmont Zei M., 1993. Benthic Foraminifera of the Gulf of Naples (Italy): systematics and autoecology. Bollettino della Società Paleontologica Italiana 32 (2), 145-264.

Soil Survey Staff, 1999. Soil Taxonomy. A basic system of soil classification for making and interpreting soil surveys; 2nd edition. Agricultural Handbook 436; Natural Resources Conservation Service, USDA, Washington DC, USA, pp. 869.

Somoza L., Barnolas A., Arasa A., Maestro A., Rees J.G., Hernandez-Molina F.J., 1998. Architectural stacking patterns of the Ebro delta controller by Holocene high-frequency eustatic fluctuations, delta-lobe switching and subsidence processes. Sedimentary Geology 117, 11-32.

Spallanzani L., 1795. Viaggio alle Due Sicilie e in alcune parti dello Appennino. Tomo 5, 75. Pavia.

Stefani M., Vincenzi S., 2005. The interplay of eustasy, climate and human activity in the late Quaternary depositional evolution and sedimentary architecture of the Po Delta system. Marine Geology 222-223, 19-48.

Tarasov P. E., Cheddadi R., Guiot J., Bottema S., Peyron O., Belmonte J., Ruiz-Sanchez V., Saadi F., Brewer S., 1998. A method to determine warm and cool steppe biomes from pollen data; application to the Mediterranean and Kazakhstan regions. Journal of Quaternary Science 13 (4), 335-344.

Toti F., Bertini A., 2018. Mediterranean pollen stratigraphy across the Early-Middle Pleistocene boundary. Alpine and Mediterranean Quaternary 31, 199-203.

Tschudy R.H., Scott R.A., 1969. Aspects of palynology. Wiley-Interscience, Wiley&Sons, 510 pp.

Tomaselli M., 1970. Note illustrative alla carta della vegetazione naturale potenziale d'Italia. Min. Agr. Foreste, Collana verde 27. Roma.

Tomaselli, M. (editor), 1987. Guida alla vegetazione dell'Emilia Romagna. Collana Annali, Facoltà di Scienze MM., FF., NN. Università di Parma.

Tzedakis P.C., Frogley M.R., Heaton T.H.E., 2003. Last Interglacial conditions in southern Europe: evidence from Ioannina, northwest Greece. Global and Planetary Change 36, 157-170.

Tutin T.G., Heywood V.H., Burges N.A., Valentine D.H., 1993. Flora europaea. Cambridge University Press.

Ubaldi D., 2003. Flora, fitocenosi e ambiente. Elementi di geobotanica e fitosociologia. CLUEB, Bologna.

Vacchi M., Marriner N., Morhange C., Spada G., Fontana A., Rovere A., 2016. Multiproxy assessment of Holocene relative sea-level changes in the western Mediterranean: sea-level variability and improvements in the defnition of the isostatic signal. Earth Science Reviews 155, 172-197.

Van Benthem F., Clarcke G.C.S., Punt W., 1984. The Northwestern European pollen flora, 33. Fagaceae. Review of Palaeobotany and Palynology 42, 87-110.

Van Wagoner J.C., Posamentier H.W., Mitchum R.M., Vail P.R., Sarg J.F., Loutit T.S., Hardenbol J., 1988. An overview of the fundamentals of sequence stratigraphy and key definitions. SEPM Special Publication. In: Wilgus C.K., Hastings B.S., Kendall C.G.St.C., Posamentier H.W., Ross C.A., Van Wagoner J.C. (Editors), Sealevel Changes: an Integrated Approach, vol. 42, pp. 39-45.

Van Wagoner J.C., Mitchum R.M., Campion K.M., Rahmanian V.D., 1990. Siliciclastic sequence stratigraphy in well logs, cores and outcrops: concepts for high resolution correlations of time and facies. American Association of Petroleum Geologists, Methods in Exploration 7, Tulsa, U.S.A, p. 55.

Veggiani A., 1974. Le variazioni idrografiche del basso corso del fiume Po negli ultimi 3000 anni. Padusa 1-2, 39-60.

Vittori E., Ventura G., 1995. Grain size of fluvial deposits and late Quaternary climate: a case study in the Po River valley (Italy). Geology 23, 735-738.

Wirth S.B., Gilli A., Simonneau A., Ariztegui D., Vannière B., Glur L., Chapron E., Magny M., Anelmetti F.S., 2013. A 2000 year long seasonal record of floods in the southern European Alps. Geophysical Research Letters, 40 (15), 4025-4029.

Woillard G.M., 1975. Grande Pile peat bog: a continuous pollen record for the last 140.000 years. Quaternary Research 9, 1-21.

ACKNOWLEDGEMENTS

Last to be mentioned but first in line are my parents and family in general, whose presence and importance really go beyond imagination and cannot be expressed in words. I can just say that, like many people around, I would not be the person I am and I would not have reached all these goals without your support and your belief in my capabilities. I really hope everything will go smoothly, especially for my grandmother Bia.

APPENDIX A: BRYOPHYTE SPORES MORPHOLOGICAL GUIDE
(after Boros et a., 1993)

Features	Mean dimensions	Taxon
Trilete spore, round, spines and processes well evident, pale.	45 μm (ø)	*Phaeoceros laevis*
Trilete spore, round, spines and processes well evident, dark.	45 μm (ø)	*Anthoceros laevis*
Atreme, round, gemmae and processes evident	93 μm (ø)	*Conocephalum conicum*
Atreme, round, finely scabrate	180 μm (ø)	*Archidium alternifolium*
Atreme, round, medium scabrate	65 μm (ø)	*Meesia uliginosa*
Atreme, round, similar to very dark fungal spores but spines evident	85 μm (ø)	*Riella helicophylla*
Atreme, round, similar to very dark fungal spores but open alveolate	120 μm (ø)	*Sphaerocarpos michelii*
Atreme, round, similar to very dark fungal spores but close alveolate	81 μm (ø)	*Targionia hypophylla*
Atreme, round, similar to greyish fungal spores but open alveolate	41 μm (ø)	*Reboulia hemisphaerica*
Atreme, round, similar to greyish fungal spores but open alveolate with perine	72 μm (ø)	*Peltolepis quadrata*
Atreme, round, similar to greyish fungal spores but with dense ornamentation and perine	66 μm (ø)	*Bucegia romanica*
Atreme, monolete-shaped, similar to greyish fungal spores but with perine	72 μm (axis >)	*Preissia quadrata*
Atreme, angular with fine reticulum	53x50 μm	*Ricia frostii*
Katalept, distally-increasing large reticulum	46 μm (ø)	*Conostomum tetragonum*
Probably katalept, labyrinthic, striate-reticulate processes	55x46 μm	*Fossombronia pusilla*
Probably katalept, labyrinthic, striate-reticulate processes with columellar orientation	45x40 μm	*Fossombronia wondrazieckii*

Table 1a: morphological guide to spores ø > 40 μm.

Features	Mean dimensions	Taxon
Atreme, very large lycopod-like reticulum but < ø	26 μm (ø)	*Mylia taylori*
Trilete, fine reticulum / highly scabrate	28 μm (ø)	*Hedwigia ciliate*
Trilete, sub-triangular, nearly psilate or with some processes (for species determination see Boros et al., 1993, Reille 1992, 1995 and 1998)	Variable ø	*Sphagnum sp.*
	μm (ø)	
Atreme, scabrate-verrucate with sparse very evident processes; thin walled	25 μm (ø)	*Ptilidium pulcherrimum*
Atreme, scabrate-verrucate with scarce evident processes and a medium reticulum	23 μm (ø)	*Aongstroemia longipes*
Atreme, scabrate-verrucate with frequent evident processes and a medium reticulum	21 μm (ø)	*Dicranum bonjeani*
Atreme, scabrate-verrucate patchiness similar to Aongstroemia, globules similar to Dicranum	24 μm (ø)	*Antitrichia curtipendula*
Atreme, scabrate-verrucate with scarce processes and a varying reticulum	29 μm (ø)	*Cynodontium polycarpon*
Atreme, scabrate-verrucate with thick-piled processes, asymmetric	29 μm (ø)	*Radula complanata*
Atreme, scabrate-verrucate with thick-piled, nearly uniform-patched processes	20 μm (ø)	*Atrichum undulatum*
Atreme, scabrate with scarse, poorly-evident processes (see Boros et al., 1993 for species determination)	15-18 μm (ø)	*Fissidentaceae*
Katalept, monolete-shaped, simil-perine but clavate	39x31 μm	*Trematodon ambiguous*
Katalept, monolete-shaped, no perine but large reticulum	28 μm (ø)	*Pterygoneum ovatum*
Katalept, monolete-shaped, no perine but scabrate-verrucate	40x30 μm	*Meesia longiseta*
Katalept, monolete-shaped, labyrinthic striate	38x31 μm	*Bartramia ityphylla*
Katalept depressed, papillate	30 μm (ø)	*Pleuridium subulatum*
Katalept evident, papillate	30 μm (ø)	*Aphanorhegma patens*
Katalept evident, digitate	25 μm (ø)	*Discelium nudum*
Katalept, papillate-thickly granulate, round leptoma	32 μm (ø)	*Desmatodon heimii*
Katalept, thickly papillate, depressed leptoma	28 μm (ø)	*Phascum cuspidatum*
Katalept, thickly papillate with medium reticulum, thick wall	31 μm (ø)	*Acaulon triquetrum*
Katalept, thickly papillate with medium reticulum, thin wall	26 μm (ø)	*Leucodon sciuroides*
Katalept, thickly papillate with fine reticulum, depressed leptoma. Thin walled, thinner than aquatic Angiosperms	32 μm (ø)	*Rhizomnium punctatum*
Katalept, thickly papillate with fine reticulum, depressed leptoma. Thin walled, thinner than Rhizomnium and aquatic Angiosperms, sub-triangular	23 μm (ø)	*Plagiomnium cuspidatum*
Katalept, thickly papillate with fine reticulum, depressed leptoma. Thin walled, thinner but wider than aquatic Angiosperms	26 μm (ø)	*Drepanocladus revolvens*
Atreme, scarcely papillate, similar to Cyperaceae but ornated	34 μm (ø)	*Bryum marratii*
Atreme, fairly papillate, similar to Cyperaceae but ornated	40 μm (ø)	*Cinclydium stygium*
Atreme with large striae with colliding walls	37 μm (ø)	*Encalypta ciliata*
Katalept, striate-globulate, thin	32 μm (ø)	*Plagiobryum zieri*

Table 1b: morphological guide to spores 20 < ø < 40 μm.

Features	Mean dimensions	Taxon
Atreme, medium reticulate – papillate similarly to Anthocerotae	19 µm (ø)	*Saelania glaucescens*
Atreme, sub-triangular, striate, dark because very thick	14 µm (ø)	*Fabronia pusilla*
Atreme, sub-triangular, thick globules similar to thick reticulum	19x16 µm	*Orthotrichum sp.*
Atreme, sub-triangular, thick globules similar to thick reticulum	25 µm (ø)	*Ulotha crispa*
Atreme, sub-triangular, thick globules similar to thick reticulum	20 µm (ø)	*Calliergon giganteum*
Atreme, sub-triangular, thick globules similar to large reticulum	18 µm (ø)	*Calliergonella cuspidata*
Atreme depressed, papillate with globules peaking through	15 µm (ø)	*Cryphaea heteromalla*
Atreme, scabrate, often crumples or irregularly-shaped, thin	13.6 µm (ø)	*Hygrohypnum luridum*
Atreme, scabrate, often crumples or irregularly-shaped, thin	17 µm (ø)	*Timmia bavarica*
Atreme, scabrate, often crumples or irregularly-shaped, thin	12 µm (ø)	*Oligotrichum hercynum*
Atreme, scabrate-reticulate, thin	16-19 µm (ø)	*Pohlia sp.*
Atreme, asymmetrically reticulate	19 µm (ø)	*Palustriella commutata*
Katalept, large leptoma, spheroidal, scabrate	15 µm (ø)	*Leucobryum glaucum*
Katalept, large leptoma, spheroidal, scabrate	20 µm (ø)	*Dicranum scoparium*
Katalept, large leptoma, spheroidal, psilate	15 µm (ø)	*Dicranella heteromalla*
Katalept, large leptoma, spheroidal, thickly papillate	20 µm (ø)	*Dicranum elongatum*
Katalept, large leptoma, spheroidal, reticulate, thin	18 µm (ø)	*Dicranella cerviculata*
Katalept, trilete leptoma, thick	17 µm (ø)	*Campylopus pyriformis*
Katalept, trilete leptoma, thin	19 µm (ø)	*Dicranella palustris*
Katalept, poorly evident leptoma, gemmate	16 µm (ø)	*Dicranella varia*
Katalept, spherical or sub-spherical, nearly psilate	23x19 µm	*Polytrichum alpinum*
Katalept, spherical or sub-spherical, rugulate, very thick	15x14 µm	*Polytrichum longisetum*
Katalept-cryptic, spherical, nearly psilate	7-10 µm (ø)	*Polytrichum sp.*
Katalept, spherical, nearly psilate	10.5x8.5 µm	*Voitia nivalis*
Katalept-fine, spherical, nearly psilate	10.5x8.5 µm	*Splachnum sp.*
Katalept, spherical or sub-triangular, nearly psilate	12-14 µm (ø)	*Bryum sp.*
Atreme, ellipsoidal Cyperaceae-like but with fine reticulum	20x15 µm	*Gymnocolea inflate*
Atreme, ellipsoidal Cyperaceae-like but with evident processes	16x13 µm	*Orthodontium gracile*

Table 1c: morphological guide to spores ø < 20 µm.

APPENDIX B – PALYNOLOGICAL TABLES

Masi Torello (FE), core EM2

Family	Latin name	Groups	38.35	35.90	28.10	25.80	25.23	24.75	24.15	23.15	22.95	22.78	22.54	21.36	20.94	20.67	20.35	20.06	19.61	18.75	17.50	16.55	16.40	15.29	14.93	13.87	13.34	13.15	12.66	11.46	11.05	10.41	9.50	7.92	7.07	6.39	4.25	3.23	2.45	0.75
CHRONOLOGY						12950±130		11455±195			9335±135				8285±55							7965±35		7900±40	7520±35		7675±85		5395±80				5170±85				3280±200	1085±100		
SAMPLES			43	40	39	38	37	36	35	34	33	32	31	29	28	27	26	25	24	44	23	22	21	20	19	18	17	16	15	13	12	11	9	8	7	6	4	3	2	1
	WOODY TAXA	T+sh																																							
ADOXACEAE	*Sambucus nigra*	sh, DT				0.69				1.89												0.91										0.29								
	Sambucus cf. racemosa	sh, DT																						0.53																
BETULACEAE	*Alnus cf. glutinosa*	T, H				0.31		0.31	0.27	0.32	0.66	4.74	11.57	18.38	11.81	5.00	9.37	7.99	4.33	8.09	11.82	13.74	5.07	6.58	12.67	2.07	15.22	10.85	4.80	11.36	25.41	12.28	24.55	26.32	8.66	34.19	11.50	12.12		0.37
	Alnus cf. incana	T, Mt													2.49	9.07	4.67	3.02	6.71	5.67	1.62			3.62	4.33			4.35	4.69	1.77		2.63	3.64	4.74	0.36		0.64			
	Alnus cf. viridis	sh, Mt						5.10					0.33		0.62	6.59	3.67	2.42	3.51	0.67	1.29			0.99	0.67			0.31	4.40		0.25				3.03	3.68				
	Alnus sp.	T, H		6.60		5.21	0.96		0.97					2.18	19.78	6.00	1.81	5.75	6.15						0.31			2.05							5.79	1.81	1.94	0.64	2.02	1.12
	Betula	T, Mt				1.39		0.64	0.31			0.95			0.31	1.10	1.33	0.32	0.67	0.32		1.28	0.53	1.32	1.33			0.25			0.82									
	Carpinus betulus	T, Q									0.33				0.55	0.33	0.60		1.00			0.66		2.00	0.26	4.35	0.29									4.74			3.51	2.02
	Corylus avellana	sh, Q	1.00	7.92	10.87			0.62	0.54	1.29	13.29	14.22	3.36	3.12	3.85	9.67	3.02	8.63	4.33	3.88	3.33	13.74		5.59	3.00	0.26	5.90	10.26	4.00	6.06	4.10	0.88	14.55	0.26	8.39	0.64				
	Ostrya carpinifolia /C. orientalis	T, Q		0.99		3.13	0.31		0.92			3.65	7.11	2.61	0.31	2.75	1.33	4.23	1.00	0.32				1.33	1.32	3.00	0.78	3.11	5.57	0.80	3.28	0.82	7.89	3.64	0.53	0.36	2.58			
	Betulaceae undiff.	T, DT	1.33		2.17	1.04	0.63		1.23	1.62	0.32	5.32	5.69	6.34		1.92	0.67	0.60		2.00			0.30					4.93	3.67				8.70	2.05				1.94	0.32	
CANNABACEAE	*Humulus lupulus*	sh, DT				0.69					0.32												0.64					0.26												
	Celtis australis	T, DT																																						
CISTACEAE	*Helianthemum*	sh, M				0.31			0.92	0.27	0.32				0.37							0.32	0.67					9.58	0.66						0.25					
EPHEDRACEAE	*Ephedra fragilis cf.*	sh		3.63		0.35	0.63			0.54				2.99						2.33		0.32	0.30					0.99					0.93				0.88	0.26		1.01
ERICACEAE	*Erica arborea type*	sh, M						0.96								0.27	0.33		0.32			0.65	0.30									0.26	0.62					0.26		
	Rhododendron cf.	sh																															0.31							
	Ericaceae undiff.	sh												0.31									0.64					0.64						0.25			0.30	0.36		
FAGACEAE	*Castanea sativa*	T, Mt				0.69	0.94	0.96	0.92	0.27	0.32	0.33			2.49	2.20	1.00			0.64		1.29							1.29		0.59	1.60				0.88			0.79	0.75
	Fagus sylvatica	T, Mt														2.20	1.67	2.42																	0.88				1.44	
	Quercus cf. cerris	T, Q					0.31												7.99		0.97										0.62		2.05				0.88			
	Quercus ilex type	T, M	1.33			0.35	4.70	0.64	8.92	8.09	10.00	24.58	26.54	7.09	8.72	7.42	4.67	4.23	9.90	2.33	4.53	6.97	7.67	4.53	10.20	5.00	1.55	9.01	6.74	6.40	9.60	3.28	11.40	5.15	8.95	3.25	3.87	1.60	13.13	1.49
	Quercus cf. pubescens	T, Q					0.63	0.64	0.31	0.27	1.29	3.32	0.95	0.75	0.62	1.37	1.00	1.81	0.64	0.67	0.97	0.91	0.33				1.24	1.47		0.76	1.64	2.63		1.84	1.01		1.29		
	Quercus cf. robur	T, Q				0.35					0.65	2.66	0.95	0.75	0.31	1.92	2.00	0.32	0.61	0.32	0.27	0.99	1.33	0.26	0.31						0.51	0.82		0.30	2.11	0.36	0.65	1.28	5.05	0.37
	Quercus sp.	T, Q	0.67			1.04	0.94		2.15	1.08	1.61	4.65	0.47		0.82	2.33	4.23	0.96	2.00	0.97			0.33	0.67				0.31	1.47	2.40			7.89	0.61	0.26			0.65	0.96	2.02	0.37
JUGLANDACEAE	*Carya*	T, DT	0.33	1.65																																				
	Engelhardtia	T, DT	1.67	0.33																																				
	Pterocarya	T, DT	0.33	1.65																																				
	Juglandaceae undiff.	T, DT		0.99																																				
LAMIACEAE	*Origanum*	sh	0.33												0.62																									
LAURACEAE	*Laurus nobilis*	sh	0.33																																					
MALVACEAE	*Tilia cordata type*	T, Q		6.27		0.35	0.31	0.32	0.31	0.27	0.65	0.33		1.12	0.62	1.92	2.33	1.21	2.88	6.67	3.88	0.30	3.19	0.27	0.33			3.67	0.26	1.24	3.23		0.25		0.88	0.30	0.26		0.65	0.37
	Tilia platyphyllos type	T, Q										0.33		0.75	0.31					2.33								1.33		0.31	0.29									
MORACEAE	*Ficus carica*	T, DT																																		0.76				
	Morus alba	T, DT																																						
OLEACEAE	*Fraxinus excelsior type*	T, Q																	0.60										1.47											
	Fraxinus ornus type	T, Q						0.63											0.60														0.59			0.88				
	Fraxinus cf. oxycarpa	T, Q													0.82			0.33				0.30		0.27								1.60								
	Fraxinus sp.	T, Q							0.32	0.31					1.10																									
PINACEAE	*Abies alba*	T, Mt									3.87	1.99						3.19	7.00			0.91				0.33			0.31				3.23				0.91			
	Picea abies	T, Mt									1.29	1.33			0.82			1.92	0.33	0.32	0.61	1.28						0.26			1.76								0.32	2.02
	Pinus cf. halepensis	T, M															0.32																							
	Pinus cf. mugo	sh, Mt	5.67	0.33		5.90	0.63	1.59	1.23	3.77	2.90	0.33				0.27	0.33	1.21	0.96	1.00	0.97		0.64			0.99	9.33	0.52	0.93	1.47		2.27		1.75	0.91	0.79			1.01	2.99
	Pinus cf. nigra	T, M																							0.33				0.29											
	Pinus cf. pinea	T, M																																						
	Pinus cf. sylvestris	T, Mt				0.69														1.21	0.32														0.82					
	Pinus sp.	T, Mt	5.00	7.92		2.78	3.45	0.64	4.92	6.74	3.87	0.66		1.12		1.37	1.33	3.02	2.88	6.33	9.39	0.61	0.96	0.27	0.33			6.00	0.26	1.24	4.11		1.26		9.65	0.91	0.26			5.60
	Pinaceae undiff.	T, Mt									3.23	0.33				0.27		0.60		0.97									2.05			0.82	0.88	1.21			0.65		3.03	1.87
RHAMNACEAE	*Rhamnaceae undiff.*	sh, Q																0.32		0.65																				
ROSACEAE	*Crataegus cf. oxyacantha*	sh, DT																										1.21												
	Prunus	T, DT																		0.33																				
	Rosa cf. canina	sh, DT																																		0.88				
SALICACEAE	*Populus*	T, H						1.23	0.81	0.32												0.64	0.67	0.32	4.24	4.79	2.13	0.99		1.03		1.47	2.40		0.82		0.72		1.01	2.24
	Salix	T, H	1.00			2.08	1.57	5.10	1.54	2.16	1.29	1.66	0.95	4.10	2.49	1.37	4.67	3.63	0.64	2.67	2.27	15.15	1.60	2.67	1.64	1.33	0.78	1.24	1.47	0.80	2.27	0.82	2.63		4.47	0.36	9.03	2.24	5.05	0.37
SAPINDACEAE	*Acer campestre type*	T, Q				0.35										0.27				0.64																				
ULMACEAE	*Ulmus minor*	T, Q				0.35	1.57	0.64		0.54	1.61	1.00	8.53	1.49	3.43	1.92	2.33	2.42	7.03	4.00	0.97	5.15	4.47	1.87	1.32	3.33	0.78	2.48	1.47	1.60	2.27	0.82		0.61	1.05	0.36	2.58	0.32		1.12

Table 1a: arboreal pollen percentages of EM2 dataset.

Masi Torello (FE), core EM2

Family	Latin name	Groups	43	40	39	38	37	36	35	34	33	32	31	29	28	27	26	25	24	44	23	22	21	20	19	18	17	16	15	13	12	11	9	8	7	6	4	3	2	1
CHRONOLOGY						12950±130		11455±195			9335±135				8285±55								7965±35		7900±40	7520±35		7675±85			5395±80			5170±85				3280±200		1085±100		
DEPTH (m)			38.35	35.90	28.10	25.80	25.23	24.75	24.15	23.15	22.95	22.78	22.54	21.36	20.94	20.67	20.35	20.06	19.61	18.75	17.50	16.55	16.40	15.29	14.93	13.87	13.34	13.15	12.66	11.46	11.05	10.41	9.50	7.92	7.07	6.39	4.25	3.23	2.45	0.75
SAMPLES			43	40	39	38	37	36	35	34	33	32	31	29	28	27	26	25	24	44	23	22	21	20	19	18	17	16	15	13	12	11	9	8	7	6	4	3	2	1
	HERBACEOUS TAXA	*E*																																						
ALISMATACEAE	*Sagittaria sagittifolia* type	hel					0.31															0.30																		
AMARANTHACEAE	*Beta vulgaris* type	cc, hal	0.33			0.63	0.96	1.23	0.27			0.47	0.37	0.31			0.60								0.59			0.25									0.53	1.08		4.10
	Chenopodium	As	1.00			0.63	4.46	0.31	0.54					0.37		0.67			0.33									0.25						0.88	0.30			1.81	1.01	6.72
	Chenopodiaceae undiff.	As	2.67	0.99		1.04	1.57	0.96		0.27	0.32	1.66						0.33											0.31							0.30			1.01	1.49
AMARYLLIDACEAE	*Allium* type								0.92	0.81	1.94			0.31		1.33	0.60					0.30		0.80																
APIACEAE	*Ammi* cf. *visnaga*	As						3.50																																
	Bupleurum falcatum type							4.46																																
	Falcaria vulgaris type	pm			0.69																																			
	Apiaceae undiff.		1.00	5.94		6.60	5.33	9.87	2.15	1.35		0.33		0.37		0.82			1.92			0.32		1.28	0.27	0.33		0.62	0.29	1.26	0.82		0.61	0.53		1.08		0.96	2.02	2.61
ARACEAE	*Acorus calamus*	hyd									0.32				0.31	0.27						0.61		0.53	0.66		2.58													0.37
	Arum cf.										0.30															0.52			0.80											
	Lemna	hyd	0.33							0.65				0.37					0.32		0.33	0.32						0.62	0.80	0.51						0.30	0.26	0.96	1.01	1.49
ARISTOLOCHIACEAE	*Aristolochia clematis* type	As	0.33																																					
ASPARAGACEAE	*Asparagus* cf.								0.66										0.64																					
	Scilla type									0.65																														
ASTERACEAE	*Artemisia*	Mt, hal		1.32		2.43	3.13	3.18	1.23	1.08	2.26	1.00	0.47	0.37		0.55	0.67	0.60			0.33	0.32		0.96	0.80	0.99	0.67	0.52	1.55	0.59	2.40	1.01	1.64		0.91		0.36	1.29	0.64	0.75
	Aster tripolium type	As																																						
	Bellis cf. *perennis*	As	0.33	0.99		0.69	0.31	0.64		0.54					1.33	1.21					0.30	0.32		0.66					0.29		1.01								1.44	
	Centaurea nigra type	As	0.67	2.97	2.17	1.04				0.33												1.00			0.31						0.51									
	Tussilago farfara type	As	1.33				0.31		0.27				0.75																											
	Asteroideae undiff.	pm	3.67	3.63	4.35	4.51	1.57	0.32	0.62	0.81	1.29		0.47	2.61				0.32	0.33			1.62		0.32	0.99	0.33	1.03	1.86	0.29	0.80	3.28	1.64	0.61	1.05		0.65			2.02	3.36
	Sonchus cf. *oleraceus*	As																0.33																						
	Cichorioideae undiff.	pm	4.33	9.90	10.87	3.47	2.82	1.27	1.23	5.66	1.61		0.47	2.24	0.62			0.33	1.21			1.67	1.29		0.99	4.00		0.93	0.59		2.02	0.82	0.88	0.91	1.58	1.08			2.02	31.72
BORAGINACEAE	*Myosotis arvensis* type																																			0.79				
	Symphytum officinale type																																							
	Boraginaceae undiff.						0.31																																	
BRASSICACEAE	*Hornungia* type		0.33				1.57		0.92	0.27	0.32	0.33	1.42	0.75			0.27		0.60			0.32		0.53	0.66			0.31			0.51		1.21	1.32	1.44			0.32		1.87
	Sinapis type					0.94		1.85	1.89	9.68	1.00	0.95	1.12	0.62	0.27				2.88			2.12	0.96	1.07	1.64		0.26	0.31		0.76			0.91	4.47	1.08		0.65	0.64	1.01	1.87
	Brassicaceae undiff.							0.32		0.54											2.27			0.66				0.31									0.26			0.37
BUTOMACEAE	*Butomus umbellatus*	hel					0.31		0.92		0.97								0.64		0.33			0.32				0.26	0.62	0.29			0.25			0.30	0.26			0.36
CALLITRICHACEAE	*Callitriche* sp.	hyd			0.69																																			
	Callitriche obtusangula	hyd					0.31			0.27	2.26	0.33		0.31			0.60					0.30		0.32	1.60	0.33	0.67	0.26	0.31				0.25		0.88		0.26			0.37
	Callitriche stagnalis	hyd				0.35	1.25		0.31	0.81			1.66	0.47		0.75		1.65	0.67		0.60	0.91	0.64	5.33	1.32	1.00	4.65	0.62		0.76			0.91	0.26	1.44		1.28	1.01		
CAMPANULACEAE	*Campanula* type				0.35																																			
CANNABACEAE	*Cannabis sativa*	As																				0.96	1.07																0.72	
	Cannabaceae undiff.	As																				0.27																		
CAPRIFOLIACEAE	*Scabiosa columbaria* type		0.67																																					
CARYOPHYLLACEAE	*Corrigiola litoralis*	hal					0.31				0.65				0.93										0.33												0.30			
	Corrigiola thelephiifolia	hal						0.31																	0.33				0.31	0.29										
	Paronychia echinulata type						2.19		1.23	0.81									0.67						0.33	0.67														
	Spergula arvensis type	As	0.33		2.08		3.13	7.01	6.15	0.54			1.66	1.90	1.87			1.10				1.28	1.33	5.83	1.21	0.32	2.40	2.96	2.00	2.33	3.42	1.17								
	Caryophyllaceae undiff.		2.00				2.19		0.31	4.31	0.97	0.33	1.42	0.37	1.56							0.67		1.00				0.62					0.76			0.30	0.26			0.36
CRASSULACEAE	*Crassula*							0.32																																
	Sedum type						0.63								0.62							0.61	0.32			0.67					1.52									
CYPERACEAE	*Carex* type	hyg						0.32		0.27	0.97				1.56								1.07																	
	Cladium mariscus	hyg																			0.33																			
	Cyperus	hyg					0.31		1.54	2.43				0.37								0.66	3.33	1.03	1.86		2.40	2.02			0.61	1.05		1.08						
	Eleocharis cf.	hel																												1.26									
	Scirpus maritimus	hel																			0.33															0.36				
	Cyperaceae undiff.	hyg	17.67	1.65		5.90	7.21	1.27	16.92	13.21	5.16	2.99	1.42	0.37	2.49	0.82	4.33	8.46	0.96	11.67	6.15	2.12	0.64	1.33	1.64	1.67	6.20	0.62		11.20	1.01	0.82	10.53	0.91	0.79	0.36	3.23	2.88	3.03	1.12
EUPHORBIACEAE	*Euphorbia*																												0.99											
	Mercurialis	As																																			1.29			
	Euphorbiaceae undiff.																																						0.72	
FABACEAE	*Astragalus danicus* type	pm														0.27						0.27																		
	Lotus type					0.69	0.63	1.27		0.54				0.31	0.27	0.33									1.32	1.33												2.89		0.37
	Trifolium cf. *hybridum*	pm												0.75								0.53		0.99	0.67															
	Trifolium cf. *repens*	pm							0.62																															
	Vicia sp.	pm			0.35									0.31																										
	Fabaceae undiff.	pm	1.33	0.99		1.04	0.63	3.50	0.62	0.81			1.90	1.12	0.31				0.33			0.32				0.91			0.67				0.91	0.53				1.81		1.49
GERANIACEAE	Geraniaceae undiff.	As								0.27																														
HIPPURIDACEAE	*Hippuris vulgaris*	hyd																								0.91														
HYDROCHARITACEAE	*Hydrocharis morsus-ranae*	hyd					0.31		1.85	1.08											0.33								0.67			0.88								
HYPERICACEAE	*Hypericum perforatum* type			2.31	2.17	0.35	0.63	1.91																		0.67							0.59								
JUNCACEAE	*Juncus* cf. *conglomeratus*	hel													0.31										7.75						5.60	1.01								
	Luzula campestris	pm					0.31							0.37																			0.91	0.53				0.32		1.01
	Juncaceae undiff.		0.33				0.31		1.54	0.54			0.47	0.37			0.60		1.00							0.31			0.29			0.88	0.91	0.53			0.65	0.32		0.75

Table 1b: herbaceous pollen percentages (Alismataceae – Juncaceae) of EM2 dataset.

Masi Torello (FE), core EM2

Family	Latin name	Groups	43	40	39	38	37	36	35	34	33	32	31	29	28	27	26	25	24	44	23	22	21	20	19	18	17	16	15	13	12	11	9	8	7	6	4	3	2	1
CHRONOLOGY						12950±130		11455±195			9335±135				8285±55							7965±35		7900±40	7520±35		7675±85				5395±80			5170±85			3280±200		1085±100		
DEPTH (m)			38.35	35.90	28.10	25.80	25.23	24.75	24.15	23.15	22.95	22.78	22.54	21.36	20.94	20.67	20.35	20.06	19.61	18.75	17.50	16.55	16.40	15.29	14.93	13.87	13.34	13.15	12.66	11.46	11.05	10.41	9.50	7.92	7.07	6.39	4.25	3.23	2.45	0.75
SAMPLES			43	40	39	38	37	36	35	34	33	32	31	29	28	27	26	25	24	44	23	22	21	20	19	18	17	16	15	13	12	11	9	8	7	6	4	3	2	1
HERBACEOUS TAXA		*E*																																							
LAMIACEAE	*Lamium amplexicaule* type	As																							0.33																
	Mentha type									0.27	0.33															0.33									0.76						
	Thymus type	pm														0.27																									
	Lamiaceae undiff.				0.33			0.31			0.66											0.33						0.33													
MENYANTHACEAE	*Menyanthes trifolia*	hyd																																						0.36	
NYMPHAEACEAE	*Nymphaea* cf. *alba*	hyd								2.26	2.33		1.12	0.62	0.27	0.33	0.60		4.00						1.29						0.80	0.25	0.88	0.61	0.53					
	Nuphar lutea	hyd							0.54										0.67														0.88							
	Nymphaeaceae undiff.	hyd			0.69																														0.53					
PAPAVERACEAE	*Papaver argemone* type	As								0.54																														
	Papaver rhoeas type	As													0.31				1.28						0.53	0.99														
	Papaveraceae undiff.	As	1.00								0.32														0.33						0.80	1.26			0.30					
PLANTAGINACEAE	*Linaria* type	As																						0.30							0.25						1.08			
	Plantago sp.	As																													0.82									
	Plantaginaceae undiff.	As		0.99									0.47											0.32																
PLUMBAGINACEAE	Plumbaginaceae undiff.																				0.32																			
POACEAE	*"Avena-Triticum"* group	cc, pm																																			0.26			
	"Hordeum" group	cc, pm		0.99	2.17	1.39	0.31		0.62		0.33				0.62		0.60				0.33			3.19	0.53	0.66	0.33	1.81	0.62			0.51	0.88		0.79		0.65	1.60	1.01	2.61
	Poaceae spontaneous group	pm	32.33	15.51	32.61	25.69	30.72	17.83	23.08	20.22	11.94	7.97	11.85	30.22	24.61	7.14	28.33	24.77	7.35	10.33	18.45	18.18	8.95	37.33	28.95	11.00	49.10	16.46	13.78	37.60	30.30	38.52	12.28	19.09	8.68	45.85	10.97	36.10	25.25	11.57
POLYGONACEAE	*Polygonum aviculare* group	As					0.31																																	1.12
	Polygonum persicaria group	As	0.67						0.31		0.66					0.67																	0.91					0.26		0.75
	Rumex acetosa type	As		0.33							0.33																	0.59												
	Polygonaceae undiff.	As																0.32			0.32																	0.64	1.01	
POTAMOGETONACEAE	*Potamogeton* type	hyd	1.00							1.35	0.32		0.47	1.87				0.60							1.60	0.33	0.33					0.25						0.72		
PRIMULACEAE	*Anagallis* cf. *arvensis*	As																																			0.61			
	Androsace elongata type	Mt					0.31																																	
	Cyclamen hederifolium type							1.59																																
	Lysimachia vulgaris type	hyg															0.31																							
	Primulaceae undiff.		0.33			0.69			0.32													0.32		0.32													0.30			
RANUNCULACEAE	*Aconitum napellus* type		0.67																																		1.44			
	Caltha palustris type	hyg						1.27																																
	Aquilegia cf. *vulgaris*	pm																	1.28					0.91																
	Ranunculus sp.				0.35										0.31	0.27								3.94																
	Ranunculaceae undiff.		2.33	0.33		1.04	0.31	2.23		0.54	1.29	3.65	0.47		0.62	0.27	0.67								1.21			0.33		0.26							0.26	1.29	1.01	0.37
ROSACEAE	*Dryas octopetala*	Mt				0.35	0.94			0.32																														
	Rosaceae undiff.		0.67	5.61		0.35			0.31	0.27						0.37			0.33							0.33		0.31					0.88							
RUBIACEAE	*Galium* type		0.67	1.65	6.52	0.69	0.94	4.46	0.31	0.27	0.32	0.66						0.32	0.67		0.32							0.52				0.82		0.61		0.65				
	Rubiaceae undiff.				2.17			0.32										0.64														0.88		0.61					1.01	
SAXIFRAGACEAE	*Saxifraga granulata* type						0.94																																	
	Saxifraga stellaris type	Mt				0.35	0.63	0.32										0.32																						
	Saxifragaceae undiff.	Mt				1.39																				0.33														
SCROPHULARIACEAE	*Scrophularia* type																													0.26										
	Verbascum cf.	As									0.32				1.25									0.32	1.33				0.26										1.01	
	Scrophulariaceae undiff.					0.94									0.62							1.29	0.30	6.39	2.67					0.80						0.61		0.36	1.94	0.37
SMILACACEAE	*Smilax aspera*		0.33			0.94				0.27	2.90	0.33			0.31	0.27			1.00						0.27		0.33					0.80		0.61		0.72			0.37
TOFIELDIACEAE	*Tofieldia calyculata*	hyg																							0.52				0.80											
TYPHACEAE	*Sparganium emersum* type	hyd	1.33		2.19			1.23		3.23	1.94	0.66	1.42	0.75	4.05	1.37	2.67	2.42				5.33	1.64	1.33	5.43	0.62			1.60	1.01	4.10			1.52	2.63	2.89	1.29	15.34	1.01
	Sparganium erectum type	hel			1.57			1.54	1.35	0.97			0.47	3.73	4.36	0.55	0.67	1.21							2.30		0.26	0.93	0.80	0.76	4.10				1.58	3.25	1.29	8.31	2.02
	Sparganium sp.	hel					0.31																													0.26			
	Typha latifolia	hel	0.33		0.31				0.31	0.54	3.23	0.33	0.47		1.25	1.10	0.33				0.33												0.91	0.26	1.08	0.65	3.51		0.37
	Typha minima	hel			0.31				0.31		3.55			0.37	0.31		0.33				0.61														0.30	0.36			0.37
	Typhaceae undiff.	hel									1.61																		1.24								1.29		
URTICACEAE	*Parietaria*	As						3.18		0.32								0.32				1.29	0.30	2.56	5.60	0.33	0.33	0.26	0.31			0.82				0.36	0.65		0.37
	Urtica atrovirens	As													0.31																	0.82							
	Urtica dioica type	As	0.33	5.28	23.91	7.29		2.87	0.62		0.32		0.95		0.37	0.31	0.27	0.33			0.64	2.91	1.21	2.56	1.33			0.52		0.25	1.64		0.30			1.08	0.64		0.37
	Urtica membranacea	As					0.94			0.54			1.12												0.66															
	Urtica pilulifera type	As												0.37	0.31																									
	Urticaceae undiff.	As	0.33					2.23	0.92	0.54	1.29	2.33	0.47		1.25				0.64		0.33	4.53			1.60		0.33	0.52			2.40		0.82			2.17	0.65	0.32	1.01	0.75
XANTORRHOEACEAE	*Simethis mattiazzi*	pm				0.31				0.27	0.32																									0.80	0.65			
UNDETERMINABLE GRAINS			9.09	6.77	14.81	5.26	9.38	6.27	9.72	13.11	8.55	7.38	4.52	9.76	1.83	3.96	5.36	3.50	4.57	4.46	6.36	2.08	1.57	2.60	8.43	7.98	3.25	5.57	5.87	2.34	6.16	2.40	9.52		7.99	6.10	4.32	2.80	9.17	3.94
PTERIDOPHYTES																																								
ASPLENIACEAE	*Asplenium adiantum nigrum*	P (hyg)														0.33	1.17																			0.80				
	Asplenium petrarchae	P (hyg)																								0.28													
	Asplenium trichomanes	P (hyg)																															0.22						
	Asplenium indiff.	P (hyg)																											0.56										
ATHYRIACEAE	*Cystopteris fragilis*	P (hyg)													9.11	0.66																				9.51				
DRYOPTERIDACEAE	*Dryopteris filix-mas*	P (hyg)																	0.58								1.56	0.31												
EQUISETACEAE	*Equisetum*	P (hyg)									0.31													0.87					0.50								0.50			
HYPOLEPIDACEAE	*Pteridium aquilinum*	P (hyg)	0.25											0.70					0.62							0.62	0.56	0.29					0.22							
ISOETACEAE	*Isoetes durieui*	P (hel)									0.35				0.80				1.88							0.31				1.32										
	Isoetes sp.	P (hel)							0.30					1.05	3.83				0.62							0.62	5.04		1.45	0.53	1.33						2.24	2.28	0.94	1.40
	Isoetes hystrix	P (hel)													2.08			0.58									0.84										0.21			
	Isoetes lacustris	P (hyd)													1.12						0.29																	1.44		
MARSILEACEAE	*Marsilea quadrifolia*	P (hel, hyd)																																		0.44	5.56		1.89	
OPHIOGLOSSACEAE	*Botrychium*	P (hyg)																												1.33					0.25			2.15		
POLYPODIACEAE	*Polypodium vulgare* type	P (hyg)		0.33				0.94					0.45		0.90							1.23	4.93		0.94	0.52				1.24			0.53	7.97			1.03			
SELAGINELLACEAE	*Selaginella*	P (hyg)																											1.40											
THELYPTERIDACEAE	*Thelypteris palustris*	P (hyg)																											0.28											
FILICALES MONOLETE		P (hyg)	24.31	0.98	2.13	0.34	1.23		1.50	1.30	2.18	3.76	2.71	2.10	2.41	33.23	1.64	2.92			4.92	2.61		0.31		3.70	5.04	1.74	3.48	7.11		7.96	24.69	6.40			34.77	1.27	56.01	1.89	3.51
FILICALES TRILETE		P (hyg)	0.25			0.69	0.92	0.63	0.60	2.08	0.93	1.88	1.36	2.10							0.80			0.31	1.16	0.30		0.26	0.93	2.80	0.50	1.45	0.79	1.45	1.11		2.40		2.49		1.89	1.05
TOTAL			24.81	1.30	2.13	1.03	2.15	1.57	2.40	3.39	3.43	5.64	4.52	6.29	3.31	41.85	1.64	3.50	1.88		7.69	10.43	0.30	1.57	2.34	6.17	15.97	3.97	6.67	10.26	9.42	12.39	24.69	8.80		5.47	43.00	1.27	60.43	6.60	5.96

Table 1c: herbaceous pollen percentages (Lamiaceae – Xantorrhoeaceae; Pteridophytes) of EM2 dataset.

Masi Torello (FE), core EM2

Family	Latin name	Groups	38.35	35.90	28.10	25.80	25.23	24.75	24.15	23.15	22.95	22.78	22.54	21.36	20.94	20.67	20.35	20.06	19.61	18.75	17.50	16.55	16.40	15.29	14.93	13.87	13.34	13.15	12.66	11.46	11.05	10.41	9.50	7.92	7.07	6.39	4.25	3.23	2.45	0.75
CHRONOLOGY ±100						12950±130		11455±195			9335±135				8285±55						7965±35		7900±40	7520±35		7675±85				5395±80		5170±85			3280±200		1085±100		
DEPTH (m)			38.35	35.90	28.10	25.80	25.23	24.75	24.15	23.15	22.95	22.78	22.54	21.36	20.94	20.67	20.35	20.06	19.61	18.75	17.50	16.55	16.40	15.29	14.93	13.87	13.34	13.15	12.66	11.46	11.05	10.41	9.50	7.92	7.07	6.39	4.25	3.23	2.45	0.75
SAMPLES			43	40	39	38	37	36	35	34	33	32	31	29	28	27	26	25	24	44	23	22	21	20	19	18	17	16	15	13	12	11	9	8	7	6	4	3	2	1
ALIA																																								
Pseudoschizaea circula											0.64	0.33			0.31				0.60	0.32	0.66	0.32		0.63	1.83	0.33	0.66	1.02	0.31	0.87		0.25		0.87	1.20	0.26	0.72	1.27		1.98	27.37
HYSTRICOSPHAERIDIA				2.57																		0.32																		
SECONDARY GRAINS																																								
	Abies alba										1.52																												
	Alnus sp.																																			0.32			0.37
	Asteroideae undiff.																	0.63																					
	Betulaceae undiff.		0.33								0.36																												
	Carya				3.77	0.33															0.95	0.58				0.32	0.32					0.79			1.56				
	Corylus avellana																																		1.56				
	Engelhardtia				2.61																4.34											0.92			0.78		0.32		
	Ephedra cf.																																					1.00	0.37
	Ericaceae undiff.																																		5.50				
	Filicales monolete									0.27				0.36														0.96							1.62		1.26		
	Filicales trilete						0.31				0.53		0.47	1.45							1.59				0.65	0.32		0.31	0.29				0.78		0.30		0.65		
	Juglandaceae undiff.				9.43	2.94					0.27								0.63	3.76															0.65			
	Picea excelsa										1.52																												
	Pinaceae undiff.										3.34																					0.58				0.89	0.97		
	Pinus sp.		1.64				0.62		0.31	0.53	0.91			1.09							2.22				0.65	2.56		0.31											0.37
	Pinus mugo																																		0.30				
	Poaceae undiff.						0.31																														0.97		
	Polypodiaceae undiff.																																				0.32		
	Pterocarya																			2.02																0.59			
	Quercus sp.																																			0.30			
	Rubiaceae undiff.																						0.32															
	Taxodium																																						
	Triatriopollenites						0.31																																
	Urticaceae undiff.																																				0.32		
	Zelkova						0.31																																
	Underterminable grains		4.59	3.96	16.98	3.92	8.05	5.41	2.15	4.24	1.82	0.33	4.25	2.90		0.27	2.33	1.21	6.03	9.52	14.16	0.61	5.11	0.27	3.88	6.07	0.52	6.12	3.49	0.79	0.25	2.34	1.75	3.86	0.53	6.47	17.09	2.52	21.00	11.11
	TOTAL		6.56	3.96	30.19	9.80	9.91	5.41	2.45	5.84	9.12	0.33	4.72	6.16	0.27	2.33	1.21	6.67	14.92	24.86	0.61	5.11	0.27	5.50	10.54	0.52	7.65	4.36	1.59	0.25	7.03	1.75	6.23	0.53	17.48	18.99	3.79	22.00	12.22
	SAMPLES		43	40	39	38	37	36	35	34	33	32	31	29	28	27	26	25	24	44	23	22	21	20	19	18	17	16	15	13	12	11	9	8	7	6	4	3	2	1
	AGE						13	11.5			9.3				8.3						8	7.9	7.5			7.6					5.4		5.2			3.3		1.1		
PLANT ECOLOGICAL GROUPS		FACIES	lev	fpl	f-ch	f-ch	crs	pdf	sw2p	sw2	sw1	sw2	pdf	sw2	sw1	sw2	sw2	sw2	crs	sw2	crs	sw2	crs	sw1	sw2	crs	sw1	sw2	crs	sw1	sw2	sw2	d-ch	d-ch	sw2	sw1	lev	sw1	fpl	fpl
WOODY		T++sh	19.00	38.28	13.04	27.43	17.55	17.83	26.46	29.11	36.45	67.11	71.09	44.40	47.35	81.87	56.00	54.68	77.32	61.33	51.78	53.94	67.41	24.00	44.08	63.33	10.85	63.35	75.95	27.20	43.69	41.80	69.30	62.12	67.37	18.41	69.68	24.92	50.51	19.03
TREES		T	17.33	26.73	2.17	25.69	16.61	11.78	24.92	25.88	34.52	53.49	56.87	37.69	42.68	71.15	41.00	46.83	64.22	53.33	44.98	47.88	42.81	19.47	35.86	59.67	10.08	55.28	61.00	23.20	36.87	37.70	66.67	44.24	62.89	17.69	61.29	24.28	49.49	19.03
SHRUBS		sh	1.67	11.55	10.87	1.74	0.94	6.05	1.54	3.23	1.94	13.62	14.22	6.72	4.67	10.71	15.00	7.85	13.10	8.00	6.80	6.06	24.60	4.53	8.22	3.67	0.78	8.07	14.96	4.00	6.82	4.10	2.63	17.88	4.47	0.72	8.39	0.64	1.01	
QUERCETUM		Q	1.67	15.18	10.87	5.56	4.39	1.27	4.92	2.70	7.10	29.57	32.23	10.82	8.72	15.38	19.33	18.73	30.99	24.33	12.94	10.61	24.60	8.27	10.86	18.33	2.58	19.88	26.39	10.40	13.38	8.20	21.93	20.00	11.05	1.44	16.77	6.71	10.10	2.24
MEDITERRANEANS		M	1.53			0.35	4.70	0.64	8.92	8.09	10.00	24.58	26.54	7.09	8.72	7.42	4.67	4.23	10.22	2.35	4.53	6.97	7.67	4.53	10.20	5.00	1.55	9.01	6.74	6.40	9.60	3.28	11.40	5.15	8.95	3.25	3.87	1.60	13.13	1.49
WOODY HYGROPHYTES		H	1.00	6.60		7.29	1.88	6.05	3.08	3.23	2.90	2.33	5.69	15.67	23.05	32.97	15.67	14.80	15.02	7.67	16.83	31.21	20.13	9.87	9.21	14.00	3.88	16.77	13.78	8.80	13.89	27.87	16.67	25.45	36.58	11.55	45.16	14.38	20.20	4.10
OTHER DECIDUOUS TREES		DT	3.67	4.62	2.17	2.43	0.63		1.23	3.50	0.65	5.32	5.69	6.34		1.92	0.67	0.60		2.33		2.42	0.64	0.53	4.93	3.67	0.26	8.70	2.35		0.76		1.94	0.32						
QUERCETUM + OTHER DT		Q+other DT	5.33	19.80	13.04	7.99	5.02	1.27	6.15	6.20	7.74	34.88	37.91	17.16	8.72	17.31	20.00	19.34	30.99	26.67	12.94	13.03	25.24	8.80	15.79	22.00	2.84	28.57	28.74	10.40	14.14	8.20	24.56	20.61	11.05	1.44	18.71	7.03	10.10	2.24
HERBS		E	81.00	61.72	86.96	72.57	82.45	82.17	73.54	70.89	63.55	32.89	28.91	55.60	52.65	18.13	44.00	45.32	22.68	38.67	48.22	46.06	32.59	76.00	55.92	36.67	89.15	36.65	24.05	72.80	56.31	58.20	30.70	37.88	32.63	81.59	30.32	75.08	49.49	80.97
HERBACEOUS HYGROPHYTES		hyg	17.67	1.65		5.90	7.52	2.87	18.46	15.90	6.13	2.99	1.42	0.75	4.36	0.82	4.33	8.46	0.96	11.67	6.15	2.12	0.64	2.40	2.63	5.33	7.24	2.48	3.52	15.20	3.28	0.82	10.53	1.52	2.89	1.44	3.87	3.19	3.03	1.87
HYDROPHYTES		hyd	2.67			1.74	4.08		3.38	7.28	7.74	4.98	2.37	4.85	5.30	3.57	3.67	4.83	0.32	5.73	0.96	14.40	4.28	14.21	2.17	0.88	3.20	3.03	4.10	2.63	3.33	4.47	1.52	3.16	5.42	1.29	17.57	3.03	2.24	
HELOPHYTES		hel	0.33				2.82		3.38	1.89	10.32	0.33	0.95	4.10	6.23	1.65	1.33	1.21	0.64	0.67		0.91	0.32		2.30	0.33	8.27	2.80	0.29	6.40	3.28	4.10		1.52	3.16	5.78	3.23	12.14	2.02	0.75
TOTAL HYGROPHYTES		Hyg	18.67	8.25		13.19	9.40	8.92	21.54	19.14	9.03	5.32	7.11	16.42	27.41	33.79	20.00	23.26	15.97	19.33	22.98	33.33	20.77	12.27	11.84	19.33	11.11	19.25	17.30	24.00	17.17	28.69	26.97	39.47	13.00	49.03	17.57	23.23	5.97	
TOTAL AQUATICS		Aq	3.00			1.74	6.90		6.77	9.16	18.06	5.32	3.32	8.96	11.53	5.22	5.00	6.04	0.96	6.00	0.32	3.64	1.28	14.40	6.58	4.33	22.48	4.97	1.17	9.60	6.31	8.20	2.63	4.85	7.63	11.19	4.52	29.71	5.05	2.99
PASTURE-MEADOW		pm	41.67	30.03	47.83	35.76	36.36	22.93	26.46	27.76	15.16	7.97	14.69	37.31	25.86	7.42	29.00	25.98	9.27	12.33	21.36	20.00	9.27	38.13	31.91	16.67	50.13	19.25	14.66	39.20	35.61	40.98	13.16	22.42	12.37	48.74	12.26	36.42	30.30	48.13
HALOPHYTES		hal	1.33	1.32		2.43	4.70	8.60	3.08	1.89	2.90	1.00	0.95	1.12	1.25	0.55	1.33	1.21		0.67	0.32		0.96	0.80	0.99	1.33	0.52	1.86	1.47	2.40	1.52	1.64	0.88	1.21	0.53	3.25	1.29	0.64	1.01	11.57
MONTANE TAXA		Mt	10.67	8.25		14.93	9.72	11.15	9.23	11.32	16.45	5.98	0.95	1.12	10.90	28.30	16.00	13.90	22.04	21.67	18.77	2.12	4.15	0.80	7.57	22.00	4.91	7.14	27.57	4.80	5.56	2.46	15.79	10.61	11.84	4.69	4.52	1.92	6.06	12.69
HERBACEOUS ANTHROPIC SPONTANEOUS		As	9.00	11.55	26.09	12.15	7.21	24.84	8.31	4.04	2.90	6.98	3.79	4.85	3.74	1.37	2.33	1.21	4.47	3.00	14.89	3.33	7.67	14.13	6.25	4.00	3.88	4.35	2.05	3.20	3.54	4.92	0.88	2.42	0.26	8.66	2.58	1.60	5.05	11.57
CULTIVATED		cc	0.33	0.99	2.17	1.39	0.94	0.96	1.85	0.27		0.33	0.47	0.37	0.93				1.21		0.33			3.19	0.53	0.66	0.33	1.81	0.62	0.59		0.76				1.58	1.08	0.65	1.60	6.72
ANTHROPIC INDICATORS		Ai	9.33	12.54	28.26	13.54	8.15	25.80	10.15	4.31	2.90	7.31	4.27	5.22	4.67	1.37	2.33	2.42	4.47	3.33	14.89	3.33	10.86	14.67	6.91	4.33	5.68	4.97	2.64	3.20	4.29	4.92	1.75	2.42	1.84	9.75	3.23	3.19	6.06	18.28
HYGROPHILOUS PTERIDOPHYTES		P (hyg)	24.81	1.30	2.13	1.03	2.15	1.57	2.10	3.39	3.43	5.64	4.52	4.90	3.31	4.33	2.30	3.50		7.08	9.57	0.30	1.26	2.34	5.56	10.92	3.97	5.22	8.42	9.42	20.35	24.69	8.80		3.23	35.80	1.27	58.15	3.77	4.56
AQUATIC PTERIDOPHYTES		P (aq)							0.30					1.40				7.83			1.88	0.62	0.87		0.31		0.62	5.88		1.45	1.84		1.77			2.24		7.20	2.28	2.83	1.40
COUNTED GRAINS																																								
TRACHEOPHYTA		S+P	399	307	47	291	326	319	333	384	321	319	221	286	322	626	305	343	319	325	345	331	318	384	324	357	403	345	380	138	452	162	375	330	402	486	157	791	106	285
SPERMATOPHYTA (pollen sum)		S	300	303	53	310	319	315	325	372	310	301	211	268	321	381	324	349	316	300	314	331	313	375	304	300	387	322	341	341	341	122	342	330	380	278	155	313	99	268
PTERIDOPHYTES		P	99	4	1	3	7	5	8	13	11	18	10	18	11	262	5	12	6	25	36	1	5	9	20	57	16	23	39	13	56	40	33		22	209	2	478	7	17
SECONDARY GRAINS			19	12	16	30	30	17	8	22	25	1	10	16		1	7	4	21	45	86	2	16	1	17	32	2	25	15	2	1	9	6	20	2	52	30	12	22	32
TRACHEOPHYTE TAXA		Total	48	32	12	50	61	45	56	60	58	49	35	47	52	53	43	44	48	54	53	44	45	46	57	58	47	54	47	32	60	29	33	47	53	50	34	34	36	47
ABSOLUTE POLLEN FREQUENCY (grains/g)																																								
APF TRACHEOPHYTA			73034	122978	349	14711	9381	45302	22898	13334	189972	93299	11398	13886	325405	100998	40613	11260	32423	7944	11777	61464	60501	251457	27332	15180	17776	80846	18007	669667	18482	27972	5182	30286	160651	391031	39929	1828062	8367	10619
APF SPERMATOPHYTA			54913	121376	394	15672	9179	44734	22348	12917	183462	88035	10882	13012	314624	61470	43143	11457	32118	7333	10719	61464	59550	245563	25645	12756	17070	75456	16159	1654757	13943	21065	4726	30286	151859	223676	39421	723367	7815	9985
APF PTERIDOPHYTES			18121	1602	7	152	201	710	550	451	6510	5265	516	874	10782	42271	666	394	610	611	1229	186	951	5894	1687	2424	706	5390	1848	63085	2290	6907	456		8792	168160	509	1104695	553	633
APF SECONDARY GRAINS			3478	4807	119	1517	863	2414	550	764	14795	292	516	777		161	932	131	2134	1100	2936	371	3044	655	1434	1361	88	5858	711	9705	41	1554	83	1836	799	41839	7630	27733	1737	1192

Table 1d: alia, secondary grains and plant ecological groups of EM2 dataset.

Pisa, Pianura Arno 1

Family	Latin name	Groups	25.3	25.18	24.95	24.47	24.13	23.82	23.48	23.15	22.83	22.05	21.8	21.32	19.15	18.67	18.45	17.97	17.8	17.25	16.9	16.35	15.35	14.35	13.35	12.35	11.35	10.35	9.5	8.25	7.45	6.7	6.6	5.97	5.5	5.25	5.1	4.9	4.3	3.75	1.9	0.85	0.5
CHRONOLOGY																					9826±130				7356±68								4682±160	3768±75									
SAMPLES			55	54	53	52	51	50	49	48	47	64	46	44	41	40	39	37	36	33	32	31	30	29	28	27	26	25	24	22	21	19	18	16	12	11	10	9	8	7	5	2	1
	WOODY TAXA	T+sh																																										
ADOXACEAE	*Sambucus* sp.	sh, DT						0.97																																			1.31
BETULACEAE	*Alnus* cf. *glutinosa*	T, H	0.78	0.49	1.33	2.74	3.79	6.80	2.32	1.69		3.57		4.11	1.00			0.70	2.30	6.58	11.11	2.33	8.26	5.32	3.55	13.91	7.99	8.56	5.76	10.97	5.56	5.81	2.78	1.69	2.75	5.15	1.59	2.34	2.07	1.52			
	Alnus cf. *incana*	T, Mt					0.63				1.60						1.40	1.97	0.31	3.70	2.33	2.75	0.35	4.84	2.63	4.44	4.11	3.64	9.03	1.75	3.23		0.34		0.69			0.67	0.69				
	Alnus cf. *viridis*	sh, M			1.33		0.32		1.93		2.24									0.66		1.23	2.75	0.35	5.81	0.38	1.18	1.37	5.45	4.19	0.29	1.94			0.34			0.34	1.67	0.76		0.95	
	Alnus sp.	T, H	0.78			0.44		3.09						1.00	2.08				0.99		0.31		2.75	3.90	3.23	4.89	2.37	0.68	0.91	1.94	3.51	2.58	0.31				2.14	0.34	0.63	0.67	0.34	4.55	1.90	1.58
	Betula	T, Mt				0.44		4.10	0.49	0.39							1.40								7.34	3.23		0.89	0.68	5.45								0.69	0.32					
	Carpinus betulus	T, Q							0.77	1.69	1.60		2.63							0.63					0.32		0.59			1.94	2.63	1.94	0.31					0.34	0.95	1.00	0.34			
	Corylus avellana	sh, Q	0.78	0.49	0.44	4.11	5.68	17.96	3.47	5.08	2.24		1.32			2.08		2.45	3.95	6.58	11.42	3.49	5.50	2.13	4.84	8.65	4.73	4.45	4.55	0.97	3.51	1.94						0.32	0.33	1.03	1.52	1.04		0.95
	Ostrya carpinifolia /C. orientalis	T, Q				2.74	2.52	5.83	2.32		4.17	3.57							0.66		1.25	0.93		2.75	1.06	2.58	1.13	3.25	1.71	0.91	2.90	0.29						0.69						
	Betulaceae undiff.	T, DT	0.78		1.77	1.37		0.97	2.70						2.08		4.20	1.32	0.31		2.33			1.42	0.97	1.88	1.18	2.05	0.91	0.65	0.88							0.34		0.33	0.69			0.26
CANNABACEAE	*Celtis australis*	T, DT					3.15		0.39		1.28									0.33			2.33	0.92							0.29													
	Humulus lupulus	sh, DT																	0.31				0.35		0.38													0.31		0.33				
CISTACEAE	*Helianthemum*	sh, M					0.32													0.66		0.63	0.93		0.97																			0.40
CORNACEAE	*Cornus mas*	T, Q					0.32																																					
EPHEDRACEAE	*Ephedra fragilis* cf.	sh, M	0.78			0.44	0.32				1.28				1.00								5.81		0.35					0.30	1.29				0.32	0.31					1.00			1.90
ERICACEAE	*Erica arborea* type	sh, M			1.37		6.94	7.77	7.72	22.03	17.95		2.63							0.66	1.88	3.40		0.92	0.71		0.32	0.38		1.13	0.89	1.71	0.61		0.97		0.34		0.34		0.34			2.61
FAGACEAE	*Castanea sativa*	T, Mt					0.95								4.00					0.33							0.32	0.38							0.32		0.32	0.33	0.69		0.78			
	Fagus sylvatica	T, Mt				0.44	1.37	0.63		0.39	1.69								0.99	0.31			0.35		0.38				2.73	5.16	11.70	1.94	0.31		0.69			0.33			1.52			
	Quercus cf. *cerris*	T, Q					1.37	0.32												0.33	1.57		3.49		1.06			0.89	0.68	0.91	1.94	1.17	0.32		0.68						0.26			
	Quercus ilex	T, M	0.78			3.10	4.11	13.88	16.99	8.11			11.22			2.08		1.40	6.58	6.58	8.02	9.30	8.26		11.29		1.13		9.25	8.79	10.00	8.77	2.26	2.78	3.72	1.22	2.06	5.08	2.68	0.69	4.55		2.86	0.40
	Quercus cf. *pubescens*	T, Q	0.78	1.95			5.36	0.97	2.32							2.08			0.99	2.82	4.01		2.48			1.13	0.59	1.03	1.21			1.17	0.97	1.23	0.34	0.92		0.34						0.79
	Quercus cf. *robur*	T, Q					0.63														0.62											1.75	0.65	0.62										
	Quercus sp.	T, Q	3.10	8.29	6.19	2.74	2.52	0.97	12.74	6.78	9.62	3.57		2.00	8.33	3.57		2.80	0.99	2.82		0.31	5.81	1.83	3.90	0.65	3.38	4.14	0.34	3.94	1.29	1.75	2.90		4.94	1.69	0.61	2.75	3.81	2.68	2.07	3.79	3.39	
JUGLANDACEAE	*Carya*	T, DT							1.93																																			
	Pterocarya	T, DT							1.16																																			
MALVACEAE	*Tilia cordata* type	T, Q							0.39									0.35	0.66	0.94	0.31			1.83	0.35	0.97	0.75	0.30	0.34					0.32	0.29					0.33		0.76	0.26	
	Tilia platyphyllos type	T, Q					0.32								1.00										0.35									0.32	0.32			0.33						
MORACEAE	*Morus alba*	T, DT			0.44				0.77																																			
MYRICACEAE	*Myrica*	sh, M																							0.29													0.34						
OLEACEAE	*Fraxinus* cf. *angustifolia*	T, Q					0.49																		0.88																			
	Fraxinus excelsior type	T, Q				2.74		0.97	0.39		2.24	3.57													2.75			0.68	0.30															
	Fraxinus ornus type	T, Q					1.37	3.40										0.35	0.33	0.31	0.62		0.92					0.65												0.76				
	Oleaceae undiff.	T, DT					1.37	0.49		3.39													1.83				1.03																	
	Olea europaea	T, M						2.43																																				
	Phillyrea	sh, M						1.94															0.92					0.34										0.34						
PINACEAE	*Abies alba*	T, Mt								3.53										0.66				1.83	0.35						0.88	0.32	0.31				0.34							
	Larix decidua	T, Mt															5.36						0.92																					
	Picea abies	T, Mt							1.54					2.74												0.30	0.68			0.88										0.78			
	Pinus cf. *cembra*	T, M																																			0.76			0.40
	Pinus cf. *halepensis*	T, M																					0.92																			
	Pinus cf. *mugo*	T, M				3.54	1.37	0.63		0.39		3.53	7.14							12.50	7.14	0.33		0.92			1.18	0.34										0.33	2.27		0.95	0.40	
	Pinus cf. *pinea*	T, M																										0.29															
	Pinus cf. *sylvestris*	T, Mt																										0.29															
	Pinus sp.	T, Mt	6.20	2.44	2.65	2.74	0.63		3.09	3.39	11.86	14.29	17.11	38.36	42.00	12.50	14.29	0.35	2.96	0.94	2.47		2.75	5.67	4.84	1.13	1.48	1.37	0.30	0.97	4.09	0.32	1.85		0.34	1.22	1.03	1.59	0.33	2.41	15.91	3.39	4.76	2.37
	Pinaceae undiff.	T, Mt	0.78	0.98			1.37	1.58	1.93			1.79			20.55	6.00	4.17			0.33	0.31											0.32	2.05					0.34	0.32	0.33	0.34			
RHAMNACEAE	*Rhamnus* type	sh, Q			0.44				0.39																																			
ROSACEAE	*Pyracantha coccinea*	sh, M						0.49																																				
SALICACEAE	*Populus*	T, H		0.49													3.57	0.35	0.33				0.97													0.31					3.09	0.95		
	Salix	T, H			1.95	12.33	1.89	4.37	5.79	1.69	4.49							1.05	2.30	1.57	1.23	3.49		2.84	1.94	2.63	0.89	2.40	2.12	4.19	3.80	5.16	23.15	23.31	59.63	10.31	3.49	5.35	2.41	1.52	2.09	2.86	0.79	
SAPINDACEAE	*Acer campestre* type	T, Q																					1.06		0.38		0.68										0.34						
ULMACEAE	*Ulmis glabra*	T, Q						1.94	4.25	5.08		5.26	2.00										0.92	1.77		0.75	1.78	0.68	0.91	1.29	0.58	0.32					0.34		0.33	0.69			
	Ulmus minor	T, Q	0.78		2.65	10.09	2.91	1.93	3.39	1.60		7.89		1.00	4.17			0.35	0.99	1.88	0.93			0.92		0.97			0.89	0.34	0.30	1.29	1.75	1.94	0.93	0.68			0.32	1.00	1.38			0.95
VITACEAE	*Vitis vinifera*	sh, DT																							0.29													0.34						

Table 2a: Arboreal pollen percentages of PA1 dataset.

Pisa, Pianura Arno 1

Family	Latin name	Groups	25.3	25.18	24.95	24.47	24.13	23.82	23.48	23.15	22.83	22.05	21.8	21.32	19.15	18.67	18.45	17.97	17.8	17.25	16.9	16.35	15.35	14.35	13.35	12.35	11.35	10.35	9.5	8.25	7.45	6.7	6.6	5.97	5.5	5.25	5.1	4.9	4.3	3.75	1.9	0.85	0.5
CHRONOLOGY																					9826±130				7356±68								4682±160		3768±75								
SAMPLES			55	54	53	52	51	50	49	48	47	64	46	44	41	40	39	37	36	33	32	31	30	29	28	27	26	25	24	22	21	19	18	16	12	11	10	9	8	7	5	2	1
HERBACEOUS TAXA		*E*																																									
AMARANTHACEAE	*Beta vulgaris* type	cc, hal	1.55		3.54	1.37	1.26	0.97		0.96		1.32						0.66			1.54		0.92	6.38	0.97	1.50	2.66	3.77	2.73	1.61						2.41	3.81	0.67	2.76	9.09	17.23	2.86	0.79
	Chenopodium	As			3.10	1.37	1.58	1.94							1.00				1.97					4.32		2.75	2.48	1.94	1.50	1.78			0.91	0.32	0.29	0.65	0.31		0.63	0.34	1.52	2.09	2.86	6.32
	Suaeda type	hal					0.32													0.62																							
	Chenopodiaceae undiff.	As																4.17	0.35			0.31	3.49		1.42		0.38	0.30		0.30	0.58						1.53				3.79		0.79
AMARYLLIDACEAE	*Allium* type																	0.70	0.99						0.65													0.69		0.76			
APIACEAE	Apiaceae undiff.		4.65	1.46	0.44		0.63	1.46	0.39						1.00			2.80	1.97	0.94	1.23				0.35	0.32	0.75		0.34		0.29					0.31	1.03		1.03		0.52	6.67	1.58
ARACEAE	*Arum* cf.			1.46														0.66		0.31						0.97																	
	Lemna	hyd							0.77			10.71																												0.34	0.34		
ASPARAGACEAE	*Asparagus* cf.																												0.32														
ASTERACEAE	*Artemisia*	Mt, hal			0.44	7.89	1.46	2.32	5.08		3.57						1.79	1.75	0.33		1.85		4.59	0.35	0.97	0.75	1.48	0.34	0.30	0.97	0.29	0.32					0.34	0.32	0.67		0.95	5.93
	Aster tripolium type	As			0.44												1.79					0.35			0.91	0.65		0.32									0.34	0.33	0.34			
	Bellis cf. *perennis*	As	1.55	0.98							3.57	3.95	2.00					5.36	5.94	1.32	5.02	0.62	1.16	0.92	0.71	1.94		0.38		1.71		0.32	0.58		0.93			0.92	1.03	0.95	0.76	0.78	
	Centaurea nigra type	As	0.78	0.49	0.44	1.37									1.00			3.15	0.66			0.31			0.92	0.35		0.30			0.29							0.76		0.95			
	Tussilago farfara type	As										2.08														0.30							0.58						0.69				
	Asteroideae undiff.	pm	3.88	2.44								1.79	11.84		5.00		3.57	4.20	0.33	1.88			3.49			0.30			0.30			0.32			1.01			0.67	1.03		2.61	1.90	1.98
	Cichorium intybus type	cc, As, pm																								0.61																	
	Sonchus cf. *oleraceus*	As																																								0.34	1.90
	Tragopogon pratensis ttype	pm																								0.30																	
	Cichorioideae undiff.	pm	2.33	0.98	15.93	6.85	2.52	1.16	5.08		3.57	2.63	2.74	3.00				1.75	2.30	1.88	0.93	8.14			0.71	0.65	0.75	0.30	0.34	2.42	0.32	1.75	2.26	0.93	0.31	0.34	0.32	1.34	6.90	6.06	11.49	22.86	17.79
BORAGINACEAE	*Cerinthe minor* type	As																														0.31	0.34										
BRASSICACEAE	*Hornungia* type				1.77	0.32		1.16		1.28								0.70	0.66						1.42		0.38	0.59	1.37		1.29	0.29	1.69				0.34	0.34		1.04	0.95	14.23
	Sinapis type				0.88	0.95						0.32			1.00							0.35					0.38	0.30					0.65	1.35				0.63			1.04	7.51
	Brassicaceae undiff.								0.39																		0.38					0.32									0.26	0.79
BUTOMACEAE	*Butomus umbellatus*	hel			0.88	0.63												0.35	1.32				2.33	0.92						1.17									2.70	0.61	1.03	0.95	1.58
CALLITRICHACEAE	*Callitriche obtusangola*	hyd																0.35	0.33				3.49	1.83																			
	Callitriche stagnalis	hyd	1.55			1.37									1.37			0.35	0.66						0.71	0.65	0.38	0.30	1.03				0.88		0.62	1.22	0.69	1.27	1.34	1.38	0.76	1.90	1.98
	Callitriche sp.	hyd							0.39																																		
CAPRIFOLIACEAE	*Valeriana officinalis* ttype																	1.40																									
CARYOPHYLLACEAE	*Corrigiola litoralis*	hal		0.49	0.44						2.88	3.57						2.45	3.62	5.02					1.88											0.34		0.34					
	Corrigiola telephiifolia	hal								1.69									0.99	11.60							0.38		0.68	1.21	0.32	1.17			1.01								
	Herniaria glabra type	As							0.39																																		
	Paronychia echinulata type		1.55	1.46	0.44		0.32	0.49				5.26						3.50	1.97	0.31					0.35			0.30	0.68	1.21	0.29					1.29	1.23			1.59		0.34	0.78
	Sagina procumbens group	As	1.55			1.37					3.57	1.32	3.00						5.26								0.38		0.32									0.34					
	Silene dioica type								0.39									4.20																									0.40
	Spergula arvensis type	As			3.54		0.95	0.49	0.39	0.96			4.00						1.97	5.02	12.04		2.75	2.48	2.58	6.02	13.91	9.93	2.73	5.16	2.92	0.65	0.31	2.03		1.37						1.04	
	Caryophyllaceae undiff.												1.32	2.74	2.08								3.49	0.92																			0.79
CRASSULACEAE	*Crassula*																															0.91	0.88				1.35						
	Sedum type					0.63	0.97																										3.55	2.12			0.31	0.68					
	Crassulaceae undiff.																																	2.12									
CYPERACEAE	*Carex* type	hyg		8.78	3.54																0.31				0.35	0.32		0.30	0.34			3.23	0.93	2.03				0.69		1.59	1.67	1.38	
	Schoenoplectus type	hel	1.55	20.98		1.58	0.77								1.00		2.08	5.94	0.99		0.31	3.49	0.92		1.77	3.23			0.68	0.61	0.32	1.17	2.26	4.01	2.36	0.61	1.03	1.59	1.67	5.86	0.76	1.04	
	Scirpus maritimus	hel							0.39																							0.32											
	Cyperaceae undiff.	hyd	7.75	14.63	3.98	6.85	0.32	0.49	0.39			1.32			12.50	17.86	2.80	3.29			1.54	2.33	2.75	1.06					0.68		2.63	4.52	12.35	6.76	3.36	11.34	24.76	20.74	28.28	5.30	15.67	5.71	3.95
EUPHORBIACEAE	*Mercurialis*	As																							2.58													0.97					
FABACEAE	*Lotus* type																				2.75								0.34	1.21	0.97	0.29	0.30					0.34	0.92	0.34		0.76	0.78
	Ononis type	pm, As																	0.66														0.58										
	Trifolium cf. *repens*	pm																							0.31						0.32									0.32			
	Fabaceae undiff.	pm																		0.71																				0.32			0.95
HALORAGACEAE	*Myriophyllum spicatum* type	hyd							1.16																	0.30									0.93				0.63		0.76		
HYDROCHARITACEAE	*Hydrocharis morsus-ranae*	hyd																0.66							0.65							0.91	0.88										0.79
HYPERICACEAE	*Hypericum perforatum* type				0.49	2.65	1.37	0.63																								4.55	0.88		0.31	1.69		0.34					0.79
JUNCACEAE	Juncaceae undiff.		2.33															0.70																									

Table 2b: herbaceous pollen percentages (Amaranthaceae – Juncaceae) of PA1 dataset.

168

Pisa, Pianura Arno 1

Family	Latin name	Groups	25.3	25.18	24.95	24.47	24.13	23.82	23.48	23.15	22.83	22.05	21.8	21.32	19.15	18.67	18.45	17.97	17.8	17.25	16.9	16.35	15.35	14.35	13.35	12.35	11.35	10.35	9.5	8.25	7.45	6.7	6.6	5.97	5.5	5.25	5.1	4.9	4.3	3.75	1.9	0.85	0.5
CHRONOLOGY																				9826±130				7356±68								4682±160		3768±75									
DEPTH (m)			25.3	25.18	24.95	24.47	24.13	23.82	23.48	23.15	22.83	22.05	21.8	21.32	19.15	18.67	18.45	17.97	17.8	17.25	16.9	16.35	15.35	14.35	13.35	12.35	11.35	10.35	9.5	8.25	7.45	6.7	6.6	5.97	5.5	5.25	5.1	4.9	4.3	3.75	1.9	0.85	0.5
SAMPLES			55	54	53	52	51	50	49	48	47	64	46	44	41	40	39	37	36	33	32	31	30	29	28	27	26	25	24	22	21	19	18	16	12	11	10	9	8	7	5	2	1
HERBACEOUS TAXA		E																																								
LAMIACEAE	*Mentha* type									0.96																0.32												0.34					
	Teucrium																		0.33								0.59	0.68			0.29												
	Lamiaceae undiff.																						0.65																			
LILIACEAE	*Streptopus amplexifolius*								0.77																																		
	Liliaceae undiff.			0.49																																							
LINACEAE	*Linum maritimum*	hyg, hal																	0.94																								
	Linum sp.	hyg																			0.35																						
NYMPHAEACEAE	*Nymphaea* cf. *alba*	hyd									21.43									0.33	0.63	0.93																		0.26			
	Nuphar lutea	hyd																						0.65																			
PAPAVERACEAE	*Papaver rhoeas* type	As																						0.97																			
PLANTAGINACEAE	*Linaria* type	As																		0.66							2.42				0.97	0.93											
	Odontites cf.																										0.30															
	Plantago undiff.	As	0.78									1.16	1.69							0.94								2.26															
POACEAE	*"Hordeum"* group	cc, pm			0.88		0.32									1.00		1.79		0.66											0.29		0.31								1.04		1.19
	Poaceae spontaneous group	pm	46.51	25.37	28.76	19.18	9.46	10.19	7.34	25.42	7.05	7.14	31.58	20.55	13.00	14.58	3.57	27.97	19.74	20.69	13.27	25.58	8.26	13.83	5.81	12.03	11.24	10.96	7.27	7.74	9.65	33.87	18.52	13.85	14.07	31.27	27.30	28.43	27.93	16.67	19.58	22.86	17.39
POLYGONACEAE	*Polygonum persicaria* group	As																	2.08	21.43	0.35	0.31																					
	Rumex acetosa type	As		0.49			0.95					0.39				1.00			1.05	2.63	0.31			0.92		3.55	2.42	1.17					0.68										
POTAMOGETONACEAE	*Potamogeton* type	hyd								0.96																													0.63	0.33			
PRIMULACEAE	*Anagallis* sp.																										0.30		0.29														
	Cyclamen hederifolium type																								0.32				3.94														
	Primula veris type																																										
	Primula sp.																				2.13					1.88	2.66	3.08	0.65														
RANUNCULACEAE	*Aconitum napellus* type					0.32	0.49					1.28								3.62	0.94	4.94		5.50	3.55	4.52		1.78	1.37	0.91	1.29	0.29	2.26	1.85	1.35	0.61	1.37	1.59		0.76			
	Caltha palustris type	hyg					0.49													0.99		1.54			1.42			0.30	1.03		1.29		0.97	3.70	3.04	0.31	1.03		0.67				
	Helleborus viridis type																			0.33																							
	Helleborus sp.										0.32																																
	Ranunculus sp.												3.57																														
	Thalictrum flavum type						0.32																		0.32													0.34			1.03	1.34	0.34
	Ranunculaceae undiff.				0.44							0.96								1.32	2.19	0.93			0.71	1.29	0.38	0.30		0.91		2.63	0.32	0.34	0.31	0.34	0.32	1.00	0.34	1.52			0.79
ROSACEAE	*Alchemilla* type																				0.63				1.42			0.30		0.32										0.26		
	Potentilla type																								1.18																	
	Rosaceae undiff.																	0.35							1.06		1.13	0.59	0.34				0.31		0.31	0.34		1.34					0.79
RUBIACEAE	*Galium* type				0.88															0.35					1.42	0.32	0.38	0.30		0.30			0.32		0.34	0.34	0.32						
SAXIFRAGACEAE	*Saxifraga* sp.	Mt																							1.06	1.94	0.30																
SCROPHULARIACEAE	Scrophulariaceae undiff.																6.25								0.97								0.31										
SMILACACEAE	*Smilax aspera*			0.49		1.37				1.69														0.35							0.29										1.52		
TYPHACEAE	*Sparganium emersum* type	hyd	0.78	0.49	0.88	9.59	0.32	0.97	3.86					1.37					1.05	0.33		0.62		0.35	0.65	3.01	0.89	2.74	0.61	0.65	1.75	1.29	4.01	12.16	3.67	3.78	7.94	10.37	1.38	1.52	2.09		
	Sparganium erectum type	hel							0.49	1.16		1.69								0.33						0.34		0.32			2.90	4.01	5.41	1.83	6.87	2.22	4.35	0.34		0.76	0.26		
	Sparganium sp.	hel													2.74				0.35																								
	Typha minima	hel									1.54										0.63			0.92	0.65								0.58	0.65									
	Typha latifolia type	hel				1.37																						0.34										0.32			4.18	1.90	0.79
URTICACEAE	*Parietaria*	As							0.39										1.05									0.30			0.29		0.97		0.93	0.68							
	Urtica atrovirens	As														2.08															0.91												
	Urtica dioica tipo	As		0.98					0.39	1.69			2.74	2.00					10.71	0.66	0.63							2.58		0.34	1.82		0.97	0.58		1.54	0.34		0.32	0.34	1.52	0.52	0.95	1.19
	Urtica membranacea	As	0.78																6.64	1.64											0.32	0.58							0.31					
	Urtica pilulifera	As							0.49																																		
	Urticaceae undiff.	As	3.88			1.37			0.49					2.63						0.35			2.33															0.34				0.26	
XANTHORRHOEACEAE	*Simethis mattiazzi*	M																		0.33	0.63						0.32						0.30		0.32								
UNDETERMINABLE GRAINS			16.23	15.98	20.70	7.59	6.49	2.83	11.90	3.28	7.14	9.68	11.63	12.05	7.41	12.73	11.11	26.67	17.39	11.39	2.99	18.87	4.39	13.23	7.19	18.15	16.13	16.33	6.78		8.80	11.93	4.71	8.07	4.39	17.56	18.39	16.94	21.62	6.38	10.72	7.08	8.00
PTERIDOPHYTES		P																																									
ASPLENIACEAE	*Asplenium adiantum nigrum*	P (hyg)		0.34			0.58												0.60	1.11		0.30		0.35			0.74				0.29		1.11		0.32								
CYSTOPTERIDACEAE	*Cystopteris fragilis*	P (hyg)																	0.56	2.02		0.30																					
DENNSTAEDTIACEAE	*Pteridium aquilinum*	P (hyg)		0.34																		0.30											0.88										
DRYOPTERIDACEAE	*Polystichum* type	P (hyg)																								0.30																	
	Dryopteris filix-mas	P (hyg, umb)																													0.29												
ISOETACEAE	*Isoetes* sp.	P (hyg)		2.73	4.10																						1.11																
	Isoetes durieui	P (hyg)	4.29	21.50	0.75		3.78	5.45	0.37	3.17	0.92								8.63	1.94																		0.31		0.30		0.26	
	Isoetes hystrix	P (hel)					1.45																	0.83			0.74	0.29															
	Isoetes lacustris	P (hyd)																	2.38	3.06	1.44	1.49																					
MARSILEACEAE	*Pilularia globulifera*	P (hyd)									0.31									0.28				0.83																			
OPHIOGLOSSACEAE	*Botrychium lunaria* type	P (hyg)			0.37				0.37																		0.29											0.34		0.30			
	Ophioglossum vulgatum type	P (hyg)					0.29																																				
POLYPODIACEAE	*Polypodium vulgare* type	P (hyg)					0.29													0.28				0.83																			
PTERIDACEAE	*Adiantum capillus-veneris*	P (hyg)			1.02					0.31																																	
	Pteris sp.	P (hyg)			0.37																																						
	Pteris cretica	P (hyg, umb)					0.29			0.61										0.28							0.29															2.73	0.38
SALVINIACEAE	*Salvinia natans*	P (hyg)			0.68																																						
SELAGINELLACEAE	*Selaginella*	P (hyg)					0.29																																				
FILICALES MONOLETI		P (hyg)	3.57	2.39	9.33	7.59	0.87	0.91	1.50	3.17	2.15	3.28	1.30	6.41	0.99	6.56	2.08	7.22	4.61	1.19	3.37	6.67	1.05	5.76	0.74	2.02	0.34	1.17	1.27	1.94	1.27	3.85	0.34	1.02	1.25	3.86	11.21	10.74	1.79	1.82	1.92		
FILICALES TRILETI		P (hyg)		1.02	0.75				0.75						4.92		2.04	1.64	1.19	0.83							0.29		0.83		0.32		0.30		0.34			0.30		0.30		0.67	0.77
PTERIDOPHYTA - TOTAL		P	7.86	30.03	15.67	7.59	7.85	6.36	3.00	6.35	4.29	8.20	1.30	6.41	0.99	2.04	8.20	14.88	15.56	8.07	3.57	3.37	9.17	1.40	6.06	2.21	2.59	0.34	3.23	1.27	5.00	1.90	4.14	0.67	0.30	1.36	1.56	3.86	12.12	11.41	2.05	4.55	3.07
ALIA																																											
ALGAE	*Pseudoschizaea circula*		4.44			1.35	0.31												1.75	4.67	0.98	0.93	0.61								0.32		0.31				0.68	0.32	0.99	3.01	2.94	4.25	0.78
ANIMALIA	Nematoda (eggs)																																								3.32	0.63	0.33
DINOFLAGELLATA									43.70				1.75																												0.75		
FUNGI	*Glomus*																																0.32					0.34	0.33				

Table 2c: herbaceous pollen percentages (Lamiaceae – Xantorrhoeaceae; Pteridophytes) and alia of PA1 dataset.

Pisa, Pianura Arno 1

			25.3	25.18	24.95	24.47	24.13	23.82	23.48	23.15	22.83	22.05	21.8	21.32	19.15	18.67	18.45	17.97	17.8	17.25	16.9	16.35	15.35	14.35	13.35	12.35	11.35	10.35	9.5	8.25	7.45	6.7	6.6	5.97	5.5	5.25	5.1	4.9	4.3	3.75	1.9	0.85	0.5
CHRONOLOGY																					9826±130				7356±68								4682±160		3768±75								
DEPTH (m)			25.3	25.18	24.95	24.47	24.13	23.82	23.48	23.15	22.83	22.05	21.8	21.32	19.15	18.67	18.45	17.97	17.8	17.25	16.9	16.35	15.35	14.35	13.35	12.35	11.35	10.35	9.5	8.25	7.45	6.7	6.6	5.97	5.5	5.25	5.1	4.9	4.3	3.75	1.9	0.85	0.5
SAMPLES			55	54	53	52	51	50	49	48	47	64	46	44	41	40	39	37	36	33	32	31	30	29	28	27	26	25	24	22	21	19	18	16	12	11	10	9	8	7	5	2	1
Family	**Latin name**	**Groups**																																										
BRYOPHYTA																																												
AMBLYSTEGIACEAE	*Drepanocladus revolvens*	hel					0.31																										0.31											
	Hygrohypnum luridum	hyg			2.00			0.96	0.74																																			
ANEURACEAE	*Aneura pinguis*	hyd																						0.32																				
ANTHOCEROTHACEAE	*Phaeoceros laevis*	hyg	0.74	4.76	2.80													0.90	0.60		0.60			0.65	0.61							0.64								0.34		1.02		
AYTONIACEAE	*Reboulia hemisphaerica*	Mt, umb		0.63																																								
BRYACEAE	*Bryum marratii*	hel		0.63																																								
	Bryum sp.	igro			0.40																1.29																							
	Leptobryum pyriforme	As																		4.76																								
	Orthodontium gracile	hum		1.90	0.40	1.53												0.90	0.30	0.31					0.61																			
CODONIACEAE	*Fossombronia pusilla*	hyg			0.40																																							
	Fossombronia wondraczekii	hyg									1.72																																	
CONOCEPHALACEAE	*Conocephalum conicum*	hyg, umb								0.37																																		
DICRANACEAE	*Aongstroemia longipes*	Mt, hyg																0.30																										
	Campylopus pyriformis	hyg, umb			0.63					0.37																	0.29	0.62																
	Cynodontium polycarpon	Mt																										0.31															
	Dicranella cerviculata	hyg													4.44	0.92												0.62																
	Dicranella palustris	hyd, helio																								0.29																		
	Dicranella varia	helio																0.30																										
	Dicranoweisia crispula	Mt, helio													4.44																													
	Dicranum bonjeani	hel																1.51																										
	Dicranum scoparium	umb																0.30																										
	Saelania glaucescens	Alia		0.63																								0.31																
	Trematodon ambiguus	hyg			0.40																																							
	Dicranaceae undiff.	Alia		2.22														0.60						0.65				0.31																
DISCELIACEAE	*Discelium nudum*	hyg																0.30																										
ENCALYPTACEAE	*Encalypta ciliata*	hel		0.32																																								
HEDWIGIACEAE	*Hedwigia ciliata*	Mt		0.63																																								
FABRONIACEAE	*Fabronia pusilla*	Mt		0.32																																								
FISSIDENTACEAE	*Fissidens adianthoides*	hel																1.20																										
	Fissidens rufulus	hyg		3.17											5.56			0.30																										
FUNARIACEAE	*Funaria hygrometrica*	As																0.30																										
JUNGERMANNIACEAE	*Mylia taylori*	Mt								0.37														0.32	0.36							1.16	0.64											
LEUCODONTACEAE	*Cryphaea heteromalla*	Mt, umb			0.80																																							
LOPHOZIACEAE	*Gymnocolea inflata*	hyg		1.90	0.40													0.60	0.30																									
MEESIACEAE	*Meesia longiseta*	hel		0.95																				0.97																				
	Meesia uliginosa	hyg, helio																										0.31															
MNIACEAE	*Cinclidium stygium*	hel		0.63																																								
	Plagiomnium cuspidatum	umb				0.31														0.62																								
	Rhizomnium punctatum	hyg, umb		0.32						0.37																		0.31															
ORTHOTRICHACEAE	*Ortotrichum anomalum*	M, helio								0.37																																		
POLYTRICHACEAE	*Atrichum undulatum*	umn		1.27																								0.31															
	Polytrichum longisetum	hyg						0.48	0.37															0.32				0.31																
POTTIACEAE	*Pterygonum ovatum*	M, helio			1.20																																							
PTILIDIACEAE	*Ptilidium pulcherrimum*	umb				0.31																																						
SPHAGNACEAE	*Sphagnum capillifolium*	hel		1.90																																								
	Sphagnum fimbriatum	hel		1.90																			1.20	0.97		3.60	1.73	4.62		2.75										0.33				
	Sphagnum palustre	hel		0.32																																								
	Sphagnum recurvum	hel			0.80		0.31			1.11					2.22									0.65																				
	Sphagnum sp.	hel	1.47	1.90		1.33	0.31							1.30				0.30						0.32	0.61	0.36	0.29			1.53									0.34	0.32	0.33		0.26	1.17
SPLACHNACEAE	*Splachnum sp.*	Alia																0.30																										
	Splachnum sphaericum	hyg																	3.57																									
BRYOPHYTA UNDIFF.		Alia	2.94	7.94		1.33			0.37	3.28	1.58	1.72	2.22	7.34				5.72		0.62	0.60			2.58	3.07			1.85		0.92									0.34				
BRYOPHYTA TOTAL			5.15	34.92	9.60	2.67	3.06	1.44	4.43	3.28	1.58	3.45		1.30	18.89	8.26		13.86	9.52	1.54	2.41			9.03	4.91	4.32	2.59	10.15		5.20	1.16	1.27						1.02	0.32	0.66	1.02	0.26	1.17
SECONDARY GRAINS																																											
	Abies alba																																					0.29					
	Alnus sp.																	1.68					0.55	3.13				3.94										3.31	2.65	3.65	5.34		0.21
	Asteroideae undiff.																														0.28							0.25	0.60		1.25		
	Betulaceae undiff.												3.30					2.36					8.47	4.13		3.41											0.30		0.30	1.02		
	Carya				3.33								1.10		1.92																								0.29	0.25			
	Chenopodiaceae undiff.																				0.34						0.28											0.30	0.29	0.30	0.51		
	Cichorioideae undiff.																																	0.56		0.30					0.51		
	Corylus avellana						0.95						1.10														2.84	0.56										0.60	0.29	0.61	2.04		
	Engelhardtia																																				0.30					
	Erica arborea type																														0.33									1.88		
	Filicales monolete												1.10																	0.28							0.30					
	Filicales trilete		0.64																1.75					0.55																0.25	0.71	0.63	
	Ostrya c./ Carpinus o.																																							0.25			
	Piceapollenites mesophyticus				3.04	1.11																																						
	Pinaceae (Cretaceous)				18.24	2.22																																						
	Pinaceae undiff.									0.95																												0.30		0.30	1.78		1.25
	Pinus sp.				1.11																						0.28			0.29												5.67	0.63
	Poaceae undiff.																										0.28										1.22	0.25			0.63	0.93
	Pterocarya																						0.55				0.28										0.30					
	Sequoiadendron																																				0.29					
	Tilia sp.																																								0.21		
	Tsuga																													0.28								0.30	0.61			
	Zelkova																																							0.93		0.21
	Undeterminable grains		16.67	6.39	2.36	11.11	6.49	0.95		3.28	0.63	3.45	9.89		5.77	1.38	2.56	3.92	1.22	2.27	1.80	0.67	0.32	1.36	1.10	6.53	1.79	6.76	0.57	1.20	1.00	0.30			6.93	3.83	2.13	13.74	13.15
	TOTAL		17.31	6.39	23.65	18.89	6.49	1.90		3.28	1.58	3.45	16.48		7.69	1.75	1.38	2.56	3.92	1.22	2.27	1.80	5.05	0.32	9.83	6.89	17.05	1.79	12.68	2.01	2.70	1.33	0.30			12.35	7.08	9.12	26.21	6.38	20.04	1.87

Table 2d: Bryophytes and secondary grains of PA1 dataset.

170

Pisa, Pianura Arno 1

PLANT ECOLOGICAL GROUPS	SAMPLES	25.3	25.18	24.95	24.47	24.13	23.82	23.48	23.15	22.83	22.05	21.8	21.32	19.15	18.67	18.45	17.97	17.8	17.25	16.9	16.35	15.35	14.35	13.35	12.35	11.35	10.35	9.5	8.25	7.45	6.7	6.6	5.97	5.5	5.25	5.1	4.9	4.3	3.75	1.9	0.85	0.5
CHRONOLOGY																			9826±130					7356±68								4682±160				3768±75						
SAMPLES (no.)		55	54	53	52	51	50	49	48	47	64	46	44	41	40	39	37	36	33	32	31	30	29	28	27	26	25	24	22	21	19	18	16	12	11	10	9	8	7	5	2	1
WOODY	T+s h	16.28	17.07	25.66	45.21	67.51	79.13	72.59	55.93	82.05	37.50	36.84	65.75	61.00	52.08	33.93	17.13	32.57	38.56	51.54	40.70	61.47	50.00	52.26	64.66	56.51	56.51	50.00	70.32	62.57	37.42	40.12	35.14	68.81	30.58	20.32	23.08	16.55	43.18	16.19	18.10	7.11
TREES	T	14.73	16.59	23.01	39.73	53.94	48.54	59.07	28.81	58.33	37.50	32.89	65.75	60.00	50.00	33.93	14.69	26.64	29.15	34.57	31.40	51.38	44.33	40.65	48.87	43.20	37.67	39.09	55.16	58.19	32.26	39.81	34.12	68.50	26.46	18.41	19.40	15.17	40.91	12.53	14.29	6.72
SHRUBS	sh	1.55	0.49	2.65	5.48	13.56	28.16	13.51	27.12	23.72		3.95		1.00	2.08		2.45	5.92	9.40	16.98	9.30	10.09	5.67	11.61	15.79	13.31	18.84	10.91	15.16	4.39	5.16	0.31	1.01	0.31	4.12	1.90	3.68	1.38	2.27	3.66	3.81	0.40
QUERCETUM+other DT	Q+other DT	6.20	10.73	11.95	17.81	30.91	37.86	35.91	25.42	22.76	10.71	17.11		6.00	18.75	3.57	10.49	10.53	19.44	19.14	17.44	20.18	15.96	11.29	18.42	18.34	14.04	13.94	13.55	17.25	11.29	8.02	3.72	1.83	4.81	5.40	6.69	6.55	6.82	6.53	1.90	0.79
OTHER DECIDUOUS TREES	DT	0.78		2.21	2.74	3.15	2.43	6.95	3.39	1.28					2.08		4.20	1.64	0.63		4.65	2.75	1.77	0.97	2.26	1.18	3.08	0.91	0.65	1.46			0.34	0.31	0.34		0.67	0.69		1.57		
QUERCETUM	Q	5.43	10.73	9.73	15.07	27.76	35.44	28.96	22.03	21.47	10.71	17.11		6.00	16.67	3.57	6.29	8.88	18.81	19.14	12.79	17.43	14.18	10.32	16.17	17.16	10.96	13.03	12.90	15.79	11.29	8.02	3.38	1.53	4.47	5.40	6.02	5.86	6.82	4.96	1.90	0.79
MEDITERRANEANS	M	1.55		3.54	5.48	21.45	29.61	15.83	22.03	30.45		2.63		1.00	2.08		1.40	8.22	9.72	12.35	15.12	11.01	14.89	12.58	19.92	17.46	22.26	10.00	20.32	9.36	3.55	3.09	4.05	1.22	5.84	6.67	4.01	1.03	5.30	2.61	4.76	0.79
WOODY HYGROPHYTES	H	1.55	2.93	1.77	15.07	5.68	11.17	11.20	3.39	4.49	3.57		4.11	2.00	2.08	3.57	2.10	5.92	8.15	12.65	5.81	11.01	12.06	9.68	21.43	11.24	11.64	8.79	17.10	12.87	13.55	26.54	25.00	64.53	15.81	5.71	8.36	4.83	9.85	2.09	4.76	2.37
HERBS	E	83.72	82.93	74.34	54.79	32.49	21.84	27.41	44.07	17.95	62.50	63.16	34.25	39.00	47.92	66.07	82.87	67.43	61.44	48.46	59.30	38.53	50.00	47.74	35.34	43.49	43.49	50.00	29.68	37.43	62.58	59.88	64.86	31.19	69.42	79.68	76.92	83.45	56.82	85.12	81.90	92.89
PASTURE-MEADOW	pm	52.71	28.78	44.69	26.03	11.99	10.19	8.49	30.51	7.05	12.50	46.05	23.29	21.00	14.58	7.14	33.92	23.03	24.45	14.51	37.21	8.26	15.25	6.45	12.78	11.83	11.30	10.91	8.39	11.99	36.45	19.44	14.86	14.37	31.62	28.25	30.43	35.86	22.73	33.68	48.57	39.13
UMBROTROPHICS	omb		2.86	0.80		0.90		1.11		0.61							0.30	0.28	0.62					0.58	1.23	0.29															2.73	0.38
HELIOPHILOUS	helio		1.20					0.37						4.44			0.30							0.59	0.31																	
HERBACEOUS HYGROPHYTES	hyg	7.75	23.41	7.52	6.85	0.32	0.97	0.39			1.32			12.50	17.86	0.30	2.80	4.28	0.94	3.40	2.33	2.75	3.19	0.32		0.99	2.05		1.29	2.63	8.71	16.98	11.82	3.67	13.06	26.35	23.08	29.66	5.30	15.93	5.71	3.95
TOTAL HYGROPHYTES	Hyg	9.30	26.34	9.29	21.92	5.99	12.14	11.58	3.39	4.49	3.57	1.32	4.11	2.00	14.58	21.43	4.90	10.20	9.09	16.05	8.14	13.76	15.25	10.00	21.43	11.83	13.70	8.79	18.39	15.50	22.26	43.52	36.82	68.20	28.87	32.06	31.44	34.48	15.15	18.02	10.48	6.32
HELOPHYTES	hel	1.55	20.98	0.88	1.37	2.21	0.49	3.86	1.69				2.74	1.00	2.08		6.64	2.63	0.63	0.31	5.81	2.75	1.77	3.87		1.37	0.91	0.65	2.92	6.13	8.02	10.47	3.06	7.90	4.13	6.02	7.24	1.52	5.48	2.86	2.37	
HYDROPHYTES	hyd	2.33	0.49	0.88	9.59	0.32	0.97	6.18		0.96	32.14		2.74				1.75	2.30	0.63	1.54	3.49	1.83	1.06	2.58	3.38	1.18	3.77	1.82	0.65	3.51	1.29	5.56	12.16	4.89	4.81	10.48	12.04	3.10	3.03	2.09	1.90	2.77
AQUATICS	Aq	3.88	21.46	1.77	10.96	2.52	1.46	10.04	1.69	0.96	32.14		5.48	1.00	2.08		8.39	4.93	1.25	1.85	9.30	4.59	2.84	6.45	3.38	1.18	5.14	2.73	1.29	6.43	7.42	13.58	22.64	7.95	12.71	14.60	18.06	10.34	4.55	7.57	4.76	5.14
HALOPHYTES	hal	1.55	0.49	7.52	2.74	11.04	4.37	2.32	6.78	3.85	7.14	1.32		1.00			4.20	7.57	17.55	8.33		8.26	9.22	3.87	6.02	5.92	4.79	5.15	3.23	1.75	0.97	0.31	1.35		0.69	0.95	0.67	0.34	1.52	2.09	3.81	12.25
MONTANE TAXA (no Pinus)				5.75	2.74	7.26	0.49	4.63	1.69	12.50	7.14		2.74	4.00	12.50	12.50	2.80	4.93	0.63	4.94	2.33	16.51	2.48	16.13	3.76	8.28	7.19	17.27	18.39	16.96	8.71	0.62	2.03		2.75	0.63	3.34	1.38	5.30	1.57	1.90	0.79
MONTANE TAXA	Mt	6.98	3.41	8.41	6.85	9.46	0.49	9.65	5.08	24.36	23.21	17.11	61.64	52.00	29.17	26.79	3.15	8.22	1.88	7.41	2.33	19.27	8.16	20.97	4.89	9.76	8.56	17.58	19.68	23.10	9.03	2.47	2.36	1.22	4.12	2.54	4.01	4.14	21.21	4.96	6.67	3.16
HERBACEOUS ANTHROPIC SPONTANEOUS	As	9.30	2.93	4.87	4.11	9.78	2.91	5.41	8.47	0.96	10.71	7.89	2.74	13.00	10.42	39.29	20.63	15.79	12.23	15.12	6.98	10.09	5.67	15.16	7.89	16.27	12.33	13.03	10.97	8.48	4.19	4.94	4.39	2.75	3.09	1.59	1.00	2.07	8.33	2.87	9.52	10.67
CULTIVATED	cc																											0.61							2.41	3.81	0.67	2.76	9.09	17.23	2.86	2.77
TOTAL ANTHROPIC SPONTANEOUS	Ai	9.30	2.93	4.87	4.11	9.78	2.91	5.41	8.47	0.96	10.71	7.89	2.74	13.00	10.42	39.29	20.63	15.79	12.23	15.12	6.98	10.09	5.67	15.16	7.89	16.27	12.33	13.64	10.97	8.48	4.19	4.94	4.39	2.75	5.50	5.40	1.67	4.83	17.42	20.10	12.38	13.44

COUNTED GRAINS

		25.3	25.18	24.95	24.47	24.13	23.82	23.48	23.15	22.83	22.05	21.8	21.32	19.15	18.67	18.45	17.97	17.8	17.25	16.9	16.35	15.35	14.35	13.35	12.35	11.35	10.35	9.5	8.25	7.45	6.7	6.6	5.97	5.5	5.25	5.1	4.9	4.3	3.75	1.9	0.85	0.5
TRACHEOPHYTA	S+P	140	293	268	79	344	220	267	63	326	61	77	78	101	49	61	336	360	347	336	89	120	286	330	272	347	293	341	314	360	316	338	298	328	295	320	311	330	149	391	110	261
SPERMATOPHYTA (pollen sum)	S	129	205	226	73	317	206	259	59	312	56	73	73	100	48	56	286	304	319	324	86	109	282	310	266	338	292	330	310	342	310	324	296	327	291	315	299	290	132	383	105	253
PTERIDOPHYTA	P	11	88	42	6	27	14	8	4	14	5	1	5	1	1	5	50	56	28	12	3	11	4	20	6	9	1	11	4	18	6	14	2	1	4	5	12	40	17	8	5	8
BRYOPHYTA	Br	7	110	24	2	10	3	12	2	5	2		17	9			46	32	5	8		28	16	12	9	33		17	4	4				3	1	2						3
SECONDARY GRAINS		27	14	70	17	22	4		2	5	2	15			4	1	4	8	13	4	2	2	15	1	29	25	60	6	45	7		9	4	1	41	24	30	103	9	96		2

ABSOLUTE POLLEN FREQUENCY (grains/g)

		25.3	25.18	24.95	24.47	24.13	23.82	23.48	23.15	22.83	22.05	21.8	21.32	19.15	18.67	18.45	17.97	17.8	17.25	16.9	16.35	15.35	14.35	13.35	12.35	11.35	10.35	9.5	8.25	7.45	6.7	6.6	5.97	5.5	5.25	5.1	4.9	4.3	3.75	1.9	0.85	0.5
APF TOTAL		5282	49456	16177	6890	61155	431672	4384	166681	13757	19032	1552	3011	82	1131	1430	78074	17921	143443	434218	112363	133274	11477	11553	6842	10244	16337	41142	21298	21519	30945	27596	329761	420907	28176	30914	23264	22572	3582	7550	1728	3606
APF SPERMATOPHYTA		4635	25158	12520	6210	54763	398764	4070	151205	12967	16917	1513	2314	75	1108	1312	58454	13898	129995	408972	108575	121057	10308	10351	6408	9726	14633	39815	19947	20218	29978	26453	327548	419624	27514	30336	22223	19658	3173	7377	1649	3455
APF PTERIDOPHYTA		395	10799	2327	510	4664	27100	126	10257	582	1510	20	158	1	23	117	10219	2560	11410	15147	3788	12217	146	668	145	50	1327	257	1064	580	1143	2213	1283	378	482	892	2711	409	154	79	109	
APF BRYOPHYTA		252	13499	1330	170	1728	5807	189	5129	208	604	20	539	7			9402	1463	2038	10098		1023	534	289	259	1654		1094	236	387				284	96	149	203					41
APF SECONDARY GRAINS		970	1718	3878	1446	3801	7743		5129	208	604	299			92	23	818	366	5298	5049	2525	2221	548	33	699	719	3007	724	2896	414		735	4426	1283	3876	2311	2230	6982	216	1849		1

Pteridophyta-Briophyta groups

		25.3	25.18	24.95	24.47	24.13	23.82	23.48	23.15	22.83	22.05	21.8	21.32	19.15	18.67	18.45	17.97	17.8	17.25	16.9	16.35	15.35	14.35	13.35	12.35	11.35	10.35	9.5	8.25	7.45	6.7	6.6	5.97	5.5	5.25	5.1	4.9	4.3	3.75	1.9	0.85	0.5
MONTANE	Mt		0.63					0.37						4.44			0.30					0.32		0.36		0.31									1.16	0.64						
MEDITERRANEANS	M		0.95	2.00				0.37																																		
HYGROPHYTES	hyg	10.06	42.73	22.07	8.93	6.70	7.80	5.21	6.35	3.99	9.92	2.60	16.41	1.91	2.04	8.20	15.21	16.69	6.63	2.69	3.37	7.29	1.83	2.88	3.23	2.80	5.00	2.54	4.14	0.67	0.30		2.04	1.88	4.19	13.15	11.41	2.31	4.55	4.24		
helophytes	hel	1.47	8.57	0.80	1.33	2.37		1.11				1.30	2.22				3.01			1.20		0.83	2.90	0.61	4.69	2.31	4.92		4.28						0.34	0.32	0.66			1.17		
hydrophytes	hyd								0.61								4.76	6.67	2.88	2.98		1.67	0.32		0.29																	
AQUATICS	Aq	1.47	8.57	0.80	1.33	2.37		1.11	0.61		1.30	2.22				7.77	6.67	2.88	4.18		2.50	3.23	0.61	4.69	2.59	4.92		4.28						0.34	0.32	0.66				1.17		
OMBROTROPHIC	omb		2.86	0.80		0.90		1.11		0.61							0.30	0.28	0.62					0.58	1.23	0.29													2.73	0.38		
HELIOPHILOUS	helio		1.20					0.37						4.44			0.30							0.29	0.31																	
HUMICOLOUS	hum		1.90	0.40		1.53											0.90	0.30	0.31						0.61																	
DISTURBANCE	As																0.30	4.76																								
ALIA	Alia	2.94	10.16		1.33			0.37	3.28	1.58	1.72		2.22	7.34			6.63			0.62	0.60			3.23	3.07			2.15		0.92						0.34						

Bryophyta groups

		25.3	25.18	24.95	24.47	24.13	23.82	23.48	23.15	22.83	22.05	21.8	21.32	19.15	18.67	18.45	17.97	17.8	17.25	16.9	16.35	15.35	14.35	13.35	12.35	11.35	10.35	9.5	8.25	7.45	6.7	6.6	5.97	5.5	5.25	5.1	4.9	4.3	3.75	1.9	0.85	0.5
MONTANE	Mt		0.63					0.37						4.44			0.30					0.32		0.36		0.31									1.16	0.64						
MEDITERRANEANS	M		0.95	2.00				0.37																																		
HYGROPHYTES	hyg	2.21	12.70	6.40	1.33	0.31	1.44	2.21			1.72	1.30	10.00	0.92			2.71	4.46		0.60			2.90	1.23	0.36	0.58	2.46		1.53			0.64				0.68	0.32	0.33	1.02		0.26	1.17
HELOPHYTES	hel	1.47	8.57	0.80	1.33	0.92		1.11				1.30	2.22				3.01			1.20			2.90	0.61	3.96	2.02	4.92		4.28						0.34	0.32			0.26			1.17
HYDROPHYTES	hyd								0.31								2.38	3.33	1.44	1.49		0.83	0.32		0.29																	
OMBROTROPHIC	omb		2.86	0.80		0.61		1.11									0.30		0.62							0.29	1.23															
HELIOPHILOUS	helio		1.20					0.37						4.44			0.30							0.29	0.31																	
HUMICOLOUS	hum		1.90	0.40		1.53											0.90	0.30	0.31						0.61																	
DISTURBANCE	As																0.30	4.76																								
UNDIFF.	Alia	2.94	10.16		1.33			0.37	3.28	1.58	1.72		2.22	7.34			6.63			0.62	0.60			3.23	3.07			2.15		0.92						0.34						

Table 2e: plant ecological groups of PA1 dataset.